

Conjugates of Fragmented Proteins and Polysaccharides as Food Emulsifiers

Yue Ding

Submitted in accordance with the requirements for the degree of Doctor of
Philosophy

The University of Leeds
School of Food Science and Nutrition

October 2020

The candidate confirms that the work submitted is her own and that appropriate credit has been given where reference has been made to the work of others.

This copy has been supplied on the understanding that it is copyright material and that no quotation from the thesis may be published without proper acknowledgement.

The right of Yue Ding to be identified as Author of this work has been asserted by Yue Ding in accordance with the Copyright, Designs and Patents Act 1988.

©2020 The University of Leeds and Yue Ding

Acknowledgements

Firstly, I would love to thank my primary supervisor Dr. Rammile Ettelaie. I learnt most of the essentials of the field of food colloids, particularly the theoretical calculations, from him. Without his great guidance and support, this Ph.D project could not have been completed. I would also like to thank my second supervisor Dr. Mahmood Akhtar for his help with my experiments. Additionally, I would like to express my special thanks to Prof. Jianshe Chen from Zhejiang Gongshang University, who previously worked in School of Food Science and Nutrition, University of Leeds, for his constructive suggestions during my exchange visit to his laboratory in China.

Particularly, I would like to take this opportunity to thank my parents and other family members for their wholehearted love and patience. Last but not least, I would like to thank my friends and colleagues for their encouragements throughout my entire journey of Ph.D.

Publications from thesis

Manuscript in progress:

Ding, Y., Chen, L., Shi, Y.G., Akhtar, M., Chen, J.S., & Ettelaie, R. (2020). Emulsifying and emulsion stabilizing properties of soy protein hydrolysates, covalently bonded to polysaccharides: The impact of enzyme choice and the degree of hydrolysis. *Food Hydrocolloids*, under revision.

Attended conferences and accepted abstracts

Ding, Y., & Ettelaie, R. A theoretical study of mediated steric interactions by fragmented soy proteins conjugated with polysaccharides. *BIOPOLYMERS 2017: Key Ingredients for the Food Transition*, Tour, Bretagne in Nantes, France, 29th November to 1st December 2017.

Ding, Y., & Ettelaie, R. A theoretical study of stabilizing properties of conjugated vegetable protein fragments as food emulsifiers. *The 3rd Annual Food Science & Nutrition PhD Conference* – University of Leeds, Leeds, West Yorkshire, UK, 22nd November 2017.

Ding, Y., & Ettelaie, R., & Akhtar, M. A theoretical study of mediated steric interactions by fragmented soy proteins conjugated with polysaccharides. *The 17th Food Colloids Conference* – University of Leeds, Leeds, West Yorkshire, UK, 8th to 11th April 2018.

Ding, Y., & Ettelaie, R., & Akhtar, M. Conjugated soy protein as food emulsifiers. *The 4th Edwards Symposium: Emerging Trends in Soft Matter* – University of Cambridge, Cambridge, UK, 4th to 6th September 2019.

Ding, Y., & Ettelaie, R., & Akhtar, M. Conjugated soy protein as food emulsifiers. *Physics in Food Manufacturing 2020 Conference* – IOP Liquids and Complex Fluids, Leeds, West Yorkshire, UK, 15th to 17th January 2020.

Abstract

Protein based emulsifiers play an important role in food colloids. Modified proteins derived from animal sources, formed by covalent bonding with polysaccharide via Maillard reaction, have been reported in the literature to have excellent emulsifying and stabilizing abilities under harsh environmental stresses (e.g. high ionic strengths, freeze-thaw cycles, acidic pH conditions). On the contrary, conjugates based on plant derived proteins, have presented an incomplete, and often confusing picture of their colloidal stabilizing behaviour.

In the current study, milk whey protein isolate (WPI) and commercial soy protein isolate (SPI) were used as respective typical representatives of animal and plant sourced proteins. Careful comparisons were made between these two materials, undergoing exactly the same modification process (i.e. hydrolysis of proteins followed by conjugation with maltodextrin). The aim is to explore the possibility of and the difficulties in obtaining suitable conjugated plant proteins which have comparable emulsifying efficiency to their animal derived counterparts in producing stable and fine submicron sized oil-in-water (O/W) emulsion systems.

Two enzymes (i.e. trypsin and alcalase) were used to digest protein, particularly in order to improve the poor solubility and emulsifying property of SPI. Various degrees of hydrolysis (i.e. DH = 2.5%, 5.5% and 8.0%) were attempted. It is seen that for both WPI and SPI, trypsin, which has a higher level of selectivity at cleaving peptide bonds than alcalase, is more beneficial in producing polypeptides with improved emulsifying and colloidal stabilizing performance. The optimal DH was found to be roughly 2.5% and 8.0% for WPI and SPI, respectively.

Furthermore, by using an uncharged, linear and relatively small maltodextrin with no special surface functionalities (e.g. emulsifying, gelling or stabilizing properties) on its own, the impacts of conjugation with this polysaccharide on the colloidal stabilizing capacities of proteins and their hydrolysates under various pH conditions were investigated. Consistent with the literature, conjugated whey protein materials offered excellent flocculation stabilization to emulsion droplets in the absence of sufficient electrostatic repulsion. The situation was slightly different with regard to modified soy protein materials. The emulsion droplets coated by the conjugated biopolymers, based

on fragmented soy protein, only exhibited limitedly enhanced flocculation stability. This is attributed to the inefficient level of Maillard reaction between protein/hydrolysates and maltodextrin. For soy protein (and probably most plant derived proteins), the major issue of synthesizing Maillard reaction products (MPRs) is the presence of particulate proteins in the sample, which is not desirable for achieving a molecular-scale intimate mixing of protein materials and polysaccharide, thus not facilitating the covalent bonding between those two species.

Last but not least, theoretical calculations were also performed, evaluating the impact of the size of a protein fragment and polysaccharide on the colloidal stabilizing capacity of emulsifiers made from these two components. The predicted theoretical results, together with experimental results, demonstrated that short peptides (and conjugated polymers derived from them) fail to deliver proper emulsifying and stabilising functionalities, as they are not able to adsorb sufficiently at the droplet surface (even though they may have a large proportion of hydrophobic amino acid residues). The critical size of a polypeptide to fulfil the role of strongly anchoring the composite polypeptide + maltodextrin biopolymer at the O/W interface was found to be roughly 10 kDa from the experiments. For conjugated polymer that can adsorb substantially, the size of its polysaccharide attachment now becomes predominant in controlling the colloidal stabilizing ability of this hybrid polymer species.

This study highlights the benefits of using highly selective enzymes, such as trypsin, in producing plant protein fragments with good colloidal performances. It also demonstrates that the major obstacle for obtaining suitable plant based conjugated emulsifier is the aggregated state of the protein material. Thus, an important prerequisite is a reasonable solubility of plant protein, which allows for a uniform mixture of protein materials with polysaccharide, prior to their Maillard reaction via heating process.

Table of Contents

Acknowledgements	iii
Publications from thesis	iv
Attended conferences and accepted abstracts	v
Abstract	vi
Table of Contents	viii
List of Tables	xiii
List of Figures	xiv
Chapter 1 Introduction	- 1 -
1.1 Foundation of research	- 1 -
1.1.1 Colloidal state of matter	- 1 -
1.1.2 Surface free energy	- 2 -
1.1.3 Colloidal interactions	- 3 -
1.1.3.1 Van der Waals force	- 4 -
1.1.3.2 Electrostatic repulsion and DLVO theory	- 5 -
1.1.3.3 Steric repulsion and total interaction potential	- 6 -
1.1.3.4 Bridging and depletion attractions	- 7 -
1.1.3.5 Hydrophobic interactions	- 8 -
1.1.4 Stability of emulsions	- 8 -
1.1.4.1 Creaming	- 8 -
1.1.4.2 Flocculation	- 9 -
1.1.4.3 Coalescence	- 10 -
1.1.4.4 Ostwald ripening	- 11 -
1.1.5 Emulsifiers and stabilizers	- 11 -
1.2 Protein-polysaccharide conjugates as food emulsifiers	- 12 -
1.2.1 Stabilizing mechanism of protein-polysaccharide conjugates	- 13 -
1.2.2 Preparation of protein-polysaccharide conjugates	- 14 -
1.2.3 Conjugates based on animal-derived proteins	- 18 -
1.2.4 Conjugates based on plant-derived proteins	- 20 -
1.3 Aims and objectives	- 26 -
1.4 Thesis outline	- 27 -
Chapter 2 Theoretical and Experimental Methods	- 29 -
2.1 Introduction	- 29 -
2.2 Theoretical methods	- 29 -

2.2.1 Statistical and thermal physics	- 30 -
2.2.2 SCF theory applied to dense adsorbed interfacial layers	- 31 -
2.3 Experimental methods	- 35 -
2.3.1 Degree of hydrolysis	- 36 -
2.3.2 Gel electrophoresis	- 37 -
2.3.3 Solubility	- 38 -
2.3.4 Sulfhydryl (-SH) content	- 39 -
2.3.5 Particle sizing	- 40 -
2.3.5.1 Sizing of emulsifiers	- 40 -
2.3.5.2 Sizing of emulsion droplets	- 42 -
2.3.6 Zeta potential	- 43 -
2.3.7 Rheological measurements	- 45 -
Chapter 3 A Theoretical Study of the Colloidal Stabilizing Ability of Emulsifiers Influenced by Structural Properties of Polypeptide and Polysaccharide	- 48 -
3.1 Introduction	- 48 -
3.2 Models	- 49 -
3.3 Results and Discussions	- 54 -
3.3.1 The impact of the structural properties of a protein fragment on its emulsion stabilizing capacity	- 54 -
3.3.2 The impact of the grafted hydrophilic chain on the emulsion stabilizing capacity of a protein fragment	- 62 -
3.4 General Conclusions	- 68 -
Chapter 4 Characteristics and Functional Properties of Modified Whey Protein as Food Emulsifiers at Various pH Conditions	- 70 -
4.1 Introduction	- 70 -
4.2 Materials and Methods	- 70 -
4.2.1 Materials	- 70 -
4.2.2 Hydrolysis of WPI by trypsin and alcalase	- 71 -
4.2.3 Preparation of protein-polysaccharide conjugates	- 72 -
4.2.4 Electrophoresis analysis	- 72 -
4.2.5 Protein solubility	- 73 -
4.2.6 Determination of sulfhydryl content	- 73 -
4.2.7 Preparation of emulsions	- 74 -
4.2.8 Storage stability of emulsions at different pH conditions	- 74 -
4.2.9 Statistical analysis	- 75 -

4.3 Results and Discussions	- 75 -
4.3.1 Molecular weight profiles	- 75 -
4.3.2 Solubility	- 77 -
4.3.2.1 Solubility of WPI and WPHs samples	- 78 -
4.3.2.2 Solubility of conjugated WPI and WPHs samples	- 80 -
4.3.3 Morphology and stability of emulsions at different pH conditions ..	- 83 -
4.3.3.1 Emulsions based on WPI and WPHs samples	- 84 -
4.3.3.2 Emulsions based on conjugated WPI and WPHs samples ...	- 91 -
4.4 General Conclusions	- 95 -
Chapter 5 Characteristics and Functional Properties of Modified Soy Protein as Food Emulsifiers at Various pH Conditions	- 97 -
5.1 Introduction	- 97 -
5.2 Materials and Methods	- 98 -
5.2.1 Materials	- 98 -
5.2.2 Hydrolysis of SPI by trypsin and alcalase	- 98 -
5.2.3 Preparation of protein-polysaccharide conjugates	- 99 -
5.2.4 Particle sizing of protein/polypeptide dispersions	- 100 -
5.2.5 Electrophoresis analysis	- 100 -
5.2.6 Protein solubility	- 100 -
5.2.7 Dissociation of insoluble MRPs made from SSPI	- 100 -
5.2.8 Preparation of emulsions	- 101 -
5.2.9 Storage stability of emulsions at different pH conditions	- 101 -
5.2.10 Statistical analysis	- 101 -
5.3 Results and Discussions	- 101 -
5.3.1 Protein particle size	- 102 -
5.3.2 Molecular weight profiles	- 106 -
5.3.3 Solubility	- 108 -
5.3.3.1 Solubility of SPI, SSPI and SSPHs samples	- 108 -
5.3.3.2 Solubility of conjugated SPI, SSPI and SSPHs samples ...	- 111 -
5.3.4 Morphology and stability of emulsions at different pH conditions ..	- 116 -
5.3.4.1 Emulsions based on unconjugated soy proteins/hydrolysates	- 116 -
5.3.4.2 Emulsions based on conjugated soy hydrolysates	- 124 -
5.4 General Conclusions	- 132 -

Chapter 6 Emulsifying and Stabilizing Properties of Soy Peptides Produced by Ultrafiltration and Covalently Bonded with Maltodextrin	135 -
6.1 Introduction	135 -
6.2 Materials and Methods	136 -
6.2.1 Materials	136 -
6.2.2 Hydrolysis of WPI and SPI by trypsin	136 -
6.2.3 Fractionation of polypeptides by membrane ultrafiltration	136 -
6.2.4 Preparation of protein-polysaccharide conjugates	137 -
6.2.5 Electrophoresis analysis	138 -
6.2.6 Preparation of emulsions	138 -
6.2.7 Storage stability of emulsions at different pH conditions	138 -
6.2.8 Statistical analysis	138 -
6.3 Results and Discussions	138 -
6.3.1 Molecular weight profiles	138 -
6.3.2 Morphology and stability of emulsions	141 -
6.3.2.1 Emulsions based on conjugates made from WR30 and SR30 (fragmented whey and soy protein of molecular size larger than 30 kDa)	141 -
6.3.2.2 Emulsions based on conjugates made from WR10 and SR10 (fragmented whey and soy protein of molecular size between 10~30 kDa)	144 -
6.3.2.3 Emulsions based on conjugates made from WP10 and SP10 (fragmented whey and soy protein of molecular size less than 10 kDa)	147 -
6.4 General Conclusions	149 -
Chapter 7 General Discussions and Conclusions	151 -
7.1 Introduction	151 -
7.2 Improved emulsion stability induced by protein-polysaccharide conjugate	152 -
7.3 The impact of the molecular size of a polypeptide	153 -
7.4 The impact of the degree of hydrolysis (DH) and the choice of enzyme	154 -
7.5 The impact of the protein structure	155 -
7.6 Conclusions and outlook	156 -

List of Abbreviations	- 158 -
Appendix I	- 161 -
Appendix II	- 168 -
Appendix III	- 171 -
Appendix IV	- 172 -
Bibliography	- 173 -

List of Tables

Table 1.1 Classification of a two-phase colloidal system.	- 2 -
Table 3.1 The list of the Flory-Huggins interaction parameters (in the unit of $k_B T$) between different types of monomers and the pK_a values for the groups of charged amino acid residues. The numbers (0 to 8) in this table indicate the nine types of monomers in the model system: solvents (0), five groups of amino acid residues (1 to 5), glucose residues of maltodextrin (6) and ions (7 and 8). A list of the classification of amino acid residues in this study is provided in Appendix II.	- 52 -
Table 3.2 The characteristic properties of the selected soy polypeptides.	- 54 -
Table 3.3 The predicted total amount of adsorption (in the unit of mg/m^2) for various polypeptides at the droplet surface, obtained from SCF calculations. The results are produced at a background electrolyte volume fraction of 0.001 and at $\text{pH} = 5.5$.	- 59 -
Table 4.1 ζ-potential (mV) of freshly made and stored (for 60 days) emulsion droplets, stabilized by WT1 sample as emulsifiers. Results are shown at different pH conditions.	- 86 -
Table 4.2 ζ-potential (mV) of freshly made and stored (for 60 days) emulsion droplets, stabilized by WT1-MD sample as emulsifiers. Results are shown at different pH conditions.	- 93 -
Table 5.1 ζ-potential (mV) of freshly made and stored (for 60 days) emulsion droplets, stabilized by SST3 sample as emulsifiers. Results are shown at different pH conditions.	- 121 -
Table 5.2 ζ-potential (mV) of freshly made and stored (for 60 days) emulsion droplets, stabilized by SST3-MD sample as emulsifiers. Results are shown at different pH conditions.	- 129 -

List of Figures

Figure 1.1 Schematic illustration of the kinetically stable and thermodynamically stable state of a two-phase dispersed system.	- 3 -
Figure 1.2 Schematic illustration of the interactions between two identical droplets according to DLVO theory. The total pair potential, the potentials derived from van der Waals attraction and electrostatic double layer repulsion are plotted as a function of the separation between droplets.	- 5 -
Figure 1.3 Schematic illustration of the interactions between two identical droplets which are sterically stabilized by adsorbed macromolecules. The total pair potential, the potentials derived from van der Waals attraction and steric repulsion are plotted as a function of the separation between droplets.	- 7 -
Figure 1.4 Schematic illustration of bridging attraction (A) and depletion attraction (B).	- 7 -
Figure 1.5 Schematic illustration of the deformation of droplets and the formation of the liquid film of the continuous phase as the droplets approach and/or stay close.	- 10 -
Figure 1.6 Schematic comparison of oil droplet stabilized by proteins and conjugates respectively. The red dot in the conjugates represents the covalent bonding between protein and polysaccharide.	- 13 -
Figure 1.7 Basic chemical reaction mechanism for the formation of protein-polysaccharide conjugate in the initial stage of Maillard reaction. The highlighted groups in red colour on the structures of polysaccharide and protein are the sites involved in Maillard reaction.	- 16 -
Figure 1.8 Preparation of protein-polysaccharide conjugates via wet-heating (A) and dry-heating (B) pathways.	- 17 -
Figure 2.1 (A) Schematic illustration of two approaching dispersed phases with the space in between. (B) Magnified two-dimensional lattice model of this space and the different species existing in between.	- 33 -
Figure 2.2 Schematic illustration of the migration of proteins on the solid polyacrylamide gel support during electrophoresis. The green arrow indicates the direction of protein movement.	- 37 -
Figure 2.3 The chemical reaction mechanism of Biuret assay for quantification of protein solubility.	- 38 -
Figure 2.4 The chemical reaction mechanism of Ellman's reagent for analysis of the free sulfhydryl content of protein materials.	- 39 -
Figure 2.5 Schematic illustration of the basic setup for Dynamic Light Scattering (DLS) technique.	- 40 -

Figure 2.6 Schematic illustration of the hydrodynamic size of a particle. · - 42 -

Figure 2.7 Schematic illustration of the basic setup for Light Diffraction technique. - 43 -

Figure 2.8 Schematic illustration of the basic principles of zeta potential measurement. - 44 -

Figure 2.9 (A) The three types of flow behaviour. (B) Schematic illustration of the shear-thinning flow behaviour. - 46 -

Figure 2.10 The double gap cylinder geometry measuring system. - 47 -

Figure 3.1 Primary structure representing soy peptide Met³²²-Lys³⁵⁵ in the SCF calculations. A list of the full names of the amino acids shown here in abbreviations is provided in Appendix II. - 51 -

Figure 3.2 The interaction potentials, plotted against the inter-droplet separation distance, resulting from the adsorbed layers of five different soy polypeptides (i.e. Met³²²-Arg³³⁴, Met³²²-Lys³⁵⁵, Asn³⁵⁶-Arg⁴²⁵, His¹⁶⁰-Arg²⁹⁰ and Glu⁹³-Arg³⁰²) respectively. The diameter of oil droplets is 1 µm. The results are produced at a background electrolyte volume fraction of 0.001 and at pH = 5.5. - 55 -

Figure 3.3 The average distance of each monomer residue that makes up the adsorbed soy polypeptides (i.e. Met³²²-Arg³³⁴, Met³²²-Lys³⁵⁵ and Asn³⁵⁶-Arg⁴²⁵), away from a hydrophobic surface, plotted against the sequence number of monomers starting with the first monomer at *N*-terminus of a protein fragment. The results were calculated at a background electrolyte volume fraction of 0.001 and at pH = 5.5. - 57 -

Figure 3.4 Density profiles of the five different polypeptides (i.e. Met³²²-Arg³³⁴, Met³²²-Lys³⁵⁵, Asn³⁵⁶-Arg⁴²⁵, His¹⁶⁰-Arg²⁹⁰ and Glu⁹³-Arg³⁰²) adsorbed at an isolated droplet, plotted against the distance away from the hydrophobic surface. The inset graph is a magnification of the same graph by a factor of 2500, so as to illustrate more clearly the result for the smallest peptide Met³²²-Arg³³⁴ (black line). All the data were calculated at a background electrolyte volume fraction of 0.001 and at pH = 5.5. - 58 -

Figure 3.5 The average distance of each monomer residue that makes up the adsorbed soy polypeptides (i.e. His¹⁶⁰-Arg²⁹⁰ and Glu⁹³-Arg³⁰²), away from a hydrophobic surface, plotted against the sequence number of monomers starting with the first monomer at *N*-terminus of a protein fragment. The results are produced at a background electrolyte volume fraction of 0.001 and at pH = 5.5. - 61 -

Figure 3.6 Density profiles of the conjugated polymers made from three polypeptides (i.e. Met³²²-Lys³⁵⁵, Asn³⁵⁶-Arg⁴²⁵ and Glu⁹³-Arg³⁰²), respectively bonded with a hydrophilic chain ($L = 60 a_0$), adsorbed at an isolated droplet, plotted against the distance away from the hydrophobic surface. The results are produced at a background electrolyte volume fraction of 0.001 and at pH = 5.5. - 63 -

- Figure 3.7 The interaction potential, plotted against the inter-droplet separation distance, resulting from the adsorbed layers of the conjugates made from three polypeptides (i.e. Met³²²-Lys³⁵⁵, Asn³⁵⁶-Arg⁴²⁵ and Glu⁹³-Arg³⁰²), respectively bonded with a hydrophilic chain ($L = 60 a_0$). The diameter of oil droplets is 1 μm . The results are produced at a background electrolyte volume fraction of 0.001 and at pH = 5.5. - 65 -
- Figure 3.8 The interaction potential, induced by the conjugate made from polypeptide Asn³⁵⁶-Arg⁴²⁵ and a hydrophilic chain of various lengths ($L = 30, 60$ and $180 a_0$), between two oil droplets (diameter 1 μm), plotted against the separation distance. The results are produced at a background electrolyte volume fraction of 0.001 and at pH = 5.5. - 67 -
- Figure 4.1 Reducing SDS-PAGE analysis of the protein/peptide profiles for various whey protein samples. Lane 0 is intact WPI. Lane 1-3 are polypeptides produced by trypsin digestion at increasing DH (i.e. WT1 at 2.5%, WT2 at 5.5% and WT3 at 8.0%, respectively). Lane 4-6 are polypeptides produced by alcalase digestion, from lower to higher DH (i.e. WA1 at 2.5%, WA2 at 5.5% and WA3 at 8.0%, respectively). Lane M is the molecular weight ladder (with values presented in the unit of kDa). A sample post conjugation with maltodextrin (i.e. WT1-MD) is also shown at lane 8 to compare with its unconjugated counterpart (i.e. WT1) at lane 7. - 76 -
- Figure 4.2 The solubility of intact WPI and WPHs samples hydrolysed by trypsin (A) and alcalase (B) at various DH, plotted as a function of pH. - 79 -
- Figure 4.3 The visual appearance of 1% (w/v) WT1 sample solution at various pH conditions. - 80 -
- Figure 4.4 The visual appearance of 1% (w/v) WT1-MD sample solution at various pH conditions. - 81 -
- Figure 4.5 The solubility of conjugates made from intact WPI and those from WPHs at various levels of hydrolysis, produced by either trypsin (A) or alcalase (B), plotted as a function of pH. - 82 -
- Figure 4.6 Free sulfhydryl (-SH) content of protein and hydrolysates prior to and post dry-heating Maillard reaction. - 83 -
- Figure 4.7 The average droplet size $D_{4,3}$ of freshly made and stored (60 days) emulsions, fabricated by intact and hydrolysed whey protein, at various pH conditions (i.e. pH 7.5, 4.5 and 3.0). - 84 -
- Figure 4.8 Micrographs of WT1 fabricated emulsion, stored at pH 7.5, on day 1 (A) and after 60 days of storage (B). The droplet size distribution and the mean droplet size $D_{4,3}$ are also provided on each photo. - 85 -

Figure 4.9 Micrographs of WT1 fabricated emulsion, stored at pH 4.5, on day 1 (A) and after 60 days of storage (B). The droplet size distribution and the mean droplet size $D_{4,3}$ are also provided on each photo. - 88 -

Figure 4.10 Apparent viscosity of the emulsions fabricated by WT1, stored for 1 day at pH 7.5 and pH 4.5, plotted against shear rate. - 89 -

Figure 4.11 Micrographs of WT1 based emulsion stored at pH 4.5 after 60 days. (A) and (B) respectively display the microstructure when this stored emulsion was adjusted to pH 3.0, or when it was diluted in 5% SDS. The droplet size distribution and the mean droplet size $D_{4,3}$ are also provided in each photo. - 90 -

Figure 4.12 The average droplet size $D_{4,3}$ of freshly made and stored (60 days) emulsions, fabricated by conjugates made from WPI/WPHs + maltodextrin, at various pH conditions (i.e. pH 7.5, 4.5 and 3.0). The scale in this graph is kept the same as that in Figure 4.7 for the ease of comparison. However, a more detailed version is also shown in the inset. - 91 -

Figure 4.13 Micrographs of WT1-MD fabricated emulsion, stored at pH 4.5, on day 1 (A) and after 60 days of storage (B). The droplet size distribution and the mean droplet size $D_{4,3}$ are also provided on each photo. - 92 -

Figure 5.1 The visual appearance of various 0.5% (w/v) soy protein dispersions at pH 7.5. SPI and SSPI refer to intact and ultrasonicated soy protein isolate, accordingly. SSPI digested by trypsin and alcalase at different levels of hydrolysis (i.e. 2.5%, 5.5% and 8.0%) are denoted as SST1, SST2, SST3 and SSA1, SSA2, SSA3, respectively. - 102 -

Figure 5.2 The average protein particle size of SSPI and its hydrolysates post digestion by trypsin (A) and alcalase (B), accordingly. - 103 -

Figure 5.3 The schematic picture of the processes of protein hydrolysis by alcalase (A) and trypsin (B). - 105 -

Figure 5.4 Reducing SDS-PAGE analysis of the protein/peptide profiles for various soy protein samples. Lane 0 is ultrasonicated SPI. Lane 1-3 are polypeptides produced by trypsin digestion at lower to higher DH (i.e. SST1, SST2 and SST3, respectively). Lane 4-6 are polypeptides produced by alcalase digestion at lower to higher DH (i.e. SSA1, SSA2 and SSA3, respectively). Lane M is the molecular weight ladder (with values presented in the unit of kDa). A sample post conjugation with maltodextrin (i.e. SST3-MD) is also shown at lane 8 to be compared with its unconjugated counterpart (i.e. SST3) at lane 7. - 106 -

Figure 5.5 The solubility of SPI, ultrasonicated SPI (i.e. SSPI), and SSPHs samples hydrolysed by trypsin (A) or alcalase (B) at various DH, plotted as a function of pH. - 110 -

Figure 5.6 The visual appearance of 1% (w/v) SST3 sample, dispersed under various pH conditions.	111 -
Figure 5.7 The solubility of conjugates made from ultrasonicated SPI (i.e. SSPI-MD), and those made from fragmented soy protein produced by either trypsin (A) and alcalase (B) at various levels of hydrolysis, plotted as a function of pH.	112 -
Figure 5.8 Effects of addition of SDS, DTT, or both to a dispersion of otherwise insoluble MRPs, produced from ultrasonicated soy protein + maltodextrin (i.e. sample SSPI-MD). Ultrasonicated soy protein without conjugation (SSPI) was dissolved in deionized water and is included for comparison on the left. SSPI-MD was dissolved in different solvents (from left to right): deionized water, buffer (pH 9.0, 0.086 M Tris, 0.09 M Glycine), 5% SDS + buffer, 0.5 M DTT + buffer, 5% SDS + 0.5 M DTT + buffer.	113 -
Figure 5.9 The visual appearance of 1% (w/v) SST3-MD sample, dispersed under various pH conditions.	114 -
Figure 5.10 Average droplet size $D_{4,3}$ of freshly made and stored (for 60 days) emulsions, fabricated using intact SPI, ultrasonicated SPI (i.e. SSPI) and SSPHs, at various pH conditions (i.e. pH 7.5, 4.5 and 3.0).	117 -
Figure 5.11 Micrographs of SST3 fabricated emulsion, stored at pH 7.5, on day 1 (A) and after 60 days of storage (B). The droplet size distribution and the mean droplet size $D_{4,3}$ are superimposed on each photo.	118 -
Figure 5.12 The change of mean droplet size $D_{4,3}$ of O/W emulsion, stabilized by SST3, stored at pH 7.5.	119 -
Figure 5.13 Apparent viscosity of O/W emulsions fabricated by SST3 stored at pH 7.5 for 1 day and 60 days.	120 -
Figure 5.14 Micrograph of WT1 based emulsion stored at pH 7.5, with addition of 0.03% soy lecithin (i.e. 3 g soy lecithin/100 g WT1), following 60 days of storage.	122 -
Figure 5.15 Micrographs of SST3 fabricated emulsions, stored at pH 4.5, on day 1 (A) and after 60 days of storage (B). The droplet size distribution and the mean droplet size $D_{4,3}$ are also provided on each photo.	123 -
Figure 5.16 The average droplet size $D_{4,3}$ of freshly made and stored (60 days) emulsions, fabricated by conjugates made from SSPHs + maltodextrin, under various pH conditions (i.e. pH 7.5, 4.5 and 3.0).- ...	124 -
Figure 5.17 Micrographs of SST3-MD fabricated emulsions, stored at pH 7.5, on day 1 (A) and after 60 days of storage (B). The droplet size distribution and the mean droplet size $D_{4,3}$ are also provided on each photo.	125 -

Figure 5.18 Micrographs of emulsions stored at pH 7.5 after 60 days. The emulsions were stabilized by conjugated SST3 + maltodextrin DE4-7 ($M_w = 65$ kDa) and SST3 + dextran ($M_w = 500$ kDa), which are displayed in (A) and (B), respectively. The droplet size distribution and the mean droplet size $D_{4,3}$ are also provided on each photo. ... - 126 -

Figure 5.19 Micrographs of SST3-MD fabricated emulsion, stored at pH 4.5, on day 1 (A) and after 60 days of storage (B). The droplet size distribution and the mean droplet size $D_{4,3}$ are also provided on each photo. - 127 -

Figure 5.20 Apparent viscosity of freshly made O/W emulsions fabricated by SST3 and SST3-MD, stored at pH 7.5 and pH 4.5. - 128 -

Figure 5.21 Micrographs of emulsions produced by SST3-MD conjugates as emulsifiers, after adjustment of pH to 3.0 (A), then to 2.0 (B). The emulsion sample was kept at the intermediate pH for only a few minutes. The droplet size distribution and the mean droplet size $D_{4,3}$ are also provided on each photo. - 131 -

Figure 5.22 Micrographs of emulsion produced by SST3-MD as emulsifiers, stored at pH 7.5, on day 1 (A) and after 60 days of storage (B). This emulsion was subjected to an acid treatment by adjustment of pH to 4.5, then back up to 7.5. The emulsion sample was kept at pH 4.5 for only a few minutes. The droplet size distribution and the mean droplet size $D_{4,3}$ are also provided on each photo. - 132 -

Figure 6.1 Reducing SDS-PAGE analysis of the peptide profiles for various fractionated protein samples. Lane W is intact WPI and lane S is ultrasonicated SPI. Lane 1, 2, 3 are the fractions of polypeptides derived from WPI (produced by trypsin digestion) of molecular size larger than 30 kDa, between 10~30 kDa and less than 10 kDa, respectively. Lane 1*, 2*, 3* are the fractions of polypeptides derived from ultrasonicated SPI (produced by trypsin digestion) of molecular size larger than 30 kDa, between 10~30 kDa and less than 10 kDa, respectively. Lane M is the molecular weight ladder (with values presented in the unit of kDa). - 139 -

Figure 6.2 Micrographs of conjugated WR30 fabricated emulsion. The freshly made and stored (for 60 days) samples at pH 7.5 are shown in (A) and (B), respectively. The samples adjusted to and stored at pH 4.5 on day 1 (C) and after 60 days of storage (D) are also displayed. The droplet size distribution and the mean droplet size $D_{4,3}$ are provided on each photo. - 141 -

Figure 6.3 Micrographs of conjugated SR30 fabricated emulsion. The freshly made and stored (for 60 days) samples at pH 7.5 are shown in (A) and (B), respectively. The samples adjusted to and stored at pH 4.5 on day 1 (C) and after 60 days of storage (D) are also displayed. The droplet size distribution and the mean droplet size $D_{4,3}$ are provided on each photo. - 142 -

Figure 6.4 Micrographs of conjugated WR10 fabricated emulsion. The freshly made and stored (for 60 days) samples at pH 7.5 are shown in (A) and (B), respectively. The samples adjusted to and stored at pH 4.5 on day 1 (C) and after 60 days of storage (D) are also displayed. The droplet size distribution and the mean droplet size $D_{4,3}$ are provided on each photo. - 144 -

Figure 6.5 Micrographs of conjugated SR10 fabricated emulsion. The freshly made and stored (for 60 days) samples at pH 7.5 are shown in (A) and (B), respectively. The samples adjusted to and stored at pH 4.5 on day 1 (C) and after 60 days of storage (D) are also displayed. The droplet size distribution and the mean droplet size $D_{4,3}$ are provided on each photo. - 146 -

Figure 6.6 Micrographs of freshly made emulsion samples fabricated with conjugated WP10 (A) and conjugated SP10 (B) at pH 7.5. The droplet size distribution and the mean droplet size $D_{4,3}$ are provided on each photo. - 147 -

Figure 6.7 Micrograph of freshly made emulsion samples fabricated using conjugated WP10, after adjustment of pH to 4.5. The droplet size distribution and the mean droplet size $D_{4,3}$ are provided on the photo. - 148 -

Chapter 1 Introduction

This chapter will start with a brief description of colloidal science and the so called colloidal state of matter. Focus will be placed on the oil-in-water (O/W) emulsion stabilized by macromolecules (e.g. proteins), which is the most commonly seen form of colloids in foods and is also the system of main concern in this project. A review of previous work regarding protein-polysaccharide conjugates as food emulsifiers will follow to demonstrate the significance of the current study in the context of the work done so far in the literature. At the end of this chapter, the aims and organisation of the thesis are discussed, illustrating the general flow of the theme of this project through different chapters and how they relate to each other.

1.1 Foundation of research

1.1.1 Colloidal state of matter

Solid, liquid and gas have been largely regarded as the three states of matter for centuries. This classification applies to systems where pure or molecularly-scaled mixed substances are being considered. It was only a century and half ago that the colloidal state of matter was officially recognized as potentially a different state of matter. This intermediate state of matter, colloids, has one component finely dispersed in another but the degree of dispersion does not approach a molecular level (Everett, 1988e). Colloidal systems and techniques relating to their production and characterisation have been applied in a wide variety of fields. Examples of colloids include milk, yogurt, jelly, toothpaste, ink, emulsion explosives, paint and coatings. Many biological materials are also colloids in nature (e.g. saliva and blood).

The simplest type of a colloidal system consists of a single dispersed phase and a second dispersion medium. However, more than one dispersed phase can be present simultaneously in a system (e.g. ice cream). Based on the nature of dispersed phase and dispersion medium, simple colloids, consisting of two phases, can be grouped into different types, as summarized in **Table 1.1** (Hunter, 2001b, Dickinson, 1992d, Everett, 1988e).

	Dispersed Phase	Dispersion Medium	Types	Examples
Dispersed system	Liquid	Gas	Liquid aerosol	Fog, spray
	Solid	Gas	Solid aerosol	Industrial smoke
	Gas	Liquid	Foam	Beer froth
	Liquid	liquid	Emulsion or emulsion gel	Milk, butter, yogurt
	Solid	liquid	Sol, suspension, paste	Ink, blood
	Gas	Solid	Solid foam	Bread
	Solid	Solid	Solid suspension	Stained glass
Macromolecular colloids	Macromolecules	Liquid	Gels	Jelly, glue
Association colloids	Micelles	Liquid	—	Detergent-water, liquid crystals

Table 1.1 Classification of a two-phase colloidal system.

Colloids have distinct characteristics. They can behave like solid or liquid under different circumstances. They are all heterogeneous and contain structural entities with at least one relevant dimension ranging from 1 nm to 1 μm . However, the limit of the size range is not strict. In most food colloids, the size of some dispersed particles can be outside this range. Though much larger than molecules, colloidal particles are sufficiently small for Brownian motion to still be of some significance. For instance, the Brownian motion can be sufficient to overcome the effects of gravity (Dickinson, 1992d). Colloidal-sized entities also tend to strongly scatter light. Another crucial characteristic of these systems is the large interfacial area between the dispersed phase and the dispersion medium. The physicochemical properties of a substantial amount of molecules residing at the interface will determine the behaviours of the colloidal system to a large extent (Everett, 1988e). Colloidal systems are thermodynamically unstable. They are not in their state of the lowest possible free energy. Given a long enough time (which could be days, months, years or even centuries), they will eventually revert to their phase separated components. This is different from molecular mixtures that are homogeneous and thermodynamically stable, such as salt or sugar solution (McClements, 2015v).

1.1.2 Surface free energy

The instability of colloidal systems arises from the large contact area between the two immiscible phases. Compared to bulk molecules, the molecules at the interface are experiencing unbalanced intermolecular forces (Coupland, 2014c). As a consequence, dispersed systems consisting of a large amount of surface molecules possess substantial excess free energy (Everett, 1988g). From the perspective of thermodynamics, such systems always tend to change spontaneously in the direction of lowering their free energy. Therefore, there is a tendency for them to shrink the contact area between the two phases. This eventually induces complete phase separation (McClements, 2015v).

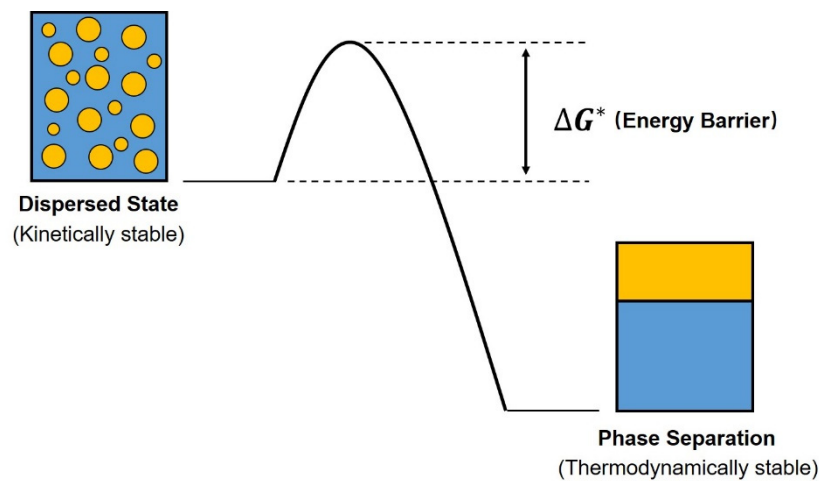


Figure 1.1 Schematic illustration of the kinetically stable and thermodynamically stable state of a two-phase dispersed system.

Nevertheless, it is possible to generate dispersed systems that are kinetically stable for a considerable length of time, by introducing an energy barrier which separates the kinetically stable and thermodynamically stable states (**Figure 1.1**). Though there are always some molecules that meet the activation energy requirements and have a chance to jump over the energy barrier to get into the lower-energy state, the transformation would be imperceptibly slow if the energy barrier is sufficiently high. The existence of such an energy barrier is the reason why the colloidal systems could be maintained in a dispersed and relatively stable state over long durations, sufficient to make colloids useful in many practical situations (McClements, 2015v, Everett, 1988f).

1.1.3 Colloidal interactions

The excess free energy of a colloidal system can be dramatically altered by the presence of molecules adsorbed and accumulated at the interface (e.g. amphiphilic macromolecules, surfactants, ions) (Coupland, 2014c, Dickinson, 1992a). In particular, for O/W emulsions in foods (e.g. milk, cream, salad dressing), the behaviours of such systems are the result of the overall free energy change when two droplets approach each other, determined normally by three major contributions, i.e. the van der Waals force, the electrostatic force and the steric force (Everett, 1988k). In some systems, other types of forces are also significant, including depletion force, bridging attraction and hydrophobic force (McClements, 2015c, Dickinson, 1992a).

1.1.3.1 Van der Waals force

This interaction is derived from the permanent or induced dipoles of molecules making up the dispersed phase. It is always attractive for molecules of the same species, and is very short ranged between two individual molecules (Everett, 1988j). However, the energy of this attractive force, when acted between two particles or droplets, becomes the sum of all the pair interactions between individual molecules within the two dispersed particles. As such, it falls much more slowly (line A in **Figure 1.2**). Due to this long-ranged attractive potential, colloidal particles under Brownian motion or shear force tend to approach and stick together, and eventually coalesce (McClements, 2015d).

1.1.3.2 Electrostatic repulsion and DLVO theory

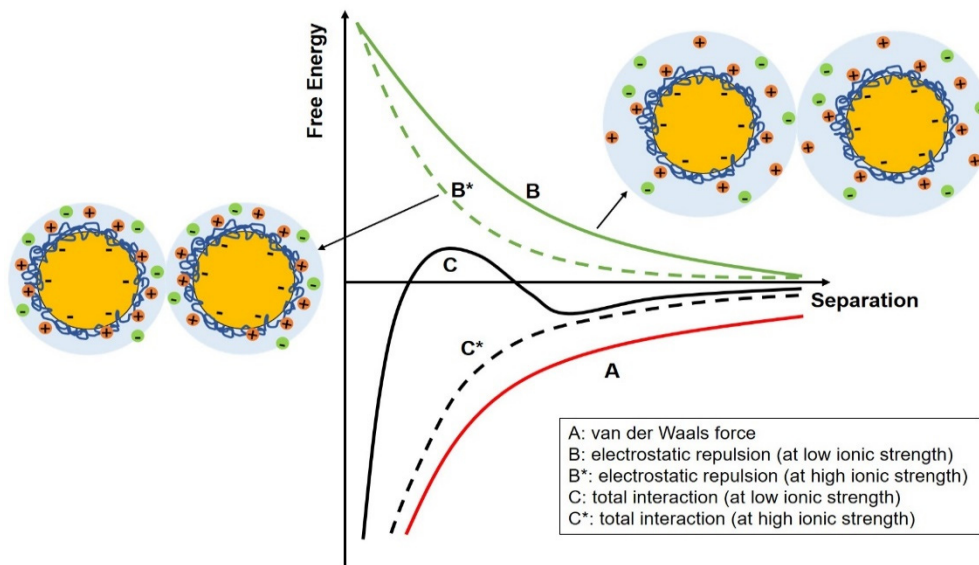


Figure 1.2 Schematic illustration of the interactions between two identical droplets according to DLVO theory. The total pair potential, the potentials derived from van der Waals attraction and electrostatic double layer repulsion are plotted as a function of the separation between droplets.

If there are repulsive forces present in the system, they can result in an energy barrier against the approach of droplets and therefore prevent dispersed droplets, under the influence of van der Waals force, from aggregating. The repulsive forces could come from the overlap of the electrical double layers that are built up around the droplets due to the adsorption of the charged species at the droplet surface. Such forces are referred to as electrostatic repulsion (Everett, 1988i). The sign and magnitude of the charge carried by the adsorbed species, and most importantly the thickness of the formed electrical double layer, would largely depend on the environmental conditions as well as the type and concentration of the emulsifiers used (McClements, 2015e).

In the classical DLVO theory (**Figure 1.2**), the overall pair potential between two dispersed droplets is the combination of van der Waals attraction and electrostatic repulsion. Van der Waals attractive energy predominates at small and large separations. This often leads to the formation of a primary and a separate secondary minimum in the droplet-droplet interaction potential. An energy barrier would exist at intermediate separations due to the electrostatic repulsion. However, in the presence

of a high ionic strength, which is often the case for most food emulsions, such an energy barrier could disappear. Then, systems that rely mainly on electrostatic repulsion for maintaining colloidal stability will become unstable to droplet aggregation (Dickinson, 1992a).

1.1.3.3 Steric repulsion and total interaction potential

In addition to electrostatic repulsion, a steric repulsive force could also be generated by the adsorbed macromolecules, irrespective of their charge. The free energy change induced by the steric force involves both entropic and enthalpic components (Everett, 1988h). The former is mainly resulted from the reduction of conformational entropy of adsorbed polymers at the interface, due to the progressively restricted space between two approaching droplets. Therefore, this is always a repulsive contribution to the inter-droplet potential. The latter component mainly arises from the change of local osmotic pressure when adsorbed polymers on two individual droplets start to interpenetrate. Whether its contribution to free energy is positive or negative depends on the solvent quality. In a good solvent, polymer-solvent contacts are more favourable than polymer-polymer contacts. The free energy will grow when the adsorbed polymers have more chance to interact as dispersed droplets come closer. In this sense, a repulsive force will be produced. Whereas in a poor solvent, the overlap of polymer layers is more favoured. Under this circumstance, the free energy of the system decreases with droplet-droplet separation distance. This will result in an attractive force between droplets as they approach (McClements, 2015f).

Generally, for hydrophilic macromolecules in good solvent, the steric force is always repulsive. The change of total interaction potential between two sterically stabilized droplets under good solvent conditions is illustrated in **Figure 1.3**. Van der Waals attractive energy predominates at large separations. A steeply increased repulsion arises at short separations, as soon as the two adsorbed layers overlap. At separations just before the overlap occurs, there is an attractive energy minimum, the depth of which is mainly dependent on the thickness of the interfacial layer formed by the adsorbed polymers. The magnitude of this energy minimum governs the colloidal behaviours of dispersed droplets (McClements, 2015g, Dickinson, 1992a).

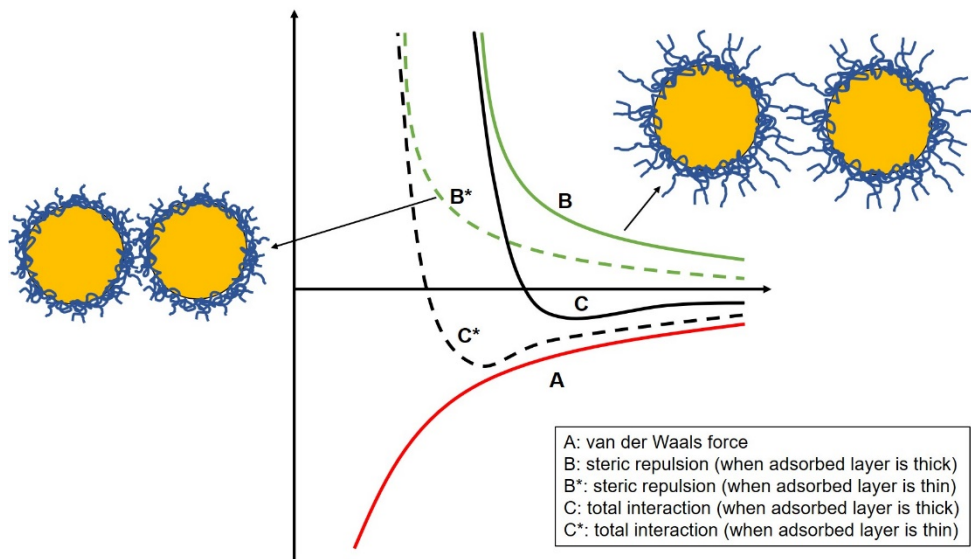


Figure 1.3 Schematic illustration of the interactions between two identical droplets which are sterically stabilized by adsorbed macromolecules. The total pair potential, the potentials derived from van der Waals attraction and steric repulsion are plotted as a function of the separation between droplets.

1.1.3.4 Bridging and depletion attractions

In contrast to a strong steric repulsion, adsorbed polymers in good solvent can also induce an attraction between droplets, under the circumstance where the droplet surface is not fully coated with polymers. Such attraction is the consequence of polymer bridging, where a polymer chain adsorbs onto the surface of two or more neighbouring droplets (**Figure 1.4A**) (Dickinson, 1992a).

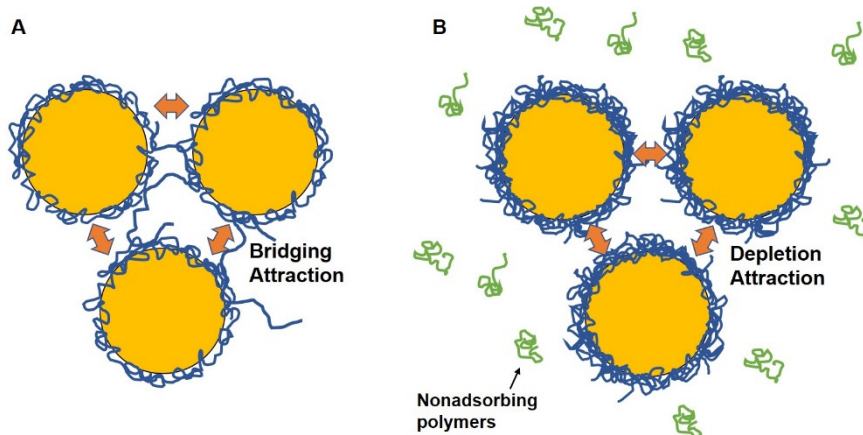


Figure 1.4 Schematic illustration of bridging attraction (A) and depletion attraction (B).

Inter-droplet attraction can also be induced by non-adsorbed polymers present in the bulk. When two droplets approach, these polymers will avoid residing in the gap between droplets, due to the loss of conformational entropy. This will create a polymer concentration gradient between the bulk and the gap, with the amount of polymers being lower in the gap. Under the influence of the resultant osmotic pressure, the solvent molecules between the gap will flow out into the bulk, making droplets approach even more closely. Such osmotic driving force, induced by non-adsorbed polymers, is referred to as depletion attraction (**Figure 1.4B**) (McClements, 2015h). The magnitude of depletion force largely depends on the size and concentration of non-adsorbed polymers (McClements, 2015t).

1.1.3.5 Hydrophobic interactions

Hydrophobic interaction is normally not believed to play an important role in determining the colloidal stability of food emulsions, but it would if the adsorbed emulsifiers at the droplet surface have some nonpolar/hydrophobic regions exposed to the aqueous phase (McClements, 2015i). Typical examples are heat-denatured globular proteins and partially unfolded proteins upon adsorption. The hydrophobic interactions induced by them can have significant impact on the flocculation stability of some food emulsions (Kim et al., 2002a, McClements, 2004).

1.1.4 Stability of emulsions

The total interaction potential between dispersed droplets discussed previously in section 1.1.3 is the major factor that governs the behaviours of dispersed droplets and the stability of O/W emulsion. Other factors (e.g. the solubility of dispersed phase in dispersion medium, the strength of interfacial layer) also play a role. Based on the underlying mechanism involved, the instability of emulsion is normally classified into creaming, flocculation, coalescence and Ostwald ripening.

1.1.4.1 Creaming

Compared to other instability mechanisms, creaming is a relatively insensitive process to inter-droplet interaction, only affected by it in an indirect manner. Creaming involves the formation of a concentrated layer of oil droplets at the top of an emulsion sample due to gravity or centrifugal force. Creaming does not involve the change of droplet

size distribution (Dickinson, 1992a), but it can indirectly aid other processes that contribute to the size change. Creaming is enhanced in dilute flocculated emulsions. While if the flocculated emulsion is concentrated, creaming is likely to be inhibited to some extent, because of the spanning network formed by the highly interconnected flocs throughout the whole system which locks the flocs in position, preventing them from moving upwards. Creaming can also be effectively controlled by reducing the droplet size or by modifying the viscosity of the dispersion medium (McClements, 2015p, Dickinson, 1992b).

1.1.4.2 Flocculation

As a precursor to creaming and coalescence in many cases, flocculation is very important to the stability of food emulsions. There are quite a few different situations where droplets can become flocculated. Most of the time, emulsion droplets completely coated with emulsifiers will flocculate when the inter-droplet pair potential is appreciably attractive at short separations. For this case, the most effective means of controlling the rate and extent of flocculation is to manipulate the colloidal interactions between droplets by introducing strong electrostatic and/or steric repulsions (McClements, 2015q).

If there are not sufficient emulsifiers to fully cover the newly created droplet surface during homogenization, bridging flocculation may occur (**Figure 1.4A**) where droplets are strongly held together by adsorbed species shared between two or more individual droplets (McClements, 2015s, Dickinson, 1992a). The presence of non-adsorbed polymers (e.g. proteins, polysaccharides) in the dispersion medium could also lead to droplet flocculation, called depletion flocculation as illustrated in **Figure 1.4B**. Depletion flocculation is negligible, if the concentration of non-adsorbed polymers is below a critical level. But it will become significant when a substantial amount of non-adsorbed polymers is present (McClements, 2015t). On the other hand, if the concentration of non-adsorbed polymers is increased to an extent that it is able to provide a substantial enhancement in the viscosity of the aqueous phase, depletion flocculation would become completely inhibited (Dickinson, 1992a). Flocculation could also result from the thermal or surface denaturation of adsorbed globular proteins that leads to nonpolar patches exposed to the aqueous phase (McClements, 2015r).

Generally speaking, any perturbations that can cause adsorbed polymers to become insoluble or aggregated (e.g. heating, change of pH and ionic strength), are likely to promote flocculation (Dickinson, 1992a). Flocculation of emulsion droplets could also be induced as a result of the competitive adsorption in a mixed polymer system or polymer/surfactant system. For instance, under environmental stresses, the displacement of initially adsorbed β -casein from the droplet surface by α_{S1} -casein (Dickinson, 1997) or low-molecular-weight surfactants (Courthaudon et al., 1991) could lead to some extent of droplet flocculation.

1.1.4.3 Coalescence

Coalescence is the irreversible merging of two or more emulsion droplets into one single droplet. It is much more severe than creaming and flocculation in terms of emulsion stability (Dickinson, 1992a). Nevertheless, coalescence becomes desirable when encapsulated components need to be released during oral processing and digestion (McClements, 2015k).

The susceptibility of an emulsion to coalescence depends on the stability of the thin aqueous film separating the two closely seated droplets (**Figure 1.5**). When droplets collide, as a result of their Brownian motion or applied forces (e.g. shear, centrifuge), or if they stay close for an extended period of time (e.g. when they are in a flocculated state), the droplets would deform and the film of the continuous phase separating the droplets tends to be squeezed out. If the thickness of the film gets below a critical value, there is a chance for subsequent film rupture and formation of holes in the film between the droplets. Eventually droplet coalescence occurs (McClements, 2015w, Dickinson, 1992a).

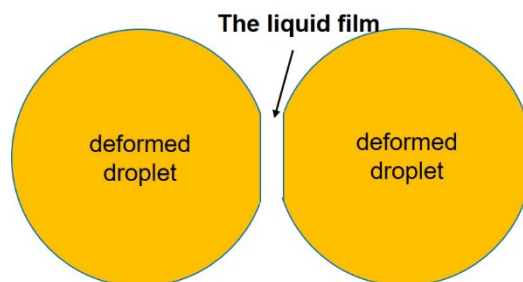


Figure 1.5 Schematic illustration of the deformation of droplets and the formation of the liquid film of the continuous phase as the droplets approach and/or stay close.

The resistance of the film to rupture is generally governed by the rate of droplet collisions, the nature of interactions between droplets, the interfacial tension and the surface rheology of the interfacial layers (McClements, 2015w). In most cases, proteins offer better coalescence stability to O/W emulsions than low-molecular-weight surfactants, mainly because proteins are able to form thicker protective interfacial layers with a much higher viscoelasticity, via the intermolecular forces (Dickinson, 1992a).

1.1.4.4 Ostwald ripening

This process describes the growth of larger droplets at the expense of smaller ones due to the mass transport of dispersed phase through the continuous medium. The thermodynamic driving force for Ostwald ripening is the chemical potential difference of the dispersed phase in large and small droplets (Dickinson, 1992a).

Ostwald ripening can be significant if the dispersed phase is sufficiently soluble in the continuous phase, such as when short-chain triglycerides, flavour oils or essential oils are incorporated in the oil phase (Li et al., 2009, Rao et al., 2012). Nonetheless, in most food O/W emulsions, Ostwald ripening is negligible, as long chain triglycerides are virtually insoluble in water (McClements, 2015u).

1.1.5 Emulsifiers and stabilizers

To obtain stable O/W emulsions, an emulsifier must be present to protect the newly formed droplets against immediate re-coalescence during vigorous homogenization.

An effective emulsifier has to first facilitate the creation of new interface by rapidly adsorbing at the interface and lowering the interfacial free energy. Then they should be able to form a protective coating around the droplets and provide sufficient repulsions between droplets for long-term stability (McClements, 2015n). There are generally two classes of emulsifiers in food, low-molecular-weight surfactants and proteins. As to the formation of emulsion droplets, surfactants tend to be more effective than proteins, due to their structure and smaller size, which enable a more rapid reduction of the interfacial tension. The reverse is true when it comes to the stabilizing ability. Compared to surfactants, proteins are able to provide a much better long-term stabilization to emulsion systems, as a result of their irreversible adsorption as well as

the formation of thicker viscoelastic interfacial layers (Dickinson, 1992d). Protein materials are the most important and widely used stabilizing agents in food colloids.

Furthermore, for proteins to display excellent colloidal emulsifying and stabilizing ability, they are required to have a sufficient solubility, hydrophobicity and flexibility. In this sense, disordered proteins with a structure more closely resembling a diblock, consisting of a strongly anchored hydrophobic train at the interface and a hydrophilic tail extending into the bulk phase (e.g. β -casein), are shown to be better candidates as food emulsifiers than the globular counterparts (e.g. soy proteins) (Dickinson, 1992f, McClements, 2015n).

Another widely used biopolymer, high-molecular-weight polysaccharides (e.g. carrageenan, xanthan gum) are only regarded as stabilizers rather than emulsifiers, as most of them cannot be used alone to produce an emulsion. The main stabilizing mechanism of polysaccharides is to modify the viscosity of dispersion medium (McClements, 2015l), inhibiting the Brownian movement of the droplets. In this respect, such polysaccharides, despite often being called stabilizers, are not true stabilizers in the sense of colloidal science. Proteins, on the other hand, fulfil both the roles of emulsifiers and true colloidal stabilizers in many cases (Dickinson, 1992d).

1.2 Protein-polysaccharide conjugates as food emulsifiers

O/W emulsion systems have been applied to a wide variety of fields. Products ranging from foods, pharmaceuticals, cosmetics, agrochemicals to personal care and cleaning products etc., rely heavily on the use of O/W emulsions to deliver different active ingredients (e.g. vitamins, essential oils, drugs, flavours and pesticides) for the purpose of improving their stability, availability as well as controlled release (Dubey et al., 2009, Burgos-Díaz et al., 2016, McClements, 2010). In addition to conventional O/W emulsions where dispersed oil droplets are shielded by a single layer of wall materials, a few newly designed structured delivering systems are created, for instance, multiple emulsion, multilayer emulsion, Pickering emulsion and emulsion gel (McClements, 2010, 2012, Ettelaie et al., 2017, Dickinson, 2015). Depending on the delivery strategy of choice, various kinds of emulsifiers are available. Nevertheless,

the scope of this research project focuses only on the application of protein fragments and their covalent conjugates as food emulsifiers, in conventional O/W emulsions.

1.2.1 Stabilizing mechanism of protein-polysaccharide conjugates

Proteins, particularly milk proteins, are effective emulsifiers by virtue of their amphiphilic characteristics which enable them to adsorb strongly to the oil-water interface, rapidly reduce the interfacial tension and protect the freshly formed oil droplets from coalescing during the emulsification process (McClements, 2015n).

The stability of protein based emulsions mainly derives from the ability of proteins to induce electrostatic stabilization, provided by virtue of the charge on the adsorbed proteins (**Figure 1.6**). Therefore, in cases involving high ionic strength or when the pH approaches pI of the protein, the colloidal stability is often lost (Dickinson, 2015, Evans et al., 2013). In order to improve the stability of protein based emulsions under such unfavourable conditions, polysaccharides are commonly incorporated to form a second protective layer deposited on top of the primary protein layer, enhancing the steric component of the repulsive force between the droplets.

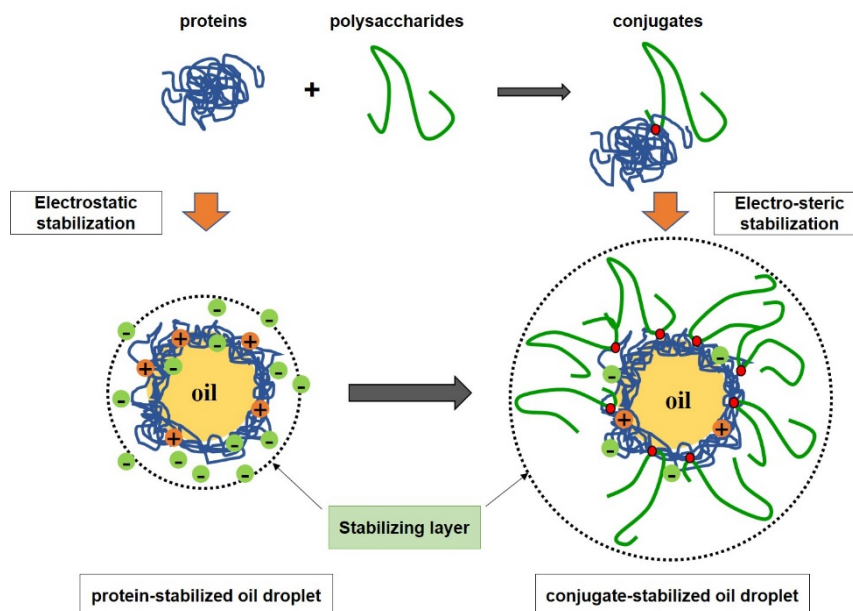


Figure 1.6 Schematic comparison of oil droplet stabilized by proteins and conjugates respectively. The red dot in the conjugates represents the covalent bonding between protein and polysaccharide.

This idea can be realised either by forming electrostatically-driven protein-polysaccharide complexes (i.e. the so-called layer-by-layer films) (McClements, 2010), or by the use of covalently bonded protein-polysaccharide conjugates (Evans et al., 2013, Wooster et al., 2007, Al-Hakkak et al., 2010). The first approach can give rise to several issues of its own, including the possibility of bridging and depletion flocculation during the deposition of polysaccharides layers (Dickinson, 2008), the breakdown of the structural integrity of the complexes induced by large pH shifts (Guzey et al., 2006, Ettelaie et al., 2017), and also the gradual mutual diffusion of biopolymers layers to form a single mixed film rather than the desired layer-by-layer preparation (Ettelaie et al., 2017, Ettelaie et al., 2012). In contrast, protein-polysaccharide conjugates behave somewhat like a copolymer. The polysaccharide moiety protrudes outwards away from the surface, thus effectively forming a second outer layer surrounding the oil droplets, while the protein part ensures the strong anchoring of the conjugated molecule to the surface of the droplets (**Figure 1.6**). This design aims to keep the integrity of the composite macromolecules, while avoiding any bridging flocculation arising from the separate loading of polysaccharides as happens in the layer-by-layer approach, irrespective of the changes in the environmental conditions (Dickinson, 2008, 2015, 2019, Akhtar et al., 2017).

1.2.2 Preparation of protein-polysaccharide conjugates

The covalent linking of protein and polysaccharide can be achieved by means of Maillard reaction (de Oliveira et al., 2016, Kato et al., 1993, Akhtar et al., 2003) or enzyme treatment (e.g. laccase, tyrosinase) (Jung et al., 2012, 2014, Liu et al., 2017).

Enzyme-catalysed conjugation of protein and polysaccharide has been reported to produce biomaterials (e.g. highly absorbent hydrogels) for medical use and in food packaging (e.g. edible films and coatings) (Milczek, 2018, Azeredo et al., 2016). Recently, its application to produce food emulsifiers has drawn much research interest (Liu et al., 2015, Liu et al., 2018b). Based on the catalysing mechanisms, enzyme-mediated crosslinking requires substrates that have certain functional groups (e.g. free amino groups, phenolic compounds). Therefore, the choice of polysaccharide for crosslinking with protein is limited to complex polysaccharides (e.g. pectin, chitosan, gum Arabic) (Milczek, 2018, Isaschar-Ovdat et al., 2018). Furthermore, enzyme-catalysed conjugation has not yet been extensively investigated for the possible

improvement of the emulsifying property of protein, under applied environmental stresses (Jung et al., 2012, 2014, Jiang et al., 2011, Zhu et al., 2015). In some cases, it can be considered as a way to modify complex polysaccharides that do not have sufficiently good emulsifying and stabilizing abilities. For example, Liu et al. (2015) and Chen et al. (2018a) reported enhanced emulsifying properties of corn fibre gum and sugar beet pectin, respectively, under a variety of harsh conditions, following their conjugation with proteins. Most importantly, crosslinking enzymes are capable of catalysing the formation of not only protein-polysaccharide conjugates, but also protein-protein conjugates and even polysaccharide-polysaccharide conjugates (Milczek, 2018). The extent of hetero crosslinking depends on the accessibility of reactive sites on protein and polysaccharide to enzymes (Selinheimo et al., 2008). Therefore, not all of these cases may result in a better emulsifier. For example, due to the formation of protein-protein crosslinks, such covalently bonded polymers display a lower emulsifying activity, compared to untreated proteins (Liu et al., 1999, Isaschar-Ovdat et al., 2015, Zhu et al., 2015). Furthermore, the dispersion of enzymatically crosslinked polymers has been reported to have a dramatically increased viscosity as compared to that formed by non-crosslinked counterparts (Jiang et al., 2010, 2011, Zhu et al., 2015, Chen et al., 2012). This significant alteration of the rheological property should be taken into account when protein-polysaccharide conjugates are being prepared as food emulsifiers by enzyme treatment.

To avoid issues mentioned above, Maillard reaction has become the most popular and straightforward approach to produce protein-polysaccharide conjugates (Zhang et al., 2019b, Akhtar et al., 2017). Maillard reaction refers to a series of complex reactions which naturally occur during cooking and are responsible for the creation of major flavour and colour compounds in most cooked foods (Ames, 1992). For the purpose of simplicity, Maillard reaction is usually summarized into three stages: early, intermediate and final (Friedman, 1996, de Oliveira et al., 2016). Only the early stage is relatively well characterized, which involves the formation of covalent bond between a free amino group of protein (usually the Lysine or *N*-terminus) and a reducing carboxylic group of a polysaccharide (**Figure 1.7**) (Kato, 2002, Oliver et al., 2006). There is no colour change at this stage of Maillard reaction. While the numerous reaction pathways and chemical transformations (e.g. oxidation, degradation, dehydration, free radical reactions) at the intermediate stage result in multiple poorly

characterized compounds which give yellow to golden brown colour and distinctive flavour to cooked foods (de Oliveira et al., 2016, Ames, 1992, Martins et al., 2000). Maillard reaction products (MRPs) formed at these two stages are food grade and are reported to have some health benefits (Gu et al., 2010, Rufián-Henares et al., 2007). At the final stage, advanced reactions will lead to the formation of highly coloured (usually dark brown coloured) nitrogenous polymers, known as melanoidins, which have detrimental health effects (de Oliveira et al., 2016, Martins et al., 2000). Therefore, incorporation of protein-polysaccharide conjugates into foods requires Maillard reaction to be conducted under controlled conditions (including temperature, incubation time, pH, etc.) in order to prevent the reactions from proceeding into more advanced stages.

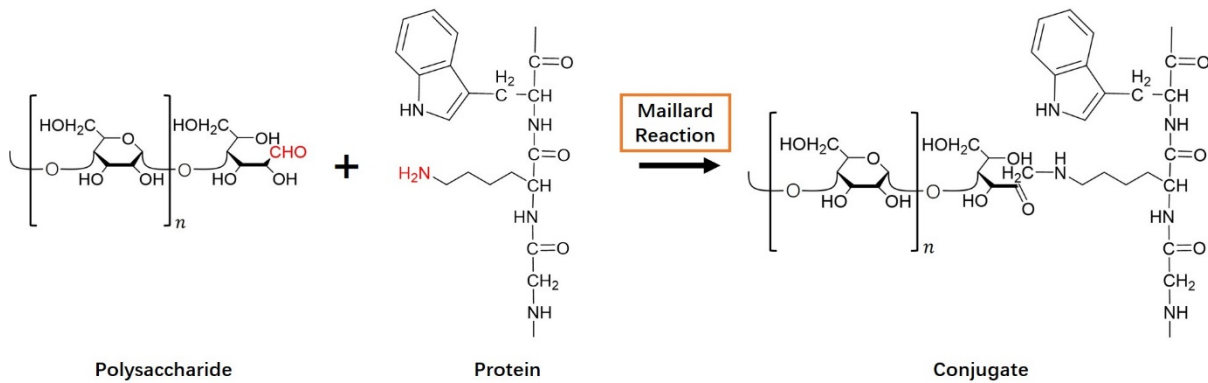


Figure 1.7 Basic chemical reaction mechanism for the formation of protein-polysaccharide conjugate in the initial stage of Maillard reaction. The highlighted groups in red colour on the structures of polysaccharide and protein are the sites involved in Maillard reaction.

Formation of conjugates by Maillard reaction can include both complex polysaccharide (e.g. pectin, gum Arabic, chitosan) as well as simple polysaccharide (e.g. dextran, maltodextrin) (Kato, 2002, de Oliveira et al., 2016). There are generally two possible routes to perform Maillard reaction, the wet-heating route and the dry-heating route. The former has only been studied in the last few years for the preparation of protein-polysaccharide conjugates as emulsifiers. It is a modification of the dry-heating route in the attempt to eliminate the energy-consuming freeze-drying process in the latter (de Oliveira et al., 2016). It is more often used than the dry-heating route when plant based MRPs are prepared (Qu et al., 2018, Li et al., 2014, Pirestani et al., 2017). The

wet-heating route is shown in **Figure 1.8A**. The MRPs formed in this way have been confirmed by various analytical methods, such as electrophoresis, amino acid analysis, FTIR (Guan et al., 2006, Zhu et al., 2008, Zhang et al., 2012b). However, there are relatively few systematic studies with regard to the emulsifying and emulsion stabilizing properties of the conjugates formed via wet-heating route, under environmental stresses. Moreover, the degree of conjugation is heavily influenced by water activity (a_w), with the optimal a_w around 0.6~0.8. Therefore, in the wet-heating approach, where excess water is present, the reaction between protein and polysaccharide is thought to be not particularly efficient (Nursten, 2005, Wrolstad, 2012).

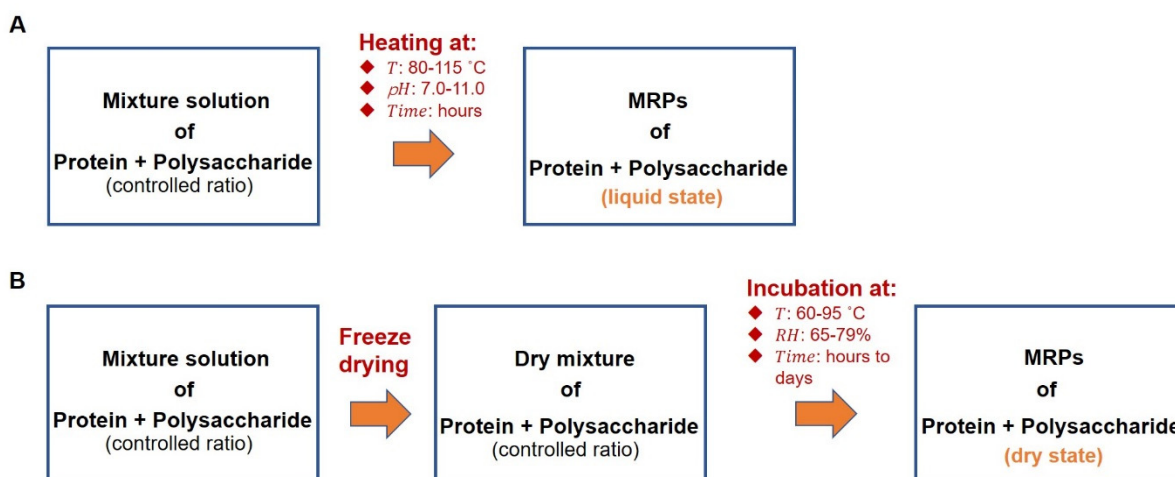


Figure 1.8 Preparation of protein-polysaccharide conjugates via wet-heating (A) and dry-heating (B) pathways.

Based on the above stated issues, dry-heating Maillard reaction remains the most effective approach to produce proper MRPs (Akhtar et al., 2017, de Oliveira et al., 2016). In practice, dry-heating Maillard reaction is usually conducted under controlled temperature and humidity, with no requirement of additional chemicals (Oliver et al., 2006, de Oliveira et al., 2016). Commonly used reaction conditions are incubation for a few days at 60°C and relative humidity (RH) of 65% (de Oliveira et al., 2016, Kato, 2002), or at a higher temperature and RH (e.g. 80°C and 75% RH) for only a few hours (de Oliveira et al., 2016, Akhtar et al., 2017). The flow chart in **Figure 1.8B** demonstrates the preparation of MRPs via dry heating.

1.2.3 Conjugates based on animal-derived proteins

Since the pioneer studies on Maillard-type protein-polysaccharide conjugates in the early 1990s (Kato et al., 1992, Kato et al., 1993, Dickinson et al., 1992), their excellent functionalities and potential use in the food industry have steadily attracted the attention of many researchers. In the past thirty years, glycoproteins made by dry heating have been extensively studied with a diverse combination of animal-derived proteins and polysaccharides (de Oliveira et al., 2016, Dickinson, 2015), including milk β -lactoglobulin-maltodextrin conjugates (Wooster et al., 2007), sodium caseinate-maltodextrin conjugates (O'Regan et al., 2010a), egg white-pectin conjugates (Al-Hakkak et al., 2010), and lysozyme-xanthan gum conjugates (Hashemi et al., 2014).

Protein conjugates have been reported for their remarkably improved solubility (Jiménez-Castaño et al., 2007, Wang et al., 2012) as well as superior emulsifying and stabilizing properties, compared to unmodified proteins, particularly under harsh storage and processing conditions, such as high ionic strength (Kato et al., 1992, Kato et al., 1993, Wooster et al., 2007), acidic pH (Ding et al., 2017), freeze-thaw cycles (O'Regan et al., 2010a), thermal treatment (Wooster et al., 2007, O'Regan et al., 2010a, Wang et al., 2014). In addition, Maillard-type conjugates have also been found to have some health benefits, such as enhanced antioxidant (Xu et al., 2013) and antimicrobial activities (Nakamura et al., 1991).

There are also a couple of studies involving conjugation of polysaccharide with hydrolysed animal-derived proteins. O'Regan et al. (2010b) and O'Regan et al. (2013) investigated the behaviours of hydrolysed sodium caseinate-maltodextrin conjugates under environmental stresses (e.g. elevated temperature, acidic pH), and assessed their potential as low-molecular-weight molecules in aiding emulsification as a replacement for surfactants (e.g. glycerol monostearate). In another study (Hou et al., 2017), hydrophobic casein fragments were obtained by trypsin hydrolysis and conjugated with *A. seyal* gum, so as to modify the weak emulsifying capacity of this cheap gum. Results showed that the hydrophobically modified gum has dramatically improved emulsification performance which is not far from that achievable by gum Arabic.

The factors that would influence the emulsifying and stabilizing properties of the produced conjugates have also been systematically investigated, mostly by taking milk proteins as a model. For instance, the impact of molecular mass of polysaccharides was studied. Polysaccharides of larger molecular mass were found more effective than smaller ones on preventing emulsion flocculation (Wooster et al., 2007, 2006, Dunlap et al., 2005). This is because they are capable of forming a thicker protective layer around droplets, which provides a strong steric repulsion coming into operation at larger droplet-droplet separations. In this sense, mono- and oligosaccharides showed no effect on enhancing the flocculation stability (Ding et al., 2017, Delahaije et al., 2013). Some studies estimated the critical size of polysaccharides necessary to convey effective steric stabilization to roughly be around 6~10 kDa (Shu et al., 1996, Kato, 2002, Akhtar et al., 2007). On the other hand, emulsion stability only increased with the molecular size of polysaccharides up to a certain value. Attachment of larger polysaccharides exceeding that value did not offer any further benefits in terms of the steric stability, and even started to damage the stability of emulsions, probably due to disturbing the adsorption of conjugates onto the O/W interface (Akhtar et al., 2007, Dunlap et al., 2005).

Another essential factor is the average density of carbohydrate moieties that are linked to one protein molecule. A few studies have demonstrated the improvement of emulsion stability with increasing number of polysaccharide attachments (Wooster et al., 2007, Akhtar et al., 2007). Similarly, over-attachment of polysaccharides impaired the emulsifying and stabilizing ability of conjugates (Dickinson et al., 1992, Akhtar et al., 2007), possibly due to making the conjugates too hydrophilic.

In the study by Wooster et al. (2007), the influence of the polysaccharide structure on the induced steric stabilization was investigated. It was shown that linear polysaccharides were superior to branched ones in preventing droplet flocculation, when the two kinds of polysaccharides had similar molecular mass.

In addition to the structure of polysaccharides, the distinct structure of proteins also played an important role in the performance of the final conjugated products. In an early study by Dickinson et al. (1992), three proteins (i.e. 11S globulin *Vicia faba*, bovine serum albumin (BSA) and β -casein) were conjugated with both a small (40 kDa) and a large (500 kDa) dextran in order to assess the emulsifying behaviour as a

function of the molecular size of dextran and the dextran/protein ratio. It was found that attached dextran substantially enhanced the emulsifying ability of the two globular proteins (i.e. 11S globulin and BSA), whereas its impact in the case of the disordered β -casein was detrimental. The size of dextran and the ratio of dextran/protein for the optimum colloidal performances were dependent on the combination of protein and dextran.

1.2.4 Conjugates based on plant-derived proteins

In recent years, the “green” trends in food industries have motivated a significant level of research interest in achieving completely plant based protein-polysaccharide conjugates. Plant proteins considered extensively so far for this purpose include soy protein, peanut protein, pea protein and wheat protein. However, the published work on the colloidal performances of plant based MRPs as emulsifiers is still incomplete.

Firstly, quite a few studies only assessed the emulsifying activity index (EAI) and emulsion stability index (ESI) of the produced plant protein conjugates, but detailed information on the storage stability of emulsions under harsh conditions (e.g. the change of droplet size and distribution over time, the microstructure of emulsions) has rarely been provided (Liu et al., 2012, Qu et al., 2018, Matemu et al., 2009, Li et al., 2014, Ma et al., 2020).

In a number of other studies, plant proteins were covalently bonded with complex polysaccharides, such as soy soluble polysaccharides (Yang et al., 2015), gum Arabic (Pirestani et al., 2017, Zha et al., 2019), or fenugreek gum (Kasran et al., 2013). These polysaccharides, to a greater or lesser extent, already exhibit a reasonable degree of emulsifying ability on their own (Nakamura et al., 2004, McNamee et al., 1998, Huang et al., 2001, Garti et al., 1997). Therefore, it is difficult to attribute the improvement in the functionalities of plant protein solely to the formation of covalent conjugates, and to exclude the contribution made by the presence of those already surface active polysaccharides in the system.

More importantly, the published results on emulsifying and stabilizing behaviours of MRPs derived from plant proteins provide a rather mixed picture. On one hand, a couple of studies have demonstrated dramatically modified functional properties for the conjugated plant proteins. For instance, in the study of Dickinson et al. (1992), 11S

globulin, isolated from *Vicia faba*, was conjugated with dextran (40 kDa) by incubating the dry mixture at controlled temperature and RH. The resultant hybrid polymers showed significantly enhanced emulsifying capacity. They generated a fresh O/W emulsion of smaller droplets ($D_{4,3} = 1.35 \mu\text{m}$) with a monomodal size distribution at pH 8.0 and 0.1 M ionic strength, compared to unmodified 11S globulin which produced an emulsion with a broad bimodal size distribution ($D_{4,3} = 2.2 \mu\text{m}$). In another study (Delahaije et al., 2013), isolated potato protein, called patatin, was conjugated with oligosaccharides via dry heating. The O/W emulsion made by modified patatin exhibited a remarkably improved stability to flocculation at the pH range 3.0~7.0 or in the presence of high ionic strength (0.2 M). Another good example is the conjugates made from isolated wheat protein with dextran (64~76 kDa) via dry heating (Wong et al., 2011). The O/W emulsion made from those conjugates was adjusted to pH 4.0 (approximately the *pI* of isolated wheat protein). Although the zeta-potential of the oil droplets was reduced almost to zero, the emulsion remained completely stable ($D_{4,3}$ around $1.5 \mu\text{m}$) with no change in the droplet size. This indicated the excellent steric stabilizing ability of conjugated wheat protein.

On the other hand, a large number of studies reported limited improvement of the emulsifying and stabilizing properties of conjugates based on plant derived proteins. For example, conjugation of dextran on wheat germ protein only slightly modified the solubility of protein (Niu et al., 2011). The case was the same for conjugates of rapeseed protein-dextran (Qu et al., 2018), soy protein-dextran (Diftis et al., 2006) and peanut protein-glucomannan (Li et al., 2014). The emulsion stability under acid pH conditions or high ionic strength was also found to be marginal in the studies of conjugated soy protein-dextran (Xu et al., 2009), conjugated soy β -conglycinin (Zhang et al., 2012a) and conjugated oat protein-dextran (Zhang et al., 2015). There are even a couple of cases reporting that the MRPs had significantly deteriorated solubility as well as emulsifying capacity as a result of conjugation, for instance, the MRPs of soy protein-maltodextrin (Akhtar et al., 2007) and acid soluble soy protein-dextran (Xu et al., 2009). This makes the picture emerging from these studies, involving the properties of conjugated plant protein, even more confusing.

Last but not least, conjugated plant proteins normally produce relatively coarse emulsions. The average droplet size is around a few microns (Chen et al., 2016, Diftis

et al., 2006, Diftis et al., 2005, Mu et al., 2010, Zhang et al., 2012a). It is suspected that in many cases those reported emulsions may be of Pickering type, stabilized not by molecularly adsorbed protein layers, but rather by particulate protein aggregates. This is usually the case for proteins with a poor solubility.

From the reviews of previously published studies on both animal- and plant-based conjugates, it is noticed that conjugates made from animal derived proteins are more successful with respect to their colloidal performances than those made from plant proteins. It is postulated that the key factor in synthesizing suitable covalent complexes with polysaccharides is the solubility of the original protein. The solubility of protein is not only critical in producing fine emulsions, but is also crucial to guarantee an intimately mixed blend of the two biopolymers in the first instance, so that the Maillard reaction could proceed at a sufficient level. This point is sometimes overlooked in the literature, particularly when plant based conjugates are prepared.

If the three studies aforementioned which demonstrated conjugated plant proteins with improved functionalities, are carefully examined, it is noted that the plant proteins involved in those studies all have a reasonable level of solubility to start with. The 11S globulin *Vicia faba* in the study of Dickinson et al. (1992) was reported to be able to produce a fine emulsion which had a similar mean droplet size to that made by BSA ($D_{4,3}$ for the former and the latter case is 2.2 μm and 2.0 μm , respectively), implying that the protein chains of 11S globulin were in a much less aggregated state, as compared for example to commercial isolated soy proteins which normally fabricate coarse Pickering-type emulsions ($D_{4,3}$ normally over 10 μm) (Chen et al., 2011a, 2011b) with the measured soy protein particle size in dispersion normally over a few hundred nanometres (Zhang et al., 2018). Likewise, the potato patatin used in the study of Delahaije et al. (2013) has a relatively high solubility over the pH range 3.0 to 7.0, and was found to have a comparable emulsifying property to milk β -lactoglobulin (van Koningsveld et al., 2001). The isolated wheat protein used in forming conjugates with dextran in the study of Wong et al. (2011) was indeed a modified wheat protein isolate. Modification was conducted via deamidation, in which more than 90% of the protein fraction was made quite soluble. The solubility of such deamidated wheat protein was observed to be similar to that of sodium caseinate and about seven times superior to that of isolated soy protein (Ahmedna et al., 1999).

However, most of the native plant proteins (e.g. soy proteins, pea proteins and peanut protein) have a compact and complex tertiary and quaternary structure (Chen et al., 2011a, Chen et al., 2016, Burger et al., 2019). Besides, commercially available plant proteins are normally denatured, which exposes their hydrophobic residues and causes their aggregation through hydrophobic association (and where cysteine is involved, the formation of disulphide bonds) (Dickinson, 2019). The structural properties and the aggregated state of commercial plant proteins vary according to the extraction and processing conditions that they have been subjected to (Dickinson, 2019, McClements, 2015n). This renders many plant proteins a poor solubility and limited dispersibility, which become a major obstacle in obtaining a well-blended mix of protein and polysaccharide. Such a molecularly mixed blend is the first step in order for an efficient synthesis of plant based conjugated biopolymers. Therefore, it is essential to modify the protein solubility prior to its mixing with polysaccharide in the solution and its subsequent conjugation with polysaccharide.

One effective way to achieve the above goal is to fragment plant proteins. Generated smaller peptides will not only tend to be more soluble than the original protein, but also aid the formation of fine emulsions due to the breakdown of large aggregated protein particles. Therefore, this could be a promising way to produce molecular (as opposed to Pickering-type) plant based emulsifying agents. In an early study of Kato et al. (1991), insoluble wheat gluten was first treated by protease (i.e. Pronase), and was found to have improved solubility. However, the solubility of hydrolysed gluten was still not greatly modified at acidic conditions. Following incubation with dextran via dry heating, the conjugated wheat protein peptides constantly maintained a high level of solubility over a wide pH range from 2.0 to 12.0. Unfortunately, this study did not provide information on the emulsion stabilizing capacity of the conjugated wheat gluten fragments.

In addition to fragmentation, it is noted that plant protein can also be made more soluble by deamidation reaction. This treatment introduces additional carboxyl groups (-COOH) to proteins by converting asparagine and glutamine residues into aspartic acid and glutamic acid respectively. In the meantime, the high alkaline condition required by the deamidation reaction hydrolyzes the peptide bonds. Both effects benefit the solubilization of plant proteins in neutral and alkaline conditions, whereas

the solubility in acidic conditions is not improved much. In the study of Yin et al. (2017), insoluble zein protein was deamidated under alkaline conditions. The obtained zein peptides themselves were not able to produce proper emulsions at pH 4.0, due to their low solubility and weak electrostatic repulsion. In contrast, their conjugated counterparts with maltodextrin, formed post dry heating treatment, exhibited excellent emulsifying and long-term emulsion stabilizing ability at pH 4.0. The reported droplet size of the O/W emulsions had a hydrodynamic diameter of around 200 nm and remained stable over 70 days of storage. Unexpectedly, if stored at pH 7.0, these emulsions completely broke up. At this pH condition, the peptides became highly charged and some of them became too hydrophilic, arising from the deprotonation of a large amount of carboxyl groups which were introduced during protein deamidation. Consequently, there are strong electrostatic repulsions between the polymers which made up the adsorbed layer. Also, some polymers previously anchored at the surface of oil droplets may become detached. These effects together lead to the dissociation of the interfacial films that coated the oil droplets and the eventual breakdown of emulsions. Another disadvantage of deamidation is that the cleavage of peptide bonds during this treatment normally happens at random and in a non-selective way along the protein backbone. This is likely to generate a large number of peptides which would be too small to be effective emulsifiers.

For most of the research in food colloids, the solubility of protein is improved via the strategy of enzymatic hydrolysis. There is one study in which plant protein was modified by a combination of conjugation and enzymatic hydrolysis, showing promising functionalities. Zhang et al. (2012a) first synthesized conjugated soy β -conglycinin with dextran (67 kDa). The product was then hydrolysed by trypsin in a controlled manner. Although the hydrolysis was performed post conjugation (which is the opposite way to what is being proposed in the current project), the final products at the degree of hydrolysis (DH) of 2.2% formed a fine emulsion ($D_{4,3} < 1 \mu\text{m}$). The droplets remained reasonably stable under a wide range of tested pH (pH 2.0 to 10.0), at high ionic strength (up to 0.2 M NaCl), and post thermal treatment (90°C for 30 min) for a storage period of 4 weeks. Whereas extensive hydrolysis at higher DH of 6.5% was seen to significantly deteriorate the functional properties of β -conglycinin-dextran conjugates. Unfortunately, β -conglycinin, as one of the components of isolated soy protein, is tedious to isolate and is rarely commercially available (Nagano et al., 1992,

Vu Huu et al., 1979, Thanh et al., 1975). (Particularly, as will be discussed later in this thesis, our work showed that the same technique, i.e. conjugation prior to fragmentation, does not work if commercial SPI is used instead of β -conglycinin.)

The ability of conjugated protein fragments to stabilize emulsions during repeated freeze-thaw treatments has been assessed as well. In the study by Yu et al. (2018a), soy protein isolate (SPI) was digested by trypsin. The soy hydrolysates at two different DH (2% and 5%) were conjugated with dextran (40 kDa). Emulsions made by conjugated soy peptides at DH 2% exhibited significantly better stability ($D_{4,3} = 3.13 \mu\text{m}$) subjected to three freeze-thaw cycles than both SPI/SPI-dextran based emulsions ($D_{4,3}$ about $15 \mu\text{m}$) and those made by conjugated peptides at DH 5% ($D_{4,3} = 5.61 \mu\text{m}$). Another study of conjugated soy fragments also showed positive results on the freeze-thaw stability of emulsions by evaluating the creaming index of emulsions (Zhang et al., 2019a, Lee et al., 1987).

It is also worth noting here that with regard to the conjugates made from protein fragments, there will be a few more issues of concern in addition to the solubility of proteins (e.g. the optimal degree of hydrolysis of proteins, the choice of enzyme), in order for the conjugates to display good emulsifying and stabilizing properties.

In addition, research also studied the interfacial adsorption behaviours (Li et al., 2016), the structural properties (Xu et al., 2018, Zhang et al., 2014c), and the antioxidant properties (Xu et al., 2018, Zhang et al., 2014a) of conjugated plant protein fragments.

To summarize, the picture of modification of the functional properties of plant protein/peptides with polysaccharide via Maillard reaction is far from clear. Although a few studies have provided useful information, these have not been enough for us to totally understand the contrasting results reported in the literature on the emulsifying and stabilizing abilities of plant based conjugates. In spite of that, through a careful comparison of previous studies, a couple of factors that could significantly influence the properties of conjugated products could already be identified. The most crucial one is the solubility of protein to start with, prior to Maillard reaction. Enzymatic hydrolysis of plant protein prior to conjugation would be beneficial for enhancing the protein solubility. When it comes to protein fragmentation, additional factors have to be taken into consideration, such as the degree of hydrolysis and the choice of enzyme to use.

However, various investigations in the literature have used a different enzyme and the degree of hydrolysis (DH) was also not the same. This makes a comparative analysis of how enzymatic hydrolysis affects the colloidal behaviours of protein more difficult. In order to clarify the picture, more systematic studies are required on the investigations of the emulsifying and long-term stabilizing properties of conjugated plant protein/peptides, particularly under environmental stresses.

1.3 Aims and objectives

The current project aims to systematically investigate the feasibility of conjugated polypeptides to create and stabilize fine submicron-sized O/W emulsions under challenging environments (particularly acidic pH conditions). We hope to establish guidelines for synthesizing fully plant-based food emulsifiers for this purpose. To achieve this aim, the following objectives are included in this project.

First of all, both milk whey protein isolate (WPI) and commercial soy protein isolate (SPI) are studied, as typical examples of proteins derived from animal and plant sources, respectively. WPI is a protein mixture with its *pI* value roughly around pH 4.5~5.0 (Boland, 2011). The major component of WPI is β -lactoglobulin, which makes up more than 60% of the total protein. The other important component is α -lactalbumin (Boland, 2011, Kilara et al., 2004). SPI is also a mixture of various proteins. The main protein ingredients are classified into four categories (i.e. 2S, 7S, 11S and 15S) according to their sedimentation coefficients (Fukushima, 2004). Among these, β -conglycinin (7S) and glycinin (11S) represent more than 80% of the total protein content in SPI, with the ratio of 7S to 11S varying between 0.5~1.7 depending on the type of cultivars (Tang, 2017, Nishinari et al., 2014). The *pI* value of SPI is estimated to be around pH 4.5~4.8 (Nishinari et al., 2014).

Careful comparisons are made between the observed behaviours for whey protein samples and those for equivalent soy protein samples that have undergone exactly the same enzyme treatment and the subsequent Maillard reaction process. Greater emphasis is placed on soy protein, as the picture of emulsifying and stabilizing

properties of conjugated plant protein/peptides is far from clear (as discussed in section 1.2.4). We hope to provide more clarity on this aspect.

As to the polysaccharide, a neutral, linear and relatively small maltodextrin with dextrose equivalent (DE) of 16.5-19.5 ($M_w = 8.7$ kDa) is chosen to conjugate with protein/peptides. This is to avoid the formation of electrostatically-driven complexes between protein/peptides and polysaccharides. The use of this maltodextrin also ensures that no complications, such as those coming from the emulsifying, gelling or stabilizing capabilities of polysaccharides, arise. In the meantime, we would like to maintain some level of continuity with earlier published work in our labs, on the modification of emulsifying and stabilizing properties of whey protein isolate by covalently bonding with this maltodextrin (Akhtar et al., 2003, 2007, Ding et al., 2017).

Most importantly, two distinct enzymes (i.e. trypsin and alcalase) are used to digest protein. These two enzymes dramatically differ in their overall level of selectivity of peptide bonds to cleave. Trypsin only acts on the C-terminal sides of lysine and arginine residues, whereas alcalase has a much broader range of substrates (e.g. aromatic, acidic and basic amino acid residues). The aim is to interpret the role of the selectivity of enzyme and the degree of hydrolysis in the performance of the fragmented protein materials, both prior to and post reaction with polysaccharide.

1.4 Thesis outline

The thesis is composed of 7 chapters.

Chapter 1 briefly introduced the foundation of colloidal systems, with focus on the stability of O/W emulsions made by macromolecules. Then the major literature regarding the preparation of MRPs and the emulsifying and stabilizing properties of conjugated animal- and plant-based protein/peptides was reviewed, with the research gap in this field identified. Finally, the organization of the thesis is presented.

Chapter 2 explains in detail the basic physical and chemical principles underlying the theoretical and experimental methods that were employed in this project. This builds

up a general understanding of how the theoretical calculations and the experiments were conducted.

Chapter 3 is theoretical work, which mainly discusses how the structural properties of fragmented protein (i.e. the size, the hydrophobicity and conformation) and polysaccharide (i.e. the size) would affect the emulsifying and stabilizing properties of biopolymers. This chapter serves as a theoretical foundation for the following experimental investigations.

Chapter 4 and Chapter 5 present the results for the non-conjugated and conjugated whey protein/peptides and soy protein/peptides, respectively. Results from these two chapters are compared in detail from various aspects (e.g. solubility, efficiency of conjugation, emulsifying and long-term stabilizing ability). In this way, we aim to provide a clearer understanding of the possibility and complications involved in producing suitable plant based food emulsifiers for the use of making stable and fine submicron-sized O/W emulsion systems.

Chapter 6 is a relatively short study, which provides some preliminary data on the impact of the molecular size of protein fragments on the emulsifying and stabilizing properties of conjugated products. This short study offers some experimental evidence for the theoretical results in Chapter 3, and is also helpful to interpret some of the findings in Chapter 4 and Chapter 5.

Last but not least, Chapter 7 summarizes the key findings in this project and manifests the contributions of this entire study to the understandings of the properties of not just soy protein/peptides, but plant proteins more generally.

Chapter 2 Theoretical and Experimental Methods

2.1 Introduction

Experimental investigations have played an essential role in the study of colloidal systems. They provide the solid foundation for understanding many aspects of the behaviour of the colloidal materials and systems, such as the stability, the microstructure and rheological properties of emulsions. Nevertheless, the complexity of food systems, due to the simultaneous presence of various components (e.g. dispersed particles, polymers, surfactants, salts, sugars, fats), can lead to different or even sometimes contrasting expectations of the behaviour to those actually found experimentally. On the other hand, mathematical and computer simulations can simplify those situations by offering the flexibility of changing or completely switching off certain disturbances arising from the presence of a particular type of ingredient, without altering the interactions between the others. This allows simulations to provide a unique insight and critical ability to examine possible conclusions arrived at through experiments. Mathematical and computer simulations have been broadly applied to the studies of food colloidal systems (Ettelaie, 2003), such as the structure and mechanical behaviours of food gels, and the conformational structures of protein materials at the interface (Dickinson et al., 1997a, Akinshina et al., 2008).

In this project, both experimental and simulation techniques are employed to study the performance of unconjugated and conjugated protein materials, in particular the colloidal stability that adsorbed layers of these biopolymers induce in O/W emulsion systems. The theoretical method used here is numerical based self-consistent-field (SCF) calculations, which are a valuable tool in the study of the equilibrium property of adsorbed polymers at the interface. This chapter will start with a discussion of this theoretical method first, and then continue to explain the principles of the experimental techniques that have been used in the project.

2.2 Theoretical methods

The self-consistent-field (SCF) theory and calculations are firmly based on the principles of thermodynamics. In order to get a better idea of this theory, it is necessary

to first provide a basic sense of the thermal and statistical physics involved, before moving on to a more detailed description of SCF calculations as applied to adsorbed interfacial polymer layers.

2.2.1 Statistical and thermal physics

A thermal system normally consists of an extremely large number of molecules. These molecules can exist in many different configurations, depending on their positions, velocities, orientations and other possible internal states. Each possible configuration of such an ensemble of molecules is regarded as a microstate. The number of possible microstates is extremely huge. A thermal system is not going to stay long in any of these microstates, but rather continuously evolves from one microstate to another. All the accessible microstates can be conveniently grouped into different “macrostates” which are associated with macroscale parameters that can be measured (e.g. pressure, volume, density, etc.) (Lee, 2002a).

The fundamental postulate in statistical and thermal physics is that an isolated system visits each of its accessible microstates with equal frequency. According to that, the most probable macrostate that the system will be found in is the one which has the largest number of microstates (Dill et al., 2003b). This number tends to be so overwhelmingly large for a normal thermal system that in many cases it is safe to ignore those macrostates with smaller number of microstates. In other words, an isolated system will always evolve spontaneously towards the macrostate that contains the largest number of microstates, even though it was initially put in a different macrostate (Lee, 2002a). This indeed is a statement of the second law of thermodynamics. Based on the Boltzmann Law below, the macrostate with the largest number of microstates also has the maximum entropy:

$$S = k_B \cdot \ln W \quad (2.1)$$

where S is the entropy of the system

k_B is the Boltzmann's constant ($1.38 \times 10^{-23} JK^{-1}$)

W is the number of microstates (also called multiplicity) of a specific macrostate

For the above reason, the second law of thermodynamics is also referred to as the maximum entropy principle, which is the only rule that governs how an isolated thermal

system will behave when the energy, volume and number of molecules of the system have changed (Dill et al., 2003a). A thermal system is considered to have reached the equilibrium when it is in the macrostate with the highest entropy. If left alone once this macrostate is attained, the isolated thermal system will remain in this equilibrium state forever, with various observable parameters only showing very small fluctuations around their values for this macrostate (Lee, 2002a).

When a thermal system is brought into contact with a large reservoir, the two will cooperate to maximize their combined total entropy, instead of their own. In the pursuit of doing this, the probability $P(E_i)$ of the system visiting a microstate i with an energy E_i is altered and now becomes proportional to the Boltzmann factor $\exp(-E_i/k_B T)$ that is associated with the energy E_i of the system. Compared to the fundamental postulate for an isolated system, this is called the modified postulate (Lee, 2002b). If one takes the total number W of the microstates in a specific macrostate into account, then the probability of finding the system in a macrostate j of an energy E_j is given by

$$P(E_j) \sim W(E_j) \exp\left(-\frac{E_j}{k_B T}\right) = \exp\left(-\frac{F_j}{k_B T}\right) \quad (2.2)$$

Equation (2.2) stresses that from a macroscopic point of view, the probability of a system being in a macrostate with an energy E_j is now proportional to the Boltzmann factor that is associated with the free energy F_j of the system. In other words, the most probable macrostate of a system is the one with the lowest free energy (Lee, 2002b). Another point worth noting is that the maximum entropy principle for the combined system has now been converted to a minimum free energy principle for the system of interest (Dill et al., 2003c). This conversion is of significant importance, because instead of working on the combined entropy of the system plus the large reservoir, which is barely possible to calculate and measure, one can handle the free energy more easily both in experimental and theoretical approaches (Lee, 2002b).

The above considerations are quite general, but of course apply to the equilibrium properties of dense adsorbed polymer layers at the interfaces, as will be discussed next.

2.2.2 SCF theory applied to dense adsorbed interfacial layers

There has been a great deal of efforts in theoretical modelling of the interactions between polymers (e.g. proteins and polysaccharides). With regard to Monte Carlo and Molecular Dynamics simulations, they normally deal with a relatively small number of molecules over a short period of time. However, when one considers the adsorbed layer at the interface, one molecule is very likely to interact with many other molecules. Therefore, it will be too time-consuming to apply Monte Carlo and Molecular Dynamics in such situations (Ettelaie et al., 2008, Ettelaie et al., 2012). On the other hand, the highly concentrated interfacial layer can be regarded as homogenous along the surface, and this is particularly true for flexible and disordered polymers (e.g. α_{s1} -casein and β -casein) or hydrolysed protein fragments as are considered in this project. Thus, it becomes feasible to apply the mean-field numerical self-consistent field (SCF) calculations, which are well-established in the field of polymer physics, to examine the properties of such dense interfacial layers (Ettelaie, 2003, Ettelaie et al., 2005).

The self-consistent field (SCF) calculations in this project are performed by using the Scheutjens-Fleer scheme (Scheutjens et al., 1979, 1980). It was originally introduced to the study of adsorption behaviour of protein-like chains by the work of Leermakers et al. (1996), Dickinson et al. (1997a) and Dickinson et al. (1997b). The predicted results in terms of the structures of interfacial layers formed by α_{s1} -casein and β -casein in those early works were in very good qualitative agreement with the neutron reflectometry experiments (Atkinson et al., 1995, Atkinson et al., 1996, Dickinson et al., 1993), and also provided a clear explanation for the observed differences in the colloidal stabilizing behaviours of these two proteins (Dickinson et al., 1997a, Dickinson et al., 1997b). The SCF calculations have also been successfully extended to a variety of other colloidal materials, such as interfacial layers consisting of mixed biopolymers (Parkinson et al., 2005, Ettelaie et al., 2008), protein-polysaccharide conjugates (Akinshina et al., 2008) and fragmented proteins (Ettelaie et al., 2014).

The Scheutjens-Fleer scheme for implementation of the SCF calculation is established on a 3D lattice model. **Figure 2.1** provides a simpler 2D illustration of the model. Two approaching interfaces (representing part of the surface of two dispersed droplets) are taken as two parallel planar planes with the space in between them being divided into layers ($r = 1, 2, 3, \dots, L$), each of a thickness of one monomeric size a_0 . These layers are further divided into equal-sized cubic cells. For the purpose of numerical

calculations, all the different monomeric segments making up the polymers (i.e. amino acid or glucose residues), individual ions and solvent molecules are considered to be of equal size a_0 . Each monomer occupies one lattice site, and all the sites are required to be occupied either by a polymer segment, an ion or a solvent molecule. The excluded volume (i.e. one monomer cannot land on a lattice site that has already been occupied by another monomer) is accounted for in SCF theory by putting a constraint in the calculations which ensures the sum of the volume fractions of all monomer species for each lattice site in the system has to add up to one (see Appendix I). Particularly for polymers, the excluded volume effect, arising from the conformational entropy of polymer chains, induces repulsive forces and is the basis for the steric stabilization in colloidal systems (Dill et al., 2003d, 2003e). This entropic term is inherently built in the SCF calculations for the free energy of the dispersed system. More details regarding this are provided in Appendix I.

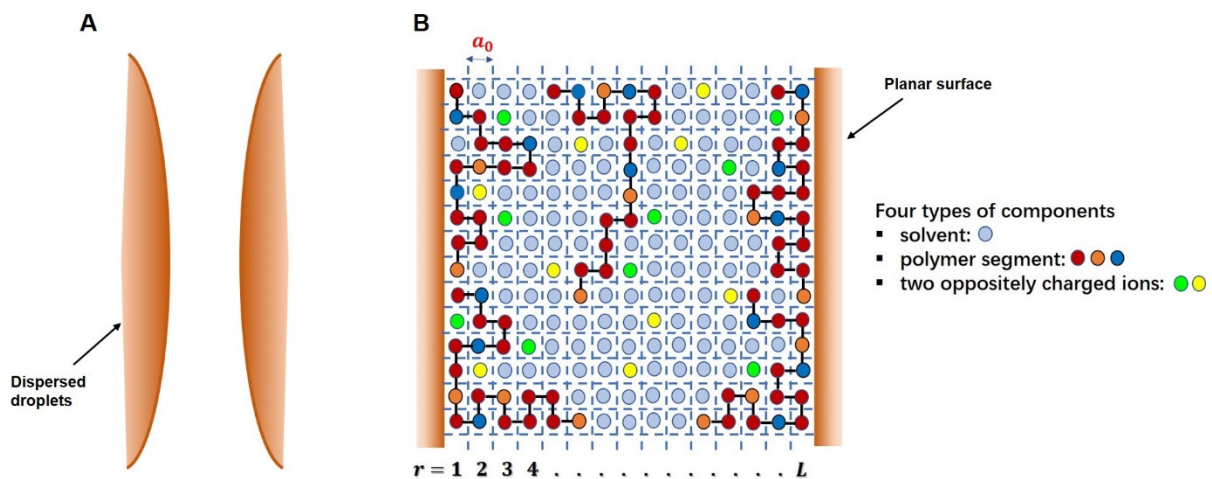


Figure 2.1 (A) Schematic illustration of two approaching dispersed phases with the space in between. (B) Magnified two-dimensional lattice model of this space and the different species existing in between.

The essential aim of self-consistent field (SCF) calculations is to determine the most probable macrostates for all the species (including polymers, solvent, ions) that exist in the gap between a pair of planar surfaces. The discussions in the previous section indicate that such states will be the ones that minimize the free energy of the system. To obtain these states, the free energy of the system is evaluated in terms of a set of concentration profiles for all different types of monomers, instead of the position or

conformation of individual molecules (Ettelaie et al., 2014). Due to the fact that in this lattice model one monomer size is chosen as one lattice size, the concentration or density is now the same thing as the volume fraction for a certain type of monomer. Furthermore, provided that the environment of all the lattice sites within a given layer is the same (see **Figure 2.1**), the density of the monomers of a certain type α is assumed to be uniform within the same layer, only varying in the direction perpendicular to the two interfaces (across the gap) but with no variation parallel to the surfaces (Ettelaie et al., 2014, Ettelaie et al., 2008, Ettelaie et al., 2005). Thus, variations in the concentration of any type of monomers can be expressed as a function of the perpendicular distance r away from one or the other planar surface.

In principle, associated with each set of concentration profiles (for all types of monomers) there is a free energy, which in line with the discussions of section 2.2.1, determines the likelihood of that set of profiles to happen. Strictly speaking, for a thermal system, all the thermodynamic quantities of interest have to be averaged over all possible outcomes, each one of which has a probability of occurring proportional to its own appropriate Boltzmann factor. Unfortunately, the task of summing over all concentration profiles with their corresponding probabilities is very difficult to carry out mathematically. Therefore, the SCF theory adopts an important approximation in that the most probable set of concentration profiles dominates the behaviour of the system, with the fluctuations around this set being negligible and hence ignored (Fleer et al., 1996, Lifshits et al., 1978, Ettelaie et al., 2014). This is a feature that SCF calculations share with all mean-field type theories. This approximation is valid for sufficiently concentrated systems with a large number of molecules present, such as the dense interfacial layers formed by adsorbed polymers in our case (Ettelaie et al., 2012, Ettelaie et al., 2014, Ettelaie et al., 2008).

The concentration profiles of different monomer species are influenced by a variety of interactions between monomers in the system, such as the electrostatic interactions and hydrophobic interactions. In SCF calculations, the net result of these interactions, experienced by a monomer, is represented by an “effective field” acting on it. For each type of monomer, a set of such fields are applied on the monomer at any layer it may sit. These fields themselves depend on how molecules are distributed in the space between the two planar surfaces. Unfortunately, neither the distributions of different

species nor the interacting fields resulting from them are known to us in advance. In order to solve this issue, an iterative process is performed. A much more detailed description of how SCF calculations are done via such an iterative procedure can be found in Appendix I. Here only a brief explanation is provided. The iteration begins with a trial set of interacting fields. Then the concentration profiles of various species are calculated under the influence of these guessed fields. Based on the calculated concentration profiles, an updated set of fields are then obtained. This procedure is repeated until the concentration profiles and the fields no longer change substantially with further iterations. At this point, the iteration process has converged and the density profiles thus obtained are the most probable profiles, representing the equilibrium density profiles.

These calculations and iteration processes can be implemented by using an already developed program available for Windows platform. The calculations are done for a series of separation distances between the two surfaces, to obtain the variations of free energy. Combined with the attractive van der Waals forces, the total colloidal interactions between two dispersed droplets coated with adsorbed polymers will be presented as a function of separation. This plot of interaction potential-distance may for example look like **Figure 1.2** or **Figure 1.3** in Chapter 1, and it will help to theoretically examine the colloidal emulsifying and stabilizing properties of a particular polymer.

Apart from the inter-droplet interaction potentials, the density profiles for each type of monomer species in the gap between two droplets, and the most probable conformation of adsorbed polymers at the droplet surface, can also be determined through SCF calculations. These will provide additional information to interpret the colloidal stability of an O/W emulsion system. An important point to note here is that the SCF calculations only predict the equilibrium properties of a dispersed system, without any kinetic factors taken into account.

2.3 Experimental methods

In this section, the basic physical and chemical principles underlying the key experimental methods used in this project are discussed. The details of how the experiments were performed (e.g. reaction time, temperature) will be given in each of the following chapters, as appropriate.

2.3.1 Degree of hydrolysis

Limited enzymatic hydrolysis has been demonstrated to be an effective way to modify the functional properties of proteins, more often with vegetable proteins. The parameter to control the proteolytic reaction in the current work is the degree of hydrolysis (DH), which is defined as the percentage of peptide bonds cleaved (Panyam et al., 1996). The advantage of using DH over other parameters (e.g. enzyme dosage, reaction time) is that the properties of hydrolysed proteins are mainly governed by DH alone (Adler-Nissen et al., 1979, Adler-Nissen et al., 1983).

There are a couple of analytical methods commonly used for determining DH, e.g. the TNBS (trinitrobenzenesulfonic acid) assay, the OPA (*o*-phthalaldehyde) assay or the pH-stat technique. As to this project, pH-stat is chosen as the preferred method, because it is a very convenient, fast, reproducible and non-destructive way to monitor DH as hydrolysis is taking place (Mat et al., 2018).

In pH-stat approach, protein is hydrolysed under constant pH and temperature. Particularly for our case, proteins will be digested by two enzymes (i.e. trypsin and alcalase) where both enzymes have optimal activity in the pH range 7.0 to 9.0. The breakdown of peptide bonds will release carboxyl groups (-COOH) and amino groups (-NH₂). At neutral or alkaline condition, the deprotonation of carboxyl groups, which is more intensive than the protonation of amino groups, will lead to a decrease of pH in the system as enzymatic hydrolysis proceeds. In order to keep the pH constant, base solution has to be added. The DH can therefore be calculated from the amount of base consumed according to the following equation (Adler-Nissen et al., 1983):

$$DH(\%) = \frac{B \times N_b}{\alpha \times M_p \times h_{tot}} \times 100\%$$

where B = consumption of base (in litre)

N_b = normality of the base

α = average degree of dissociation of the amino groups

M_p = mass of protein to be hydrolysed (in kg)

h_{tot} = total number of peptide bonds per gram of protein substrate (meqv/g)

The values of α for a series of temperature and pH conditions are given in the book of Adler-Nissen (1986). The value of h_{tot} depends on the amino acid composition of the protein. For the two proteins under investigation in this study, h_{tot} is 8.8 meqv/g for whey protein and 7.8 meqv/g for soy protein (Adler-Nissen, 1986).

2.3.2 Gel electrophoresis

After the preparation of conjugates, it is essential to confirm that protein and polysaccharide are covalently bonded. A major difference of a conjugated protein/peptide compared to its unreacted counterpart is the significant increase of the molecular weight of the former. This can be readily visualized by performing gel electrophoresis.

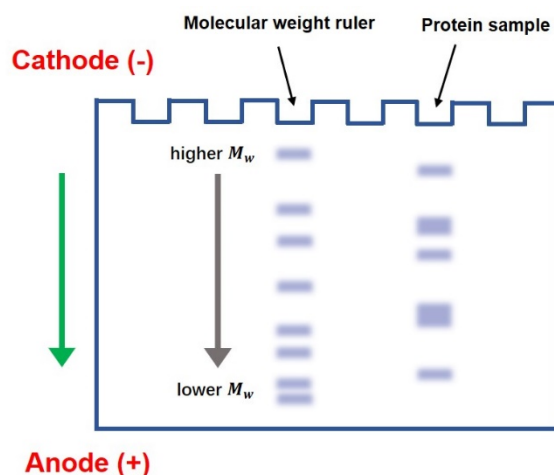


Figure 2.2 Schematic illustration of the migration of proteins on the solid polyacrylamide gel support during electrophoresis. The green arrow indicates the direction of protein movement.

In this technique, protein materials are pretreated with both an anionic detergent, i.e. SDS (sodium dodecyl sulphate), and a reducing reagent, i.e. DTT (dithiothreitol). SDS strongly associates with protein to mask the original charges on the protein backbone, so that protein obtains sufficient negative charges and will move towards the anode under an applied electric field. SDS also denatures and unfolds protein. In contrast,

DTT is added to break up the disulphide bonds in protein. The treatment with SDS and DTT makes protein materials acquire a rod-like shape. This eliminates the difference between proteins in their secondary and tertiary structure (and also quaternary structure where it applies). Therefore, protein materials will be separated based on their molecular weight alone (Srinivas, 2012). As shown in **Figure 2.2**, the difference in molecular weight of protein materials is reflected by how fast they migrate through the solid polyacrylamide gel support (i.e. PAGE) when an electric field is applied. Protein materials of larger molecular size will move more slowly and eventually appear on the upper end of a vertical gel platform, as compared to those of smaller molecular size (Srinivas, 2012). By using a standard molecular weight ruler, the molecular weight of a tested protein sample can thus roughly be estimated.

2.3.3 Solubility

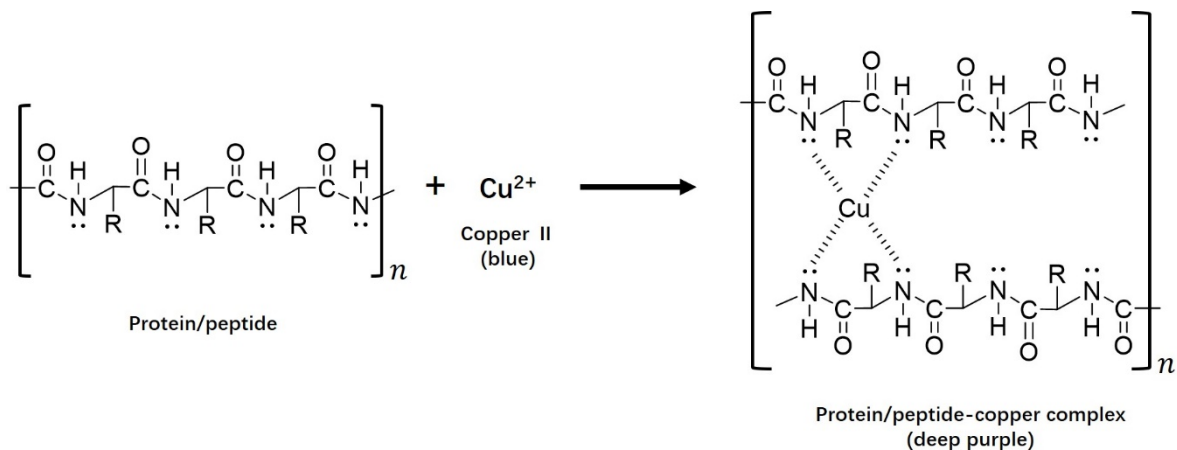


Figure 2.3 The chemical reaction mechanism of Biuret assay for quantification of protein solubility.

The solubility is one of the most important characteristics that affect the emulsifying capacity of protein materials. It is usually defined as the protein content in the supernatant after centrifugation. There are several analytical methods that can quantify the protein content in a sample, such as Kjeldahl, Biuret, Lowry, BCA (bicinchoninic acid) and Bradford assays (Moore et al., 2010). In this study, solubility is determined by Biuret assay, which is a relatively simple, rapid and accurate technique (Gornall et al., 1949).

The principle of Biuret assay is illustrated in **Figure 2.3**. In alkaline conditions, cupric ions (Cu^{2+}) in Biuret reagent will complex with the unshared electron pairs on the nitrogen atoms in peptide bonds, which produces cuprous ions (Cu^+). The shift from Cu^{2+} to Cu^+ results in the solution turning from blue to purple. The deeper the purple colour, the higher the number of peptide-copper complexes (Rocco, 2006). This is the basis of the quantitative colorimetric measurement of total protein content in the supernatant.

2.3.4 Sulfhydryl (-SH) content

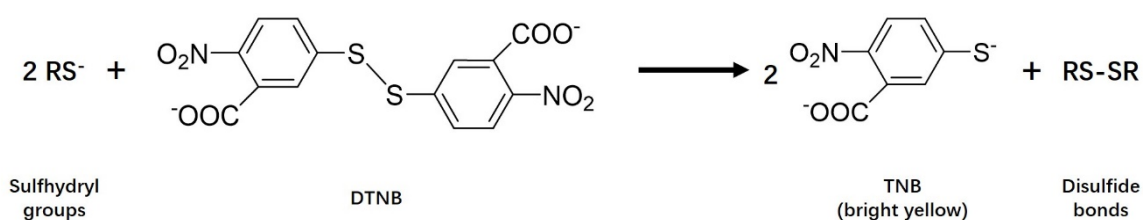


Figure 2.4 The chemical reaction mechanism of Ellman's reagent for analysis of the free sulfhydryl content of protein materials.

The change of free sulfhydryl content of a sample is detected in order to display the structural properties of different protein materials. The free -SH groups are quantified based on a stoichiometric disulphide exchange reaction (**Figure 2.4**), where the highly oxidizing disulphide bond in 5,5'-Dithiobis-(2-nitrobenzoic acid) (called DTNB or Ellman's reagent) is reduced by free -SH (Hansen et al., 2009, Winther et al., 2014). The formed compound, 5-thio-2-nitrobenzoic acid (TNB), gives bright yellow color and absorbs strongly at 412 nm. The free -SH content C_{SH} (mol/g protein) is then easily obtained from the absorbance measurement according to the following equation (Ellman, 1959):

$$C_{SH} = \frac{A_{412}}{\varepsilon} \times D/C_p$$

where A_{412} = absorbance reading at 412 nm

ε = molar extinction coefficient of TNB ($13,600 \text{ M}^{-1}\text{cm}^{-1}$)

D = dilution factor of the sample

C_p = protein content of the tested sample (g/L)

2.3.5 Particle sizing

The molecular size of emulsifiers plays an essential role in determining the emulsion droplet size. For example, surfactants and macromolecules are able to produce nano- or submicron-sized O/W emulsions, while large particles more than a few hundred nanometres can only create micron-sized Pickering emulsions. In turn, the size distribution of oil droplets formed is closely related to the behaviours of O/W emulsions, such as the creaming stability and the rheological property of an emulsion. Therefore, it is crucial to investigate the size of both the emulsifiers and the emulsion droplets. The size information can be obtained by light scattering techniques.

When a light beam hits a particle, the incident light will be scattered in a well-defined manner. The scattering pattern (i.e. mainly the angle and intensity of scattered light) is characteristically dependent on the size of the particle relative to the wavelength of the light, supposing the particle is of a spherical shape (Everett, 1988b, McClements, 2015a). This is the basis of how the particle size distribution of a sample can be derived from collecting the signals of scattered light at different angles.

2.3.5.1 Sizing of emulsifiers

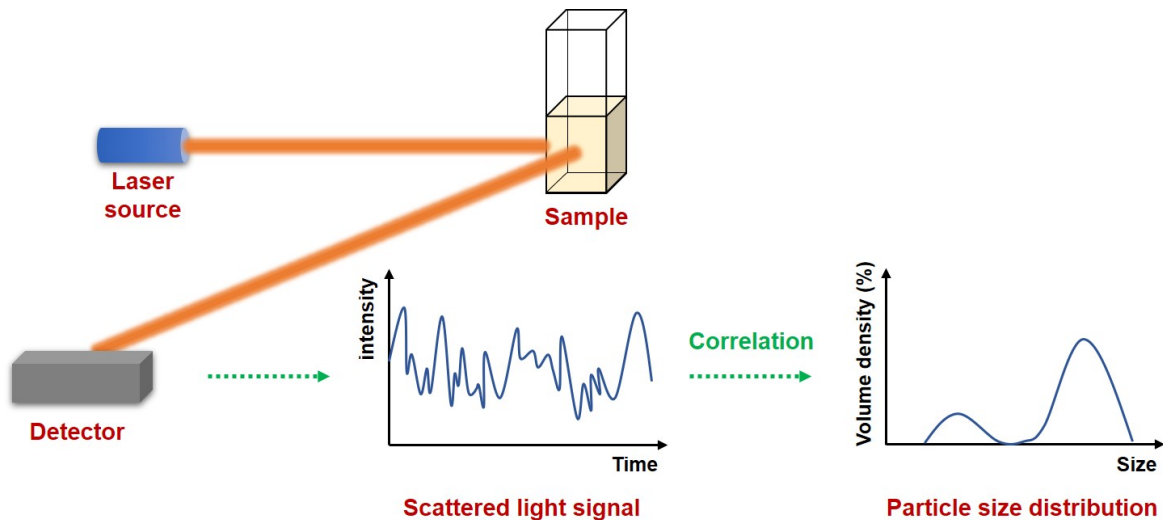


Figure 2.5 Schematic illustration of the basic setup for Dynamic Light Scattering (DLS) technique.

In this project, the sizing of protein particles was conducted by a Zetasizer Nano ZS instrument (Malvern Panalytical, USA), which is built on Dynamic Light Scattering (DLS) technique (also known as photon correlation spectroscopy).

The instrument setup is schematically shown in **Figure 2.5**. Laser is used to illuminate the particles in the sample. The signal of scattered light is collected at a fixed angle, normally either at a 90 degree (right angle) or 173 degree (back angle). In this work, the back angle detector is chosen to collect the scattered light signal. If the particles in the sample are completely still, a constant intensity of scattered light will be detected. In contrast, particles subjected to random Brownian motion will cause the intensity of scattered light to continuously fluctuate over time. How fast the fluctuations occur depends on the diffusion rate of the particle. Smaller particles diffuse more quickly, and will lead to more rapid fluctuations of scattered intensity than larger particles. Based on this, DLS technique extracts the information on the diffusion coefficient of a dispersed particle from the time-varying intensity profile of the scattered light. Then this information is used to derive the radius R of the particle by applying the Stokes-Einstein formula (see below) (Hirst, 2013a, McClements, 2015b):

$$R = \frac{kT}{6\pi\eta D}$$

where k is the Boltzmann's constant, T is the absolute temperature, η is the viscosity of the continuous phase and D is the diffusion coefficient.

One important point to note is that the particle under investigation is assumed to be spherical and the size obtained by DLS technique is defined as the hydrodynamic size (**Figure 2.6**), which comprises the particle plus anything that binds onto its surface and thus diffuses with the particle at the same rate. This can for example include solvent molecules, ions, surfactants and adsorbed polymers (Everett, 1988c). The particle size of a sample is reported as Z -average diameter which is an intensity-weighted average.

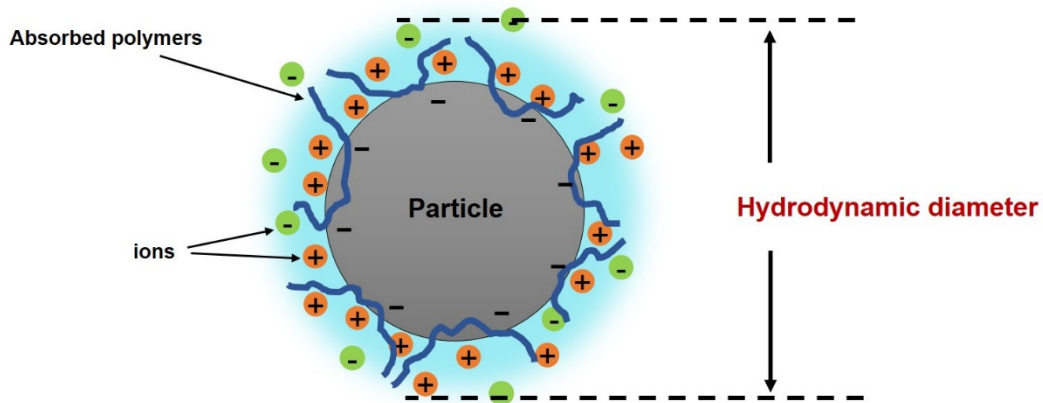


Figure 2.6 Schematic illustration of the hydrodynamic size of a particle.

2.3.5.2 Sizing of emulsion droplets

Particle size can also be measured through the Laser Diffraction technique (or Static Light Scattering). Different from the DLS technique, where the signals of scattered light are only detected at specific angles with the scattered intensity recorded and evaluated as a function of time, Laser Diffraction measures the scattered pattern using a series of detectors over a wide range of angles (**Figure 2.7**) (Hirst, 2013a). Then an intensity distribution is generated as a function of the scattering angle. This information is turned into a size distribution of particles in the sample, using an optical model called Mie scattering theory. This theory also assumes that all the particles under investigation are spherical. It enables sizing analysis over a wide range of particle size, from nanoparticles to large micron-sized particles, to be conducted quite rapidly (Hirst, 2013a, Everett, 1988b, McClements, 2015b).

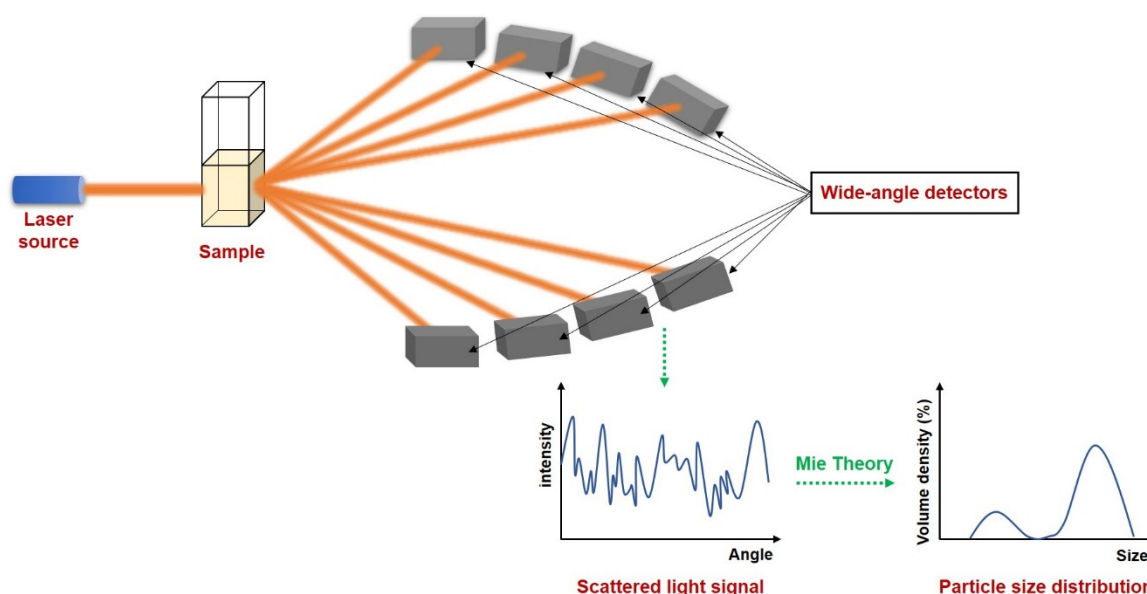


Figure 2.7 Schematic illustration of the basic setup for Light Diffraction technique.

This project determined the size of dispersed oil droplets in O/W emulsions by using a Mastersizer 3000 instrument (Malvern Panalytical, USA), which applies the Laser Diffraction technique. The results of the oil droplet sizing measurements are presented as volume-mean diameter $D_{4,3}$, as well as the size distribution plotted based on the volume ratio of droplets. For a polydisperse emulsion sample, $D_{4,3}$ value is very sensitive to the presence of large particles or aggregates (McClements, 2015j). Therefore, a full size distribution is necessary to provide a more reliable picture of the size characteristics of an emulsion system.

2.3.6 Zeta potential

Zeta potential is the electrical potential close to the surface of the particles dispersed in a specific liquid medium. It is a very useful parameter to understand the strength of the electrostatic interactions between the particles and thus to predict the stability of dispersions (Everett, 1988a). In this project, the zeta potential of emulsion droplets was obtained using a Zetasizer Nano ZS instrument (Malvern Panalytical, USA).

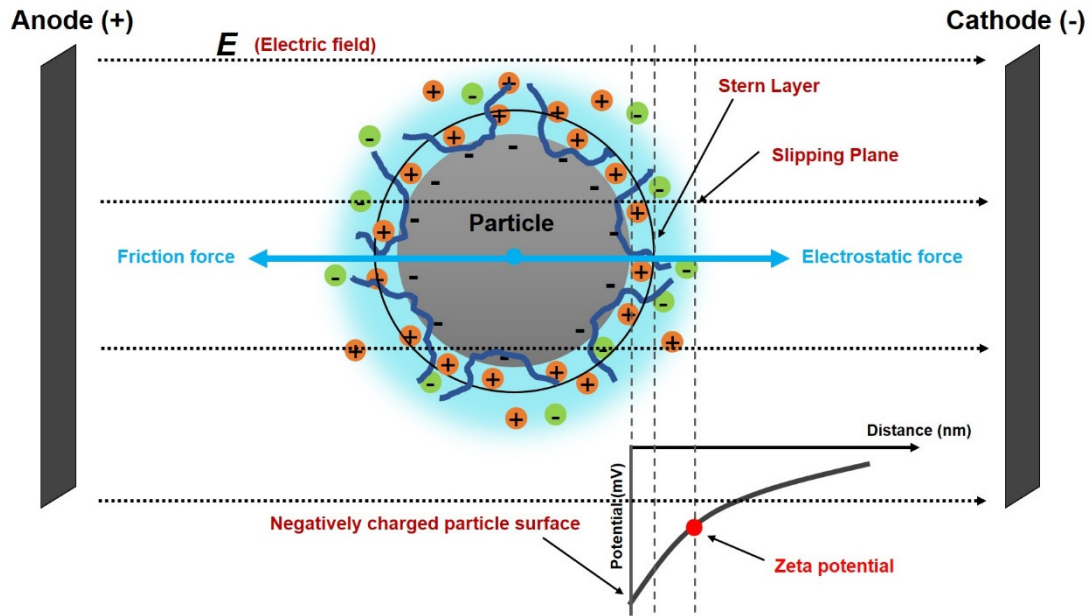


Figure 2.8 Schematic illustration of the basic principles of zeta potential measurement.

The principles of zeta potential measurement are schematically displayed in **Figure 2.8**. An electric field is applied to a sample, which causes charged particles in the sample to move towards either the anode or cathode, depending on the net charge carried by the particle. When the electrostatic force that is pulling the particle is balanced by the drag force exerted on the moving particle due to the viscosity of the medium, the particle will eventually travel at a steady speed. This process is called electrophoresis (Hirst, 2013c, McClements, 2015b). The terminal velocity of particle motion can be determined by comparing the frequency shift of the incident and scattered light, due to the Doppler effect (Everett, 1988a). From this velocity, one can derive the magnitude of the zeta potential of a particle with the aid of either Smoluchowski's or Huckel's formula. The choice of the formula depends on the thickness of electrical double layer relative to the size of the particle. In this work, Smoluchowski's equation is more suitable, on the account that there is normally a relatively thin ionic cloud around the emulsion droplets compared to the droplet size (Hirst, 2013c).

It should be noted that zeta potential refers to the potential measured at the boundary which moves with the particle under the influence of applied electric field (**Figure 2.8**). This boundary is also called the shear plane or slipping plane. Its precise location is

not so easy to define. Therefore, zeta potential is an estimated measure of the electrical potential at the particle surface (Everett, 1988a).

2.3.7 Rheological measurements

Rheology studies the flow and deformation of materials. On one extreme, there are ideally viscous fluids (e.g. water and mineral oil). At the opposite limit, one has ideally elastic solids (e.g. stone and steel). Most real materials fall between these two extremes and behave to a lesser or greater extent in a viscoelastic way. They show a combination of both viscous and elastic properties (e.g. paint, salad dressing, cosmetics, personal care products) (Everett, 1988d, McClements, 2015o).

Generally, there are two types of rheological tests available for assessment, the shear flow tests and oscillatory tests. The former are used to investigate the flow behaviour and viscous property of a liquid-like material, while the latter are for evaluating both the viscous and elastic characteristics of a material. Both types of rheological measurements can provide very useful information on the inner structure and molecular interactions, as well as the stability of a colloidal system. However, they have to be used together with other methods in order to properly interpret the structure of a material (McClements, 2015o).

In this project, controlled shear rate (CSR) rotational tests were performed on O/W emulsions using a Kinexus Ultra rheometer (Malvern Panalytical, UK). The aim is to check the inner structure of an emulsion sample by looking at its flow behaviour.

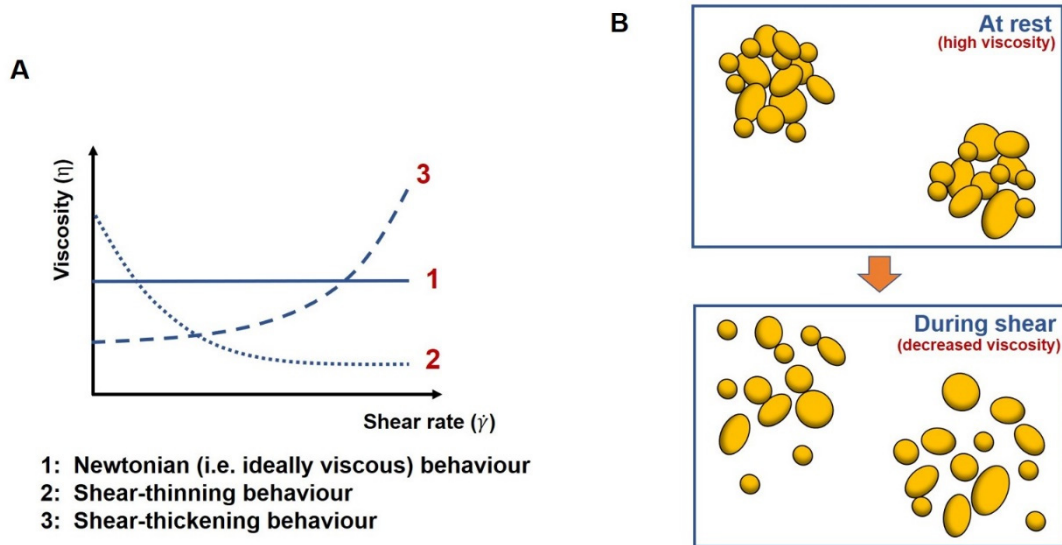


Figure 2.9 (A) The three types of flow behaviour. (B) Schematic illustration of the shear-thinning flow behaviour.

There are basically three kinds of flow behaviour in rotational tests (**Figure 2.9A**) (Hirst, 2013b). A fluid is regarded as Newtonian if its viscosity does not change with shear rate. If the viscosity decreases with increasing shear rate, the fluid exhibits shear-thinning behaviour. Shear-thinning is the most common type of non-Newtonian flow in many food and non-food products. The decreased viscosity is due to the gradual breakdown of the material structure in response to a high shear force (e.g. disintegration of colloidal aggregates), as shown in **Figure 2.9B**. The other, less common, type of non-Newtonian flow is shear-thickening, which describes an increase of viscosity with shear rate. The three types of flow behaviour are also frequently summarized with the aid of a ‘power-law’ model as given below (Dickinson, 1992g, McClements, 2015o),

$$\eta = k\dot{\gamma}^{n-1} \quad (2.1)$$

In the above equation, η is the viscosity of a sample, $\dot{\gamma}$ is the shear rate, k is known as the consistency index, while n is a parameter, called the flow behaviour index, indicating the type of flow: $n < 1$ for shear-thinning, $n = 1$ for Newtonian and $n > 1$ for shear-thickening.

Moreover, a double gap cylinder geometry was used to test the flow behaviour of our emulsion samples (**Figure 2.10**), as this measuring geometry enables testing of low-

viscosity liquids owing to the large contact area (McClements, 2015o). The rheometer collects raw data of the rotational speed and torque, which are converted into rheological parameters, i.e. shear rate ($\dot{\gamma}$) and shear stress (τ), respectively. The viscosity (η) of the sample is then calculated according to the following equation,

$$\eta = \frac{\tau}{\dot{\gamma}} \quad (2.2)$$

and presented as a η - $\dot{\gamma}$ plot in this study.

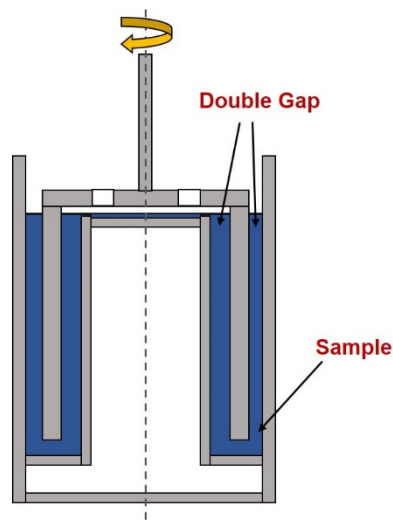


Figure 2.10 The double gap cylinder geometry measuring system.

Chapter 3 A Theoretical Study of the Colloidal Stabilizing Ability of Emulsifiers Influenced by Structural Properties of Polypeptide and Polysaccharide

3.1 Introduction

During the production of emulsifying agents based on covalent bonding of protein fragments with polysaccharide, partial hydrolysis of protein as the first step generates a multitude of polypeptides with different molecular sizes and degrees of hydrophobicity. Moreover, as the chemistry of the Maillard reaction is neither straightforward nor specific, the final products will inevitably consist of a mixture of conjugated polymers which differ from one another in the number of attached polysaccharide chains and the location of these attachments. The system is also likely to have some peptides which would not have reacted with any polysaccharides, also simultaneously present in the final product. These issues would make it difficult to interpret the experimental results obtained from such heterogeneous systems.

Concerning the question of how those factors mentioned above may influence the emulsifying and stabilizing abilities of the conjugated polymers, there have been a few theoretically established insights, involving investigation of the interfacial properties of adsorbed polymers using the so called self-consistent-field (SCF) approach. Akinshina et al. (2008) and Ettelaie et al. (2008) examined the effects of both the length and location of the grafted polysaccharide on the stabilizing ability of α_{s1} -casein under pH values close to the *pI* of the protein and high background ionic strength conditions. They found that the attachment of a short hydrophilic chain may either be detrimental or enhance the emulsion stabilizing ability of α_{s1} -casein against flocculation, depending on the location of the attachment. When the polysaccharide is attached at or close to the middle of α_{s1} -casein backbone, the colloidal performance deteriorates relative to the original non-bonded protein. Yet if the covalent bonding is made towards the end of α_{s1} -casein, the stabilizing ability improves. For a hydrophilic polysaccharide chain larger than a critical length, it was found to be always beneficial to the emulsion stabilizing properties of α_{s1} -casein, irrespective of the position where the attachment was made.

However, the influence coming from the various structural characteristics of protein fragments on the emulsion stabilizing ability of the produced conjugates has not yet been studied, although these are also important in determining whether a polypeptide and its conjugated form are able to be a good emulsifier.

Based on these research gaps, in this chapter, from a theoretical prospective, the impacts of three essential structural characteristics of a protein fragment, i.e. the molecular size, the degree of hydrophobicity (i.e. the proportion of hydrophobic amino acids) and the conformation adopted by a protein fragment at the droplet surface, on its emulsifying and emulsion stabilizing capacity, are first investigated. This allows one in turn to see the role of the degree of hydrolysis (DH) in producing suitable fragmented protein as emulsifying materials. Next, the emulsion stabilizing abilities of a modified protein fragment following its conjugation with a hydrophilic polysaccharide chain are evaluated. The respective role of the protein and polysaccharide moieties, as well as the relative importance of their structures on the colloidal performance of the conjugated polymer fabricated from them, are also discussed.

3.2 Models

All the protein fragments used in this theoretical study are derived from soybean β -conglycinin α' subunit. The primary structure of this protein chain, referred to as GLCAP-SOYBN (P11827), is found in the database UniProt (Magrane et al., 2005). This protein chain consists of 621 amino acid residues. These residues are numbered sequentially from the *N*-terminus of the protein chain. For instance, the 322nd amino acid residue on the primary structure of β -conglycinin α' subunit is Methionine, so it will be labelled as Met³²². Various protein fragments are obtained by applying ExPASy PeptideCutter Tool (Gasteiger et al., 2005) in which trypsin is used to perform the hydrolysis. Trypsin is chosen because it is one of the two enzymes that will be used in the experiments in the following chapters. Its high specificity of the amino acid substrates also eases the selection of example polypeptide. The generated polypeptides are labelled by stating the amino acid residues at both ends of a fragmented chain, starting with the one at the *N*-terminus followed by the one at the *C*-terminus. For example, Met³²²-Lys³⁵⁵ represents a polypeptide chain which is

obtained by cleaving the peptide bond between Arg³²¹ and Met³²² and that between Lys³⁵⁵ and Asn³⁵⁶. Practically, enzyme hydrolysis would produce many different types of polypeptides with a wide distribution of molecular size as well as the degree of hydrophobicity. However, here for the purpose of the theoretical study, it is assumed that only a few specific bonds are targeted, with the desired piece or set of protein fragments generated and separated from the rest of the hydrolysates. We shall not be concerned with the highly non-trivial issue of how such separation can actually be achieved in practice, in this chapter.

In the theoretical model system at its simplest (as previously illustrated in **Figure 2.1**), there are four types of components present: solvent, polymers and two oppositely charged ions. An amino acid residue of a protein fragment, a glucose segment of maltodextrin, an ion or a solvent molecule are all taken to have an equal size a_0 (i.e. the size of a lattice site). The nominal value for a_0 is roughly taken as the length of a peptide bond ~ 0.3 nm (Scheutjens et al., 1979, 1980, Ettelaie et al., 2014, Ettelaie et al., 2008).

In order to maintain a reasonably good representation of the hydrophobic and hydrophilic blocks on the protein primary structure, amino acid residues are grouped into five distinct categories based on their degree of hydrophobicity, the nature of charge and the value of their pK_a (Leermakers et al., 1996). These groups are 1) hydrophobic, 2) polar but non-charged, 3) positively charged (under neutral pH), 4) histidine and 5) negatively charged (under neutral pH). Histidine is placed in a group of its own due to its rather different pK_a value compared to all the other positively charged amino acid residues. According to this classification, the primary structure of a peptide containing 34 amino acid residues (i.e. Met³²²-Lys³⁵⁵), derived from soy β -conglycinin α' subunit (P11827), is illustrated in **Figure 3.1** as an example, showing how this polypeptide is modelled in the SCF calculation.

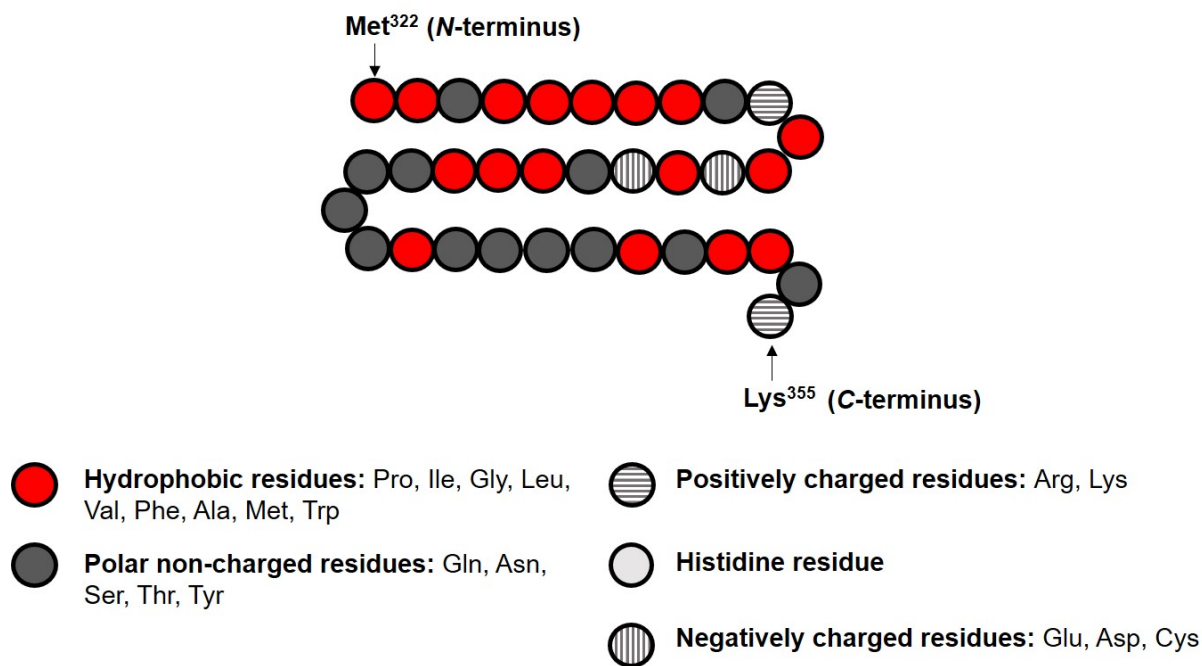


Figure 3.1 Primary structure representing soy peptide Met³²²-Lys³⁵⁵ in the SCF calculations. A list of the full names of the amino acids shown here in abbreviations is provided in Appendix II.

The maltodextrin chain is considered to be made up of a separate category of uncharged hydrophilic monomers. For a protein-polysaccharide conjugate, the primary structure of the protein moiety is kept the same. The only difference is the covalently bonded polysaccharide chain, which can either be attached to a lysine residue or to the residue at the *N*-terminus end of the polypeptide backbone, i.e. sites where a covalent bond between protein and polysaccharide is formed in the actual Maillard reaction. The maltodextrin DE16.5-19.5 ($M_w = 8.7$ kDa) that will be used in the experimental part of this project in the following chapters, is assumed here to have a size of roughly 60 hydrophilic monomers ($L = 60 a_0$), as calculated from its molecular weight. In practice, there may be more than one maltodextrin molecule reacting with and covalently bonding to a polypeptide chain. However, this theoretical study will only consider the situation where only one molecule of maltodextrin is attached per polypeptide chain for simplicity. The polydispersity in the number of attached maltodextrin chains per polypeptide molecule is a complication worth considering in future theoretical studies, but is beyond the current work. It is worth noting here that although a simple non-charged linear polysaccharide (i.e. maltodextrin) is considered here throughout this theoretical study, other characteristic aspects of polysaccharides

can be modeled in the currently available SCF calculations. These aspects include the branching and charging properties of a polysaccharide. The flexibility of a polysaccharide chain is not included in the calculations yet.

Monomer type	0	1	2	3	4	5	6	7	8
0 - solvent	0	1.0	0	0	0	0	0	-1.0	-1.0
1 - hydrophobic	1.0	0	2.0	2.5	2.5	2.5	2.5	2.5	2.5
2 - polar non-charged	0	2.0	0	0	0	0	0	0	0
3 - positively charged	0	2.5	0	0	0	0	0	0	0
4 - Histidine	0	2.5	0	0	0	0	0	0	0
5 - negatively charged	0	2.5	0	0	0	0	0	0	0
6 - glucose residues	0	2.5	0	0	0	0	0	0	0
7 - positive ions	-1.0	2.5	0	0	0	0	0	0	0
8 - negative ions	-1.0	2.5	0	0	0	0	0	0	0
surface	0	-2.0	0	0	0	0	0	0	0
pK_a values				10	6.75	4.5			

Table 3.1 The list of the Flory-Huggins interaction parameters (in the unit of $k_B T$) between different types of monomers and the pK_a values for the groups of charged amino acid residues. The numbers (0 to 8) in this table indicate the nine types of monomers in the model system: solvents (0), five groups of amino acid residues (1 to 5), glucose residues of maltodextrin (6) and ions (7 and 8). A list of the classification of amino acid residues in this study is provided in Appendix II.

Finally, there are also positive and negative ions present in the current theoretical model system. They are regarded as two further categories which are different from the six groups mentioned above (Akinshina et al., 2008, Ettelaie et al., 2008). The electrolyte is taken to be simplest monovalent type, e.g. NaCl. The presence of ions in the model, gives one the flexibility to adjust the background ionic strength in the study, when this is required.

The chemical natures of monomers in each group and their interactions with monomers from other groups, as well as those with the solvent molecules and the hydrophobic surface, are defined by a set of Flory-Huggins χ parameters. The values of these χ parameters are adopted from previously published work (Ettelaie et al., 2008, Akinshina et al., 2008, Leermakers et al., 1996), as listed in **Table 3.1**. A positive

value of χ indicates an unfavorable interaction between two types of monomers, while a negative value signifies a favorable interaction. The χ parameter of $-2 k_B T$ between a hydrophobic monomer (group 1 in the classification) and the surface is a typical value for the adsorption energy of a hydrophobic monomer onto such an O/W interface (Ettelaie et al., 2008). With no specific affinity for the surface, monomers from all the other groups (including the ions and solvent molecules) have their interaction parameter χ with the surface set to be $0 k_B T$ (Ettelaie et al., 2008, Akinshina et al., 2008). As a result of the tendency of ions for hydration by solvent molecules (assumed to be water), the ion-solvent interaction parameter χ is taken to be $-1 k_B T$ (Ettelaie et al., 2014, Akinshina et al., 2008).

In a well formulated emulsion, if the total adsorption energy for the emulsifiers is sufficiently high, most of them will tend to become adsorbed onto the hydrophobic surface of droplets, leaving only a very small fraction of the polymers remaining in the bulk phase (Ettelaie et al., 2014). Hence, the volume fraction of polymers in bulk solution is set at a low level $\Phi_p = 1.0 \times 10^{-11}$ for all the cases in this study. But it must be noted that this does not necessarily represent a low content of emulsifiers in the system.

The electrolyte volume fraction is maintained throughout this study at a low level $\Phi_s = 0.001$ (roughly corresponding to 10 mM for NaCl). The environmental pH is fixed at a value close to the isoelectric point of each protein fragment under investigation, in order to minimize the electrostatic stabilizing effect and allow us to explore the repulsion arising from the steric component.

Interaction potentials, induced by the presence of polymers in the gap between two oil droplets, are calculated using a program already developed by our school which is available for Windows platform. With the inter-droplet Van der Waals attraction also included (see Appendix I), the total interaction potentials between two emulsion droplets (of equal size of $1 \mu\text{m}$) are obtained and plotted against the inter-droplet separation distance. The configurations and density profiles of adsorbed polymers can also be obtained from our SCF calculations. These results are plotted and discussed as well to better understand the properties of the interfacial layers.

3.3 Results and Discussions

Two aspects are investigated theoretically. Firstly, the role of the size, the degree of hydrophobicity (i.e. the proportion of hydrophobic amino acids) and the adopted conformation of a protein fragment on its emulsifying and stabilizing properties is explored. In the next step, we evaluate the modification of the colloidal performance of a protein fragment by a grafted polysaccharide.

Characteristics	Met ³²² -Arg ³³⁴	Met ³²² -Lys ³⁵⁵	Asn ³⁵⁶ -Arg ⁴²⁵	His ¹⁶⁰ -Arg ²⁹⁰	Glu ⁹³ -Arg ³⁰²
Total number of amino acids	13	34	69	131	210
Number of hydrophobic residues	9	17	25	38	58
Hydrophobicity (% of hydrophobic residues)	69.2%	50.0%	36.3%	29.0%	27.6%
Isoelectric point (<i>pI</i>)	5.5	6.0	5.0	6.0	5.5

Table 3.2 The characteristic properties of the selected soy polypeptides.

In order to achieve the above purpose, five different polypeptides are carefully selected. The characteristic properties of these selected polypeptides, including their size, degree of hydrophobicity and isoelectric point, are shown in **Table 3.2**. This selection of polypeptides have a reduced proportion of hydrophobic residues as their size grows. For the ease of demonstration, these fragments were chosen to have similar isoelectric point (between pH 5.5 ~ 6.0). Nonetheless, the following discussions are also largely applicable to situations where the protein fragments may have different *pI* values.

3.3.1 The impact of the structural properties of a protein fragment on its emulsion stabilizing capacity

In this section, we have oil droplets coated by (either non-conjugated or conjugated) soy polypeptide of a single species. One way to gain an insight into the colloidal stabilizing ability of a polymer is to examine the variation of the interaction potential mediated between two emulsion droplets that are coated by these polymers as a

function of inter-droplet separation distance. At any separation distance, a decrease of interaction potential as two droplets come close or an increase as two droplets move away, indicates an overall attractive force between them. The converse cases imply a repulsive force. Consequently, droplets tend to remain in the state where no force is acting on them and they have the minimum potential energy. This state is reflected by an energy well in the plot of interaction potential as a function of separation distance (Coupland, 2014a, McClements, 2015x).

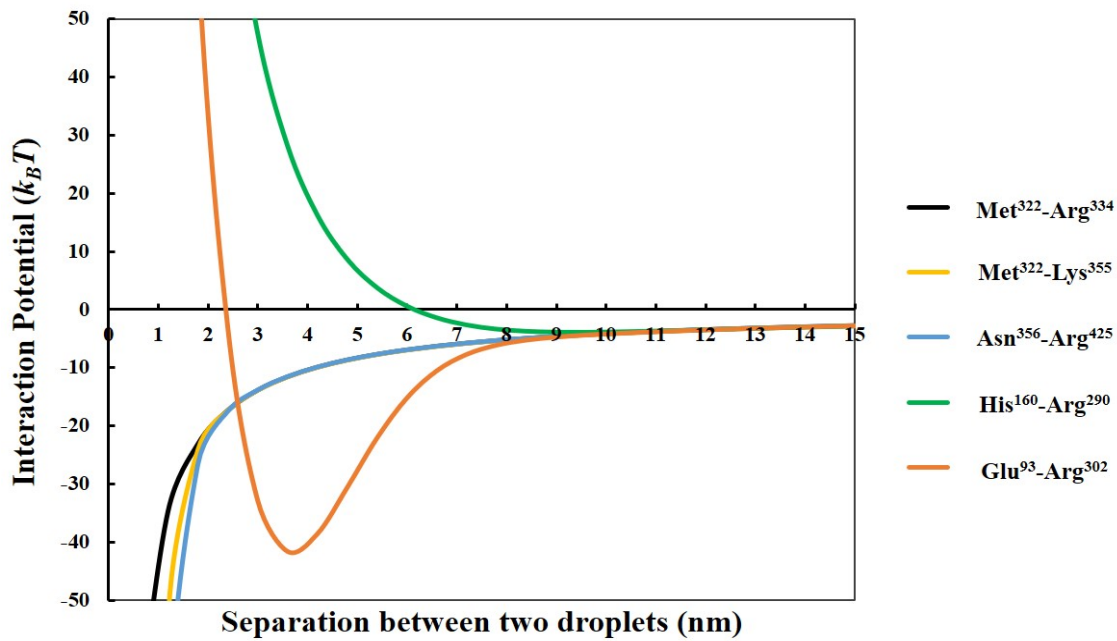


Figure 3.2 The interaction potentials, plotted against the inter-droplet separation distance, resulting from the adsorbed layers of five different soy polypeptides (i.e. Met³²²-Arg³³⁴, Met³²²-Lys³⁵⁵, Asn³⁵⁶-Arg⁴²⁵, His¹⁶⁰-Arg²⁹⁰ and Glu⁹³-Arg³⁰²) respectively. The diameter of oil droplets is 1 μm . The results are produced at a background electrolyte volume fraction of 0.001 and at pH = 5.5.

Figure 3.2 compares the profiles of total interaction potential between two oil droplets stabilized by five different soy fragments respectively. The environmental pH is set to 5.5, which is or is close to the *pI* of these polypeptides (see **Table 3.2**). For the absorbed layers formed by the three relatively short fragments (i.e. Met³²²-Arg³³⁴, Met³²²-Lys³⁵⁵ and Asn³⁵⁶-Arg⁴²⁵), the induced interaction potential profiles all look similar. In particular, no energy barrier is seen in any of these interaction potential curves to prevent the approach of two droplets coated by them. This type of profile

indicates the dominant role of the attractive Van der Waals force. This, together with the lack of a sufficient energy barrier in droplet-droplet interaction potential, will result in severe flocculation of emulsion droplets.

For the inter-droplet potential that is generated by the adsorbed fragment Glu⁹³-Arg³⁰² (see **Figure 3.2**), it is also seen that the Van der Waals attraction dominates as droplets approach. Only at very small inter-droplet separations, the repulsive force overcomes the Van der Waals attraction. This results in a deep energy minimum well ($\sim -41 k_B T$) at the separation around 4 nm. Given the depth of this well, it is unlikely that Brownian motion or even agitation of simple shear can prevent droplets from getting into this energy minimum. Under this circumstance, the droplets will also undergo severe flocculation (Ettelaie et al., 2014, Dickinson, 1992a), being trapped at a distance ~ 4 nm apart from one another in clustered aggregates. Such flocculated droplets in turn greatly increase the chance of them coalescing, with the emulsion system eventually starting to break up as a result.

In contrast to the above results, there is barely a detectable energy well (larger than $-4 k_B T$) when the emulsion droplets stabilized by soy fragment His¹⁶⁰-Arg²⁹⁰ are approaching (see **Figure 3.2**). The droplets are seen to experience a progressively increased repulsion, starting from the separation distance of around 8 nm. Then a sufficient energy barrier (over $\sim 20 k_B T$) (Dickinson, 1992a) builds up to effectively stop any two droplets from coming closer than 4 nm.

The interaction potential profile between two approaching droplets coated by a polymer can be interpreted by examining the possible conformation that the polymer takes at the interface, as well as by studying the density profile formed by that polymer as it adsorbs on an isolated interface.

Let's first look at the conformation of the polymers adsorbed at the hydrophobic surface. **Figure 3.3** presents the average distance adopted by each monomer segment that makes up the three relatively short soy polypeptides, i.e. Met³²²-Arg³³⁴, Met³²²-Lys³⁵⁵ and Asn³⁵⁶-Arg⁴²⁵. The sequence number of monomers along the backbone of a protein fragment is counted from the *N*-terminus of this fragment. It is seen that all of these three short polypeptides lie nearly flat at the droplet surface, due to the multiple small blocks, made of hydrophilic and hydrophobic residues, on the

primary structure of these polypeptides (Wijmans et al., 1994, Ettelaie et al., 2003). The average distance for any of these residues does not exceed one monomer unit a_0 away from the surface.

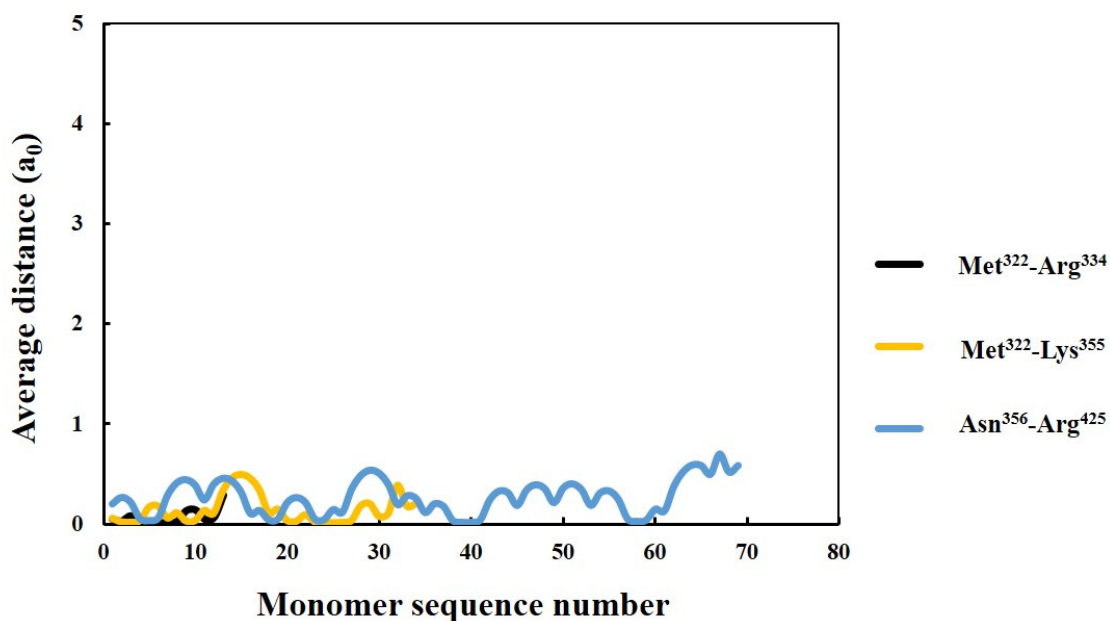


Figure 3.3 The average distance of each monomer residue that makes up the adsorbed soy polypeptides (i.e. Met³²²-Arg³³⁴, Met³²²-Lys³⁵⁵ and Asn³⁵⁶-Arg⁴²⁵), away from a hydrophobic surface, plotted against the sequence number of monomers starting with the first monomer at *N*-terminus of a protein fragment. The results were calculated at a background electrolyte volume fraction of 0.001 and at pH = 5.5.

The conformation that a polymer adopts at the interface is closely related to the interfacial structure formed by this polymer. In **Figure 3.4**, the density profile of protein fragments when they adsorb at an isolated droplet surface is displayed. The density is plotted along the distance perpendicular to the droplet surface. For the two larger polypeptides amongst those three discussed above, i.e. Met³²²-Lys³⁵⁵ and Asn³⁵⁶-Arg⁴²⁵, their flat conformation only enables them to form a rather thin coating layer with a thickness of ~ 1 nm around the oil droplet (**Figure 3.4**). In the absence of electrostatic repulsion at pH = 5.5 (where this environmental pH is close to the isoelectric point of the fragment), the hydrophobic blocks on the polypeptide can form bridges between two individual droplet surfaces, thus generating a strong attractive force, once the droplets get close into a certain separation distance (Wijmans et al., 1994). Only when the two droplets become very close to each other with their thin

interfacial layers starting to overlap, will a repulsion build. However, at such close separation, the Van der Waals attraction is already dominant, leading to a deep energy minimum (Wijmans et al., 1994).

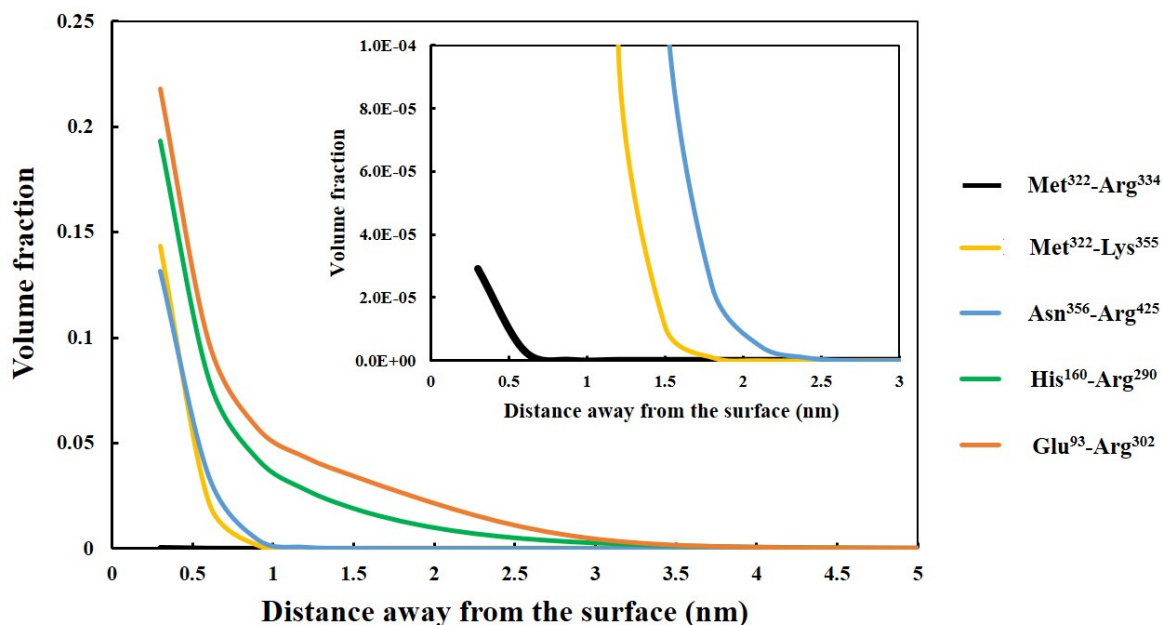


Figure 3.4 Density profiles of the five different polypeptides (i.e. Met³²²-Arg³³⁴, Met³²²-Lys³⁵⁵, Asn³⁵⁶-Arg⁴²⁵, His¹⁶⁰-Arg²⁹⁰ and Glu⁹³-Arg³⁰²) adsorbed at an isolated droplet, plotted against the distance away from the hydrophobic surface. The inset graph is a magnification of the same graph by a factor of 2500, so as to illustrate more clearly the result for the smallest peptide Met³²²-Arg³³⁴ (black line). All the data were calculated at a background electrolyte volume fraction of 0.001 and at pH = 5.5.

For the smallest fragment Met³²²-Arg³³⁴, the case is different. It is noticed from the inset graph in **Figure 3.4** that this fragment, despite having the highest degree of hydrophobicity (i.e. 69.2% of all its constituent residues are hydrophobic amino acids, see **Table 3.2**), adsorbs scantily at the droplet surface, relative to the other larger fragments. In contrast, larger peptides, although less hydrophobic, are able to adsorb at a substantially higher level on the hydrophobic surface. For instance, as to the largest two polypeptides, i.e. His¹⁶⁰-Arg²⁹⁰ and Glu⁹³-Arg³⁰², in which only 29.0% and 27.6% of their total residues, respectively, are hydrophobic amino acids (see **Table 3.2**), their total amount of adsorption is four orders of magnitude more than that of the smallest fragment Met³²²-Arg³³⁴ (see **Table 3.3**).

	Met ³²² -Arg ³³⁴	Met ³²² -Lys ³⁵⁵	Asn ³⁵⁶ -Arg ⁴²⁵	His ¹⁶⁰ -Arg ²⁹⁰	Glu ⁹³ -Arg ³⁰²
Total amount of adsorption (mg/m ²)	1.47×10 ⁻⁴	0.77	0.79	1.84	2.42

Table 3.3 The predicted total amount of adsorption (in the unit of mg/m²) for various polypeptides at the droplet surface, obtained from SCF calculations. The results are produced at a background electrolyte volume fraction of 0.001 and at pH = 5.5.

The poor adsorption of a small peptide is mainly related to its insufficient total binding energy. When a polymer adsorbs onto an interface, the equilibrium between the adsorbed and desorbed states is determined by the Boltzmann factor, $\exp(E/k_B T)$, where E is the total binding energy. In the case of a small peptide (e.g. the fragment Met³²²-Arg³³⁴, with 9 out of 13 residues being hydrophobic, see **Table 3.2**), the total binding energy per molecule is still not sufficiently large for the adsorbed state to be strongly weighted over the state of being in the bulk (Dickinson, 1992f). This is particularly true at low bulk concentrations that is considered here. This is somewhat similar to the situation seen for a small-molecular-weight surfactant. The bulk concentration for such molecules has to be much higher than that found for a large polymeric molecule, in order for the surface to attain sufficient coverage. Thus, at low bulk concentrations, the surface coverage induced by small molecules will be extremely low. In contrast, for a polymer that consists of hundreds of monomeric segments, despite only a small fraction (say one fourth or maybe even one fifth) of these having affinity for the hydrophobic surface, the total binding energy per polymer is significantly large. In such cases, the Boltzmann factor for equilibrium becomes overwhelmingly biased in favour of the adsorbed state. It is for this reason that a polymer has a progressively higher surface affinity as its molecular weight increases (Dickinson, 1992f). Particularly, for naturally-occurring proteins and polypeptides derived from them, the hydrophobic and hydrophilic amino acids are more or less evenly distributed along the backbone of the chain. As a result, the protein fragment with a larger size will normally have a greater number of hydrophobic binding groups than a smaller one and consequently can saturate the interface at much lower bulk concentrations.

A second reason for the poor adsorption of small polymers may be associated with the entropy of mixing when they dissolve in the solvent. Whether a polymer will prefer to mix with solvent and stay in the bulk or to separate out from the aqueous phase mainly depends on two factors: the enthalpic interactions and the entropy of mixing (Coupland, 2014b, Dill et al., 2003d). Provided that the enthalpic contribution to free energy of mixing is roughly the same for a certain amount (based on weight) of polypeptides dissolved in the solvent, it is then the entropy of mixing that largely determines the solubility of a polypeptide species. However, the contribution of a polymer to the entropy of mixing decreases as its molecular weight increases. This contribution becomes negligible for very large polymers. Consequently, a small polymer tends to have a better solubility than a large polymer (Coupland, 2014b). In our case, the small peptide Met³²²-Arg³³⁴ will dissolve much better in the aqueous phase, as compared to the other large polypeptides. Therefore, they become significantly less adsorbed at the surface.

The above results and discussions demonstrate a crucial criterion when it comes to the use of protein fragments as emulsifying and colloidal stabilizing agents. For a polypeptide derived from naturally-occurring proteins, the size of such protein fragment is seen more important than its degree of hydrophobicity in determining the colloidal performance of this polymer. In this respect, for a mixture of protein hydrolysates obtained by enzymatic digestion, the degree of hydrolysis (DH) could serve as a reasonable guiding parameter to control the emulsifying and stabilizing ability of the fragmented proteins, as it governs the content of large polypeptides present in the mixture. A lower level of hydrolysis will produce a distribution of fragments with a greater content of larger-sized polypeptides, while extensive hydrolysis will cause no such large chains to remain in the system. Also, due to the alternating nature of the hydrophobic and hydrophilic blocks on the backbone of a naturally-occurring protein, a small polypeptide derived from it is more likely than a large one to have an excessively hydrophilic primary structure (thus cannot adsorb at all). Consequently, in theory at least, a mixture of polypeptides tends to have a reduced overall surface affinity as the fragmentation of protein proceeds to higher levels.

We now turn attention to the interfacial structures of the two largest polypeptides, i.e. His¹⁶⁰-Arg²⁹⁰ and Glu⁹³-Arg³⁰². From the graphs of the density profiles in **Figure 3.4**,

adsorption of these polypeptides leads to the formation of a much more extended interfacial layer. For both cases, the thickness of the layer is ~ 3.5 nm. This is to be compared to that produced by the two smaller fragments (i.e. Met³²²-Lys³⁵⁵ and Asn³⁵⁶-Arg⁴²⁵, as discussed previously in **Figure 3.4**). The polypeptide Glu⁹³-Arg³⁰² is also seen to have a larger amount of adsorption, thus forming a denser layer at the interface, than the peptide His¹⁶⁰-Arg²⁹⁰ (see both **Figure 3.4** and **Table 3.3**). However, as observed previously in **Figure 3.2** for the inter-droplet potentials, the droplets stabilized by the fragment Glu⁹³-Arg³⁰², were predicted to be subject to flocculation as a result of the presence of a deep energy minimum in the mediated interaction potential. On the other hand, the droplets coated by polypeptide His¹⁶⁰-Arg²⁹⁰ were predicted to stay well dispersed. The distinct interaction potential profiles induced by these two large polypeptides, as well as the different colloidal behaviours between the emulsion droplets that are respectively coated by them, can be attributed to their conformations at the interface (see **Figure 3.5**) as discussed below.

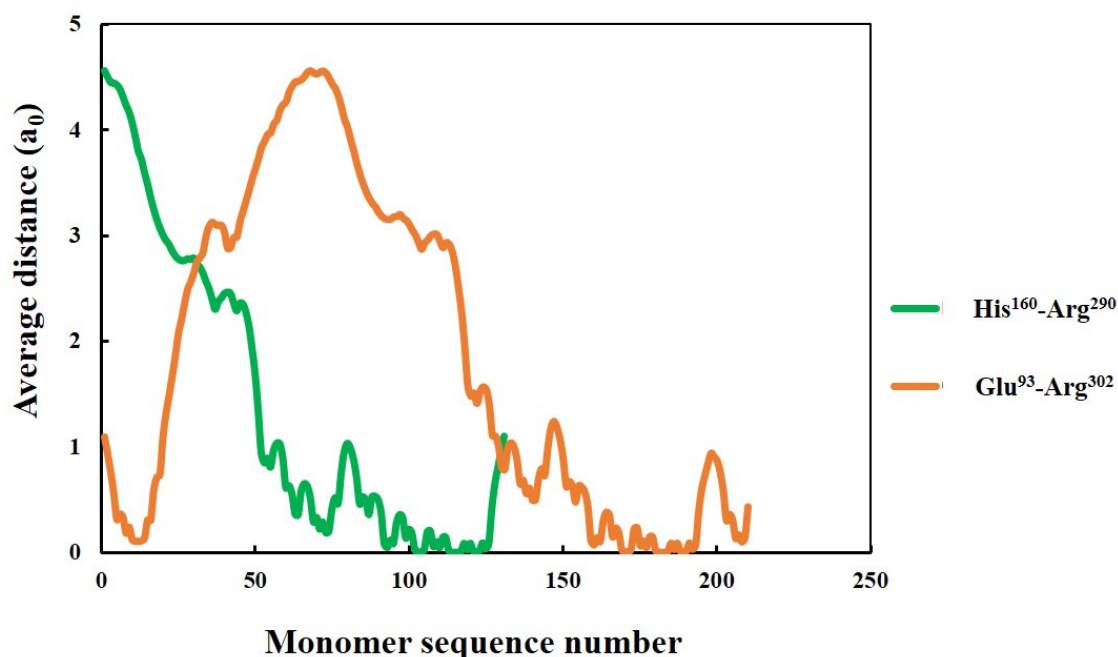


Figure 3.5 The average distance of each monomer residue that makes up the adsorbed soy polypeptides (i.e. His¹⁶⁰-Arg²⁹⁰ and Glu⁹³-Arg³⁰²), away from a hydrophobic surface, plotted against the sequence number of monomers starting with the first monomer at *N*-terminus of a protein fragment. The results are produced at a background electrolyte volume fraction of 0.001 and at pH = 5.5.

It is seen that polypeptide His¹⁶⁰-Arg²⁹⁰ adopts a diblock-like configuration, with the its *N*-terminus end extending by $\sim 4.5 a_0$ away from the surface of the droplet. This is the origin of the strong and more importantly the longer-ranged steric repulsion. This repulsive force arises when interfacial layers on neighbouring emulsion droplets overlap. In contrast, the other polypeptide Glu⁹³-Arg³⁰² behaves much more like a triblock at the interface. Although it also has its central part (called a loop) protruding outward away from the droplet surface, thus helping to form a thick interfacial layer, this polypeptide is able to also adopt a bridging conformation between two adjacent droplets over certain ranges of inter-droplet separations. This results in a strong attractive force which is not desirable (Ettelaie et al., 2003, Ettelaie et al., 2008, Wijmans et al., 1994, Akinshina et al., 2008). This situation is somewhat similar to the behaviour of α_{s1} -casein compared to that of β -casein (Dickinson et al., 1997a, Dickinson et al., 1997b).

To summarize, the emulsion stabilizing property of a protein fragment is seen closely connected with its structural characteristics. The first and foremost requirement for a protein fragment to be a potentially good colloidal emulsifying and stabilizing agent is the ability to adsorb sufficiently at the droplet surface. In this regard, the theoretical results in this section have indicated that at low bulk concentrations (i.e. the situation considered here where conventional-type O/W emulsion is prepared), the size of a polypeptide is more important than its degree of hydrophobicity. This is due to the fact that it is the overall binding energy that determines the level of adsorption of a polymeric molecule. Therefore, for a polypeptide derived from naturally-occurring proteins, a larger peptide will normally induce a stronger surface adsorption than a smaller one, thus being a more suitable candidate as an emulsifying agent. This in turn signifies the role of degree of hydrolysis (DH) as a relatively reliable parameter to control the colloidal performance of hydrolysed protein materials. In addition to a sufficient size and adsorption, a protein fragment also has to adopt a specific conformation (i.e. diblock-like, rather than flat or triblock) at the hydrophobic surface in favour of providing a steric repulsion in the absence of electrostatic stabilization.

3.3.2 The impact of the grafted hydrophilic chain on the emulsion stabilizing capacity of a protein fragment

From the above discussions in the previous section, it is clearly noted that the polypeptides obtained by the action of enzyme can exhibit various differing colloidal and interfacial behaviours. Unless by some fortunate production of diblock-like protein fragments, most of the generated polypeptides are not able to convey a very good emulsion stabilizing capacity in the absence of electrostatic stabilization (i.e. when the environmental pH is close to pI of a protein fragment). This situation will be totally modified, following covalent bonding of a hydrophilic chain to the protein fragment.

Figure 3.6 presents the density profiles of the conjugated polymers adsorbed onto an isolated droplet, plotted as a function of the distance perpendicular to the droplet surface. The results are produced for the three polypeptides that were previously showed not to have good colloidal stabilizing capacity (i.e. Met³²²-Lys³⁵⁵, Asn³⁵⁶-Arg⁴²⁵ and Glu⁹³-Arg³⁰²). These polypeptides are modified by attaching a hydrophilic chain of size 60 monomer units (i.e. maltodextrin DE 16.5-19.5 with $L = 60 a_0$) to the N -terminus end of each polypeptide. This is to minimize the influence coming from the position of hydrophilic attachment on the colloidal stabilizing performance of the polymer, as previously reported by Akinshina et al. (2008).

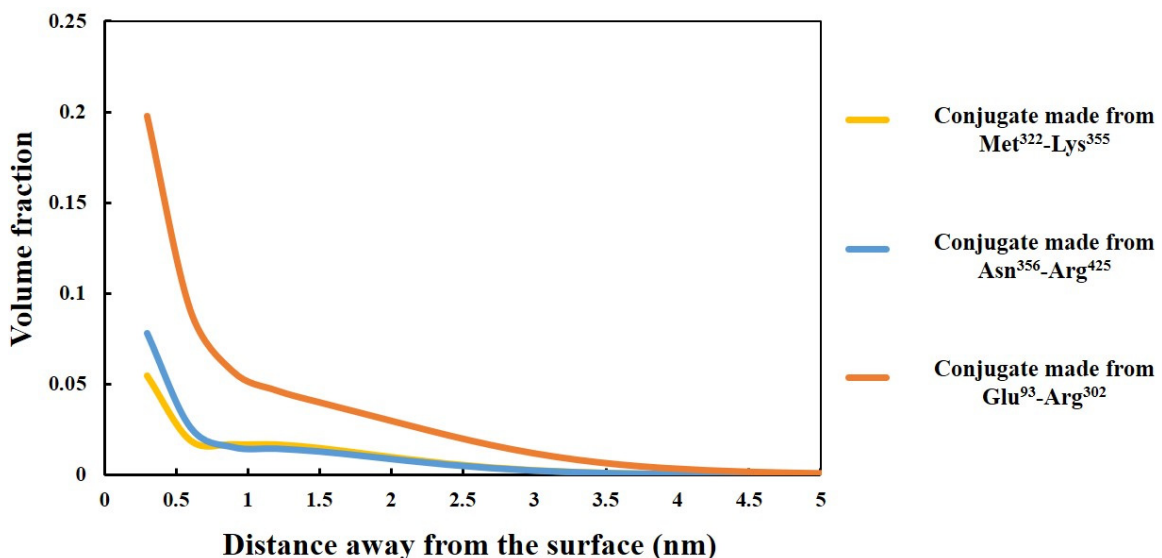


Figure 3.6 Density profiles of the conjugated polymers made from three polypeptides (i.e. Met³²²-Lys³⁵⁵, Asn³⁵⁶-Arg⁴²⁵ and Glu⁹³-Arg³⁰²), respectively bonded with a hydrophilic chain ($L = 60 a_0$), adsorbed at an isolated droplet, plotted against the distance away from the hydrophobic surface. The results are produced at a background electrolyte volume fraction of 0.001 and at pH = 5.5.

From this plot, the interfacial structure of the adsorbed polymers was examined. It is seen in **Figure 3.6** that there is a distinct modification to the structure of the interfacial layer formed by a conjugated polypeptide, when compared to that formed by its unbonded counterpart. The polypeptides with a hydrophilic attachment develop a far more extended 'two-layer like' structure around the oil droplet. The inner layer mainly consists of the protein moieties which strongly anchor at the hydrophobic surface. While the second outer layer is predominantly formed with the polysaccharide chains which protrude out into the aqueous phase. This feature is most obviously seen for conjugates made from the two shorter peptides (i.e. Met³²²-Lys³⁵⁵ and Asn³⁵⁶-Arg⁴²⁵). For both cases, the thickness of the interfacial film increases to roughly 3 nm, in comparison to the thin layer (~ 1 nm) formed by the corresponding unmodified polypeptides (see **Figure 3.4**).

The most crucial advantage due to the hydrophilic attachment is the modification of the interaction potential mediated between two approaching droplets (compare **Figure 3.2** and **Figure 3.7**). Recall from **Figure 3.2** that the three non-bonded polypeptides (i.e. Met³²²-Lys³⁵⁵, Asn³⁵⁶-Arg⁴²⁵ and Glu⁹³-Arg³⁰²) have induced a strong attraction between droplets coated by them. Their corresponding conjugates, in contrast, are observed to only generate a small energy well (see **Figure 3.7**). If the two droplets coated by the conjugated polymers were to come even closer to a distance where the overlap of adsorbed layers starts to occur (~ 3.0 nm for conjugates made from peptides Met³²²-Lys³⁵⁵ and Asn³⁵⁶-Arg⁴²⁵, and ~ 4.0 nm for conjugate made from peptide Glu⁹³-Arg³⁰², see **Figure 3.6**), the interaction potential becomes steeply repulsive. Moreover, as the energy well is relatively shallow (only around $-4 \sim -6 k_B T$ for all the three cases), being of the same order of magnitude as the kinetic energy of droplets, it can readily be overcome by the droplets via Brownian motion (Ettelaie et al., 2014, Dickinson, 1992a). Under such circumstance, the emulsion droplets are likely to maintain well dispersed (or form very weak flocs that are easy to redisperse by a modest shear force).

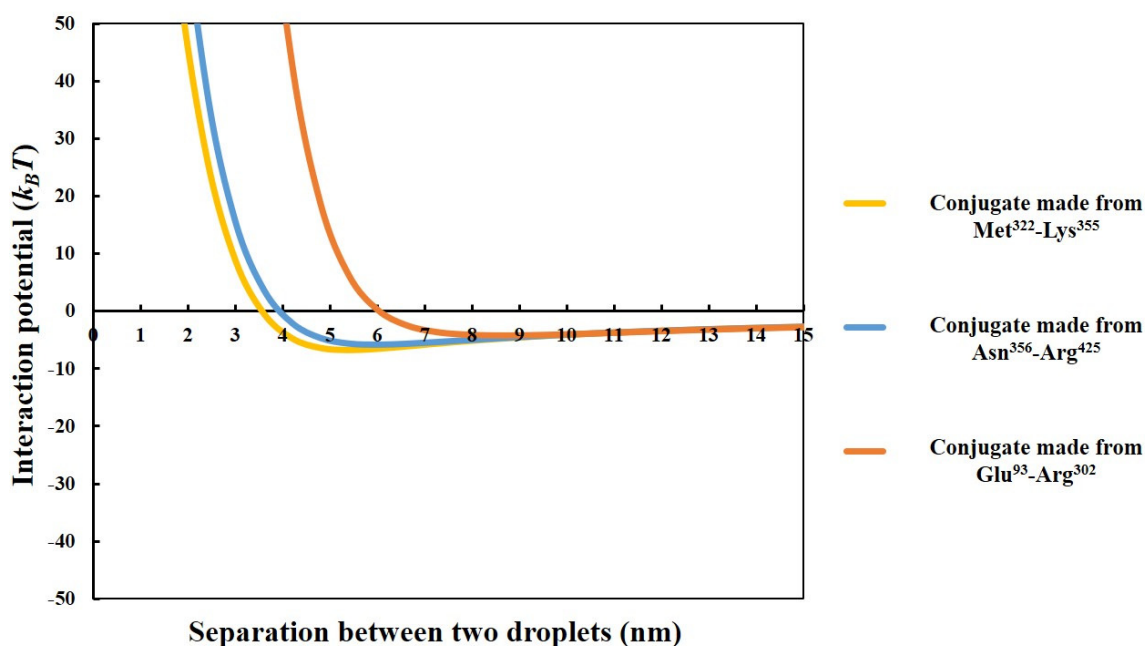


Figure 3.7 The interaction potential, plotted against the inter-droplet separation distance, resulting from the adsorbed layers of the conjugates made from three polypeptides (i.e. Met³²²-Lys³⁵⁵, Asn³⁵⁶-Arg⁴²⁵ and Glu⁹³-Arg³⁰²), respectively bonded with a hydrophilic chain ($L = 60 a_0$). The diameter of oil droplets is 1 μm . The results are produced at a background electrolyte volume fraction of 0.001 and at pH = 5.5.

It is also worth noting from **Figure 3.7** that the conjugate made from a larger polypeptide induces a profile of interaction potential with a comparable shape and magnitude to that mediated by the conjugate derived from a smaller peptide. For instance, the conjugates made from the small peptide Met³²²-Lys³⁵⁵ are seen to lead to an inter-droplet potential profile of almost the same strength as the conjugates fabricated from the larger peptide Asn³⁵⁶-Arg⁴²⁵. Similarly, for the largest polypeptide considered here, Glu⁹³-Arg³⁰² (consisting of 210 amino acid residues), though it is approximately six times larger than the smallest polypeptide Met³²²-Lys³⁵⁵ (made up of 34 residues), the depths of the energy wells for both cases ($\sim -4 k_B T$ for the former and $\sim -6 k_B T$ for the latter) are also not that different. These results indicate that as long as the conjugated polymers have the surface affinity to achieve a sufficient level of surface coverage, the O/W emulsions fabricated by them will exhibit similar level of colloidal stability, irrespective of the huge differences in the molecular size, degree of

hydrophobicity and the adopted conformation of the polypeptide components that the hybrid polymers form from.

In contrast to the above results, the molecular size of polysaccharide attachment is found to have a significantly larger impact on the stabilizing ability of the hybrid conjugated polymers. In **Figure 3.8**, the variation of the inter-droplet potentials, induced by the conjugated emulsifier formed from the protein fragment Asn³⁵⁶-Arg⁴²⁵ and a hydrophilic chain of various lengths ($L = 30, 60$ and $180 a_0$), is plotted. Recall from **Figure 3.2** that the droplets stabilized by non-bonded polypeptides Asn³⁵⁶-Arg⁴²⁵ are subjected to severe flocculation as a result of a net strong attractive force, while the same polypeptides, when modified by covalently attaching a short hydrophilic chain ($L = 30 a_0$), start to produce an increasing repulsive force at close inter-droplet separations less than 3.0 nm (see **Figure 3.8**). Unfortunately, the potential well (the depth of which is $\sim -11 k_B T$) formed prior to the energy barrier, is deep enough to trap an appreciable amount of droplets, forming flocs. Doubling the size of the hydrophilic chain (to $L = 60 a_0$) reduces the energy well to a more acceptable depth of $\sim -6 k_B T$. When the polypeptides are bonded with an even larger chain $L = 180 a_0$, which is six times the size of the short chain $L = 30 a_0$, there is hardly any perceptible energy well produced between droplets stabilized by them. Moreover, the inter-droplet repulsion now starts to come into operation from a significantly larger inter-droplet separation distance (~ 11 nm).

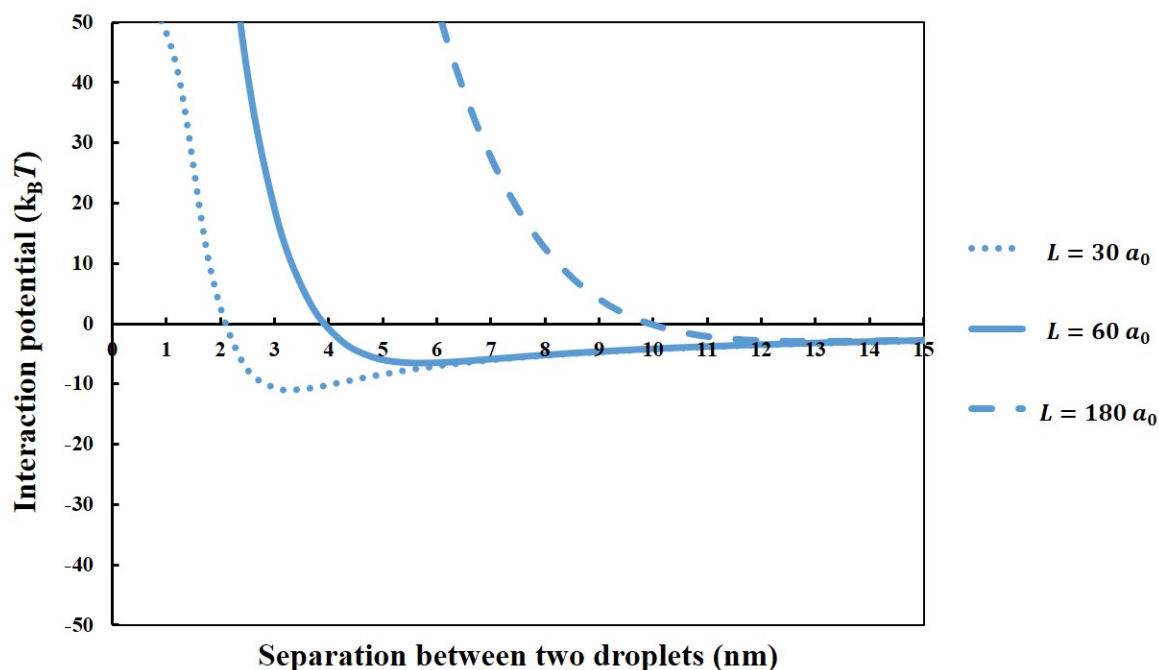


Figure 3.8 The interaction potential, induced by the conjugate made from polypeptide Asn³⁵⁶-Arg⁴²⁵ and a hydrophilic chain of various lengths ($L = 30, 60$ and $180 a_0$), between two oil droplets (diameter $1 \mu\text{m}$), plotted against the separation distance. The results are produced at a background electrolyte volume fraction of 0.001 and at $\text{pH} = 5.5$.

The results in this section suggest that in comparison to the size of the polypeptide, the length of the grafted hydrophilic attachment plays a much more crucial role in modulating the interactions between emulsion droplets and thus the emulsion stability against droplet flocculation. A dramatic improvement to the stability of the colloidal system is associated with the size of the grafted polysaccharide chain. The two approaching droplets coated by conjugated polymer with a short hydrophilic chain (i.e. $L = 30 a_0$), will probably undergo some extent of flocculation (see **Figure 3.8**). While the adsorbed polypeptide bonded with a larger hydrophilic chain (i.e. $L = 60 a_0$ or $180 a_0$) will prevent any droplet flocculation from happening (see **Figure 3.8**). The main job of the protein moiety in a conjugated polymer is to serve as an anchor, so as to entice the whole hybrid molecule to adsorb strongly onto the hydrophobic surface. On the other hand, it is the attached polysaccharide chain that fulfils the role of providing the steric stabilization necessary for achieving a well dispersed stable emulsion system.

3.4 General Conclusions

In this chapter, the colloidal stabilizing behaviours of various protein fragments, and how these are altered following covalently bonding with a polysaccharide attachment were examined. The investigations were done through a theoretical approach of the self-consistent field (SCF) calculations to look at the inter-droplet interaction potentials mediated by adsorbed polymers, as well as to examine the configuration and density profile of the adsorbed chains in the interfacial films.

For the polypeptides to provide a good level of colloidal stabilization, they are required to firstly adsorb sufficiently in order to fully cover the droplet surface. To meet this criterion, it is widely believed that it is essential for a polypeptide to have a sufficient degree of hydrophobicity (i.e. the proportion of hydrophobic groups), and desirable polypeptides are considered to be selected based on their hydrophobicity. However, this theoretical study highlights the significant importance of the molecular size of a polypeptide (over other characteristics, such as hydrophobicity) to its colloidal performance. It is demonstrated that small protein fragments are not suitable emulsifiers, as they fail to establish a sufficient level of adsorption, despite some having a high percentage of hydrophobic residues. This is probably due to the inadequate total binding energy for the whole molecule. According to our theoretical results, for the selection of desirable protein fragments, it would be more advantageous to base on the molecular size, rather than the degree of hydrophobicity of a polypeptide. The former approach is also more feasible than the latter in real practice.

In a mixture of protein fragments obtained by the action of a hydrolytic enzyme, various types of polypeptides are released. Nonetheless, a mixture of hydrolysates with a lower level of fragmentation will always have a greater number of larger-sized polypeptides than that obtained at a higher level of fragmentation. In this respect, the degree of hydrolysis (DH) can be used as a single reliable parameter to control the emulsifying and emulsion stabilizing ability of the protein hydrolysates. In the next two chapters, we shall examine experimentally how the colloidal behaviour of protein materials is altered when different levels of hydrolysis are applied.

For those polypeptides which are able to adsorb strongly at the droplet surface, they will have to possess a diblock-like interfacial structure as they become adsorbed at the droplet surface, in order to provide a good level of steric stabilization to colloidal systems. Otherwise, they will fail to protect emulsion droplets from severe flocculation in the absence of electrostatic repulsion (like when the environmental pH is close to the pI of a peptide). Such a situation can be totally modified by covalently grafting a polysaccharide chain (of sufficient length) to the protein fragment. These conjugated polypeptides display comparably good emulsion stabilizing performances against droplet flocculation, regardless of the large differences in the molecular size, degree of hydrophobicity and the adopted configurations at the interface of the original polypeptides. Hydrolysis of a protein, followed by conjugation of obtained peptides with a polysaccharide, in reality, leads to various different species. These above theoretical results indicate that the competitive adsorption between small and large conjugated polymers at the droplet surface (either during the emulsification or the storage of emulsion sample), is not supposed to make a significant difference with regard to the flocculation stability of the emulsion system.

Chapter 4 Characteristics and Functional Properties of Modified Whey Protein as Food Emulsifiers at Various pH Conditions

4.1 Introduction

Whey protein isolate (WPI) is one of the most extensively studied model proteins. Conjugated whey proteins with various polysaccharides have been reported to deliver good emulsifying and stabilizing abilities. Given the excellent emulsifying power of whey protein materials, normally it is not worthwhile to use the hydrolysed form of WPI as emulsifying agents, either conjugated or otherwise. Despite this, whey protein was fragmented in this study. This was to see if the conjugates made from the protein fragments could also replicate the known success of conjugated milk based proteins in stabilizing O/W emulsion at various pH conditions (Akhtar et al., 2007, Ding et al., 2017, Kato et al., 1992). This pH range includes the *pI* of the original unmodified protein, where major emulsifying functionalities of the protein itself are minimized due to the loss of charge and solubility. More importantly, the studies on WPI materials in this chapter provide us with a baseline to compare with the performance of vegetable protein based emulsifiers, undergoing exactly the same procedures (as will be described in the next chapter).

The current chapter presents and discusses the results obtained for the characteristics and emulsifying/stabilizing behaviours of the intact WPI and fragmented WPI which are produced by two enzymes with distinct levels of specificity (i.e. trypsin and alcalase). These results are then compared to those observed for their conjugated counterparts made through reaction with maltodextrin. The results presented in this chapter will be used to make comparisons with results obtained for soy protein materials in the next chapter. The aim is that these comparisons will aid better and clearer interpretations of the properties of both whey protein (milk based) and soy protein (plant based) materials.

4.2 Materials and Methods

4.2.1 Materials

The commercial isolated whey protein (WPI) was obtained from Davisco Foods International (USA). The WPI has a protein content of at least 95% (w/w) with a composition of 74% β -lactoglobulin (β -LG), 20% α -lactalbumin (α -LA) and 6% bovine serum albumin (BSA), as provided by the supplier. Porcine trypsin (T7409) in the form of lyophilized powder, and Alcalase 2.4L (from *Bacillus licheniformis*) in the form of aqueous solution, as well as all the other chemicals were purchased from Sigma-Aldrich. The materials required for electrophoresis analysis were all purchased from ThermoFisher Scientific Co. (USA), which included the pre-casted gel sheets, sample buffer, running buffer and molecular weight ladder. The deionised water from a Milli-Q water system (Millipore Co., USA) was used in all the experiments, including preparations of samples, buffers and reagents.

4.2.2 Hydrolysis of WPI by trypsin and alcalase

2.5% (w/v) 100 mL WPI solution was prepared by dissolving WPI powder in deionised water for 2 h with gentle stirring. The solution was then allowed to hydrate overnight at 4°C. For hydrolysis by trypsin, the protein solution was preheated to 37°C by incubation in a 37°C water bath for 20 min with gentle stirring. Then the pH of the solution was adjusted to 8.5 with 1 M NaOH. According to preliminary tests, trypsin was added at enzyme-to-substrate (E/S) ratios (w/w) of 1/300, 1/150 and 1/80 to achieve three different degrees of hydrolysis (i.e. DH = 2.5%, 5.5%, 8.0%), obtained within approximately 2 h. In the case of alcalase, the WPI solution was preheated to 50°C by incubation in a 50°C water bath for 20 min with gentle stirring. Then the pH of the solution was adjusted to 8.5 with 1 M NaOH. Different amounts of alcalase solution (i.e. 2.5, 4.5 and 7.5 μ L/100 mL protein solution) were added respectively, again to provide different levels of hydrolysis.

For each case, protein was hydrolysed under constant temperature and pH, controlled by a water bath and Metrohm 902 Titrand system (Metrohm Co., USA). The DH was monitored by pH-stat method according to section 2.3.1.

When the desired DH (i.e. 2.5%, 5.5%, 8.0%) was reached, the enzyme activity was immediately stopped by diluting the protein solution to 1.0% (w/v) with 4°C deionized water and incubating in an ice bath with gentle stirring for 0.5 h. The protein hydrolysates were then freeze dried over a period of 48 h. A moderate heating

treatment (80°C, 5 min) was applied to the freeze-dried samples, in order to ensure the complete inactivation of enzyme activity.

Whey protein hydrolysates (WPHs) produced by trypsin and alcalase digestion at different values of DH (i.e. 2.5%, 5.5%, 8.0%) were labelled as WT1, WT2, WT3 and WA1, WA2, WA3, respectively.

4.2.3 Preparation of protein-polysaccharide conjugates

The Maillard reaction products (MRPs) were prepared by dry heating according to Xu et al. (2009), Akhtar et al. (2007). First, maltodextrin DE16.5-19.5 (MD, $M_w = 8.7$ kDa) in the powder form was added to a 1.0% (w/v) solution of WPI and hydrolysed WPI (WPHs) with different DH, as fragmented by either trypsin (WT1, WT2, WT3) or alcalase (WA1, WA2, WA3). The ratio of the added maltodextrin (MD) to protein/polypeptides was 2:1 by weight. The protein/polypeptides + maltodextrin mixture solution was stirred for 1 h at room temperature, and the pH was adjusted to 7.5 with 1 M HCl, before being subjected to freeze drying process for 48 h. Freeze-dried samples were placed in a desiccator with saturated NaCl solution to control the relative humidity. Then the desiccator was either incubated at 90°C for 3 h, or at 60°C for 24 h, allowing the investigation of whether these two commonly used heating practices would result in any differences regarding the emulsifying and stabilizing properties of the produced conjugates.

The Maillard reaction products (MRPs) are denoted in here starting with the type of the protein/polypeptides, followed by polysaccharide. For example, the MRPs made from WT1 and maltodextrin DE16.5-19.5 is marked and referred to as WT1-MD throughout the study.

4.2.4 Electrophoresis analysis

SDS-PAGE was performed under reduced conditions on pre-casted Bolt™ Bis-Tris Plus Mini Gel 4-12%. According to the instructions from the supplier (ThermoFisher Scientific Co., USA), 65 µL of each tested sample (containing 0.15% of protein) was thoroughly mixed with 25 µL Bolt™ LDS sample buffer and 10 µL 0.5 M dithiothreitol (DTT). The resulting solution was then heated in a 70°C water bath for 10 min. A running buffer (1× Bolt™ MES SDS) was added into the chamber. Then 20 µL of each

heated sample solution was loaded per lane. An unstained broad-range protein ladder (2.5 ~ 200 kDa) was used to estimate the molecular weight of the protein materials in the samples. The electrophoresis was carried out at a constant voltage of 200 V for 22 min. The gel sheet was stained for protein by Coomassie brilliant blue for 2 h, and was then destained with deionised water until the background colour was largely washed off and the protein bands were sufficiently clear.

4.2.5 Protein solubility

The soluble protein content was determined by Biuret assay (see section 2.3.3). The Biuret reagent was prepared according to the previous literature (Gornall et al., 1949, Kim et al., 1990). 1.5 g cupric sulphate ($\text{CuSO}_4 \cdot 5\text{H}_2\text{O}$) and 6.0 g sodium potassium tartrate ($\text{NaKC}_4\text{H}_4\text{O}_6 \cdot 4\text{H}_2\text{O}$) are weighed and made totally dissolved in about 500 mL deionised water. The mixture is transferred to a 1 L volumetric flask. Then 300 mL of 10% (w/v) NaOH solution is added to it. The mixture solution is made to volume (exactly 1 L) with deionised water and then is well mixed before use. For long-term storage, the Biuret reagent should be kept in a plastic bottle and away from light. The reagent must be discarded, if there are any black or reddish precipitates in it.

Tested protein/polypeptide samples were prepared at a protein/polypeptide concentration of 1.0% (w/v) and adjusted to five different pH conditions (pH 7.5, 6.0, 4.5, 3.0 and 2.0) with 1 M NaOH or HCl. Then the samples were centrifuged at 12,000 g for 15 min. A volume of 200 μL supernatant was incubated with 1 mL Biuret reagent for 1 h at room temperature. The absorbance was read at 540 nm using a spectrophotometer UV-2600 (Shimadzu, Japan). In order to convert the absorbance into protein content (g/L), a standard curve was produced using bovine serum albumin (BSA) as a reference protein (see Appendix III).

4.2.6 Determination of sulfhydryl content

The sulfhydryl (-SH) content of the intact and hydrolysed proteins, as well as their corresponding MRPs, was determined. Sample was dissolved in Tris-Glycine buffer (0.086 M Tris, 0.090 M Glycine, 4 mM Na_2EDTA) at a protein/polypeptide content of 3 mg/ml with gentle mixing for 2 h. Then 0.2 mL Ellman's reagent (4 mg DTNB /mL buffer) was added rapidly to 4 mL of the sample. The resulting mixture was then

allowed to stand for 5 min at 20°C, before centrifuged at 12,000 g for 10 min. The absorbance of the supernatant was read at 412 nm. A reagent blank (i.e. 0.2 mL Ellman's reagent mixed with 4 mL deionised water) and a protein blank (i.e. 0.2 mL deionised water mixed with 4 mL sample) were prepared for each sample for correction. The absorbance was then converted into free -SH content C_{SH} (mol/g protein) based on the principles explained in the section 2.3.4.

4.2.7 Preparation of emulsions

1.0% (w/v, based on protein content) unconjugated and conjugated protein samples were prepared in deionised water and mixed for 2 h and then left for hydration overnight at 4°C. Sodium azide (0.02%) was added to prevent microbial activity. Then the pH of the sample was adjusted to 7.5 with 1 M NaOH. An oil-in-water emulsion (10 vol.% sunflower oil) was prepared in two steps, by a first pre-homogenization (12,000 rpm, 5 min) followed by two passes through Leeds Jet homogenizer at 300 bar (Akhtar et al., 2003, Dickinson et al., 1988b). The pH of the freshly made emulsions was then adjusted to various desired values (pH 7.5, 4.5, and 3.0) with 1 M NaOH or HCl. The emulsion samples were stored at 4°C for further investigations.

4.2.8 Storage stability of emulsions at different pH conditions

The stability of emulsions was assessed according to different measures. These included the mean droplet size $D_{4,3}$ and the size distribution of emulsions, both obtained by a Mastersizer 3000 analyser (Malvern, UK), the rheological flow properties of emulsions measured using a Kinexus Ultra rheometer (Malvern, UK), the ζ -potential of the emulsion droplets using a Nano ZS Zetasizer (Malvern, UK) and the emulsion microstructure by optical microscopy. The assessments were performed at various stages during the storage period.

More specifically, in the measure of emulsion droplet size, the refractive indices used for oil and aqueous phase were 1.47 and 1.33, respectively. The optical absorption parameter was set at 0.01. The rheological behaviour was conducted using a double gap cylinder geometry (DG25), as described in section 2.3.7. The emulsion sample was gently mixed before loading into a temperature-controlled cell. The temperature was allowed to equilibrate at 25°C for 20 min prior to any measurements. The viscosity

of an emulsion was measured at shear rates ranging from 1 to 100 s⁻¹, using the continuous shear mode of operation for the rheometer. The ζ -potential of the emulsion droplets was determined at different pH conditions, by diluting the emulsion sample 200 times (i.e. 10 μ L emulsion sample in 1.99 mL buffer) with the corresponding buffering system that has the same pH as the tested sample and a low background electrolyte concentration of 20 mM. The recipe for these buffering systems is provided in Appendix IV.

4.2.9 Statistical analysis

All the measurements were performed in triplicate. The obtained data were averaged and reported as a mean value in each case. The error bars were added as standard deviations. All the calculations were analysed by Microsoft Excel 2016.

4.3 Results and Discussions

In this section we shall focus on the data obtained for proteins that were conjugated with polysaccharides at 90°C for 3 h. The results obtained for these conjugated biopolymers are compared with those for the unconjugated equivalents. No significant differences in respect of the functional properties were found between conjugates made at 90°C for 3 h and those produced at 60°C for 24 h, except for a slightly lower level of solubility for the latter. Therefore, unless specifically stated, the discussions concerning the conjugates formed at 90°C for 3 h are understood to largely apply to those made at 60°C for 24 h.

4.3.1 Molecular weight profiles

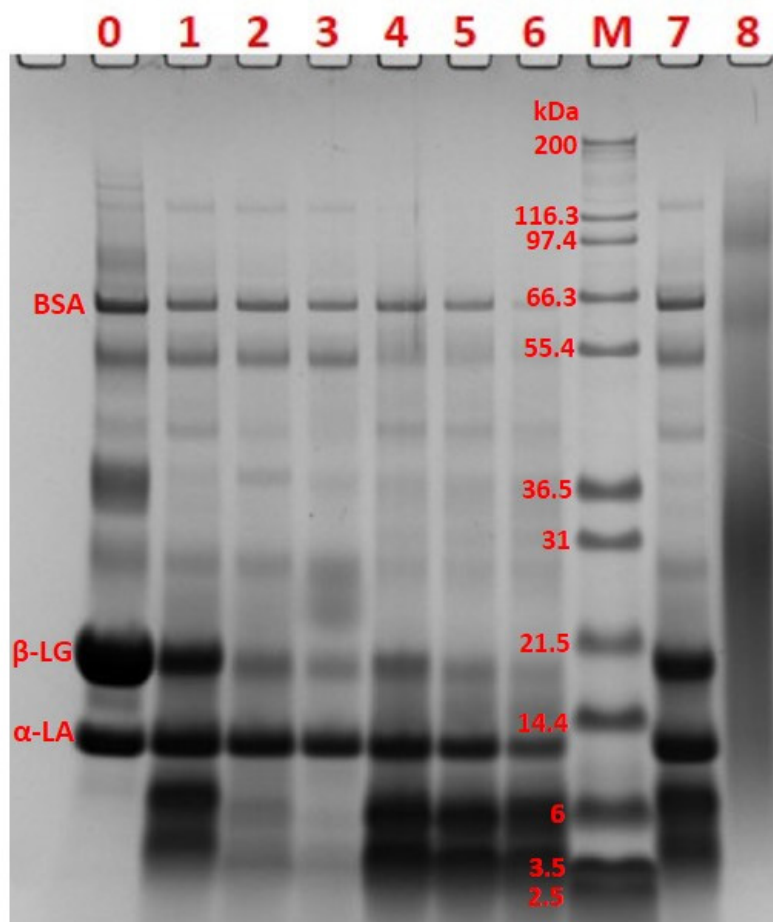


Figure 4.1 Reducing SDS-PAGE analysis of the protein/peptide profiles for various whey protein samples. Lane 0 is intact WPI. Lane 1-3 are polypeptides produced by trypsin digestion at increasing DH (i.e. WT1 at 2.5%, WT2 at 5.5% and WT3 at 8.0%, respectively). Lane 4-6 are polypeptides produced by alcalase digestion, from lower to higher DH (i.e. WA1 at 2.5%, WA2 at 5.5% and WA3 at 8.0%, respectively). Lane M is the molecular weight ladder (with values presented in the unit of kDa). A sample post conjugation with maltodextrin (i.e. WT1-MD) is also shown at lane 8 to compare with its unconjugated counterpart (i.e. WT1) at lane 7.

The peptide profiles of whey protein digested by trypsin and alcalase were analysed by reducing SDS-PAGE and were displayed in **Figure 4.1**. The major components of intact WPI, i.e. β -LG, α -LA and BSA, were marked on the gel sheet as reference (lane 0). The component α -LA showed more resistance to enzymatic attack than β -LG, which has also been reported to be the case by Cheison et al. (2011). It is clearly seen that trypsin and alcalase generated polypeptides with distinct profiles. Trypsin is found to gradually break whey protein down. This is seen as a shift of bands towards lower molecular weight range with increasing DH (lane 1-3). As for alcalase, the profiles of

hydrolysates (lane 4-6) did not show a distinct difference with increasing DH beyond 2.5%. Moreover, under SDS-PAGE reducing conditions, all the associations between peptides are broken (including disulphide bonds and hydrophobic interactions). A large number of small peptides, less than 2.5 kDa, would have also been expected to be released. However, these would be too small to show up on the gel sheet used here and therefore were not detected.

The contrasting sets of polypeptide profiles obtained by trypsin and alcalase digestion indicate that compared to the enzymes having a broader range of amino acid substrates (e.g. alcalase), the ones with a higher selectivity (e.g. trypsin in our case) seem to be more effective in breaking up the protein structure, thus causing a significant change to the distribution of polypeptides released. The influence of the actions of trypsin and alcalase on the properties of obtained peptides is much more pronounced when it comes to soy proteins. We will return to this point and provide more details in the next chapter.

Last but not least, the successful formation of conjugates was confirmed as well. The presented result here is limited to the conjugates formed using WT1, though similar data would be expected for other hydrolysed samples too. In comparison to the equivalent unmodified protein fragments (lane 7), a noticeable shift in molecular weight, towards higher values, was observed for conjugated WT1 (lane 8). This increase in molecular weight is indicative of the formation of covalent bonding of maltodextrin ($M_w = 8.7$ kDa) with the protein fragments.

4.3.2 Solubility

A reasonable level of solubility of protein/peptide is known to be a key requirement for satisfactory functioning of any good molecular (i.e. non-Pickering type) emulsifier (Dickinson, 1992e). It is also crucial when it comes to synthesising the conjugated emulsifier/colloidal stabiliser, as carefully discussed in section 1.2.4. Whether the conjugates are prepared from the dry mixture (e.g. using heat treatment (Akhtar et al., 2007, Wooster et al., 2007)) or in a solution (e.g. enzymatically (Chen et al., 2018a, Liu et al., 2018a)), it is important that the protein and polysaccharide molecules are in intimate contact, distributed homogeneously in the mixture. It is only then that the

Maillard reaction between the two can proceed to an extent that a sufficient number of conjugated emulsifiers are produced.

Additional requirements, such as preventing possible segregative phase separation (Fang et al., 2006, Banta et al., 2018) may also need some consideration, but normally can be avoided if uncharged polysaccharides are used.

Given the importance of the initial solubility of protein materials to the colloidal behaviours as well as to the efficient synthesis of conjugates, it is useful to consider how the solubility of protein fragments differs from their original intact protein, and how this alters with the choice of the enzyme, the degree of hydrolysis (DH) and the covalent attachment of polysaccharide. In this section, we shall present and discuss the results of the solubility measurements, both for hydrolysates prior to and post conjugation with maltodextrin.

4.3.2.1 Solubility of WPI and WPHs samples

Starting with intact WPI as the first example (**Figure 4.2**), the results showed that the protein has the lowest solubility at pH 4.5, which indeed is at its reported *pI* value. At all other pH conditions (i.e. pH 7.5, 6.0, 3.0 and 2.0), WPI exhibited a high level of solubility. The same trend was observed for all the hydrolysed whey protein samples produced under the action of either enzyme (i.e. WT1, WT2, WT3 and WA1, WA2, WA3).

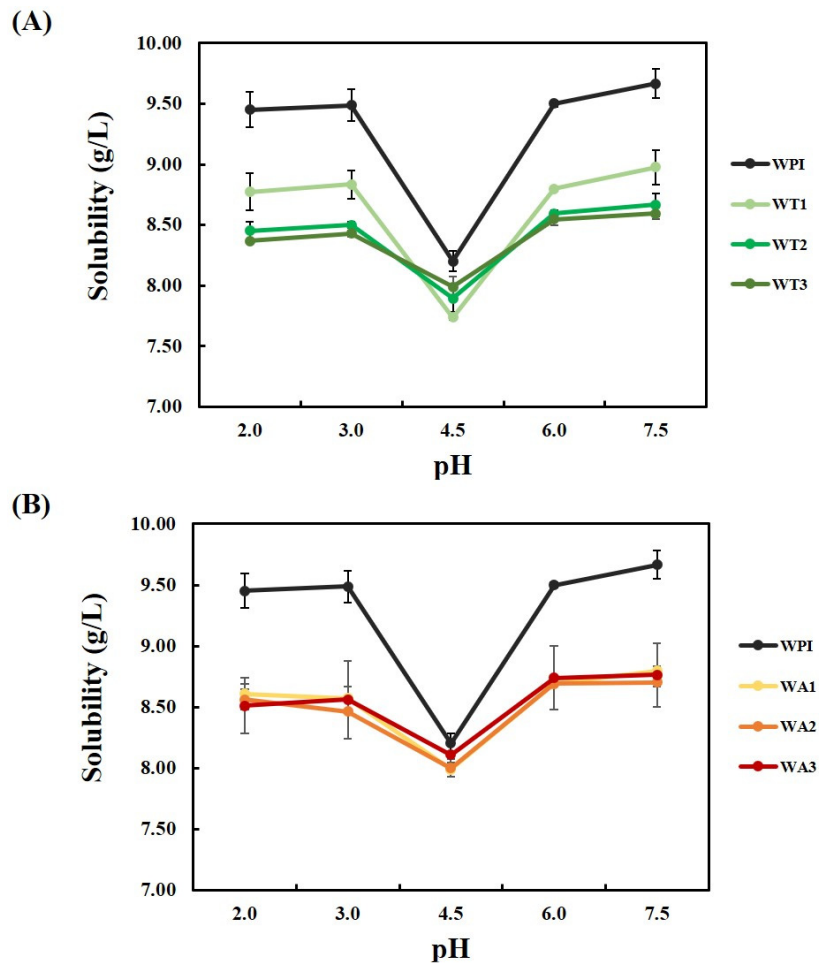


Figure 4.2 The solubility of intact WPI and WPHs samples hydrolysed by trypsin (A) and alcalase (B) at various DH, plotted as a function of pH.

The change in the solubility with pH was also seen visually in **Figure 4.3**. The figure displays the variation of the solubility of 1% (w/v) WT1 solution as a function of pH. A clear solution was obtained at all pH values except at pH 4.5. At pH = 4.5, the fragments aggregated and settled down due to their reduced net surface charge.

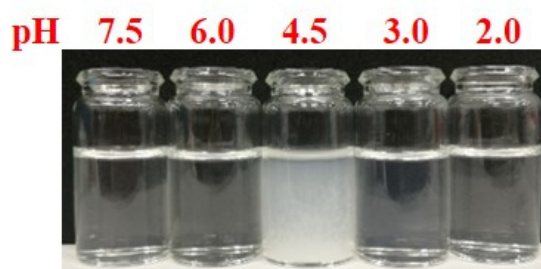


Figure 4.3 The visual appearance of 1% (w/v) WT1 sample solution at various pH conditions.

Our data also showed that a limited hydrolysis of up to DH 8.0%, by either trypsin or alcalase, caused a distinct drop in the solubility when compared to the intact WPI. This decrease was seen at all tested pH conditions (**Figure 4.2**). A likely explanation of this would be that when proteins are only hydrolysed to a limited extent (DH < 20%), the distribution of broken bonds along the protein backbone creates a mixture of polypeptides with various sizes and a range of *pI* values. As a result, each fragment would have a slightly different pH-solubility profile (Ettelaie et al., 2014), not only to other fragments but also to the original intact protein. Thus, at any pH, it is likely that a subset of the fragments is either at, or close to, their respective *pI*. Therefore, at pH conditions where the intact protein already exhibits a good level of solubility, enzyme hydrolysis is likely to serve to reduce the overall solubility. This is what is observed here for whey protein in our case. The same is also reported to be true of casein (Chobert et al., 1988), where once again the solubility of the original protein, at least away from *pI*, happens to be high. Additionally, for whey protein (though not so much for casein) the process of hydrolysis can also cause the exposure of the hydrophobic residues (Chen et al., 2011a, 2011b, Wu et al., 1998, Zhao et al., 2011). These tend to be buried deep within the interior of the globular protein. When exposed, they will probably lead to a reduction of solubility. However, it is also noticed that the solubility of WPHs at *pI* of WPI, though still not quite as good as the original protein, did gradually improve with increasing DH.

4.3.2.2 Solubility of conjugated WPI and WPHs samples

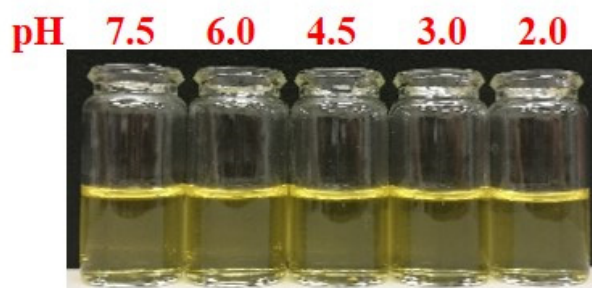


Figure 4.4 The visual appearance of 1% (w/v) WT1-MD sample solution at various pH conditions.

The solubility of WPI and WPHs that were conjugated with maltodextrin (i.e. WPI-MD, WT1-MD, WT2-MD, WT3-MD and WA1-MD, WA2-MD, WA3-MD), obtained via dry-heating Maillard reaction in accordance to the recipe in section 4.2.3, was also examined. These samples showed a golden brown colour which is typical of the characterized compounds formed during Maillard reaction (as have been discussed extensively in section 1.2.2). When dissolved in deionised water, these conjugated protein samples formed a clear golden solution at all tested pH conditions, including pI of WPI, without formation of any visible aggregates. The visual appearance of the solution involving sample WT1-MD was shown in **Figure 4.4**. This improvement in solubility at pI was also quantitatively seen in **Figure 4.5**. For example, the solubility of WT1 post conjugation with maltodextrin increased to 8.2 g/L from 7.7 g/L for unreacted WT1 sample (compare **Figure 4.2** and **Figure 4.5**). The enhanced solubility at pI is attributed to the covalent attachment of maltodextrin, which was confirmed by the increased molecular weight of the hybrid polymer on SDS-PAGE analysis (lane 7 and 8 in **Figure 4.1**).

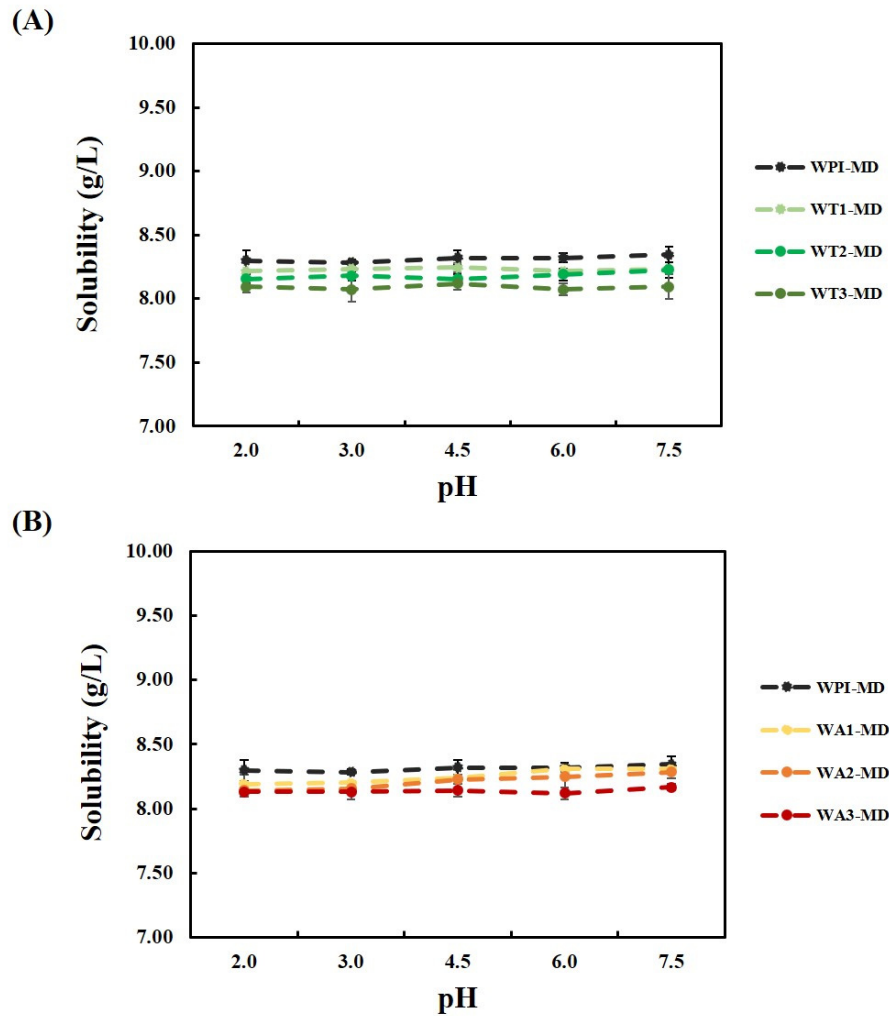


Figure 4.5 The solubility of conjugates made from intact WPI and those from WPHs at various levels of hydrolysis, produced by either trypsin (A) or alcalase (B), plotted as a function of pH.

Nonetheless, at conditions away from pI , a decrease was noticed in the solubility of the conjugates in comparison to non-reacted equivalents (compare **Figure 4.2** and **Figure 4.5**). For instance, the solubility of WT1 at pH conditions other than 4.5 was measured to be around 8.8 g/L, while that of WT1-MD was approximately 8.2 g/L at the corresponding pH conditions.

The exact reason for this decrease in solubility at conditions away from pI is not currently apparent to us. It is suspected to arise from the heat-induced intermolecular aggregation of proteins through the disulphide bond formation, which was demonstrated by the consumption of free -SH groups (**Figure 4.6**), and hydrophobic interactions (Diftis et al., 2006, McClements, 2004, Ren et al., 2009, Dickinson et al., 1992) as occurring during the synthesis of conjugates via dry heating. This point merits further investigation.

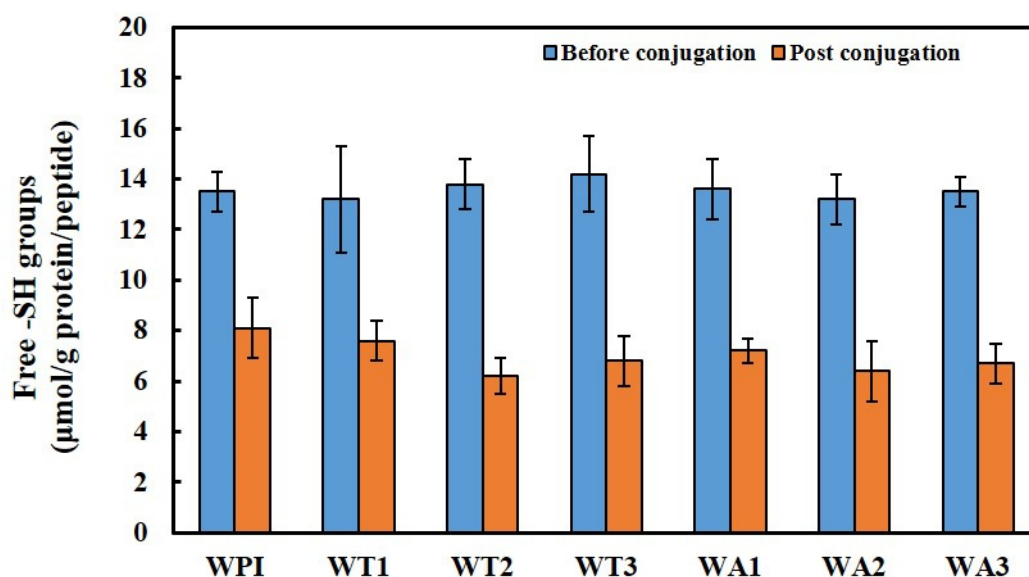


Figure 4.6 Free sulfhydryl (-SH) content of protein and hydrolysates prior to and post dry-heating Maillard reaction.

To summarise then, the solubility of the conjugated WPI and WPHs improved at pH values close to pI of WPI, but decreased at all other pH values further away from pI . Thus, the solubility profiles of conjugated samples generally displayed rather flat lines without any significant changes across the studied pH range (**Figure 4.5**). This is in contrast to the large variation seen in the solubility of unconjugated samples with changing pH (**Figure 4.2**). Despite its observed decrease at pH values away from pI , the solubility of the conjugated WPI and WPHs remained at around 8.2 g/L throughout the entire studied pH range. This is sufficient to meet this particular key requirement for having a good emulsifier.

4.3.3 Morphology and stability of emulsions at different pH conditions

The peptide distribution profile and the solubility, as investigated in the previous sections, focused on some of the key features that could influence the functional properties of a protein material as a suitable emulsifier and colloidal stabiliser. In this section, the results for the storage stability of emulsions under three pH conditions are presented. The microstructure, droplet size and distribution, ζ -potential and flow behaviour between different emulsion samples are compared. We discuss the emulsifying and stabilizing abilities of the modified protein materials, in the light of the observed attributes studied in the last two sections, as well as other possible relevant parameters.

4.3.3.1 Emulsions based on WPI and WPHs samples

At neutral pH conditions, WPI is well known to be able to form fine stable emulsions (Akhtar et al., 2007, Ding et al., 2017), as is also observed here in **Figure 4.7**. The droplet size, $D_{4,3}$, of fresh emulsion stabilized by WPI at pH 7.5 was 0.682 μm , although this increased to 0.833 μm after 60 days.

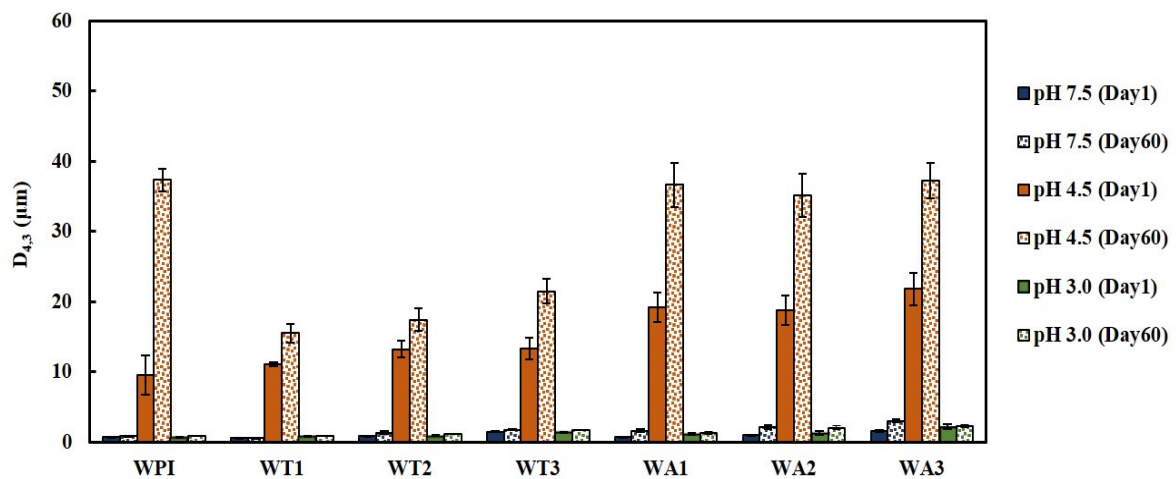


Figure 4.7 The average droplet size $D_{4,3}$ of freshly made and stored (60 days) emulsions, fabricated by intact and hydrolysed whey protein, at various pH conditions (i.e. pH 7.5, 4.5 and 3.0).

The hydrolysis by trypsin at DH 2.5% (WT1) produced fragments with improved emulsifying and stabilizing capacities compared to the intact WPI (**Figure 4.7**). The micrograph of fresh WT1 stabilized emulsion at pH 7.5 (**Figure 4.8A**), showed fine oil droplets ($D_{4,3} = 0.628 \mu\text{m}$) with a monomodal size distribution. The ζ -potential was measured to be around -55.7 mV (**Table 4.1**), indicating the presence of strong electrostatic repulsion between the droplets. The emulsion remained reasonably stable, with $D_{4,3} = 0.656 \mu\text{m}$, even after 60 days (**Figure 4.8B**). However, as WPI was further fragmented to achieve higher DH values of 5.5% and 8.0% (WT2 and WT3), the emulsifying functionality was found to suffer. The droplet sizes at day 1 were $0.837 \mu\text{m}$ and $1.49 \mu\text{m}$ for emulsions made by WT2 and WT3, respectively. These grew to $1.37 \mu\text{m}$ and $1.73 \mu\text{m}$ after 60 days of storage at pH 7.5 (**Figure 4.7**).

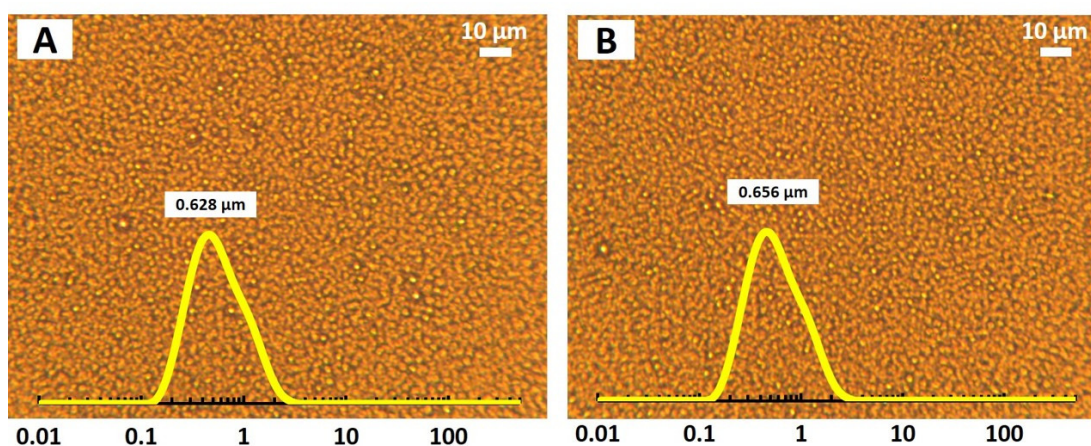


Figure 4.8 Micrographs of WT1 fabricated emulsion, stored at pH 7.5, on day 1 (A) and after 60 days of storage (B). The droplet size distribution and the mean droplet size $D_{4,3}$ are also provided on each photo.

As for fragments produced by alcalase digestion, no improvement was observed. Both the emulsifying and stabilizing properties of WPI worsened from the very onset as a result of hydrolysis. The droplet sizes, $D_{4,3}$ of fresh emulsions made by alcalase generated WPHs at day 1 were $0.713 \mu\text{m}$ (WA1), $1.02 \mu\text{m}$ (WA2) and $1.56 \mu\text{m}$ (WA3), which were noticeably larger than the ones made with the intact WPI ($D_{4,3} = 0.682 \mu\text{m}$). After 60 days of storage, these values increased to $1.65 \mu\text{m}$, $2.16 \mu\text{m}$ and $3.02 \mu\text{m}$ for WA1, WA2 and WA3 stabilized emulsions, respectively. This was to be compared to $0.833 \mu\text{m}$ found for the unmodified WPI at day 60 (**Figure 4.7**). Nonetheless, the possibility of a small improvement at even lower DH values of less

than 2.5% cannot be entirely ruled out. While this point was not investigated further, if observed it will confirm a similar trend as that found for trypsin produced WPHs. That is to say, a modest improvement at low levels of fragmentation is followed by inferior emulsifying and stabilizing properties as the protein is broken down even more.

	pH = 7.5	pH = 4.5	pH = 3.0
Day 1	-55.7 ± 5.0 mV	+11.1 ± 0.6 mV	+45.9 ± 1.5 mV
Day 60	-52.3 ± 5.2 mV	+11.9 ± 0.5 mV	+42.1 ± 2.7 mV

Table 4.1 ζ -potential (mV) of freshly made and stored (for 60 days) emulsion droplets, stabilized by WT1 sample as emulsifiers. Results are shown at different pH conditions.

The above results presented here are found to be consistent with the theoretical findings in the previous chapter. Recall from Chapter 3, it was also demonstrated that the degree of hydrolysis (DH) could serve as a guiding parameter to control the emulsifying and stabilizing abilities of the protein hydrolysates, as it governs the content of large polypeptides present in the obtained mixture of hydrolysates. A lower level of hydrolysis will produce a distribution of fragments with a greater content of larger-sized polypeptides, while extensive hydrolysis will cause fewer such large chains to remain in the system. These large protein fragments, despite only having a much lower percentage of hydrophobic amino acids in their primary structure compared to the small fragments, possess a significantly higher surface affinity and are able to adsorb substantially on the droplet surface. On the other hand, small protein fragments were seen to fail to establish a sufficient level of surface adsorption, attributed to the inadequate total binding energy of the whole molecule. Such being the case, for polypeptides (derived from naturally occurring proteins) to be good emulsifiers, they will need to have the right size. We will continue to investigate the critical size of a protein fragment that enables it to be an effective emulsifier and colloidal stabilizer in Chapter 6.

For those protein fragments that are able to adsorb sufficiently on the interface, they may well be more flexible than the intact globular protein (as long as the fragments are not too small in size), due to their lack of secondary and tertiary structures compared to the latter. They may also be more surface active than the parental

globular protein, because of the exposure of their hydrophobic amino acid residues. Thus, their presence will be beneficial for the emulsification process. However, fragmented proteins are not able to prevent possible colloidal instability (e.g. coalescence) effectively if they are made too small. During the storage of emulsions, some of the small polypeptides may be capable of gradually disturbing and even displacing large adsorbed fragments from the interface (Dickinson, 2011). These latter chains can potentially provide better steric stabilizing ability and form stronger interfacial films (Ipsen et al., 2001, Schröder et al., 2017, Chen et al., 2019). Hence, their displacement from the surface of droplets is not desired and may lead to colloidal instability for droplets stabilised by hydrolysates generated by alcalase or trypsin at higher levels of fragmentation.

The weakening in the stabilising ability, resulting from excessive hydrolysis, seems to be a general feature. It has also been observed in other studies, involving not only whey proteins (Schröder et al., 2017, Tirok et al., 2001) but also casein (Luo et al., 2014), soy proteins (Qi et al., 1997, Chen et al., 2011b, 2011a) and peanut protein (Chen et al., 2018b). The presence of a sufficiently high proportion of peptides > 2~3 kDa is demonstrated to be beneficial for the stability of emulsions (van der Ven et al., 2001, Lee et al., 1987, Schröder et al., 2017).

As seen above, the overall differences between the performances of WPI derived polypeptides produced by trypsin and alcalase, at currently investigated levels of DH, are relatively small. When considering soy protein as opposed to WPI in the next chapter, we shall see that the choice of the enzyme becomes much more critical. Hydrolysates produced by different enzymes exhibit much clearer and more pronounced variation in their colloidal performances.

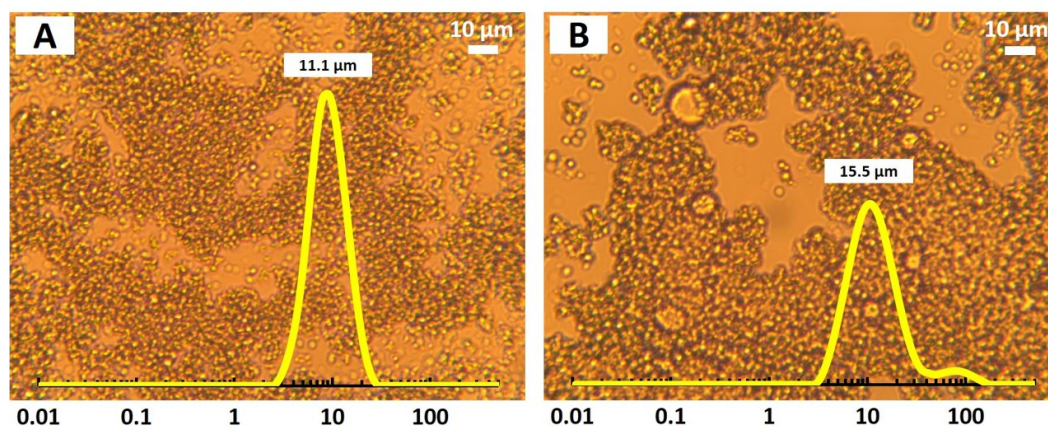


Figure 4.9 Micrographs of WT1 fabricated emulsion, stored at pH 4.5, on day 1 (A) and after 60 days of storage (B). The droplet size distribution and the mean droplet size $D_{4,3}$ are also provided on each photo.

When the pH of the whey protein based emulsions (i.e. those made from the intact WPI or WPHs produced by digestion with trypsin and alcalase) was adjusted to pH 4.5, the originally well dispersed droplets became strongly destabilized. This was illustrated by the dramatic increase in the mean droplet size, as indicated in **Figure 4.7**. For example, the measured $D_{4,3}$ rose from 0.628 μm at pH 7.5 to 11.1 μm at pH 4.5, for fresh WT1 stabilized emulsion. The micrograph of fresh WT1 stabilized emulsion at pH 4.5 displayed the formation of clusters of highly flocculated droplets (**Figure 4.9A**). A significant increase in the low shear viscosity of this emulsion was also observed, compared to that at pH 7.5 (**Figure 4.10**). These are all attributed to the reduced electrostatic stabilization between emulsion droplets (ζ -potential = +11.1 \pm 0.6 mV, see **Table 4.1**).

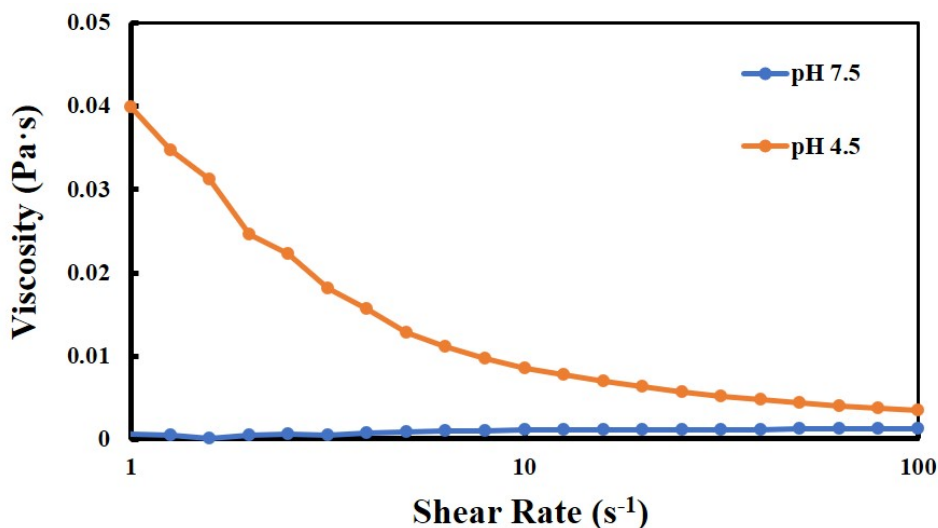


Figure 4.10 Apparent viscosity of the emulsions fabricated by WT1, stored for 1 day at pH 7.5 and pH 4.5, plotted against shear rate.

Recall from Chapter 3, the theoretical results demonstrated that adsorbed protein fragment has to adopt a diblock-like conformation at the interface, which is in favour of providing an enhanced steric repulsion, so as to deliver stabilization to emulsion systems in the absence of electrostatic repulsion. However, the action of enzyme mostly generates polypeptides with various primary structures and differing colloidal and interfacial behaviours. Unless by some fortunate production of diblock-like fragments, most of the generated polypeptides, which take either a flat, triblock- or multiblock-like conformation at the interface, are not able to convey a good emulsion stabilizing capacity under the circumstances where the electrostatic repulsion is largely reduced, thus leading to droplet flocculation. Such situations were seen, from a theoretical perspective, to be totally modified following covalent bonding of a hydrophilic chain to the protein fragment. The performance of the conjugated protein/polysaccharide will be investigated experimentally in the next section.

After 60 days of storage, a few large droplets were observed in the micrograph of WT1 stabilized emulsion stored at pH 4.5 (**Figure 4.9B**). This is the result of expected droplet coalescence following the earlier droplet aggregation (Dickinson, 1992h, Tcholakova et al., 2006). However, it should be noted that the coalescence process here proceeded at a much slower rate, in comparison to the initial rapid droplet aggregation. This is a feature seen in quite a few of the samples studied here, where the loss of colloidal stability following a change in pH was observed.

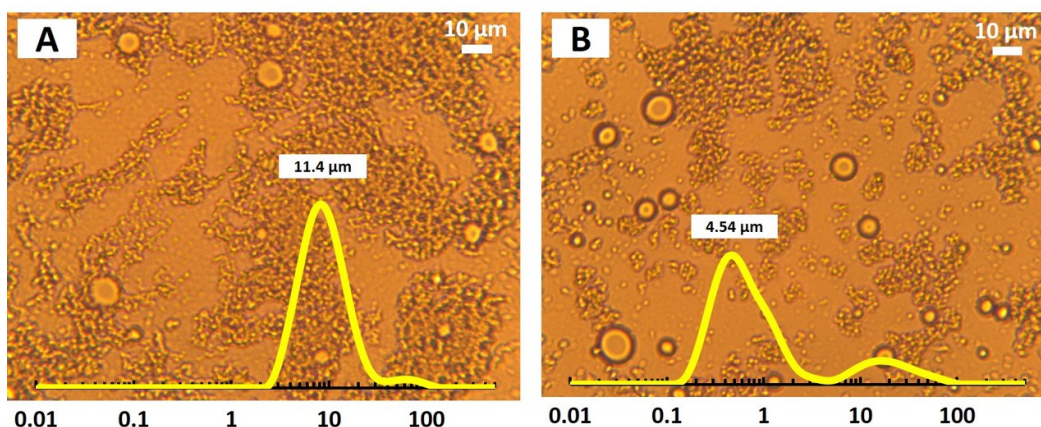


Figure 4.11 Micrographs of WT1 based emulsion stored at pH 4.5 after 60 days. (A) and (B) respectively display the microstructure when this stored emulsion was adjusted to pH 3.0, or when it was diluted in 5% SDS. The droplet size distribution and the mean droplet size $D_{4,3}$ are also provided in each photo.

If the pH was subsequently lowered down to 3.0, reasonably quickly (i.e. within 5 min) following its previous adjustment to pH 4.5, the flocculated droplets were seen to redisperse to a large extent. This observation was true of WPI and all WPHs based samples. It can be seen from the much smaller size measured following such an adjustment of pH, as indicated by the average sizes $D_{4,3}$ at pH = 3.0 and pH = 4.5 presented in **Figure 4.7**. For example, the droplet size $D_{4,3}$ of the WT1 stabilized emulsion dropped down from 11.1 μm at pH 4.5 back to 0.856 μm at pH 3.0. This was attributed to the fact that while the droplets aggregated at pH 4.5, they did not immediately coalesce. Thus, when a sufficient degree of surface charge was regained at pH 3.0 (ζ -potential = $+45.9 \pm 1.5$ mV, see **Table 4.1**), the clusters broke down. The same did not happen if the systems were retained at pH 4.5 for a period longer than a few days, prior to adjustment of pH to 3.0. In this case, flocs of droplets were only slightly dissociated (**Figure 4.11A**), with a relatively small change in the measured size distribution, as the pH was adjusted down to 3.0 (compare **Figure 4.11A** with **Figure 4.9B**). Yet, when the stored emulsion at pH 4.5 was diluted in 5% SDS, a vast majority of the droplet clusters were seen to break up (**Figure 4.11B**). The droplet size distribution following the treatment with SDS indicates that a substantial number of submicron droplets were still present in the system, although of course larger droplets were also clearly visible in the micrograph for the same sample. The overall $D_{4,3}$ was 4.54 μm, as compared to 11.4 μm prior to addition with SDS (**Figure 4.11**). This

indicates that the associations between the flocculated droplets were mainly hydrophobic in origin. These are likely to arise from the conformational rearrangements of adsorbed proteins/peptides on the surface of the droplets, via exposure of their hydrophobic residues during the aging of the emulsions (McClements, 2004, Freer et al., 2004, Kim et al., 2002a, 2002b).

Moreover, when emulsions are stored at pH = 4.5 for long periods (more than a couple of days), the rearrangement and mutual diffusion of the polypeptides between adjacent surface layers might result in the formation of interfacial films shared between neighbouring droplets. Once such layers are formed, switching the electrostatic repulsion back on between the droplets by adjustment of pH, is no longer sufficient to redisperse the emulsion system. On the other hand, the shared layers would not have formed if the storage time (at pH = 4.5) is kept short. Then, as clearly found here, the flocs were able to break up and fall apart as soon as a sufficient level of electrostatic repulsion between the droplets was operational. As an aside, the fact that a large number of small droplets were still present following dilution with SDS, shows that the coalescence kinetic was slow, even in these highly flocculated and sufficiently aged emulsions at pH 4.5.

4.3.3.2 Emulsions based on conjugated WPI and WPHs samples

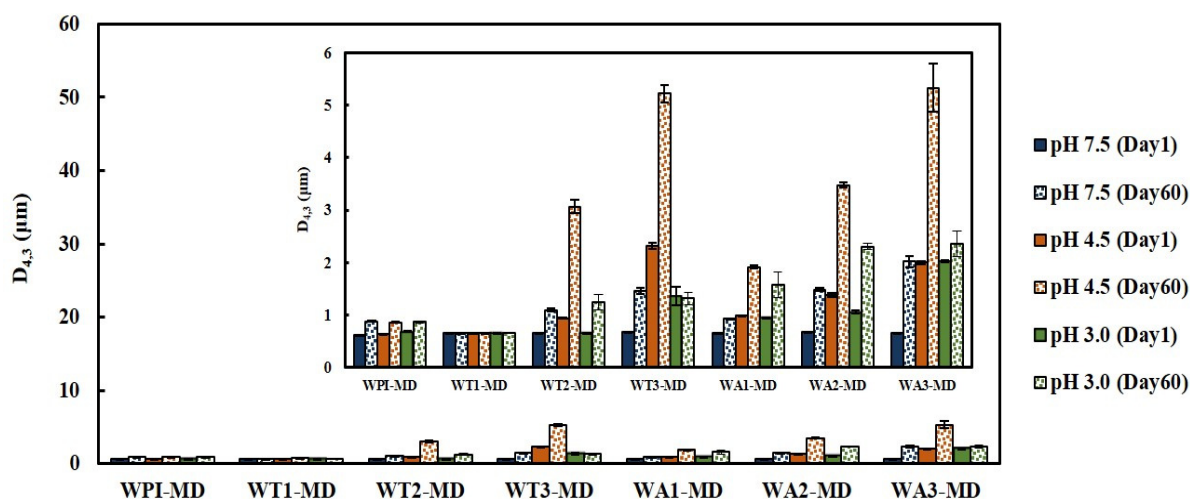


Figure 4.12 The average droplet size $D_{4,3}$ of freshly made and stored (60 days) emulsions, fabricated by conjugates made from WPI/WPHs + maltodextrin, at various pH conditions (i.e. pH 7.5, 4.5 and 3.0). The scale in this graph is kept the same as that in Figure 4.7 for the ease of comparison. However, a more detailed version is also shown in the inset.

When WPI/WPHs were conjugated with maltodextrin, both the emulsifying and stabilizing abilities were enhanced substantially at all tested pH conditions (**Figure 4.12**). The difference was particularly pronounced at pH 4.5 where emulsion droplets stabilised by unconjugated WPI/WPHs became strongly aggregated. For example, unlike the highly flocculated state of WT1 stabilised emulsion at pH 4.5, the conjugated WT1 based emulsion sample stayed well dispersed throughout the whole storage period, with no change in droplet size ($D_{4,3}$ was $0.660 \mu\text{m}$ at day 1 and $0.657 \mu\text{m}$ at day 60, see **Figure 4.13**). Since the ζ -potential measured at pH 4.5 was only $+1 \sim +2$ mV (**Table 4.2**), the excellent stability to flocculation and coalescence for WT1-MD stabilised emulsion is not the result of electrostatic repulsion. It must be due to the strong steric stabilization, operating between the adsorbed layers of conjugated polypeptides.

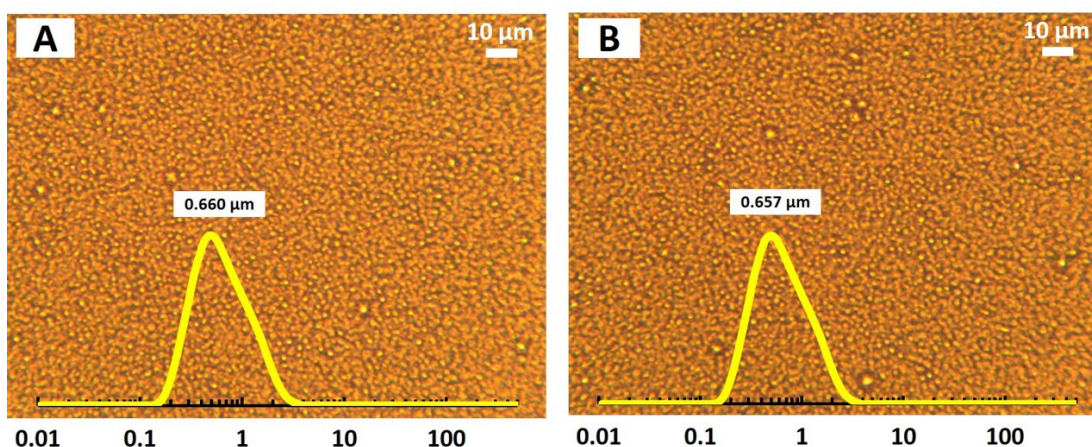


Figure 4.13 Micrographs of WT1-MD fabricated emulsion, stored at pH 4.5, on day 1 (A) and after 60 days of storage (B). The droplet size distribution and the mean droplet size $D_{4,3}$ are also provided on each photo.

The steric stabilization is the result of the excluded volume effect arising from the polysaccharide attachments (Dickinson, 2008, Ettelaie et al., 2017, Ettelaie et al., 2012, Dickinson, 1992e), and will not be significantly altered by the change of background pH or the high concentration of electrolytes. Nonetheless, in order for the steric stabilization to remain sufficiently strong so as to ensure an excellent long-term storage stability of an emulsion, the attached polysaccharide is required to have the right size. As demonstrated theoretically in Chapter 3, short hydrophilic attachments, although starting to produce a steric repulsion between two approaching emulsion

droplets coated by them, still create a relatively deep energy well which is able to trap a sizable amount of droplets and therefore induces some degree of droplet flocculation. Only sufficiently large polysaccharides are able to generate a sufficiently strong energy barrier that builds up before the inter-droplet Van der Waals attractive force dominates. Some experimental work in the literature has evaluated the critical size of a polysaccharide to convey a reasonably good steric stabilization to an emulsion system (Wooster et al., 2006, 2007).

	pH = 7.5	pH = 4.5	pH = 3.0
Day 1	-28.1 ± 2.4 mV	+2.5 ± 0.2 mV	+22.2 ± 1.5 mV
Day 60	-31.1 ± 2.7 mV	+1.8 ± 0.1 mV	+20.9 ± 1.7 mV

Table 4.2 ζ -potential (mV) of freshly made and stored (for 60 days) emulsion droplets, stabilized by WT1-MD sample as emulsifiers. Results are shown at different pH conditions.

It was also suggested that the polysaccharide chain should have an appropriate size so that the hydrophilic-hydrophobic balance of most of the composite polymers continues to favour their adsorption onto the O/W interface (de Oliveira et al., 2016, Oliver et al., 2006, Panyam et al., 1996). As for our study, fragmentation of proteins at the initial stage probably has enabled the exposure of hydrophobic residues in parental globular proteins, as has been reported by many other researchers (Zhang et al., 2012a, Chen et al., 2011a, 2011b, Wu et al., 1998, Zhao et al., 2011). This increased hydrophobicity gets balanced by covalent attachment of hydrophilic chains. This not only renders the hybrid polymers to become more surface active (Zhang et al., 2012a), but also strengthens colloidal stability against flocculation and coalescence due to the large hydrophilic polysaccharide sections of the adsorbed molecules. However, at high DH values, the generated peptides become significantly smaller and less surface active (Zhang et al., 2012a, Chen et al., 2011b, 2011a, Wu et al., 1998, Zhao et al., 2011). When synthesised from such small fragments, the produced conjugated biopolymers may become excessively hydrophilic and lose their interfacial properties (Zhang et al., 2012a, Oliver et al., 2006), particularly considering the much larger size of polysaccharide relative to the small polypeptide part. This will leave the surface of the droplets insufficiently protected.

Moreover, the conjugated protein fragments in our studied systems will inevitably consist of polymers of different sizes, as well as containing both unconjugated peptides and those fragments bonded with polysaccharides. The coexistence of a spectrum of varying polymers will lead to some degree of competitive adsorption occurring both during emulsification and the storage period of emulsion. As shown by the theoretical findings in Chapter 3, competitive adsorption and displacement between conjugated biopolymers are not likely to make a significant difference to the stability of an emulsion system. This is because the length of the grafted hydrophilic attachment was seen much more crucial in manipulating the interactions between dispersed droplets, compared to the size of the polypeptide. Therefore, conjugated polymers (as long as they can achieve a sufficient level of adsorption at the droplet surface) were found to exhibit a similar level of colloidal stabilizing capacity, irrespective of the huge differences in the molecular size, degree of hydrophobicity and the adopted conformation of the polypeptide moieties that the hybrid polymers are made from. As opposed to that, the competition between conjugated fragments and those unconjugated ones would possibly change the emulsion stability. This is particularly true for the emulsion system fabricated using the mixture of protein hydrolysates obtained at higher DH values. In those cases, there will be a lot more small polypeptide chains which will no longer have many suitable amino acid residues (i.e. lysine) to form covalent bonds with polysaccharide. When these small non-bonded fragments are present in the system, they can still adsorb onto the oil-water interface and may displace the more desired large conjugated molecules, therefore are not conducive to provide strong and long-range steric repulsion upon their adsorption, both due to their lack of any attached polysaccharide part as well as their small size and weak ability to form strong interfacial films. This may be another factor in explaining the increase of droplet size in some of our emulsion samples during storage.

According to the above discussions, the destabilization of emulsions is more likely to happen in systems with conjugates produced from the more highly fragmented proteins. This is also what we have observed in our emulsion samples (see **Figure 4.12**). For instance, the mean droplet size $D_{4,3}$ of fresh emulsion made with WT3-MD at pH 7.5 and 4.5 was 0.682 μm and 2.32 μm respectively, but grew to 1.47 μm and 5.22 μm accordingly after the storage period of 60 days. While the emulsion made by

WT1-MD stored at both pH 7.5 and 4.5 kept completely stable during storage ($D_{4,3}$ = 0.661 μm and 0.660 μm for fresh emulsion at pH 7.5 and 4.5 respectively, and 0.658 μm and 0.657 μm accordingly for day 60).

4.4 General Conclusions

This chapter investigated and compared the use of milk whey protein and its hydrolysates, prior to and post conjugation with maltodextrin, as emulsifying agents at various pH conditions. The impacts of the choice of enzyme and degree of hydrolysis on the solubility, molecular weight distribution and emulsifying/stabilizing properties of fragmented whey proteins were discussed.

Whey protein was hydrolysed with two very different enzymes (i.e. trypsin and alcalase). The digestion of protein by either enzyme led to a decrease in the solubility of parental protein at all pH conditions studied. Despite this, both intact whey protein and its various hydrolysates showed similar trends in their solubility-pH profile. They stayed fairly soluble at a wide range of pH conditions, except for at pH 4.5 where they formed visible aggregates. However, the solubility at pH 4.5 was seen to significantly improve by covalent linking of maltodextrin to the protein/polypeptides. The conjugated biopolymers formed clear solution at all the pH conditions (including pH 4.5).

Due to the differences in the cleavable peptide bonds by trypsin and alcalase, these two enzymes produced distinct sets of polypeptides. For those generated by trypsin, there was a gradual shift of bands towards lower molecular weight range with increasing DH. While the profiles of hydrolysates obtained by the action of alcalase did not show a significant difference as hydrolysis proceeded beyond DH 2.5%. These suggested that trypsin is more effective than alcalase with regards to breaking down the structure of globular protein. Despite this, the colloidal stabilizing properties of the resulting fragmented proteins were seen to be broadly similar for corresponding polypeptides generated by these two enzymes. In both cases, a deterioration of the emulsifying and stabilizing properties of protein was observed with increased DH above 2.5%.

When fresh emulsion made at pH 7.5, fabricated using WPI/WPHs as emulsifiers, was adjusted to acidic condition, i.e. pH = 4.5, the emulsion droplets became highly flocculated due to the loss of sufficient electrostatic repulsion. Some of the clustered droplets were seen to have undergone slow coalescence, during the storage period of 60 days. Such situation improved noticeably for all the samples made with whey protein/polypeptides post covalent linkage with maltodextrin. The improvement was particularly significant for the emulsion made from conjugated WT1. This sample maintained the same level of stability at pH 4.5 as was seen at pH 7.5, without any droplet flocculation nor coarsening during storage. The modified emulsion stability is attributed to the strongly enhanced steric stabilization offered by the polysaccharide moiety of the conjugated emulsifier.

In summary, we replicated with fragmented whey proteins the well-known success of (milk derived) protein-polysaccharide conjugates in delivering excellent emulsion stability against flocculation and coalescence, under a wide range of pH conditions. The contrasting polypeptide profiles produced by the two different enzymes, trypsin and alcalase, were also seen. This is a preliminary step towards synthesising a suitable Maillard-type emulsifier based on plant protein (as will be discussed in the next chapter).

Chapter 5 Characteristics and Functional Properties of Modified Soy Protein as Food Emulsifiers at Various pH Conditions

5.1 Introduction

In recent years, the “green” trends in the food industries have motivated a significant level of research interest in achieving completely plant based protein-polysaccharide conjugates. The most popular plant protein being considered for this purpose is isolated soy protein (SPI). Commercial isolated soy protein is the by-product of the soybean oil industry. They are amphiphilic molecules, with a high nutritional value and abundance, therefore are expected to be a suitable source of food emulsifiers, as an alternative to colloidal materials derived from milk. However, they turn out to exhibit poor emulsifying capability compared to milk derived proteins (e.g. casein or whey protein). This is due to the compact globular structure and, more importantly, the insoluble nature of commercial SPI (Dickinson, 2019, Tang, 2017).

Solubility of protein is not only critical in producing fine emulsions, but is also a key in synthesizing suitable covalent complexes with polysaccharide. It is crucial that a well-mixed blend of the two biopolymers is achieved in the solution in the first instance, and remains so once the solution is freeze-dried prior to the heat induced Maillard reaction. Thus, the lack of sufficient solubility of many plant proteins becomes a major stumbling block in obtaining such an intimate mix, leading to a reduction in the efficiency of bond formation between the protein and the polysaccharide molecules.

Our approach to overcome the poor solubility of commercial SPI is to hydrolyse it prior to its conjugation with polysaccharide. The hypothesis is to unfold the protein structure and also to produce smaller polypeptides which are expected to be more soluble and surface active (Ettelaie et al., 2017, Ettelaie et al., 2014, Chen et al., 2011a). The covalent bonding of these polypeptides with polysaccharides may therefore be a promising way to produce molecular level plant-based emulsifying agents.

The idea is not entirely new and has been explored in a few studies in relation to the interfacial adsorption behaviour (Li et al., 2016), emulsion stability during freeze-thaw cycles (Yu et al., 2018b) and protection against oxidation offered by these composite macromolecules (Zhang et al., 2014b). However, the focus of these studies, unlike the

present work, had not been the long-term emulsion stability, particularly at acidic conditions.

Moreover, the synthesis of the current type of conjugates based on the use of plant protein fragments, also requires an understanding of the role of the type of enzyme used and the degree of hydrolysis (DH) in producing the polypeptides. For previous investigations, each used a different enzyme, which makes a comparative analysis more difficult. To the best of our knowledge, very few studies have systematically examined these factors.

The present work investigates the possibility of creating stable submicron O/W emulsions at acidic pH conditions, using commercial isolated soy proteins. We consider soy protein fragments, obtained at various degrees of hydrolysis by two very different enzymes, trypsin and alcalase. The first acts on a rather selective set of peptide bonds, while the latter is much more indiscriminate. The emulsifying and emulsion stabilizing abilities of the polypeptides resulting from the action of these enzymes, both prior to and post the formation of covalent bonds with an electrically neutral and surface inactive polysaccharide, namely maltodextrin, are examined. The observed behaviours of these soy materials are carefully compared to those seen for whey protein hydrolysates (in the previous chapter), undergoing exactly the same enzyme treatment and the subsequent Maillard reaction process.

5.2 Materials and Methods

5.2.1 Materials

Commercial isolated soy protein (SPI) powder was purchased from Shandong Yuwang Industrial Co. (China). The sample contains approximately 90% (w/w) protein according to the supplier. The two enzymes, i.e. trypsin and alcalase, as well as all the other chemicals used in this chapter are the same as those already described in Chapter 4.

5.2.2 Hydrolysis of SPI by trypsin and alcalase

2.5% (w/v) 100 mL SPI dispersion was prepared by dissolving SPI powder in deionised water for 2 h with gentle stirring. The dispersion was then allowed to hydrate overnight at 4°C. Before enzymatic hydrolysis was conducted, the dispersion (100 mL/batch, contained in a cylinder beaker of 150 mL) was treated with ultrasonication (200W, 25kHz) for 10 min. The probe of the sonicator was sunk 4 cm into the protein dispersion. An ice bath was used to control the temperature increase during the ultrasonication treatment.

For hydrolysis by trypsin, the dispersion was preheated to 37°C by incubation in a 37°C water bath for 20 min with gentle stirring. Then the pH was adjusted to 8.5 with 1 M NaOH. According to preliminary tests, trypsin was added at enzyme-to-substrate (E/S) ratios (w/w) of 1/200, 1/100, 1/50 to achieve three different degrees of hydrolysis (i.e. DH = 2.5%, 5.5%, 8.0%), obtained within approximately 2 h. In the case of alcalase, the SPI dispersion was preheated to 50°C by incubation in a 50°C water bath for 20 min with gentle stirring. Then pH was adjusted to 8.5 with 1 M NaOH. Different amounts of alcalase solution (i.e. 3, 7 and 15 µL/100 mL protein dispersion) were added respectively, again to provide different levels of hydrolysis.

For each case, protein was hydrolysed under constant temperature and pH, controlled by a water bath and Metrohm 902 Titrando system (Metrohm Co., USA). The DH was determined according to the pH-stat method according to section 2.3.1.

When the desired DH (i.e. 2.5%, 5.5%, 8.0%) was reached, the enzyme activity was immediately stopped by diluting the dispersion to 1.0% (w/v) with 4°C deionised water and incubating in the ice bath with gentle stirring for 0.5 h. The protein hydrolysates were then freeze dried over a period of 48 h. A moderate heating treatment (80°C, 5 min) was applied to the freeze-dried samples, in order to ensure the complete inactivation of enzyme activity.

Ultrasonicated soy protein hydrolysates (SSPHs) by trypsin and alcalase at different values of DH (i.e. 2.5%, 5.5%, 8.0%) were labelled as SST1, SST2, SST3 and SSA1, SSA2, SSA3, respectively.

5.2.3 Preparation of protein-polysaccharide conjugates

The Maillard reaction products (MRPs) were prepared between maltodextrin DE16.5-19.5 (MD, $M_w = 8.7$ kDa) and different soy protein samples (i.e. ultrasonicated SPI, SST1, SST2, SST3 and SSA1, SSA2, SSA3) by dry heating. The preparation process followed the same procedure to that described in section 4.2.3.

The Maillard reaction products (MRPs) are denoted and identified here using the same convention as those for whey protein based materials in Chapter 4, starting with the type of the protein/peptides, followed by polysaccharides. For example, the MRPs made from SST1 with maltodextrin DE16.5-19.5 is marked and referred to as SST1-MD throughout the study.

5.2.4 Particle sizing of protein/polypeptide dispersions

Ultrasonicated SPI (SSPI) and soy protein hydrolysates (SSPHs) samples with different degrees of hydrolysis (DH = 2.5%, 5.5% and 8.0%) caused by trypsin (SST1, SST2, SST3) and alcalase (SSA1, SSA2, SSA3) were diluted 25 times (i.e. 40 μ L 2.5 (w/v) protein dispersion in 960 μ L buffer) using a pH 7.5 buffering system (with a low background electrolyte concentration of 20 mM). The recipe for this buffering system is provided in Appendix IV. Protein particle size was measured by Nano ZS Zetasizer (Malvern, UK) and was given as *Z*-average diameter (nm). The measurements were conducted at 25°C. The refractive indices used for protein and aqueous phase were 1.45 and 1.33, respectively.

5.2.5 Electrophoresis analysis

SDS-PAGE was performed under reduced conditions, in order to study the molecular weight profiles of produced polypeptides. The details of the procedure were the same to those provided in section 4.2.4.

5.2.6 Protein solubility

The protein solubility is defined as the soluble protein content remaining in the supernatant after a certain level of centrifugation. It was determined by the Biuret method according to the procedure described in section 4.2.5.

5.2.7 Dissociation of insoluble MRPs made from SSPI

Since the MRPs made from ultrasonicated SPI and maltodextrin (i.e. SSPI-MD) were found to be quite insoluble, despite their hydrophilic polysaccharide attachment, the interactions involved in the formation of SSPI-MD were evaluated using a method according to the study of Liu et al. (2014). An amount of 0.05 g SSPI-MD sample was incubated in 10 mL of several different solvents: buffer (pH 9.0, containing 0.086 M Tris, 0.090 M Glycine), SDS (5% SDS in buffer), DTT (0.5 M DTT in buffer) and SDS + DTT (5% SDS plus 0.5 M DTT in buffer). The incubation was allowed for 3 h at 25 °C with gentle stirring. Then the improvement in the solubility of the tested sample in different solvents was visually assessed.

5.2.8 Preparation of emulsions

O/W emulsions (10 vol.% sunflower oil), made by unconjugated and conjugated protein samples, were prepared in the same way as those prepared with whey protein materials (see section 4.2.7). The pH of the freshly made emulsions was then adjusted to various desired values (pH 7.5, 4.5, and 3.0) with 1 M NaOH or HCl. The emulsion samples were stored at 4°C for further investigations.

5.2.9 Storage stability of emulsions at different pH conditions

The stability of emulsion was assessed by various measures same as those that have been done for emulsion samples stabilized by whey protein materials (see section 4.2.8). These included the sizing and ζ -potential measurements of emulsion droplets, the rheological flow properties and the microstructure of emulsions. The assessments were performed at various stages during the storage period.

5.2.10 Statistical analysis

All the measurements were performed in triplicate. The obtained data was averaged and reported as a mean value in each case. The error bars were added as standard deviations. All the calculations were analysed by Microsoft Excel 2016.

5.3 Results and Discussions

This section displays the alteration of a few important characteristic properties (including protein particle size, solubility, profiles of hydrolysates, and colloidal functionalities) of commercial isolated soy protein post the modification of enzymatic digestion followed by covalent conjugation with polysaccharide. Again, we shall focus on the data obtained for protein/peptides that were conjugated with polysaccharide at 90°C for 3 h, since these conjugated biopolymers were found to be not significantly different from those conjugates made at 60°C for 24 h in respect of their colloidal functional properties, except for a slightly lower level of solubility for the latter. Therefore, unless specifically stated, the discussions concerning the conjugates formed at 90°C for 3 h are understood to largely apply to those made at 60°C for 24 h.

5.3.1 Protein particle size

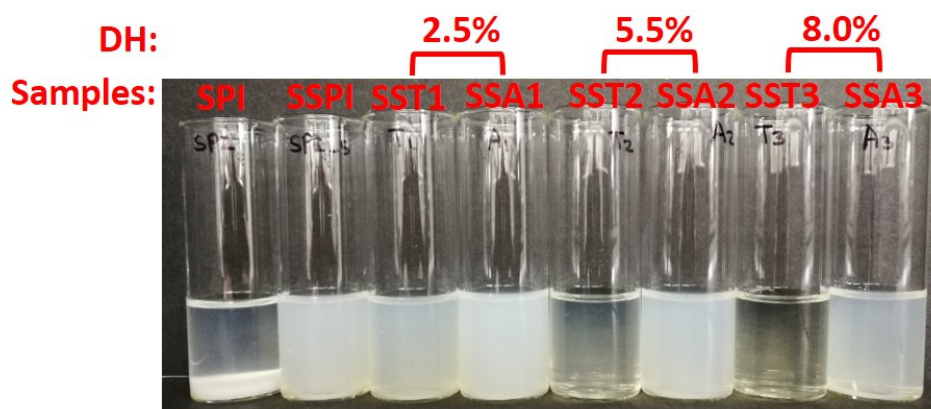


Figure 5.1 The visual appearance of various 0.5% (w/v) soy protein dispersions at pH 7.5. SPI and SSPI refer to intact and ultrasonicated soy protein isolate, accordingly. SSPI digested by trypsin and alcalase at different levels of hydrolysis (i.e. 2.5%, 5.5% and 8.0%) are denoted as SST1, SST2, SST3 and SSA1, SSA2, SSA3, respectively.

Figure 5.1 shows the visual appearances of the intact, as well as partially hydrolysed, SPI dispersions in water. As can be seen from the sample SPI in **Figure 5.1**, the intact SPI dispersion rapidly settled down because of its very poor solubility. Due to various processing conditions applied to the commercial SPI, the extracted proteins become totally or partially denatured (Adler-Nissen, 1976). Resultant exposure of the hydrophobic amino acid residues leads to significant clustering of the protein molecules. Thus, commercial SPI is normally present in a highly aggregated form,

giving it poor solubility and inferior dispersibility (Wagner et al., 2000, Dickinson, 2019, Tang, 2017).

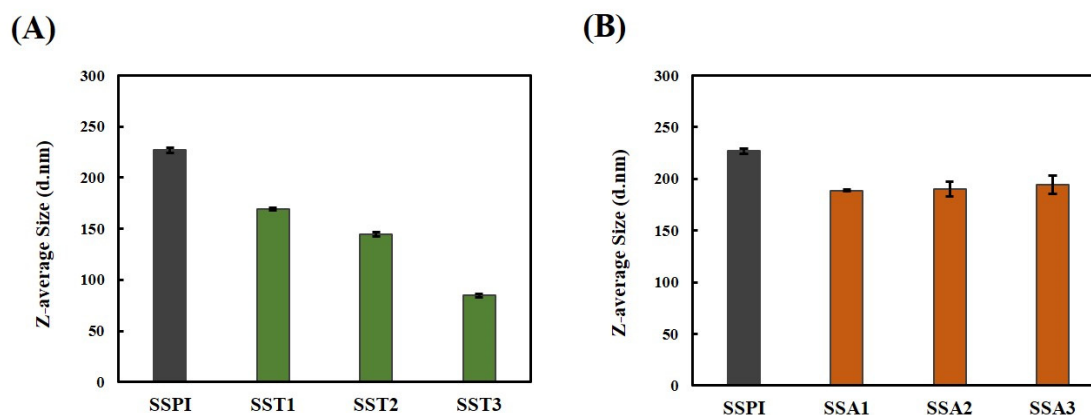


Figure 5.2 The average protein particle size of SSPI and its hydrolysates post digestion by trypsin (A) and alcalase (B), accordingly.

After ultrasonication treatment (see SSPI in **Figure 5.1**), a stable and homogenous dispersion formed. The size of protein aggregates was found to reduce to 226 nm in diameter (see SSPI in **Figure 5.2A**). Ultrasonication is a low-cost treatment which is known to be able to break up the non-covalent inter- and intra-molecular interactions (e.g. hydrogen bonding, hydrophobic interactions), resulting in protein denaturation as well as dissociation of protein aggregates. Therefore, ultrasonicated proteins have been reported to be more accessible for enzymatic hydrolysis than their untreated counterparts (Chen et al., 2011a, Jia et al., 2010).

SSPI was then hydrolysed by two distinctly different enzymes, trypsin and alcalase. Our choice of these two enzymes was based on their differing levels of selectivity to cleave various peptide bonds. Trypsin is one of the most specific enzymes, which tends to only break the peptide bonds at the C-terminal of lysine (Lys) and arginine (Arg) (Tavano, 2013). On the other hand, alcalase has a much broader range of amino acid substrates as compared to trypsin (Doucet et al., 2003). The dispersions of SSPHs samples obtained from different levels of hydrolysis by trypsin (i.e. SST1 at DH 2.5%, SST2 at DH 5.5% and SST3 at DH 8.0%), exhibited a marked reduction in their degree of turbidity (**Figure 5.1**). This was particularly noticeable at DH 5.5%, and even more at DH 8.0%. In comparison, those samples hydrolysed by alcalase (i.e.

SSA1 at DH 2.5%, SSA2 at DH 5.5% and SSA3 at DH 8.0%) continued to remain rather opaque (**Figure 5.1**).

The observed changes in turbidity are the result of a reduction in the aggregated protein particle size (**Figure 5.2**). The mean protein particle size was reduced from 226 nm (SSPI) down to 84 nm (SST3) by trypsin. In contrast, the protein particle size was only slightly reduced to around 200 nm at the early stage of alcalase hydrolysis (SSA1), and then stayed more or less unchanged as hydrolysis proceeded further (SSA2 and SSA3).

A rational explanation of the distinct alterations of the soy protein particle size by the action of the two enzymes is proposed as follows. At a low degree of hydrolysis, one would presume that most of the cleavable bonds will reside close to the surface of the aggregated protein particles. As DH increases, this is likely to continue to be the case for alcalase, given its less selective nature and higher ability to break peptide bonds of various types. On the other hand, trypsin will begin to run out of specific bonds it can hydrolyse near the surface. If it is to achieve the same degree of hydrolysis, trypsin is required to diffuse deeper into the core of the protein particles to find further bonds to break. Though it may take longer to achieve the same value of DH (i.e. the same number of broken bonds), the breakage would be more uniformly distributed on the protein particles for trypsin case.

The breakage of bonds leads to the formation of a spectrum of polypeptides with not only a distribution of molecular weights, but also varying *pI* values. At any pH, some of these protein fragments will be more soluble than the intact protein. Their presence in the interior of the protein aggregates may be able to aid the breakup of protein particles, and progressively lead to the reduction in the aggregated protein particle size. This is indeed what is seen in **Figure 5.1** and **Figure 5.2A** when hydrolysis took place using trypsin. In contrast, for the protein aggregates exposed to alcalase, most of the cleaved bonds occur close to the surface of the aggregates and the core of the protein particles remains much less affected. Therefore, a much smaller reduction in the particle size was found, at least at the levels of hydrolysis considered here (**Figure 5.2B**).

The arguments presented above also indicate that trypsin hydrolysis probably favours the generation of a large number of intermediate-sized polypeptides. The ability of trypsin to more uniformly decrease the molecular size of plant proteins than alcalase can also be seen in the studies of Kim et al. (1990) and Tamm et al. (2016). In comparison, alcalase hydrolysis is likely to produce much smaller-sized peptides, which we assume are mostly produced from the fragmentation of protein chains close to the surface of the protein aggregates. The majority of the protein chains residing further down inside the aggregates are probably less impacted by the action of alcalase during such limited hydrolysis (DH < 20%).

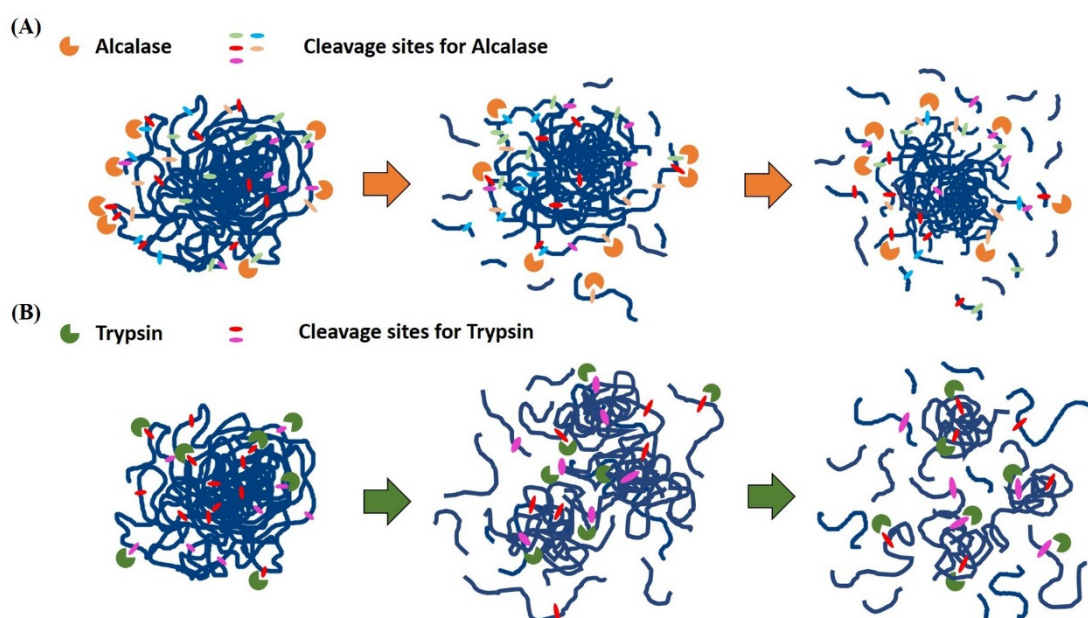


Figure 5.3 The schematic picture of the processes of protein hydrolysis by alcalase (A) and trypsin (B).

Figure 5.3 shows a schematic picture summarizing the proposed mechanism in the size reduction of the protein aggregates and the resulting generated polypeptides, arising from the actions of the two contrasting enzymes. The molecular weight distribution of produced fragments is discussed in the next section.

It should also be pointed out that, in addition to the differences in molecular size of the produced polypeptides by trypsin and alcalase, these enzymes are also known for their respective preference to cleave at hydrophilic and hydrophobic amino acid residues (Doucet et al., 2003, Tavano, 2013). Therefore, the hydrolysates produced

by them are expected to have other contrasting properties too, such as different charges and hydrophilic-hydrophobic balances (Panyam et al., 1996). All of these intrinsic properties of protein fragments are of importance in determining their solubility, and thus have a bearing on their interfacial properties and emulsifying and colloidal stabilizing abilities.

5.3.2 Molecular weight profiles

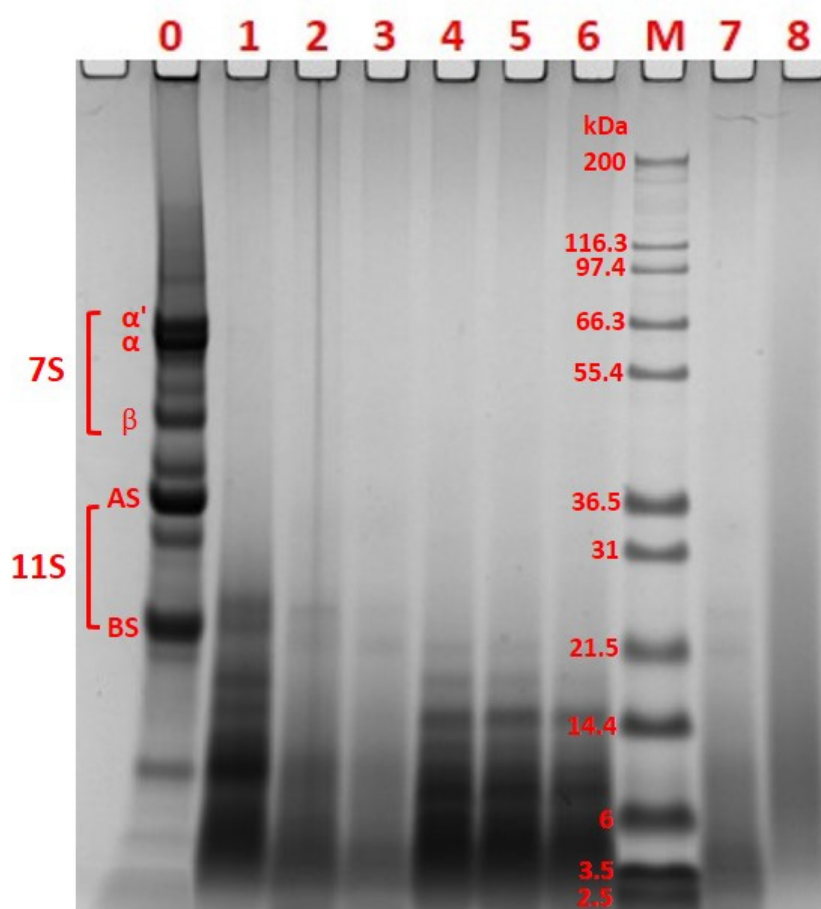


Figure 5.4 Reducing SDS-PAGE analysis of the protein/peptide profiles for various soy protein samples. Lane 0 is ultrasonicated SPI. Lane 1-3 are polypeptides produced by trypsin digestion at lower to higher DH (i.e. SST1, SST2 and SST3, respectively). Lane 4-6 are polypeptides produced by alcalase digestion at lower to higher DH (i.e. SSA1, SSA2 and SSA3, respectively). Lane M is the molecular weight ladder (with values presented in the unit of kDa). A sample post conjugation with maltodextrin (i.e. SST3-MD) is also shown at lane 8 to be compared with its unconjugated counterpart (i.e. SST3) at lane 7.

The composition of soy protein isolate has been discussed extensively by the excellent review of Nishinari et al. (2014) on this subject. The profile of hydrolysed soy proteins was analysed here by reducing SDS-PAGE. The two major components of intact SPI (Samoto et al., 2007, Kuipers, 2007, Nishinari et al., 2014), i.e. 7S (β -conglycinin) and 11S (glycinin), including their constituent subunits (i.e. α , α' and β subunits of 7S, acidic and basic subunits of 11S), were marked in lane 0 of **Figure 5.4** for comparison.

It is clearly seen that trypsin and alcalase generated polypeptides with distinct profiles. Similar to the observation by Kim et al. (1990), trypsin was also found here to be able to gradually break soy protein down. This was seen as a shift of bands towards lower molecular weight range with increasing DH (see lane 1-3 in **Figure 5.4**). As for alcalase, the profiles of hydrolysates (see lane 4-6 in **Figure 5.4**) did not show a distinct difference with increasing DH beyond 2.5%. Recall from Chapter 4 that the profiles of the fragments of whey protein obtained from treatment by trypsin and alcalase (see **Figure 4.1** in section 4.3.1), exhibited similar patterns to the corresponding ones produced for soy protein hydrolysates.

These results from SDS-PAGE on molecular size profiles of WPHs and SSPHs were consistent with the discussions in the previous section, suggesting that by the end of the hydrolysis, the mixture of protein fragments obtained by trypsin treatment would probably consist of a large content of intermediate-sized polypeptides. Due to the highly selective nature of peptide bonds broken by trypsin, this enzyme has to get deep into the core of the structure of the protein aggregates in order to achieve the required degree of hydrolysis. This means that the protein chains would be chopped down throughout the whole body of the protein aggregate particles. On the other hand, alcalase hydrolysis was highly likely to produce large amounts of very small fragments, which we suspect are predominantly produced here from a subset of protein chains residing close to the surface of the protein aggregates, due to the low selectivity of this enzyme (Tamm et al., 2016).

The successful formation of conjugates was also confirmed using SDS-PAGE analysis. The presented result here is limited to conjugates formed using SST3, though similar data would also be expected for other hydrolysed samples too. In comparison to the equivalent unmodified protein fragments (lane 7 in **Figure 5.4**), a noticeable shift in molecular weight, towards higher values, was observed for

conjugated SST3 (lane 8 in **Figure 5.4**), due to the covalent bonding of maltodextrin ($M_w = 8.7$ kDa) with the protein fragments.

5.3.3 Solubility

As have been emphasized, a relatively good solubility of protein materials is crucial for being a good molecular (i.e. non-Pickering type) emulsifier with satisfactory colloidal functionalities (Dickinson, 1992e). Recall from Chapter 4 that the covalent bonding of whey protein or their fragments with a highly soluble polysaccharide, i.e. maltodextrin, has rendered the conjugated biopolymers a sufficient level of solubility when the solubility of the non-bonded protein or fragments is not particularly high at their *pI*.

Despite this enhancement of protein solubility due to polysaccharide attachment, it does not mitigate the requirement for protein to have a good solubility to start with, when it comes to synthesising the conjugated emulsifier/colloidal stabiliser, as already discussed in section 1.2.4. A reasonable solubility guarantees a well-mixed state of protein, or hydrolysates as the case may be, and polysaccharide, so as for a sufficient level of reaction between those two types of molecules.

Additional considerations, when it comes to synthesizing vegetable protein based conjugates, perhaps involve the aggregated state of proteins. Protein in an aggregated form may not allow for adequate exposure of all its reactive sites (i.e. lysine or *N*-terminal residue) to polysaccharide. However, a satisfactory functional property can only be achieved when the Maillard reaction can proceed to an extent where a sufficient number of conjugated emulsifiers are produced.

This section will present and discuss how the solubility of soy protein fragments differs from the original intact proteins, and how this alters with the choice of the enzyme and increasing DH. These results are compared with those for their conjugated counterparts. Moreover, comparisons are made with equivalent whey protein samples where it is necessary.

5.3.3.1 Solubility of SPI, SSPI and SSPHs samples

As shown in **Figure 5.5**, ultrasonication treatment of intact soy protein broke up the non-covalent intermolecular interactions within large protein aggregates. This produced an apparent improvement in the solubility of the protein at all tested pH conditions, with exception of pH 4.5 (i.e. the isoelectric point of SPI).

The word apparent is used here, as it is suspected that a large portion of ultrasonicated proteins still remain in the form of aggregates, but with a much-reduced particle size ~ 226 nm (see **Figure 5.2**). However, protein material in these aggregates is not truly dissolved. At pH conditions away from pI , the fine protein particles are sufficiently charged to stay colloidally stable. In fact, the aggregates are probably small enough not to be completely separated by the centrifugation process. Their continued presence in the supernatant leads to a higher perceived level of solubility, than otherwise the case if they could have been removed. Of course, this issue does not arise at pH 4.5 where the total net charge on both SPI and SSPI is largely lost. This leads to complete precipitation, with neither any small aggregates nor individual protein molecules remaining in the solution.

The enzymatic hydrolysis, particularly by trypsin, noticeably enhanced the protein solubility at all tested pH values. This was especially so at pI , irrespective of which enzyme was used (**Figure 5.5**). At pH 4.5, the solubility improved to around 5 \sim 6 g/L from a value well below 1 g/L for SSPI. In contrast, whey protein fragments, produced by either enzyme, displayed reduced level of solubility at the entire tested pH range, compared to intact WPI (see **Figure 4.2** in section 4.3.2.1).

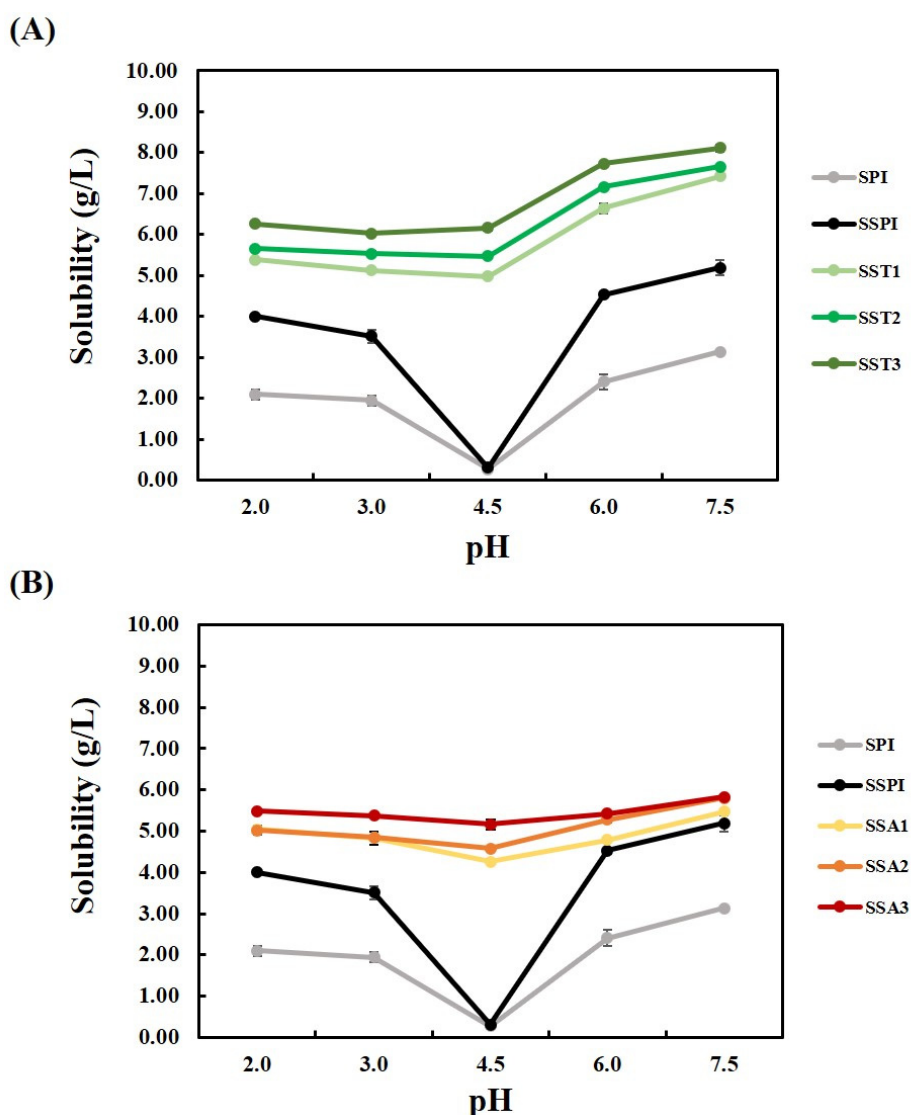


Figure 5.5 The solubility of SPI, ultrasonicated SPI (i.e. SSPI), and SSPHs samples hydrolysed by trypsin (A) or alcalase (B) at various DH, plotted as a function of pH.

A likely explanation of the contrasting impacts of protein fragmentation on the solubility of soy and whey protein can be rationalised as follows. As mentioned in previous sections, the process of hydrolysis produces various polypeptides with a variety of different pI values. Instead of a sharp well-defined pH value associated with the isoelectric point of the intact protein, now one has a more smeared distribution of pI values for various fragmented chains, following hydrolysis. Thus, at any pH, some fragments are away from their respective pI so as to be reasonably soluble, while others are not. For the whey protein sample, which is already highly soluble, this effect tends to reduce the solubility of protein hydrolysates compared to the intact protein.

However, by the same token, the averaging effect induced by fragmentation tends to improve the solubility, if the original protein is not especially water soluble to begin with. This is indeed the behaviour that is observed here for soy protein. The improved solubility of SSPHs throughout the entire tested pH range, as in comparison to SSPI, is also partially attributed to the breakdown of soy protein aggregate particles. The measured apparent solubility is expected to increase when these aggregates are broken down more effectively. This is probably why soy fragments hydrolysed by trypsin exhibited a higher solubility (5 ~ 8 g/L in **Figure 5.5A**) in comparison to those produced by alcalase (4 ~ 6 g/L in **Figure 5.5B**). Kim et al. (1990) also found a similar result that soy peptides obtained by trypsin digestion were more soluble than those obtained by alcalase.

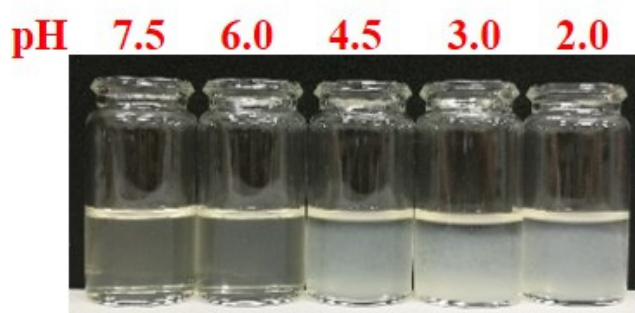


Figure 5.6 The visual appearance of 1% (w/v) SST3 sample, dispersed under various pH conditions.

The visual appearance of 1% (w/v) SST3 sample as a function of pH was shown in **Figure 5.6**. At pH values below 6.0, a substantial formation of precipitates was observed due to reduced electrostatic repulsion between the fragmented chains. But a stable and homogenous particulate protein dispersion was formed at higher pH. The situation was the same for all the SSPHs samples. Therefore, the mixture of soy protein hydrolysates and maltodextrin in water was produced at pH 7.5, in order to ensure a homogenous and well-mixed system of the two biopolymers, prior to its freeze drying.

5.3.3.2 Solubility of conjugated SPI, SSPI and SSPHs samples

The synthesis of conjugates was carried out according to the procedure outlined in section 5.2.3 and section 4.2.3. The solubility of various conjugated samples was displayed in **Figure 5.7**.

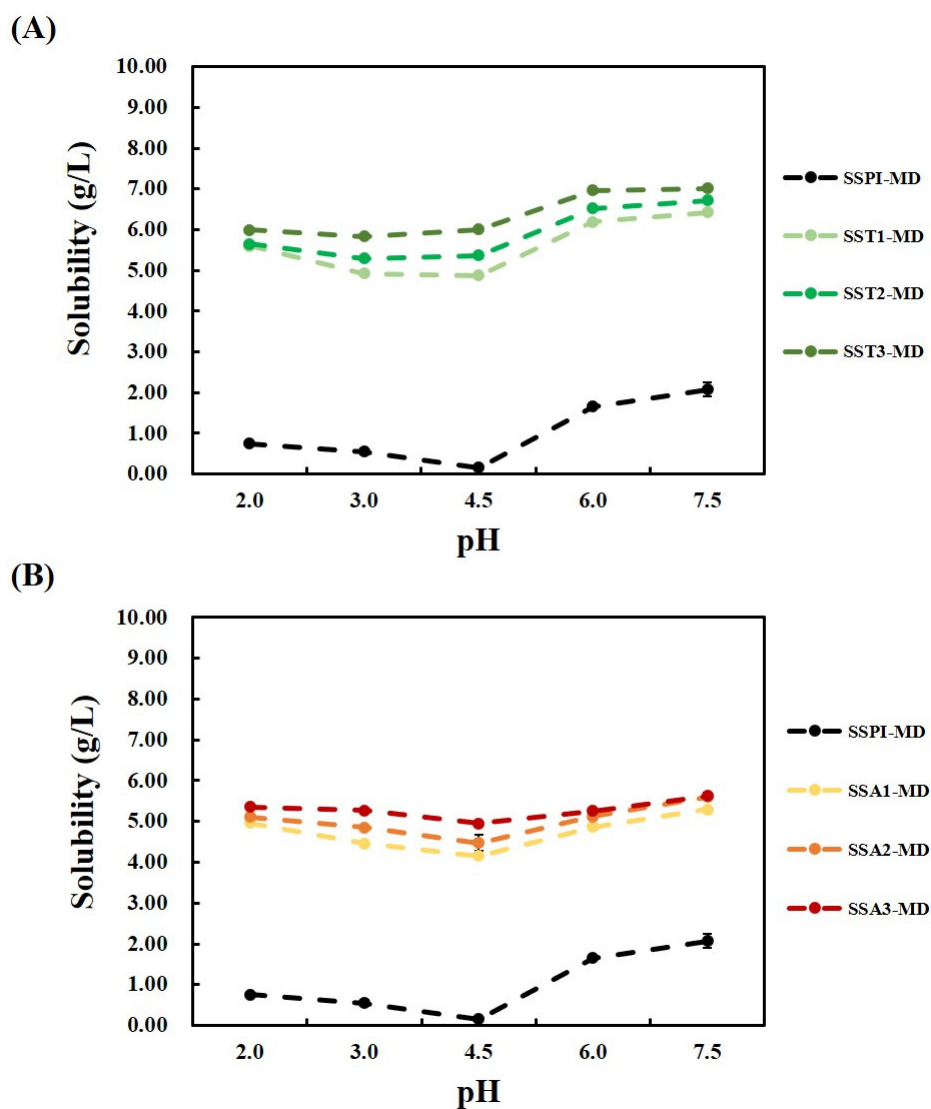


Figure 5.7 The solubility of conjugates made from ultrasonicated SPI (i.e. SSPI-MD), and those made from fragmented soy protein produced by either trypsin (A) and alcalase (B) at various levels of hydrolysis, plotted as a function of pH.

The conjugates SSPI-MD, formed between the ultrasonicated soy protein and maltodextrin, may have been expected to have a better solubility than SSPI on its own. Instead, a dramatic decrease in the dispersibility was found for SSPI-MD (~2 g/L) compared to SSPI (~5 g/L) at pH 7.5 (see **Figure 5.5** and **Figure 5.7**), with highly insoluble products formed from the dry-heating Maillard reaction (**Figure 5.8**). This result was replicated for conjugates formed at 90°C, as well as at 60°C.

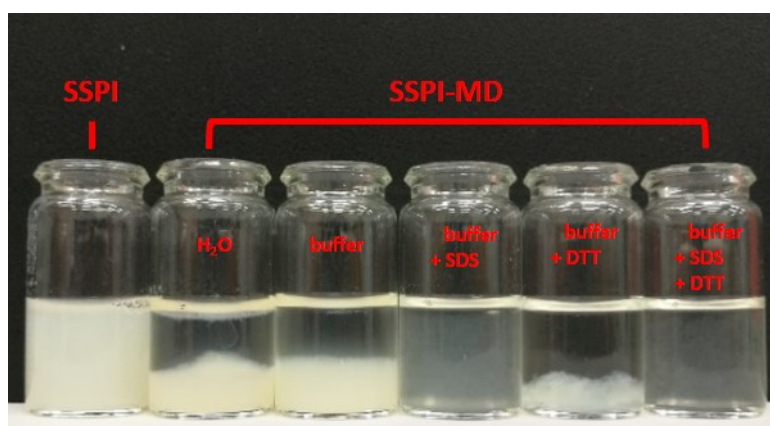


Figure 5.8 Effects of addition of SDS, DTT, or both to a dispersion of otherwise insoluble MRPs, produced from ultrasonicated soy protein + maltodextrin (i.e. sample SSPI-MD). Ultrasonicated soy protein without conjugation (SSPI) was dissolved in deionized water and is included for comparison on the left. SSPI-MD was dissolved in different solvents (from left to right): deionized water, buffer (pH 9.0, 0.086 M Tris, 0.09 M Glycine), 5% SDS + buffer, 0.5 M DTT + buffer, 5% SDS + 0.5 M DTT + buffer.

The formation of such kind of insoluble products has been reported in the literature (Akhtar et al., 2007, Xu et al., 2009). In order to investigate this issue further, SSPI-MD was dissolved in various denaturing solvents, including those with added SDS and DTT (**Figure 5.8**). These help the dissociation and breakup of different types of inter- and intra-molecular bonds, such as hydrophobic interactions and disulphide bonds. The SSPI-MD conjugates remained insoluble in Tris-Glycine buffer at pH 9.0. This indicates that the poor solubility of SSPI-MD is not merely due to the lack of electrostatic repulsions between the conjugated biopolymers, since they would have acquired sufficient charges at such alkaline condition. In a buffer solution with the presence of 5% SDS, insoluble flakes of SSPI-MD started breaking into smaller pieces, due to the disturbance of the hydrophobic associations by SDS (Ren et al., 2009). The inclusion of 0.5 M DTT, which aids to break the disulphide bonds under

alkaline conditions (pH > 8.0) (Liu et al., 2014, Singh et al., 1995), also proved helpful in dispersing SSPI-MD aggregates. However, the effect was not quite as strong as that seen with SDS. When both SDS and DTT were present, SSPI-MD aggregates were broken down into much smaller particles as can be seen in **Figure 5.8**.

These results taken together, suggest that hydrophobic interactions are likely the main driving force in the extensive aggregation of SSPI-MD, occurring during the dry-heating Maillard reaction phase. Exchange of disulphide bonds provides further contribution to this process. Nevertheless, no matter how much denaturing agents were added, SSPI-MD could never be made to completely dissolve. This indicates the rather tight and dense structure of the formed SSPI-MD aggregates, which does not allow for easy penetration of small-molecular-weight reagents (i.e. SDS and DTT) deep into the aggregates, at least not within the time scale of the current experiments here (~ 3 h).

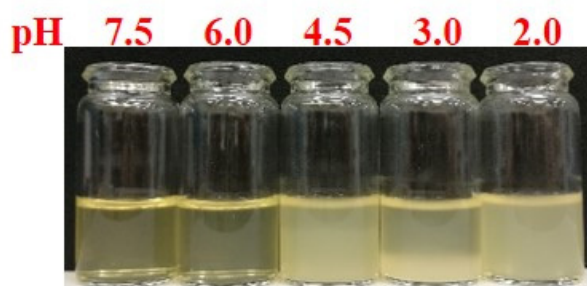


Figure 5.9 The visual appearance of 1% (w/v) SST3-MD sample, dispersed under various pH conditions.

Unlike insoluble SSPI-MD, the conjugated soy hydrolysates with maltodextrin (see **Figure 5.9**) stayed easily dispersible, without any noticeable formation of insoluble products as that seen in SSPI-MD post Maillard reaction. However, they also did not show any improvement in their solubility relative to the unreacted fragments either, at the whole tested pH range (compare **Figure 5.5** and **Figure 5.7**). Visible aggregates were observed both at *pI* and other acidic pH conditions (**Figure 5.9**). Separately, the solubility of conjugates made from WPI/WPHs and maltodextrin was seen to improve (**Figure 4.4** in section 4.3.2.2), with conjugates forming a clear golden brown solution at *pI* of whey protein materials (i.e. pH 4.5). In contrast, the unconjugated equivalents lacking the sufficient charge under this pH condition, settled down out of the solution

(**Figure 4.3** in section 4.3.2.1). The absence of precipitation at pI confirmed the formation of covalent bonds between WPI/WPHs and maltodextrin.

As for conjugated soy fragments, the formation of large visible aggregates at pI and other low pH values generally, could be an indication of the fact that a sizeable portion of protein fragments did not form the required covalent bonds with maltodextrin, at least not under the same heating regime as that used for the WPI/WPHs + maltodextrin. Prolonged heating time, and addition of a higher amount of maltodextrin (i.e. the weight ratio of peptide/maltodextrin increasing to 1:3, 1:4 and 1:5), were both tried, in the hope of facilitating conjugation between soy protein fragments and maltodextrin. However, these did not improve the situation dramatically, neither with respect to the solubility nor emulsifying and stabilizing abilities of conjugates (as will be discussed in the next section).

The difficulty for soy protein to form covalent bonds with maltodextrin, in contrast to whey protein, is presumably related to its distinct and more complex structure. When protein conjugates are made via heating of the dry mixture of protein and polysaccharide, two main competing processes occur simultaneously in the system. Firstly, the required Maillard reaction between protein and polysaccharide, involving free α -NH₂ groups of the protein. The second is the undesirable heat-induced protein aggregation (Akhtar et al., 2007, Dickinson et al., 1992). It is suggested that due to the structural characteristics and the aggregated state of the soy protein materials, the heat-induced associations between protein molecules via hydrophobic interactions, as well as exchange of disulphide bonds, tend to take place at a much more rapid and intense rate than the Maillard reaction.

Substantial associations between soy protein molecules tend to shield the chemically reactive sites on protein (i.e. free α -NH₂), making the bonding between protein and polysaccharide much harder (Mulcahy et al., 2017). Under such circumstances, insoluble products are formed, which are simply aggregates of protein molecules, rather than the desired MRPs. It is obvious that improving this situation needs a homogeneous dry mixture, with intimate contacts between the two biopolymers on length scales of individual chains. Existence of large protein particles during the preparation of protein + polysaccharide solution, present even before the freeze drying phase, is clearly not conducive in achieving a complete and efficient synthesis of

conjugates. This situation seems to improve for hydrolysed soy protein (SSPHs). As the compact structure of soy protein is broken down, protein particulate aggregates fall apart. Then the preparation of a well-blended homogenous mixture of protein fragments and polysaccharides becomes more feasible.

Additionally, protein fragmentation also causes unfolding of protein structure and allows for more reactive sites on protein chains to become exposed. This again increases the chance for their bonding with polysaccharides. However, we must keep in mind that extensive hydrolysis above a certain level can have a detrimental effect on the emulsifying and stabilizing properties of protein fragments, as well as their conjugated derivatives. This adverse effect has already been observed in whey protein based samples and discussed with details in Chapter 4. It is noted that this implies a possible optimal value for DH, where the above-mentioned benefits of hydrolysis are achieved, but yet the resulting fragmented proteins are still not made too small to lose their functionalities.

5.3.4 Morphology and stability of emulsions at different pH conditions

The particle size, the peptide distribution profile and the solubility, as investigated in the previous sections, illustrated some of the key features of various modified soy protein materials. This section will present and discuss the emulsifying and long-term stabilizing capacities of those soy protein samples under various pH conditions, in the light of the observed attributes studied in the last sections, as well as other possible relevant parameters. Similar to Chapter 4, we shall include results of the microstructure, droplet size and distribution of emulsions, ζ -potential of emulsion droplets, and flow behaviour of emulsion samples. In the meantime, the colloidal behaviours of soy protein materials are also compared to their whey protein counterparts.

5.3.4.1 Emulsions based on unconjugated soy proteins/hydrolysates

The relatively large aggregated protein particles in SPI and SSPI samples manifested themselves by their rather poor emulsifying abilities. The emulsion droplet sizes obtained for intact soy protein, used for fabricating emulsions in the absence of or with

prior ultrasonication treatment, were $D_{4,3} = 28.4 \mu\text{m}$ and $9.8 \mu\text{m}$ at pH 7.5, respectively (Figure 5.10).

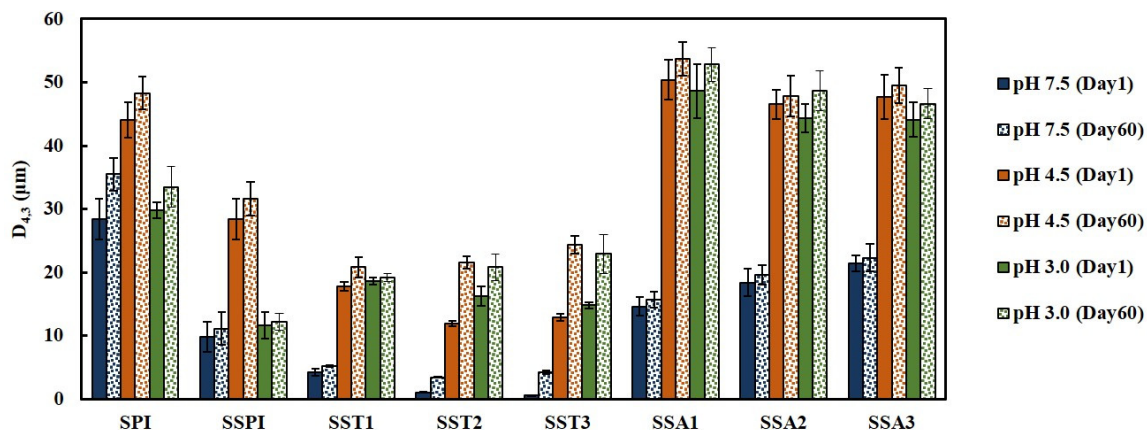


Figure 5.10 Average droplet size $D_{4,3}$ of freshly made and stored (for 60 days) emulsions, fabricated using intact SPI, ultrasonicated SPI (i.e. SSPI) and SSPHs, at various pH conditions (i.e. pH 7.5, 4.5 and 3.0).

The droplet size decreased dramatically as soy protein was progressively broken down by trypsin, before its use as emulsifiers (Figure 5.10). From the micrographs (Figure 5.11A), it was observed that soy fragments with the highest DH 8.0% (SST3) were able to produce a finely dispersed submicron-sized emulsion. The average size $D_{4,3}$ was found to be $0.608 \mu\text{m}$, at pH 7.5. This is comparable to the emulsions stabilized by WPHs (e.g. $D_{4,3} = 0.628 \mu\text{m}$ for WT1). On the other hand, alcalase digestion progressively worsened the emulsifying capacities of SSPI, leading to the formation of larger droplets ($D_{4,3} = 9.8 \mu\text{m}$, $14.6 \mu\text{m}$, $18.4 \mu\text{m}$ and $21.4 \mu\text{m}$, for fresh emulsions made at pH 7.5 by SSPI, SSA1, SSA2 and SSA3, respectively). It was clear that the more the soy protein was hydrolysed with alcalase, the poorer its emulsifying performance became.

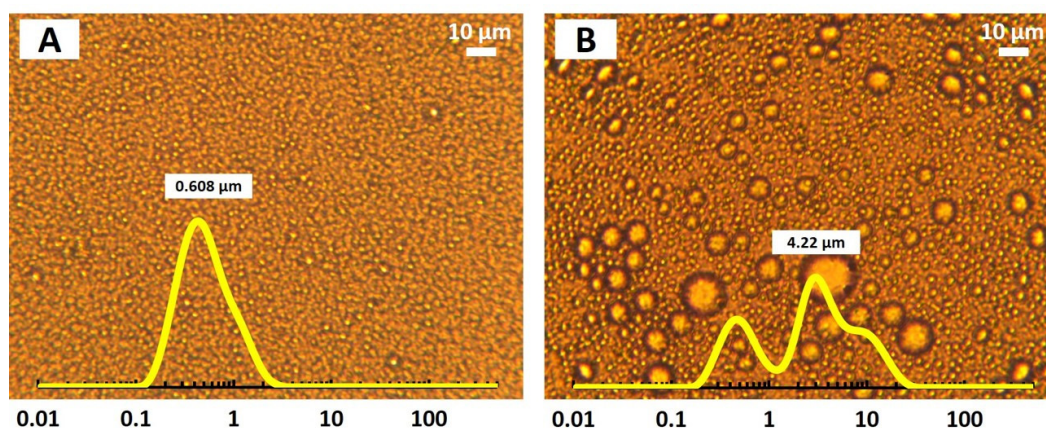


Figure 5.11 Micrographs of SST3 fabricated emulsion, stored at pH 7.5, on day 1 (A) and after 60 days of storage (B). The droplet size distribution and the mean droplet size $D_{4,3}$ are superimposed on each photo.

On the contrary, recall from Chapter 4 that for whey protein materials, hydrolysis by trypsin up to DH of 2.5% moderately enhanced the emulsifying/stabilizing capacities of WPI. This trend did not continue with further fragmentation, where the required emulsifying properties were instead seen to rather suffer. The worsening of the functional properties of whey proteins was observed from the very onset for alcalase treatment, even at DH 2.5% (see **Figure 4.7** in section 4.3.3.1). Despite this small difference at DH = 2.5%, the overall trend between the performances of hydrolysates produced by the two enzymes upon increasing DH was otherwise similar.

The striking contrasts in the observed performances of SSPHs and WPHs, resulting from the action of two different types of enzymes, trypsin and alcalase, are likely to be sought in the distinct structures of SSPI and WPI when present in the solution. The former exists in the form of dispersed protein aggregates of particle size ~ 226 nm (after ultrasonication), which remain hard to break down further by ultrasonication treatment. WPI on the other hand is relatively well dissolved. As discussed in section 5.3.1, hydrolysis of SSPI aggregates by trypsin tends to mostly produce intermediate-sized fragments, at the DH values studied here. In contrast, at the same comparable DH, alcalase is likely to generate rather small peptides from the exterior of soy protein aggregates. The remaining unhydrolyzed parts of the soy protein aggregates, post alcalase digestion, are probably still of fairly large size (see **Figure 5.2B**). While it is conceivable that those remaining particles may be able to stabilize oil droplets through

Pickering type action, it is not clear that they will be very useful in the fabrication of submicron-sized fine oil droplets. It also seems that the simultaneous presence of small peptides and protein particles contributes to a deterioration of functional properties of SSPI. In contrast, trypsin digestion, where the protein chains tend to be broken in a more uniform manner, resulting in a mixture of intermediate-sized polypeptides, proves to be a much better approach for modification of soy proteins. The differences between the actions of the two enzymes did not arise significantly for WPI, probably because whey protein is well dissolved and not dispersed as particulate aggregates. Thus, for WPHs with the same DH, the emulsifying abilities remained broadly comparable for fragments generated by trypsin and alcalase.

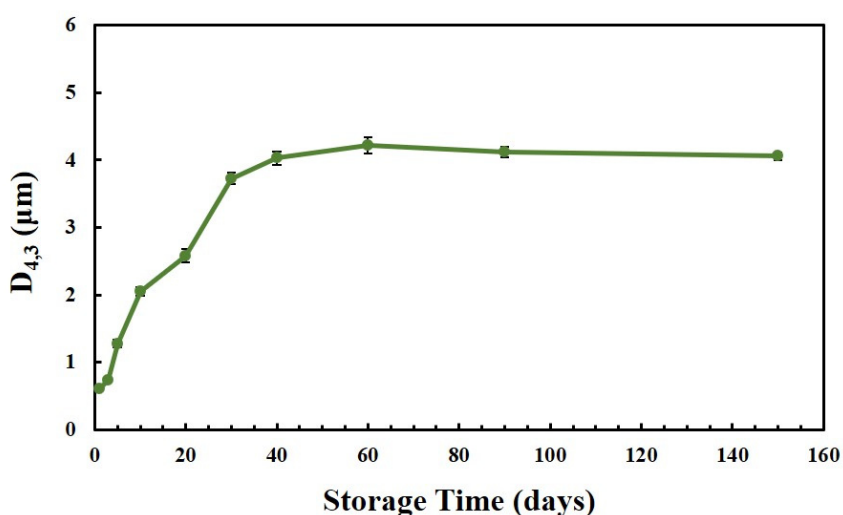


Figure 5.12 The change of mean droplet size $D_{4,3}$ of O/W emulsion, stabilized by SST3, stored at pH 7.5.

As the aim of this whole project is to produce plant based emulsifying agents for the preparation of fine submicron sized O/W emulsion system, our discussions will from now on be limited largely to trypsin generated soy fragments.

Let us now turn attention to the long-term storage stability of emulsions stabilised by soy protein fragments generated by the action of trypsin. At pH 7.5, there was a gradual increase of mean droplet size for all SSPHs stabilised emulsions during the storage, with the growth most clearly seen in the emulsion stabilised by SST3 (**Figure 5.10**). The droplet size $D_{4,3}$ of SST3 based emulsion sample started to dramatically rise from around day 3, but began to slow down from the 30th day onwards (**Figure**

5.12). In the micrograph (**Figure 5.11B**), quite a few large droplets were visible, with the average size $D_{4,3}$ measured to be $4.22 \mu\text{m}$ at the end of 60 days of storage. The size distribution was also observed to become bimodal after this period. Nonetheless, it was also noticed that this emulsion had a relatively Newtonian flow behaviour (**Figure 5.13**) and the droplets remained highly charged, with ζ -potential around $-46 \sim -50 \text{ mV}$ (**Table 5.1**). Thus, it was unlikely for such growth of droplets to be the result of emulsion flocculation, and indeed no significant evidence for any droplet aggregation was seen in the micrograph for this sample (**Figure 5.11B**).

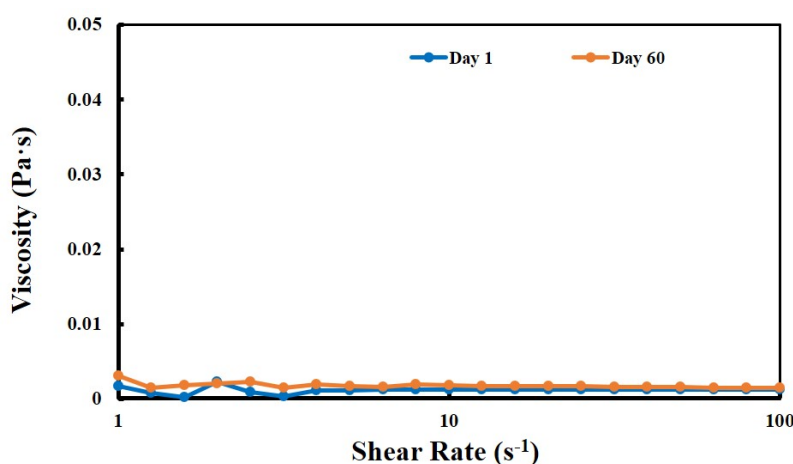


Figure 5.13 Apparent viscosity of O/W emulsions fabricated by SST3 stored at pH 7.5 for 1 day and 60 days.

Furthermore, in protein-stabilized emulsions when the droplets are in a non-flocculated state, there is normally a high level of stability against coalescence, too. This is because the aggregation of droplets is often the first required step towards their coalescence. Yet, with a high level of surface charge, no evidence for flocculation, and adsorbed proteins forming viscoelastic protective interfacial layers around the droplets, coalescence is unlikely to be the main reason responsible for the development of large emulsion droplets in our sample here (Murray, 2011, Dickinson et al., 1988a, Bos et al., 2001).

	pH = 7.5	pH = 4.5	pH = 3.0
Day 1	-50.9 ± 3.3 mV	-6.7 ± 0.9 mV	+17.3 ± 3.5 mV
Day 60	-46.5 ± 3.0 mV	-6.5 ± 0.4 mV	+16.5 ± 3.7 mV

Table 5.1 ζ -potential (mV) of freshly made and stored (for 60 days) emulsion droplets, stabilized by SST3 sample as emulsifiers. Results are shown at different pH conditions.

It is tempting then to associate the coarsening of the droplets to Ostwald ripening. Recall from section 1.1.4.4 that the process of Ostwald ripening is fairly insensitive to the type of emulsifier used, but is mainly controlled by the solubility of the dispersed phase in the dispersion medium (McClements, 2015u). For this process to be significant, the oil phase is required to be sufficiently soluble in the aqueous phase, as this phenomenon involves the mass transportation of oil molecules from smaller to larger droplets (Dickinson, 1992c, Tcholakova et al., 2006). In our case, sunflower oil was used to prepare emulsions, which is fairly hydrophobic and insoluble in water. Moreover, the emulsion sample made from WT1 stored at pH 7.5 was extremely stable, showing no evidence of Ostwald ripening during the 60 days of storage period (see **Figure 4.8B** in section 4.3.3.1). These facts suggest that the formation of larger droplets in our soy protein hydrolysates stabilised samples is not the result of a straightforward Ostwald ripening process, at least not one driven by the direct migration of oil molecules between the droplets through the continuous medium.

At present we have no definitive evidence for the underlying process driving the observed gradual formation of these larger droplets in the system. Nonetheless, a possibility worth further investigation concerns the presence of soy phospholipids on the emulsion stability, as suggested by the observations of Tirok et al. (2001), Drapala et al. (2016) and Drapala et al. (2015). This point is discussed below.

Soy phospholipids are a mixture of low-molecular-weight surfactants and are important constituents of the oil bodies in soybeans. During the extraction of soybean oil, they form complexes with soy storage proteins (Matsumura et al., 2017). It has proved a difficult and expensive process to completely remove all the soy phospholipids from commercial SPI. A typical residual soy phospholipid of 3% (w/w) is often reported in commercial SPI (Arora et al., 2011, Samoto et al., 2007).

Similar to other kinds of low-molecular-weight surfactants, soy phospholipids facilitate the emulsification process. However, the interfacial coatings they form around the oil droplets are rather thin and not sufficient to guarantee the long-term stability of emulsions. This is why emulsion droplets stabilized by such small-molecular-weight surfactants are susceptible to gradual coalescence during their storage (Bos et al., 2001, McClements, 2015x). In our fragmented soy protein based emulsions, the residual soy phospholipids (also known as soy lecithin), while only present in small amounts, are nonetheless able to partially displace proteins from the surface of droplets. This could disturb the viscoelastic network of protein films at the oil droplet surface and introduce small patches at the interface that may lack sufficient degree of protection from proteins (Bos et al., 2001, Petkov et al., 2000, Pugnaroni et al., 2004, Pugnaroni et al., 2003).

Furthermore, and perhaps more significantly, it is known that nonpolar molecules can be transported between dispersed oil droplets via solubilization in surfactant micelles (McClements, 2015m, Moulik, 1996). Although this micelle solubilization effect is still a slow process, it nonetheless allows for the transportation of oil molecules between dispersed phases to proceed at a somewhat faster speed than otherwise in the absence of soy phospholipids.

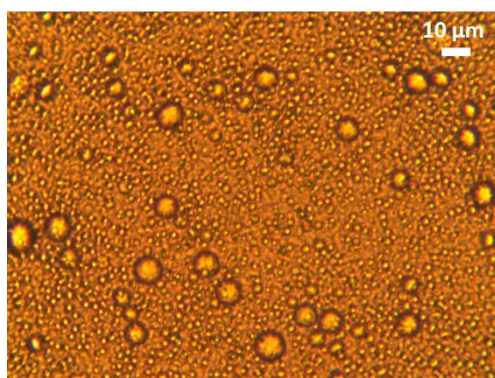


Figure 5.14 Micrograph of WT1 based emulsion stored at pH 7.5, with addition of 0.03% soy lecithin (i.e. 3 g soy lecithin/100 g WT1), following 60 days of storage.

Irrespective of the actual mechanisms responsible for the formation of the large oil drops, we have found experimental evidence that soy phospholipids can accelerate the growth of emulsion droplets during storage. A particularly clear example of this

phenomenon occurs in the otherwise very stable hydrolysed whey protein stabilized emulsions, upon addition of soy phospholipids. We were able to confirm this result by spiking the WT1 stabilised emulsion (found here to be stable at pH 7.5 over 60 days) with a small amount of soy lecithin (i.e. 3 g lecithin/100 g WT1). The micrograph taken for the system after 60 days (**Figure 5.14**) looked remarkably similar to that obtained for fragmented soy protein stabilised emulsion (**Figure 5.11B**).

One may speculate then that if the commercial isolated soy protein used here was further purified from the residual lecithin, the storage stability for (trypsin produced) SSPHs based emulsions may have been just as impressive as those obtained with WPI or its low DH hydrolysates. The exact role played by soy phospholipids in causing the formation of large droplets is worthy of a future work, but is beyond the scope of the present study.

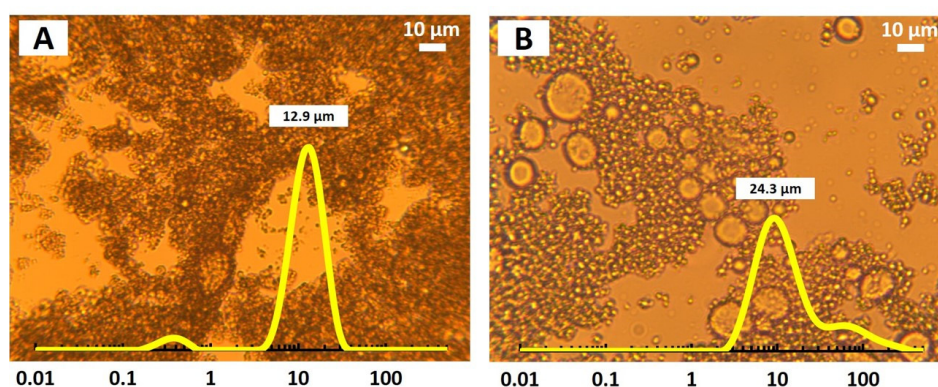


Figure 5.15 Micrographs of SST3 fabricated emulsions, stored at pH 4.5, on day 1 (A) and after 60 days of storage (B). The droplet size distribution and the mean droplet size $D_{4,3}$ are also provided on each photo.

So far, the discussion of emulsions stabilised by trypsin fragmented SSPHs was limited to the pH values away from pI . Next, the impact of pH variation on the colloidal stability of the SSPHs stabilised systems will be considered. Fresh emulsions adjusted to acidic pH conditions, exhibited a marked rapid increase in droplet size (**Figure 5.10**). For instance, the droplets became flocculated and the value of $D_{4,3}$ jumped to 12.9 μm at pH 4.5 for SST3 stabilized emulsion sample (**Figure 5.15A**). This is expected due to an insufficient level of surface charge, where the ζ -potential was found to be -6.7 ± 0.9 mV (**Table 5.1**). Thus, so far, this behaviour is similar to what has been found for WPHs stabilised emulsions (see **Figure 4.7** and **Figure 4.8** in

section 4.3.3.1). However, differences arose when the pH was further lowered to 3.0, with the system retained at the intermediate pH of 4.5 for only a short period (< 5 mins). Unlike the WPHs based systems, where the droplets became well dispersed at pH 3.0 once regaining sufficient charge (see **Figure 4.7** and **Table 4.1** in section 4.3.3.1), on this occasion the flocs did not break down into individual oil droplets for any of the emulsion samples stabilised by SSPHs (**Figure 5.10**). For example, the droplet size of fresh SST3 stabilized emulsion at pH 3.0 was 14.8 μm , which was not all that different from 12.9 μm at pH 4.5. These values are to be compared to $D_{4,3}$ of 0.608 μm at pH 7.5, prior to any pH adjustment.

The same phenomenon also occurred for conjugated SSPHs stabilized emulsions considered in the next section. A discussion of these observations will be provided once the data for the stability of emulsions made by SSPHs and maltodextrin covalent complexes are also presented below.

5.3.4.2 Emulsions based on conjugated soy hydrolysates

When soy protein hydrolysates were conjugated with maltodextrin, all modified SSPHs samples delivered significantly improved emulsifying and stabilizing capabilities, in comparison to their unconjugated counterparts. This was true at all tested pH conditions (**Figure 5.16**).

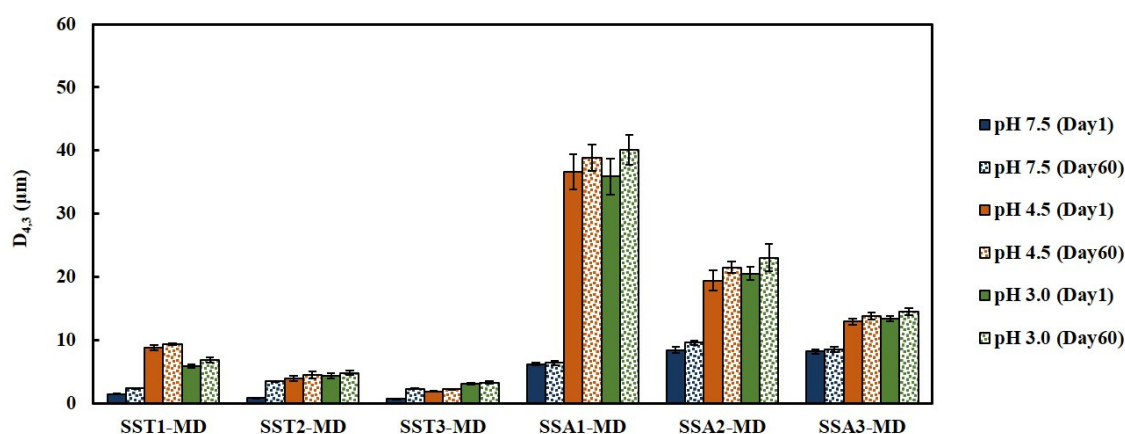


Figure 5.16 The average droplet size $D_{4,3}$ of freshly made and stored (60 days) emulsions, fabricated by conjugates made from SSPHs + maltodextrin, under various pH conditions (i.e. pH 7.5, 4.5 and 3.0).

We present as an example here the results for soy protein hydrolysates, generated by trypsin digestion at DH = 8.0%. It is seen that initially the conjugated and non-conjugated fragments (i.e. SST3-MD and SST3) produced fine emulsions with similar average droplet sizes of 0.638 μm and 0.608 μm at pH = 7.5. The droplet size distributions of the two emulsions closely resembled each other too (compare **Figure 5.17A** and **Figure 5.11A**). However, after 60 days of storage, a significantly higher number of larger droplets was visible in the emulsion sample stabilized by non-conjugated SST3 (compare **Figure 5.17B** and **Figure 5.11B**). The size distributions of the two emulsions are also seen to diverge, reflecting again the formation of a larger number of bigger droplets in the emulsion made by SST3. In the conjugated sample (**Figure 5.17B**), the secondary peak for the part of the distribution curve occurring at sizes larger than 1 μm , remained small relative to that for sizes less than 1 μm . The opposite was observed for the emulsion based on unconjugated SST3 (**Figure 5.11B**). While both emulsions exhibited some degree of coarsening, the average droplet size $D_{4,3}$ was only 2.29 μm for the conjugated polypeptides, whereas it increased to 4.22 μm for the non-bonded fragments.

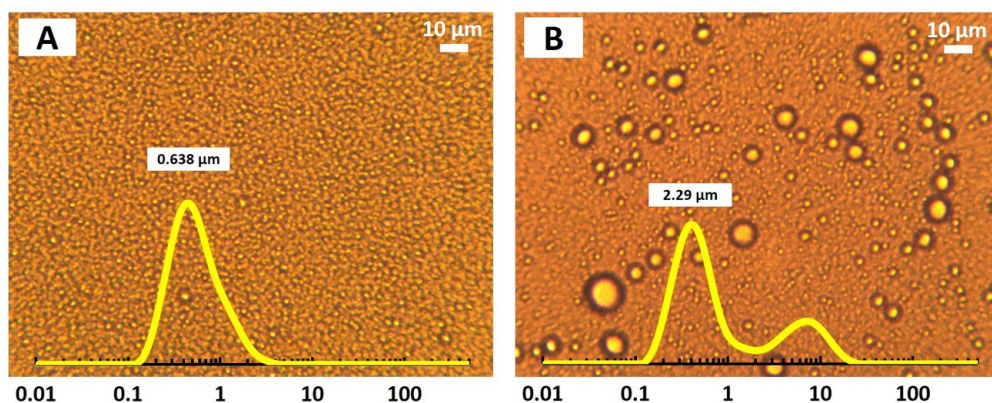


Figure 5.17 Micrographs of SST3-MD fabricated emulsions, stored at pH 7.5, on day 1 (A) and after 60 days of storage (B). The droplet size distribution and the mean droplet size $D_{4,3}$ are also provided on each photo.

The most likely reason for this superior behaviour of the conjugated system is the provision of enhanced steric repulsion as well as the physical hindrance, due to the presence of the polysaccharide moiety of these composite biopolymers (Tcholakova et al., 2006, Dickinson et al., 1988a, McClements, 2015u). If this assertion is true, it

may be possible to further improve the stabilizing ability of our emulsifiers by attachment of larger molecular weight (M_w) polysaccharides (Wooster et al., 2006, 2007, Dunlap et al., 2005). To demonstrate this, conjugated SST3 with maltodextrin DE4-7 (MD7, $M_w = 65$ kDa) and dextran (DX, $M_w = 500$ kDa) were prepared. It was observed that the long-term emulsion stability at pH 7.5 progressively improved with an increase in M_w of the polysaccharide (**Figure 5.18**). For the conjugated soy peptides with polysaccharide of the highest M_w used here, the emulsion remained reasonably stable post 60 days of storage, with $D_{4,3} = 0.665 \mu\text{m}$ as compared to $0.598 \mu\text{m}$ on day 1.

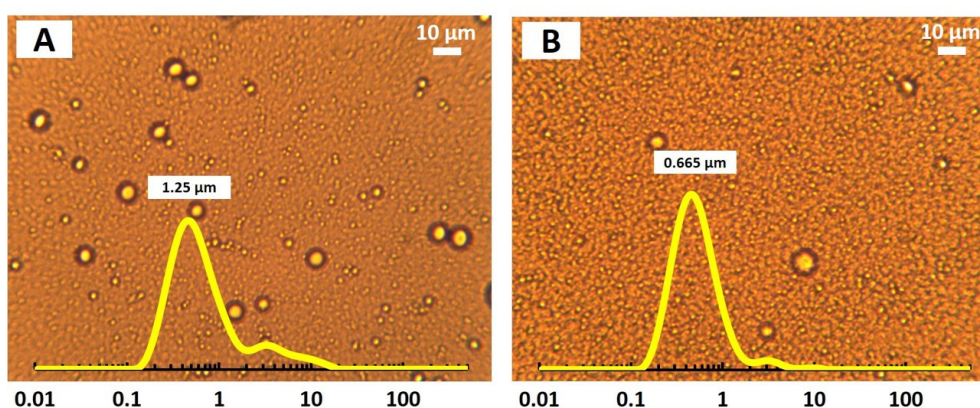


Figure 5.18 Micrographs of emulsions stored at pH 7.5 after 60 days. The emulsions were stabilized by conjugated SST3 + maltodextrin DE4-7 ($M_w = 65$ kDa) and SST3 + dextran ($M_w = 500$ kDa), which are displayed in (A) and (B), respectively. The droplet size distribution and the mean droplet size $D_{4,3}$ are also provided on each photo.

The primary reason for conjugating a protein with a polysaccharide is to improve the stabilizing properties of the former, particularly at pH values close to its isoelectric point. Recall that our results indicated a poor stability against aggregation at pH = 4.5, when droplets were stabilized by the non-bonded SSPHs, or WPHs. However, for the WT1 fragments, covalent bonding with maltodextrin was seen to vastly improve the performance of the emulsifier, to the extent that the emulsion stability at pH = 4.5 was similar to that found at pH = 7.5 (see **Figure 4.13** in section 4.3.3.2). Nonetheless, recall from previous discussions in Chapter 3 and Chapter 4 that the released small peptides at high levels of DH will either start to have insufficient overall adsorption energy or become excessively hydrophilic following covalently bonding with the polysaccharide attachment. In both cases, the presence of too small peptides were

seen to be detrimental to the stability of emulsions, due to their loss of the surface affinity for adsorption onto the surface of oil droplets. Moreover, the existence of a wide spectrum of varying polymer species are likely to lead to some degree of competitive adsorption in these systems. Both effects were demonstrated by the experimental results in Chapter 4 to have induced instability during the long-term storage in emulsion systems fabricated with conjugates derived from the more highly fragmented proteins (see **Figure 4.12** in section 4.3.3.2). These results suggest that in achieving suitable vegetable protein based conjugates, in order to match the excellent performance of WT1-MD, one needs a careful optimisation of the degree of fragmentation of soy proteins. This result is likely to be general and applies equally to most storage plant proteins.

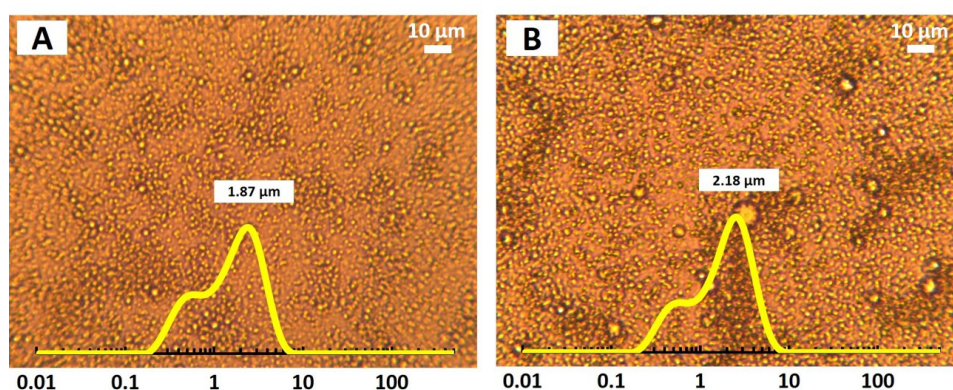


Figure 5.19 Micrographs of SST3-MD fabricated emulsion, stored at pH 4.5, on day 1 (A) and after 60 days of storage (B). The droplet size distribution and the mean droplet size $D_{4,3}$ are also provided on each photo.

Let us now turn attention to the stability of emulsions made of SSPHs + maltodextrin conjugates at pH values close to the isoelectric point of protein/peptides. In general, the flocculation stability of fresh emulsions fabricated with conjugated SSPHs remained somewhat poorer at pH = 4.5, relative to that seen for them at pH = 7.5 (**Figure 5.16**). This can also be observed by comparing the micrographs of the freshly made emulsions stored at pH 4.5 (**Figure 5.19A**) and at pH 7.5 (**Figure 5.17A**), both produced using SST3-MD emulsifier. Clear evidence for some level of droplet clustering was seen in the emulsion sample at pH 4.5, with the average particle size changing from 0.638 μm to 1.87 μm upon pH adjustment. Further support for the flocculation in the system at pH = 4.5 came from a study of the rheological behaviour

(Figure 5.20). The low shear viscosity of this emulsion was markedly higher at pH = 4.5 compared to at pH 7.5. Also, the emulsion sample exhibited shear-thinning behaviour (flow behaviour index = 0.492) at acidic condition, while it was closer to Newtonian at pH = 7.5.

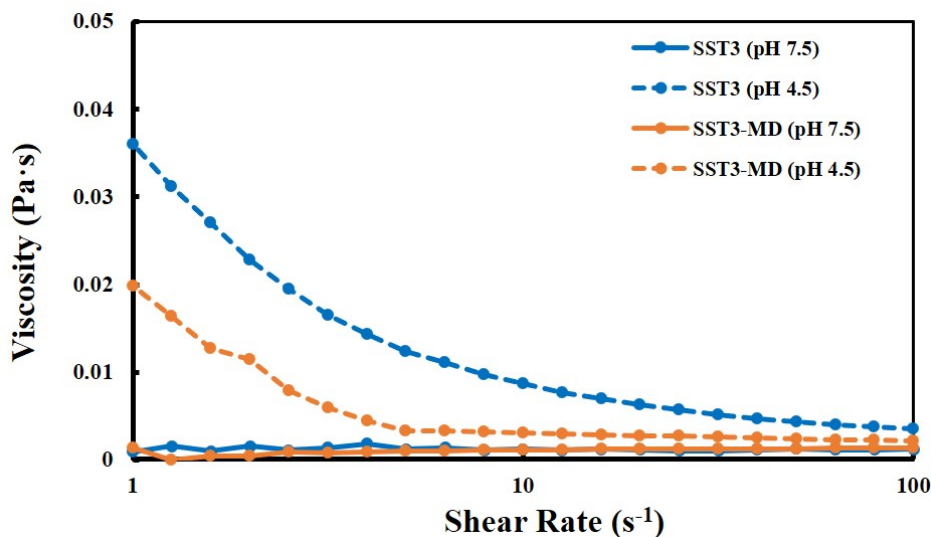


Figure 5.20 Apparent viscosity of freshly made O/W emulsions fabricated by SST3 and SST3-MD, stored at pH 7.5 and pH 4.5.

Despite this result, it has to be said that in comparison with their non-bonded counterparts (i.e. SST3), the conjugated hydrolysates SST3-MD still did offer a significant enhancement in the emulsion stabilising properties against droplet flocculation. The micrograph and the size distribution at pH = 4.5 indicate that the majority of droplet clusters were small and less than 3 μm for the SST3-MD based system, with average size $D_{4,3} = 1.87 \mu\text{m}$ (Figure 5.19A). On the other hand, the non-conjugated SST3 based system showed a much more extensive level of aggregation, with the measured average droplet size being a far larger value at pH 4.5 ($D_{4,3} = 12.9 \mu\text{m}$, see Figure 5.15A). Consistent with those results, the viscosity at low shear rate was also seen to be considerably lower for the emulsion system stabilized by SST3-MD than that of the emulsion stabilized by SST3. This indicates a modification in the flocculated state of the emulsion droplets in the former system, in comparison to the latter (Figure 5.20).

Even with its aggregated morphology, the SST3-MD based emulsion at pH = 4.5 showed far less evidence for the formation of large droplets than was the case at pH = 7.5, following 60 days of storage (compare **Figure 5.19B** and **Figure 5.17B**). As mentioned before, we believe that the formation of larger droplets at such long storage time is largely the result of a limited micelle-solubilization-effect induced Ostwald ripening process. As such, the more compact and aggregated adsorbed protein films formed at pH = 4.5, may resist Ostwald ripening and the shrinkage of droplets more effectively than the more extended but sparsely configured layers at pH = 7.5 (Murray, 2002, Rivas et al., 1984, Graham et al., 1980, Pezennec et al., 2000, Meinders et al., 2001, McClements, 2015u).

The above set of results indicates that the strength of the steric forces provided by adsorbed layers made of SST3-MD, fall somewhat short of those achieved by WT1 (DH = 2.5%) based conjugates. This is likely due to the limited number of covalent bonds formed between soy fragments and polysaccharides, at the value of DH = 8.0%. The conjugated and the unreacted polypeptides will tend to compete with each other for adsorption onto droplet surfaces. This may result in mixed layers, leaving the surface of droplets not sufficiently covered with the desired additional protection from polysaccharides. Thus, as the droplet surface charge is lost at pH 4.5 (ζ -potential = -3.7 ± 0.5 mV, see **Table 5.2**), the lack of electrostatic repulsion between the droplets, coupled with an insufficient steric stabilization, can no longer prevent aggregation of the droplets.

	pH = 7.5	pH = 4.5	pH = 3.0
Day 1	-43.2 ± 4.2 mV	-3.7 ± 0.5 mV	$+16.9 \pm 0.5$ mV
Day 60	-41.1 ± 2.7 mV	-2.8 ± 0.3 mV	$+14.9 \pm 2.7$ mV

Table 5.2 ζ -potential (mV) of freshly made and stored (for 60 days) emulsion droplets, stabilized by SST3-MD sample as emulsifiers. Results are shown at different pH conditions.

It is tempting to follow the same recipe as WT1 to produce MRPs by using SSPHs with lower DH, thus hoping to improve the yield of the Maillard-type biopolymers. For WPI fragments, conjugates made with WT1 (i.e. hydrolysates at DH = 2.5%) was seen to perform far better than those based on WT3 having higher DH of 8.0%. However, one

has to remember that fragmentation of soy protein is a necessary step for the breakup of the aggregated protein particles to ensure a homogenous dry mixture with intimate contacts between protein/peptides and polysaccharide as well as the exposure of chemical reactive sites on the soy protein, prior to Maillard reaction. If the degree of hydrolysis is too low, then this latter requirement would not be met.

A degree of hydrolysis of 2.5% or 5.5% is simply not sufficient to achieve this for soy protein. This point is clearly seen from **Figure 5.16** that for SSPHs having lower levels of fragmentation (i.e. SST1 at DH 2.5% and SST2 at DH 5.5%), their conjugated form did not offer better flocculation stability. Following pH adjustment to 4.5, the droplet size $D_{4,3}$ of fresh emulsions made by SST1-MD and SST2-MD increased to 8.82 μm and 3.87 μm , from 1.45 μm and 0.787 μm (at pH 7.5) respectively. Those data suggested a higher extent of droplet flocculation at pH 4.5, compared to the emulsion made by SST3-MD ($D_{4,3} = 1.87 \mu\text{m}$ at pH 4.5), attributed to the low yield of conjugated biopolymers for systems derived from SST1 and SST2.

In order to improve the degree of conjugation between maltodextrin and soy fragments with high DH of 8.0%, we prepared conjugated SST3 at increased weight ratio of maltodextrin (i.e. the ratio of SST3/MD = 1:3, 1:4 and 1:5). Unfortunately, there was no significant enhancement in the stabilizing ability against droplet flocculation at pH 4.5. This again indicates the restricted level of Maillard reaction between soy protein/peptides and polysaccharide. We believe that this relatively inefficient reaction between the two biopolymers arises mainly from the aggregated state of soy protein or its hydrolysates (i.e. the average particle size of various SSPHs samples is around 80~200 nm). In addition, the presence of non-protein substances in the form of impurities in commercial SPI, may also play a role in further reducing the degree of reaction between polypeptides and polysaccharides. These minor components bind on protein molecules through strong electrostatic and hydrophobic interactions, masking or affecting the availability and reactivity of $\alpha\text{-NH}_2$ on soy protein materials (Nash et al., 1967, Skorepova et al., 2007, Genovese et al., 2007).

For freshly made emulsion samples adjusted to even lower pH conditions (i.e. pH 3.0 and 2.0), clustered droplets already formed at pH 4.5 were not broken down (**Figure 5.21**). Even if the sample was brought back to pH 7.5 (with ζ -potential = -37.2 ± 2.6

mV) where the freshly made emulsion without acid treatment was well dispersed, the flocs of droplets still remained visible (compare **Figure 5.22A** and **Figure 5.17A**).

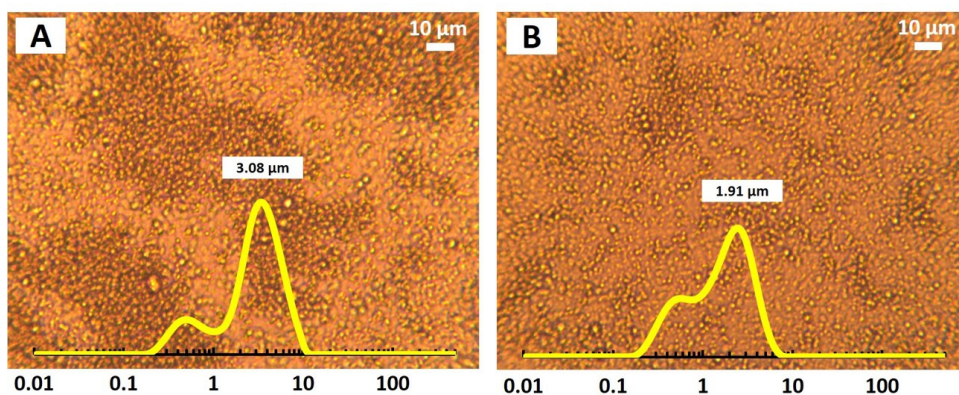


Figure 5.21 Micrographs of emulsions produced by SST3-MD conjugates as emulsifiers, after adjustment of pH to 3.0 (A), then to 2.0 (B). The emulsion sample was kept at the intermediate pH for only a few minutes. The droplet size distribution and the mean droplet size $D_{4,3}$ are also provided on each photo.

Recall from section 4.3.3.1 that this same situation did not occur in emulsions based on whey protein materials, as long as the sample was kept just a short time (< a few minutes) at pH = 4.5, before lowering pH to 3.0 or back up to 7.5 again. The same phenomenon for whey protein based emulsions, was only seen when the flocculated droplets formed at pH 4.5 were allowed to age for more than a few days (see **Figure 4.11A** in section 4.3.3.1). This phenomenon probably arises from the conformational rearrangements of adsorbed protein/peptides on the surface of the droplets, via exposure of their hydrophobic residues during the storage of emulsions (McClements, 2004, Freer et al., 2004, Kim et al., 2002a, 2002b). These rearrangements and mutual diffusion of the polypeptides between adjacent surface layers could result in the formation of interfacial films shared between neighbouring droplets. Once such layers are formed, switching the electrostatic repulsion back on between the droplets by adjustment of pH, is no longer sufficient to redisperse the emulsion system. However, it seems that the processes leading to the formation of such shared layers, happen rapidly when soy protein materials are involved, but take a while to be established with whey protein based fragments.

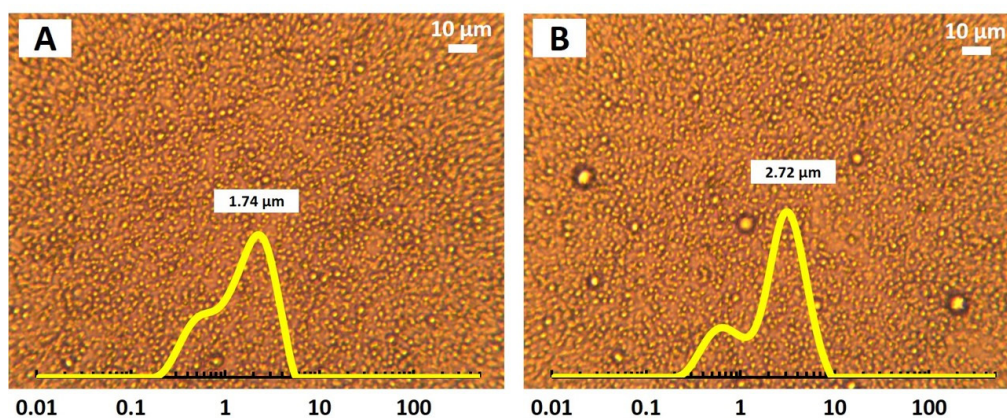


Figure 5.22 Micrographs of emulsion produced by SST3-MD as emulsifiers, stored at pH 7.5, on day 1 (A) and after 60 days of storage (B). This emulsion was subjected to an acid treatment by adjustment of pH to 4.5, then back up to 7.5. The emulsion sample was kept at pH 4.5 for only a few minutes. The droplet size distribution and the mean droplet size $D_{4,3}$ are also provided on each photo.

5.4 General Conclusions

The current study systematically evaluated the ability of commercial isolated soy protein (SPI), via a combined modification of enzymatic hydrolysis and covalent conjugation of hydrolysates with maltodextrin, to form an emulsifier capable of forming fine submicron-sized stable emulsions at various pH conditions. The dual role of the degree of hydrolysis (DH) in improving the solubility of soy protein on one hand, and the difficulties of linking soy hydrolysates to polysaccharide on the other, have been highlighted.

The hydrolysis of soy protein was conducted with two very different enzymes (i.e. trypsin and alcalase). The action of both enzymes significantly improved the (apparent) solubility of soy protein. At the same achieved DH, the soy protein fragments generated by trypsin showed distinctly superior solubility, as well as emulsifying properties, compared to those produced by alcalase. These differences were related to how efficiently soy protein, existing as aggregated colloidal particles dispersed in the solution, can be turned into polypeptides. Trypsin, due to the rather selective nature of peptide bonds it cleaves, was believed to produce a large number of intermediate-sized peptides by getting into the core of soy protein aggregates and

chopping down chains uniformly. The obtained peptides were demonstrated to be effective emulsifying agents. Soy fragments, with the highest DH used here (i.e. SST3 with DH = 8.0%), were able to produce an equally fine O/W emulsion system at pH 7.5 ($D_{4,3} = 0.608 \mu\text{m}$) as that achieved by milk whey protein materials. Alcalase, having a broad range of amino acid substrates, on the other hand, was suggested to generate a set of small peptides, leaving a large proportion of less affected protein particles in the core. Such kind of hydrolysates, with small peptides mixing with large particles, were seen to deteriorate the emulsifying and stabilizing properties of soy protein, even with low DH values.

With regards to the long-term stabilizing properties of fragmented soy protein, a development of large droplets was observed in all the emulsions made by SSPHs stored at pH 7.5. This phenomenon was attributed mainly to the Ostwald ripening, facilitated by a small amount of soy phospholipids present in commercial SPI.

When the pH of freshly made emulsion at pH 7.5 was lowered to 4.5, emulsion droplets became strongly flocculated due to reduced electrostatic repulsion. This flocculation instability at acidic conditions, as well as the coarsening of oil droplets, was seen significantly modified, when fragmented soy protein was covalently bonded with maltodextrin. Such improvement was true for all the conjugated SSPHs samples, and was most remarkable in conjugated SST3 stabilized emulsion. The value of $D_{4,3}$ was $2.18 \mu\text{m}$ for the emulsion made from SST3-MD stored at pH 4.5 for 60 days, compared to non-bonded SST3 ($D_{4,3} = 24.3 \mu\text{m}$). Despite this enhancement in emulsion stability, there were still some flocculated droplets present in the sample of SST3-MD stabilized emulsion. In contrast, the emulsion made by conjugated whey protein fragments did not exhibit any evidence of droplet clustering at pH 4.5.

The limited flocculation stability of conjugated soy protein materials at pH 4.5 is most likely due to the insufficient degree of reaction between protein chains and maltodextrin. Major obstacles come from the poor solubility and the aggregated state of soy protein materials, which fail to offer a well-blended dry mixture of protein chains and polysaccharides at a molecular scale. Under such circumstances, the Maillard reaction between these two biopolymers cannot proceed efficiently during heating, with thermal-induced protein aggregation predominating. This situation was seen

gradually ameliorated with increased level of fragmentation of soy protein (by trypsin). Nonetheless, it is noted that the improved colloidal functionalities of conjugated fragments, resulting from a higher level of hydrolysis, will be offset by further fragmentation (this point has been clearly seen and discussed for whey protein materials in Chapter 4). This leads to an optimum value of DH for plant proteins in order to synthesize the most suitable Maillard based emulsifiers. For SPI material used in this study, this value was found to be around 8%.

Another feature reported here was the irreversible aggregation of emulsion droplets stabilized by soy protein materials post acid treatment. Once the emulsion droplets became flocculated, regaining sufficient level of electrostatic repulsion was not able to effectively separate the clustered droplets into individual ones. This was completely different from the case seen with milk whey protein/peptides (discussed in Chapter 4).

To summarize, the findings in this chapter suggest that it is not easy to modify commercial isolated soy protein to be a suitable colloidal material. The difficulties are suggested to mainly originate from the structural and compositional characteristics of commercial soy protein. Enzymes having a high selectivity on cleavable peptide bonds, such as trypsin in our case, are shown to be beneficial for overcoming those obstacles. For plant based polypeptides and their conjugated form to be good emulsifiers, one needs a careful optimisation of the degree of fragmentation.

Chapter 6 Emulsifying and Stabilizing Properties of Soy Peptides Produced by Ultrafiltration and Covalently Bonded with Maltodextrin

6.1 Introduction

It has been seen from Chapter 4 and 5 that excessive hydrolysis, with large content of small peptides released at high levels of fragmentation, induced detrimental effect on the emulsifying and stabilizing properties of proteins. In this chapter, we aim to further investigate the critical size of a protein fragment for it to fulfil the role of an effective emulsifier and colloidal stabilizer, following its bonding with polysaccharide.

As trypsin generated polypeptides were demonstrated in the previous two chapters to exhibit a superior colloidal functional property than those produced by the action of alcalase (though the difference is not so huge between whey protein fragments obtained by the action of these two enzymes), only the polypeptides produced by trypsin are used in the current study in this chapter. The mixture of protein hydrolysates is first separated via membrane ultrafiltration to obtain protein fragments of three different size ranges (i.e. larger than 30 kDa, between 10~30 kDa and less than 10 kDa). Conjugated polymers are then produced from these fractions of polypeptides, and are assessed for their emulsifying and emulsion stabilizing abilities under different pH conditions.

It is useful to note here that in membrane ultrafiltration, whether a macromolecule will pass or be retained by a membrane of a given pore size depends not only on the molecular size of the macromolecule, but also on a few other factors, such as the shape (e.g. linear or globular) and the charge of the macromolecule. Moreover, membranes made from different materials, although claimed to have the same molecular-weight-cut-off value, can exhibit distinct retention behaviours, due to the distribution of their pore sizes (Schratter et al., 2004). For these reasons, membrane ultrafiltration can only be viewed as an efficient tool for a rough separation of biopolymers, in accordance to the molecular weight and size.

Nonetheless, for a given claimed cut-off value, the membrane can reject at least 90% of hypothetical globular solutes that are equal to or above this value (Schratter et al.,

2004). Therefore, using this separation technique, one can still gain a reasonably good insight into the impact of the molecular size of a polypeptide on the colloidal performance of the conjugated emulsifier made from it.

6.2 Materials and Methods

6.2.1 Materials

The commercial isolated whey protein (WPI) and soy protein (SPI), the enzyme trypsin, and all the other chemicals used in this study are the same as those used in Chapter 4 and Chapter 5. The stirred ultrafiltration cell (Amicon UFSC400001, volume 400 mL) and the disc membranes (PLC010 and PLCTK with molecular weight cut-off 10 kDa and 30 kDa, respectively) were purchased from Millipore (Merck, UK).

6.2.2 Hydrolysis of WPI and SPI by trypsin

Three batches of WPI (2.5 g/batch) were hydrolysed by trypsin to achieve three different degrees of hydrolysis (i.e. DH = 2.5%, 5.5% and 8.0%), accordingly. This is for obtaining sufficient amount of protein fragments in each of the molecular size ranges studied. The digestion of WPI was conducted following the procedure described in section 4.2.2. Those three batches of whey protein hydrolysates were then incubated in the ice bath with gentle stirring for 15 min, and then stored there for further fractionation by membrane.

For soy protein, the hydrolysis was conducted according to the procedure in section 5.2.2. Unlike the preparation of whey protein fragments, the three batches of SPI (2.5 g/batch) were all digested to achieve DH = 8.0%, for the ease of collection of the final products. This DH was chosen since according to the preliminary experiments, the hydrolysis of soy protein at low DH values (e.g. 2.5% and 5.5%) could only generate a tiny amount of soy peptides less than 10 kDa. The three batches of digested soy protein were also mixed (for 15 min) and stored in the ice bath.

6.2.3 Fractionation of polypeptides by membrane ultrafiltration

The whey protein hydrolysates were fractionated by ultrafiltration with a stirred cell and disc membrane system in a discontinuous manner. They were first separated by the 30 kDa molecular weight cut-off (MWCO) membrane in the cell. The separation was operated at 45 psi in the ice bath, and proceeded until the volume of the retentate in the stirred cell was reduced to about 100~120 mL. Then a further second separation was conducted by adding 250 mL deionised water into the stirred cell, and continued until the volume retained in the cell was concentrated down to about 100~120 mL. This procedure was repeated yet one more time, in order for a relatively complete removal of the polypeptide chains less than 30 kDa from the retentate. The protein fragments retained by the membrane were assumed to have a molecular size larger than 30 kDa (labelled as WR30). This retentate was collected and then freeze dried over a period of 48 h. At the same time, the permeate was further separated by the 10 kDa MWCO membrane, which generated a further retentate (labelled as WR10) and a permeate (labelled as WP10). The polypeptides in this retentate and permeate should then have a molecular size between 10~30 kDa and < 10 kDa, respectively. Both these two fractions of polypeptides were also collected separately and freeze dried. A moderate heating treatment (80°C, 5 min) was applied to all the freeze-dried samples, in order to ensure the complete inactivation of enzyme activity.

Soy protein hydrolysates were fractionated in the same way as the whey protein fragments, as described above. The fractions collected from this two-step separation process were labelled as SR30, SR10 and SP10 to identify the soy polypeptide chains in the size ranges of > 30 kDa, between 10~30 kDa and < 10 kDa.

6.2.4 Preparation of protein-polysaccharide conjugates

The Maillard reaction products (MRPs) were prepared between maltodextrin DE16.5-19.5 (MD, $M_w = 8.7$ kDa) and different fractionated protein samples (i.e. WR30, WR10, WP10 and SR30, SR10, SP10) using the dry heating route. The ratio of added maltodextrin to peptides was 2:1 (based on weight). The details of the preparation procedure were the same to the ones described in section 4.2.3.

The Maillard reaction products (MRPs) are denoted using the same convention as that for conjugated whey protein materials in Chapter 4, i.e. starting with the type of the polypeptides, followed by polysaccharide. For example, the MRPs made from whey

protein fragments larger than 30 kDa, conjugated with maltodextrin DE16.5-19.5, are marked as WR30-MD throughout the study.

6.2.5 Electrophoresis analysis

SDS-PAGE was performed under reduced conditions, in order to confirm the fractionation of hydrolysed protein. The detailed procedure was once again the same as the ones given in section 4.2.4.

6.2.6 Preparation of emulsions

O/W emulsions (10 vol.% sunflower oil), made by various conjugated samples, were prepared according to the procedure in section 4.2.7. The pH of the freshly made emulsions was adjusted to two pH conditions (i.e. pH 7.5 and 4.5) with 1 M NaOH or HCl. The emulsion samples were stored at 4°C for further investigations.

6.2.7 Storage stability of emulsions at different pH conditions

The stability of emulsions was assessed by sizing the emulsion droplets and examining the microstructure of the emulsion samples. The instruments involved in the measurements are the same as those applied in Chapter 4. The assessments were performed at various stages during the storage period.

6.2.8 Statistical analysis

All the measurements were performed in triplicate. The obtained data was averaged and reported as a mean value in each case. All the calculations were analysed using Microsoft Excel 2016.

6.3 Results and Discussions

6.3.1 Molecular weight profiles

In this section, the separation of protein hydrolysates is confirmed based on the molecular size. The peptide profiles of different fractions of whey protein and soy protein hydrolysates were analysed by reducing SDS-PAGE (**Figure 6.1**). Similar to

Chapter 4 and Chapter 5, the major components of intact WPI (lane W) and ultrasonicated SPI (lane S), were marked on the gel sheet as reference. The fractions of polypeptides larger than 30 kDa, between 10~30 kDa, and less than 10 kDa were respectively displayed in lane 1, 2 and 3 for whey protein and lane 1*, 2* and 3* for soy protein. Distinct differences were observed between those fractions.

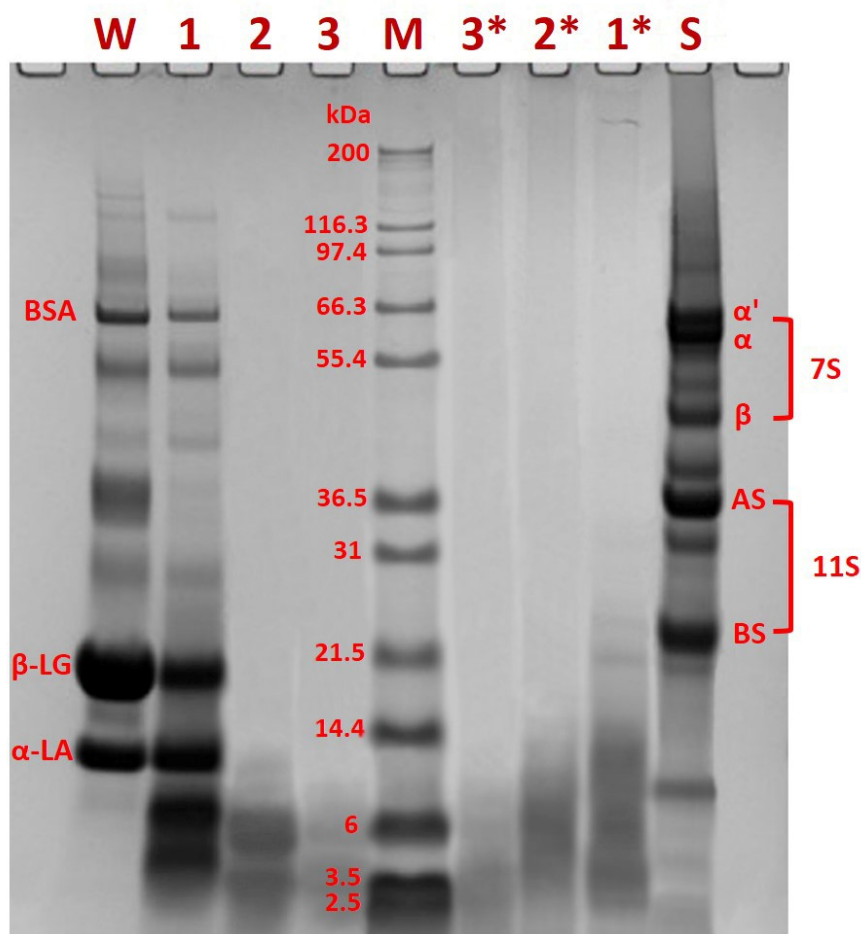


Figure 6.1 Reducing SDS-PAGE analysis of the peptide profiles for various fractionated protein samples. Lane W is intact WPI and lane S is ultrasonicated SPI. Lane 1, 2, 3 are the fractions of polypeptides derived from WPI (produced by trypsin digestion) of molecular size larger than 30 kDa, between 10~30 kDa and less than 10 kDa, respectively. Lane 1*, 2*, 3* are the fractions of polypeptides derived from ultrasonicated SPI (produced by trypsin digestion) of molecular size larger than 30 kDa, between 10~30 kDa and less than 10 kDa, respectively. Lane M is the molecular weight ladder (with values presented in the unit of kDa).

For fractionated polypeptides derived from whey protein, the pattern of the retentate WR30 (lane 1) was similar to that of the hydrolysates at low DH 2.5% (i.e. WT1, see

lane 1 in **Figure 4.1**). This indicates that a sizeable proportion of the released polypeptides in the retentate did not separate from one another after membrane ultrafiltration. This is probably due to the fact that these chains still bind with other peptides through non-covalent or covalent bonds, such as hydrophobic interactions, disulphide bonds or the less specific electrostatic interactions. This stops the passage of such associated peptides through the pores of the membrane (Wu et al., 1998), even though individual chains should have been able to go through. When these interactions are totally broken up in the reducing SDS-PAGE buffering system, all these large and small associated polypeptides eventually become free and show up on the gel sheet.

It is also seen that the bands of unaffected β -LG (18.4 kDa) and α -LA (14.2 kDa) substantially or completely disappeared from the two fractions of peptides less than 30 kDa (WR10 in lane 2 and WP10 in lane 3). This is probably due to the fact that most of these proteins cannot truly dissolve into individual molecules, but instead exist as protein aggregates. That is why they are largely retained by the membrane with a molecular weight cut-off of 30 kDa. Nonetheless, it is suspected that the aggregates they form are of very small size which consist of only a few protein molecules, since the solution formed by whey protein or its hydrolysates are generally clear without any visible particles at pH 7.5 (see **Figure 4.3**). Moreover, the bands in lane 2 and 3 were weaker than those in lane 1. This is probably because a large content of small peptides that are contained in those two fractions of peptides (< 30 kDa) are likely to be less than 2.5 kDa. Therefore, they are too small to be detected on the gel sheet, once freed due to the breakup of all the inter-molecular associations under reducing conditions.

Likewise, for soy hydrolysates, as all the covalent and non-covalent bonds are completely broken between generated polypeptides during SDS-PAGE analysis, the three fractions were seen to have different molecular weight patterns. For instance, the polypeptides in the sample of retentate SR30 (consisting of fragments more than 30 kDa, see lane 1*) were abundant in the regions of 3 ~14 kDa, as compared to the other two fractions (i.e. lane 2* and 3*). Peptides in the retentate SR10 (made of chains having a molecular size of 10~30 kDa, see lane 2*) were more prominent in the size range between 4~10 kDa. As with the fraction of whey protein peptides less than 10 kDa (WP10 in lane 3), the equivalent soy peptides (SP10 in lane 3*) also had relatively

faint bands, again indicating many released small polypeptides were beyond the limit of detection by the gel sheet.

6.3.2 Morphology and stability of emulsions

In this section, the emulsifying and emulsion stabilizing properties of the conjugated biopolymers made from maltodextrin and polypeptides in each size range are assessed. The emulsion stability is examined at two different pH conditions, i.e. pH 7.5 and pH 4.5. It is presented here the results for the average droplet size and the droplet size distribution. The microstructure of emulsion samples is also examined using optical microscopy.

6.3.2.1 Emulsions based on conjugates made from WR30 and SR30

(fragmented whey and soy protein of molecular size larger than 30 kDa)

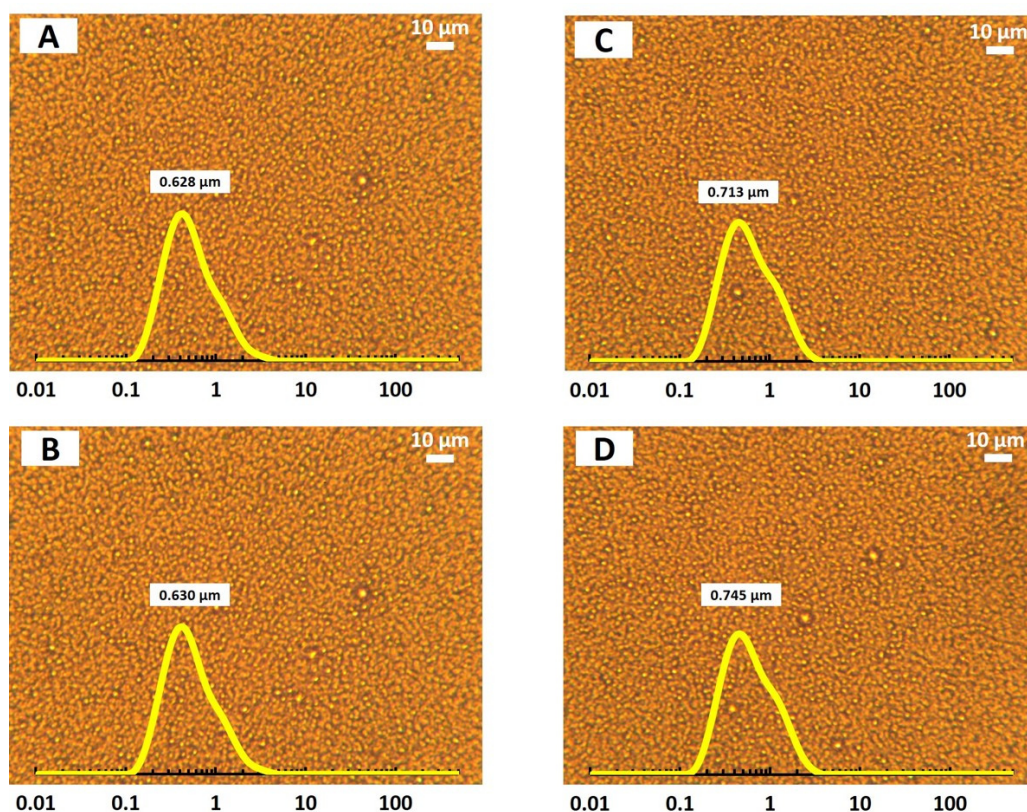


Figure 6.2 Micrographs of conjugated WR30 fabricated emulsion. The freshly made and stored (for 60 days) samples at pH 7.5 are shown in (A) and (B), respectively. The samples adjusted to and stored at pH 4.5 on day 1 (C) and after 60 days of storage (D) are also displayed. The droplet size distribution and the mean droplet size $D_{4,3}$ are provided on each photo.

Conjugated whey protein fragments (WR30-MD) delivered excellent colloidal functionalities, irrespective of the pH condition at which the emulsion was stored (**Figure 6.2**). From the micrographs, the oil droplets were observed to remain well dispersed, with $D_{4,3}$ around 600~700 nm, during the entire storage period of 60 days.

As for conjugated soy fragments (SR30-MD), these were able to form fine emulsion at pH 7.5 ($D_{4,3} = 0.683 \mu\text{m}$, see **Figure 6.3A**), which has similar mean droplet size as that fabricated by the equivalent whey protein materials (i.e. WR30-MD). However, a development of larger droplets in this emulsion sample during the storage period was clearly visible (**Figure 6.3B**).

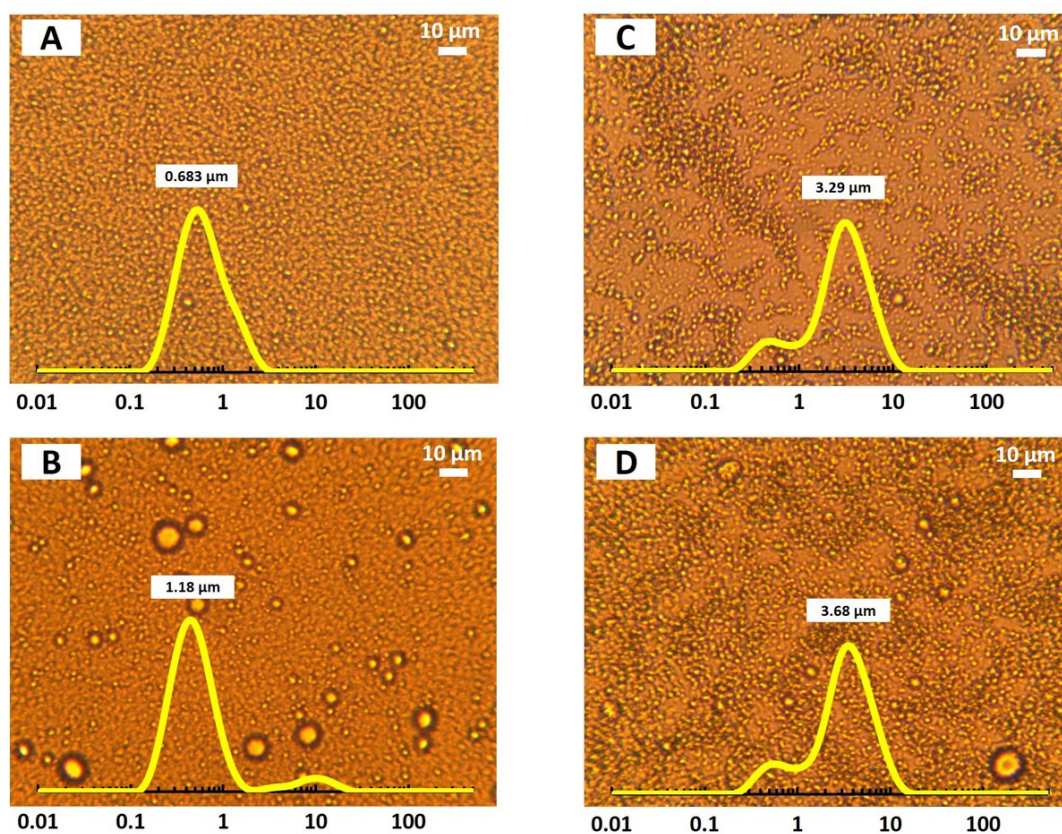


Figure 6.3 Micrographs of conjugated SR30 fabricated emulsion. The freshly made and stored (for 60 days) samples at pH 7.5 are shown in (A) and (B), respectively. The samples adjusted and stored at pH 4.5 on day 1 (C) and after 60 days of storage (D) are also displayed. The droplet size distribution and the mean droplet size $D_{4,3}$ are provided on each photo.

As most of the small fragments (less than 30 kDa) have been removed by membrane ultrafiltration from the retentate polypeptides SR30, the occurrence of large droplets in

this emulsion sample cannot simply be attributed to droplet coalescence, induced by the displacement of larger polymer chains by the smaller ones from the surface of droplets. Instead, it is more likely that it was the result of the slow Ostwald Ripening process, facilitated by the presence of a small amount of soy lecithin impurity in the system, as was discussed in Chapter 5.

Nonetheless, the growth of droplets in SR30-MD stabilized emulsion was observed to be much less pronounced, relative to that seen in the emulsion sample stabilized by SST3-MD (compare **Figure 6.3B** and **Figure 5.17B**). The droplet size $D_{4,3}$ for the former and the latter (after 60 days) were 1.18 μm and 2.29 μm , respectively. The size distribution and micrographs also showed that fewer large oil droplets were formed in the emulsion stabilized by the conjugated SR30. This is attributed to the fact that more chains of larger molecular size are present in the sample SR30-MD (conjugates made from the fraction of soy fragments larger than 30 kDa), compared to in the sample SST3-MD, when the same amount of emulsifiers (based on weight) were used to produce the emulsion. These large polymers play an important role in forming strengthened viscoelastic interfacial layers which offer a better emulsion stability (particularly against Ostwald ripening and coalescence) than smaller polymers do (as was discussed in Chapter 4) (Chen et al., 2019, McClements, 2015u, Schröder et al., 2017, Ipsen et al., 2001).

When the pH of this fresh emulsion (made using SR30-MD) was lowered to pH 4.5, some of the well dispersed oil droplets became flocculated (**Figure 6.3C**). The measured mean droplet size suggests that the flocculation in this sample was significantly worse than that seen in the SST3-MD fabricated emulsion, as displayed in **Figure 5.19A** ($D_{4,3}$ for the former and the latter were 3.29 μm and 1.87 μm , respectively). This is probably due to the lower level of reaction between the fractionated sample SR30 and maltodextrin. Given the same amount of materials (based on weight), there is supposed to be a larger content of non-fully digested protein particles remaining in the fraction of soy peptides SR30 than in the SST3 sample. As discussed in Chapter 5, the presence of such protein particles is not favourable for an intimate mixing of the protein material (in the sample SR30) with maltodextrin at molecular level, thus restricting their bonding with polysaccharide during Maillard reaction. Therefore, the oil droplets stabilized by the emulsifiers SR30-

MD lack sufficient inter-droplet repulsion to prevent them from approaching one another. This becomes particularly problematic in the absence of surface charge at pH 4.5 where electrostatic repulsion is also largely switched off. Following a storage period of 60 days, these flocculated droplets were seen to have undergone some extent of slow coalescence. The micrograph of this emulsion sample showed the appearance of a few large oil droplets (Figure 6.3D).

6.3.2.2 Emulsions based on conjugates made from WR10 and SR10 (fragmented whey and soy protein of molecular size between 10~30 kDa)

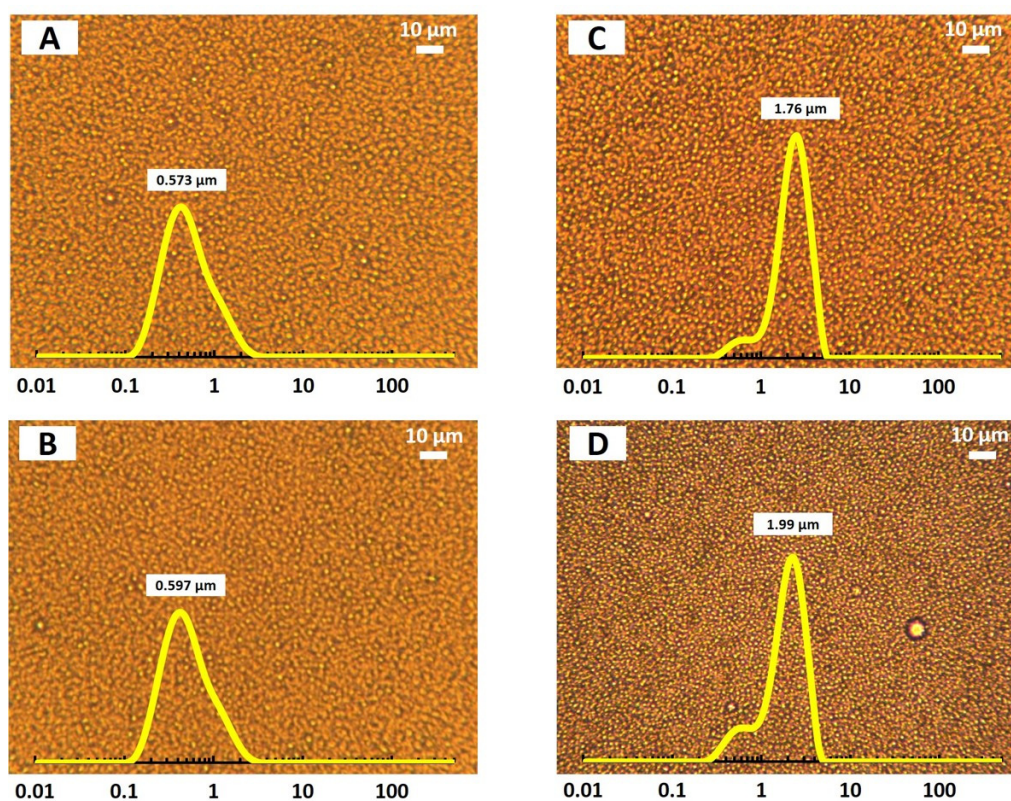


Figure 6.4 Micrographs of conjugated WR10 fabricated emulsion. The freshly made and stored (for 60 days) samples at pH 7.5 are shown in (A) and (B), respectively. The samples adjusted to and stored at pH 4.5 on day 1 (C) and after 60 days of storage (D) are also displayed. The droplet size distribution and the mean droplet size $D_{4,3}$ are provided on each photo.

Conjugated whey protein fragments (WR10-MD) were seen to have formed finely dispersed oil droplets at pH 7.5 ($D_{4,3} = 0.573 \mu\text{m}$, see Figure 6.4A), which were able

to maintain stable during the long-term storage of 60 days ($D_{4,3} = 0.597 \mu\text{m}$, see **Figure 6.4B**).

For fresh emulsion adjusted to pH 4.5, a slight extent of droplet clustering was observed in the micrograph of the sample ($D_{4,3} = 1.76 \mu\text{m}$, see **Figure 6.4C**). This indicates an insufficient level of steric stabilization between these emulsion droplets, which led to droplet flocculation. The lack of steric repulsion is likewise attributed to a large proportion of unconjugated protein fragments present in the mixture of emulsifying agents. However, it is suspected that the reason for their presence is different from that in the case of fragmented soy protein based conjugates (e.g. SR30-MD and SST3-MD). For those latter systems, a large number of soy protein chains being non-bonded with polysaccharide is mainly due to their aggregated nature, present as protein particles, which disables the intimate blending with polysaccharide and the exposure of reactive sites (i.e. lysine or *N*-terminal residue on protein materials) for Maillard reaction. In contrast, for this whey protein system (i.e. the dry mixture of WR10 + maltodextrin), the presence of excessive number of unreacted protein fragments is probably due to the shortage of maltodextrin molecules. As the molecular size of protein fragments in the fraction WR10 (fragments between 10~30 kDa) is much smaller than that in the fraction WR30 (fragments larger than 30 kDa), the total number of polypeptide chains for a fixed amount (based on weight) of WR10 sample becomes much larger than that for the same amount of WR30 sample. Given that in the current experiments, maltodextrin is always added to fragmented protein samples at the same weight ratio (i.e. 2:1), the molar ratio of protein fragments to maltodextrin in the sample WR10 + maltodextrin will be considerably bigger as compared to in the system of WR30+ maltodextrin. Therefore, at the currently used weight ratio (2:1) of maltodextrin to fragmented protein, there will certainly be a large proportion of polypeptides that find no maltodextrin molecules to bond with. Nonetheless, we did not investigate whether the flocculation stability of emulsions will be further enhanced if an additional amount of maltodextrin is introduced to the system WR10 + maltodextrin prior to Maillard reactions. Despite being slightly flocculated, this emulsion displayed a reasonable level of stability to coalescence during storage, with almost no significant formation of large droplets occurring (see micrograph in **Figure 6.4D**).

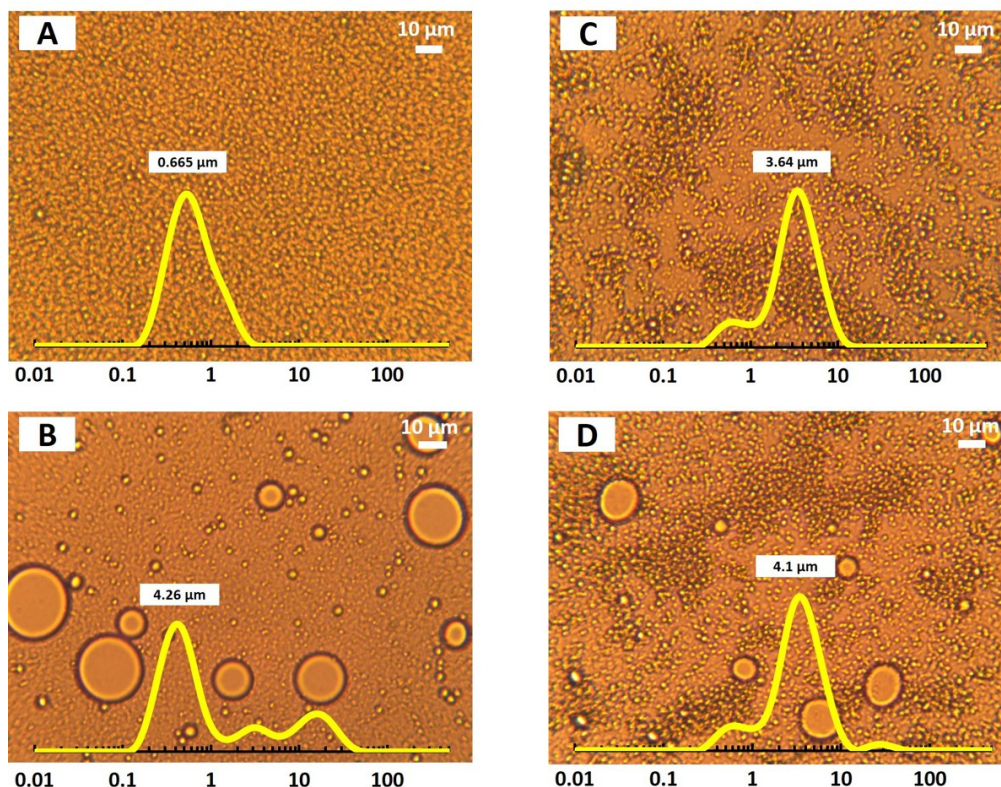


Figure 6.5 Micrographs of conjugated SR10 fabricated emulsion. The freshly made and stored (for 60 days) samples at pH 7.5 are shown in (A) and (B), respectively. The samples adjusted to and stored at pH 4.5 on day 1 (C) and after 60 days of storage (D) are also displayed. The droplet size distribution and the mean droplet size $D_{4,3}$ are provided on each photo.

Similarly, conjugated soy fragments (SR10-MD) also displayed excellent emulsifying ability at pH 7.5 ($D_{4,3} = 0.665 \mu\text{m}$, see **Figure 6.5A**). While good at producing initially fine emulsion, these conjugated polymers were not seen to be particularly good emulsion stabilizers. There were very large droplets formed (bigger than $10 \mu\text{m}$) in the emulsion sample, following a storage of 60 days (see micrograph in **Figure 6.5B**). This is probably due to the coalescence of droplets and possibly also the simultaneous Ostwald ripening process (as discussed in Chapter 5). Thus, the stability of this emulsion was worse, in contrast to the emulsion fabricated with conjugated polymers made from larger polypeptides (i.e. SR30-MD, see **Figure 6.3B**). These results indicate that the conjugated polymers made from small polypeptides are less able, than the counterparts made from large peptides, to prevent destabilization processes from taking place.

As for the stability of the emulsion (fabricated with SR10-MD) at pH 4.5, a certain extent of droplet flocculation was observed immediately after pH adjustment (with $D_{4,3} = 3.64 \mu\text{m}$, see **Figure 6.5C**), which is likewise attributed to the presence of a large proportion of non-bonded soy polypeptide chains in the system, probably because of the shortage of maltodextrin (as explained previously in this section for the system of WR10 + maltodextrin). As this fractionated soy peptides sample (SR10) forms a clear solution, this signifies that most of the large protein particles are depleted via membrane ultrafiltration. In future work, it is worth examining whether adding more maltodextrin to this fractionated soy polypeptide sample will effectively promote the yield of conjugated polymers, allowing for producing fully plant based emulsifiers that offer better stabilization to droplet flocculation under acidic conditions.

After storage for 60 days, a few large droplets were found to have developed (see micrograph in **Figure 6.5D**). The situation was worse than that seen in the emulsion sample fabricated by conjugates made from unfractionated SST3 (see **Figure 5.19B**) or fractionated soy fragments larger than 30 kDa (see **Figure 6.3D**). This again demonstrates the superior emulsion stabilizing capacity of the larger-size polymers against coalescence and Ostwald ripening over the smaller ones.

6.3.2.3 Emulsions based on conjugates made from WP10 and SP10 (fragmented whey and soy protein of molecular size less than 10 kDa)

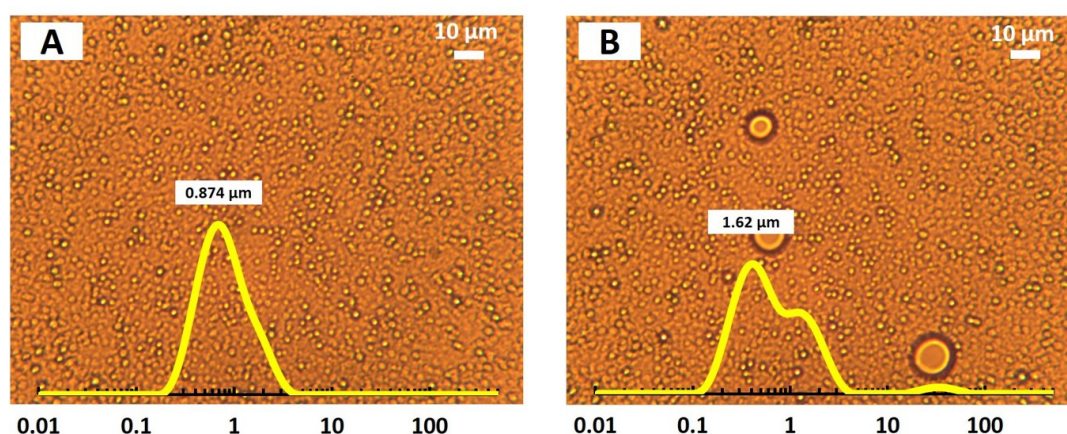


Figure 6.6 Micrographs of freshly made emulsion samples fabricated with conjugated WP10 (A) and conjugated SP10 (B) at pH 7.5. The droplet size distribution and the mean droplet size $D_{4,3}$ are provided on each photo.

Conjugated polymers made from the fraction of the smallest peptides obtained in this study, i.e. less than 10 kDa (WP10-MD and SP10-MD), were seen to have a significantly worse emulsifying ability at pH 7.5, when compared to those made from the other fractions of larger polypeptides with sizes greater than 10 kDa (i.e. WR30-MD and WR10-MD, SR30-MD and SR10-MD). This observation holds true for both conjugated whey protein materials, as well as for the corresponding soy protein materials. The mean droplet size $D_{4,3}$ of fresh emulsion fabricated using WP10-MD was 0.874 μm (**Figure 6.6A**), while the value was even larger (at 1.62 μm) for the SP10-MD stabilized emulsion system. The presence of a few big droplets in the latter system is clearly seen in micrograph of **Figure 6.6B**. Following 60 days of storage, a thin oil layer appeared on top of both emulsion samples, although the whole system was still not completely destabilized at this stage. The formation of the oil layer is the result of coalescence of emulsion droplets, suggesting that the conjugated polymers made from these small protein fragments (of less than 10 kDa) do not possess the interfacial properties that are required for a good emulsifier.

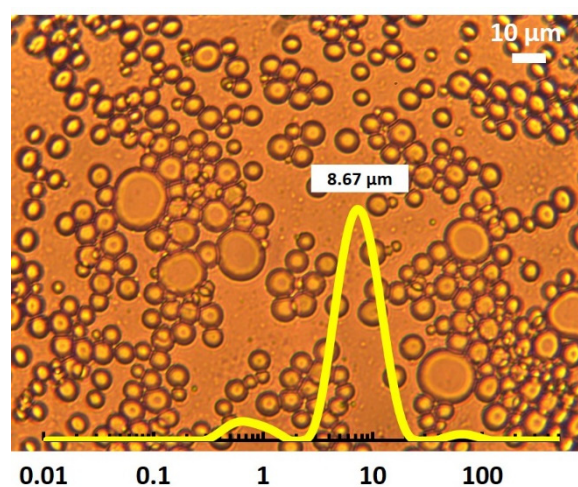


Figure 6.7 Micrograph of freshly made emulsion samples fabricated using conjugated WP10, after adjustment of pH to 4.5. The droplet size distribution and the mean droplet size $D_{4,3}$ are provided on the photo.

When the fresh emulsion sample made from conjugated WP10 was adjusted to pH 4.5, rapid coalescence was seen to occur where all the fine submicron oil droplets immediately disappeared and merged into fairly large ones within a few minutes (see micrograph in **Figure 6.7**). This rapidly destabilized emulsion sample broke down into an upper oil layer and a bottom aqueous phase after just a few days of storage. The

rapid coalescence seen in the current emulsion sample once again indicates that these conjugated polymers, made with small peptides, are unable to provide good stabilization to the emulsion droplets.

The process of droplet coalescence proceeded at an even faster speed in the emulsion sample that was fabricated by conjugated SP10 polymers, when pH was adjusted to 4.5. This emulsion sample was observed to start to show a light yellowish colour during the pH adjustment. Meanwhile, the sample also became significantly more viscous than it was at pH 7.5. A thin layer of oil appeared on the top of the emulsion after the sample was left at room temperature for a few hours. The entire emulsion system completely separated into two immiscible phases (i.e. oil and water) in just a couple of days.

6.4 General Conclusions

In this chapter, the whey and soy protein fragments were separated into three fractions based on their molecular size, i.e. > 30 kDa, 10~30 kDa and < 10 kDa. Conjugates were made using these fractions of protein fragments reacted with maltodextrin. The emulsifying and stabilizing properties of these conjugates were assessed at pH 7.5 and pH 4.5.

It was found that conjugated polymers made from protein fragments larger than 10 kDa were able to provide a reasonable level of emulsion stability. In contrast, the ones made from smaller fragments (less than 10 kDa) were observed to have lost their colloidal stabilizing functionalities. The critical size of a protein fragment for serving as an effective emulsifying and stabilizing agent, post its covalent conjugation with maltodextrin of 8.7 kDa, is found to be roughly 10 kDa.

Moreover, consistent with the findings in Chapter 4 and Chapter 5, it was demonstrated here that for conjugated whey protein materials, the larger the polypeptide size, the more effective the conjugates are as emulsifiers and stabilizers, delivering better stabilization against both flocculation and coalescence. When it comes to conjugated polymers derived from soy fragments, it was observed that the conjugates made from larger soy fragments (e.g. SR30-MD) provide better emulsion

stability against coalescence and Ostwald ripening, compared to the ones produced from smaller soy fragments (e.g. SR10-MD). However, the former is not able to offer better stabilization against droplet flocculation at acidic pH conditions, which is most likely due to the large content of particulate protein aggregates present in this portion of soy protein sample. Such protein particles are not conducive to efficiently react with maltodextrin.

The results in this chapter once again highlight the dual role of the size of soy fragments in inducing good emulsifying and stabilizing ability on one hand and in facilitating the covalent bonding to polysaccharides on the other. In this sense, in order to produce fully plant based conjugated biopolymers for the preparation of fine and stable O/W emulsion at various pH conditions, it may well be promising to remove both the large protein particles and the small peptides (less than a critical size, such as 10 kDa) remaining in the fragmented protein sample.

Chapter 7 General Discussions and Conclusions

7.1 Introduction

The study of protein-polysaccharide conjugates has a long history of more than three decades. Conjugated biopolymers based on milk proteins are typically prepared using a dry-heating Maillard reaction and have been reported to deliver excellent emulsifying and stabilizing functions even under various environmental stresses (e.g. high ionic strength, various pH conditions including pI of the original unmodified protein, temperature cycles, etc.). However, the published work so far on conjugates fabricated from plant proteins, as opposed to animal derived ones, has only provided an incomplete picture and mixed conclusions on the colloidal performances of such emulsifiers.

The current study aims to understand the possibility and the complications involved in turning vegetable proteins into suitable biopolymer-based emulsifying agents using the conjugation route. Ultimately, we hope that this work presented here will aid in producing this class of emulsifiers which rival their animal derived counterparts for making stable and fine O/W emulsions.

Taking commercial isolated soy protein (SPI) as an example of widely used plant storage proteins, the project investigated the impact of enzymatic hydrolysis, followed by conjugation with maltodextrin, on improving the emulsifying and emulsion stabilising behaviour of this protein under various pH conditions. At each stage, careful comparisons with whey protein materials, undergoing exactly the same modification process, were made in order to provide a clearer understanding of the impact of the changes made to SPI.

Hydrolysis was attempted with two enzymes having very different levels of selectivity towards cleavage of peptide bonds. Also, various degrees of hydrolysis (DH = 2.5%, 5.5% and 8.0%) were engineered, in order to examine how the choice of enzyme and DH are affecting the emulsifying and stabilizing properties of protein materials.

Furthermore, by using an electrically neutral, linear and relatively small maltodextrin with no special surface functionalities (e.g. emulsifying, gelling, stabilizing properties) of its own, the characteristics of commercial isolated soy protein and its hydrolysates

as emulsifiers, both prior to and post conjugation with this polysaccharide, were explored.

The main findings regarding the emulsifying and stabilizing performance of protein materials for fabricating stable submicron-sized O/W emulsions under various pH conditions are summarized in this chapter.

7.2 Improved emulsion stability induced by protein-polysaccharide conjugate

The emulsion stabilizing capacity of protein/polypeptide under various pH conditions is found to be significantly enhanced post covalently bonding with maltodextrin. This is demonstrated both theoretically, using self-consistent field calculations (see Chapter 3) and experimentally (see Chapter 4 and Chapter 5).

Chapter 3 displayed the alteration of the total interaction potential, mediated by the adsorbed layers of emulsifiers, between two approaching droplets. It was found that most of the produced polypeptides, unless they happen to adopt a diblock-like structure on the interface, result in a deep potential minimum between droplets, at their respective isoelectric point condition of the polypeptide. However, with a grafted hydrophilic chain (of a sufficient length), the adsorbed conjugated polymer is seen to produce a shallow energy well, followed by an established high energy barrier ($> 20 k_B T$) between the droplets at close inter-droplet separations. The presence of such energy barrier, resulting from steric repulsion, is able to inhibit the approach of droplets, in the absence of electrostatic stabilization. Our theoretical calculations also indicate that various conjugated polymers, so long as they can adsorb at a sufficient level, provide a good and similar stability against droplet flocculation in an emulsion system, regardless of the different structures of the non-bonded polypeptides. In this sense, it is suggested that the mixed interfacial layer, formed as a result of the simultaneous presence of various conjugates (derived from many different polypeptides released during enzymatic hydrolysis), has the ability to continue to provide strong steric stabilization to an emulsion system.

The points above become evident in the experiments in Chapter 4 and Chapter 5. For instance, the emulsion sample stabilized by a mixture of conjugated whey protein

hydrolysates obtained by trypsin digestion at low degree of hydrolysis (i.e. WT1-MD) maintains completely stable at pH 4.5 (i.e. the *pI* of the protein/polypeptides) during a storage period of 60 days. In contrast, the emulsion sample fabricated using the non-bonded counterparts (i.e. WT1) becomes highly clustered. This is then followed by slow droplet coalescence, under the same storage condition. Similarly, for soy protein materials (except for conjugated SSPI which will be summarized in section 7.5), conjugated emulsifiers are also seen to deliver a superior stabilization to emulsion systems.

The colloidal performance of protein/polypeptide and polysaccharide conjugates depends on several factors. The influences arising from the properties of the generated polypeptide and intact protein, the degree of hydrolysis and the choice of enzyme, are captured in the following sections.

7.3 The impact of the molecular size of a polypeptide

For a protein fragment (as well as its conjugated counterpart) to be a good emulsifying and stabilizing agent, it is essential for it to adsorb strongly and substantially on the O/W interface. The desired structural properties for a protein fragment to fulfil the role of providing a strong anchor onto the surface of droplets were theoretically evaluated in Chapter 3. The impact of the two most important characteristics of a polypeptide, i.e. the molecular size and the degree of hydrophobicity (i.e. the proportion of hydrophobic groups), were discussed. It is widely acknowledged that a certain level of hydrophobicity is an important requirement. However, our theoretical results highlight that the molecular size of a protein fragment is more crucial. This is due to the fact that the adsorbed state at equilibrium is determined by the total amount of binding energy of a polymer, instead of just the fraction of hydrophobic groups (i.e. mean binding energy per segment). For a polypeptide derived from naturally occurring proteins, where the hydrophobic and hydrophilic amino acids are relatively evenly distributed along the protein chain, a fragment of a larger size will normally also have a greater number of total binding groups than a smaller one. Consequently, highly hydrophobic but yet small peptides are seen to be unable to establish sufficient amount of adsorption around the droplet surface. Whereas large polypeptides, though with a relatively small fraction of hydrophobic segments, possess a high level of surface affinity. In Chapter 6, it was estimated experimentally that the critical size of a

polypeptide required to anchor the conjugated polymer, produced from its covalent bonding with maltodextrin ($M_w = 8.7$ kDa), was roughly ~ 10 kDa.

As the average molecular size of a mixture of protein hydrolysates obtained through enzyme digestion is governed by the level of fragmentation of proteins, it is suggested that the DH value could serve as a valid parameter to monitor and modulate the emulsifying and stabilizing abilities of fragmented proteins.

7.4 The impact of the degree of hydrolysis (DH) and the choice of enzyme

The variation of the colloidal performance of protein as a function of DH was experimentally evaluated with whey protein (in Chapter 4) and commercial isolated soy protein (in Chapter 5). The action of trypsin was observed to enhance the colloidal performance of whey protein materials at low level of fragmentation (DH = 2.5%). Nonetheless, the improvement for intact whey protein as a result of hydrolysis was quite modest at best. In contrast, the improvement was much more pronounced for intact soy protein, with the optimal DH found to be $\sim 8\%$. A higher level of hydrolysis beyond the optimal point was seen to cause a detrimental effect to the emulsifying and stabilising ability of proteins. Such effect is not limited to whey and soy protein alone, but is a general feature also seen with many other proteins. As discussed previously, this is the result of the increasing release of small peptides.

As enzyme differs in the selectivity of cleavable peptide bonds, the choice of enzyme is also crucial in addition to the degree of hydrolysis. Our experiments with whey protein (in Chapter 4) and soy protein (in Chapter 5) both showed that trypsin is advantageous in terms of the colloidal performance of the resulting fragmented protein materials. The use of alcalase, on the other hand, leads to a deterioration of the functional properties, almost from the very onset of hydrolysis. A likely explanation of the contrasting influences of these two enzymes on the performance of generated protein hydrolysates is that alcalase, having a wide range of amino acid substrates, can achieve a low value of DH ($< 20\%$) by mostly breaking bonds on the surface of protein particles, thus leaving the protein chains in the core of such aggregates less affected. On the other hand, trypsin, with a much more restricted choice of peptide bonds to cleave, has to penetrate deeper into the protein structure and cleave peptide

bonds more uniformly throughout the proteins, in order to achieve the same DH level. Consequently, the action of alcalase tends to lead to the release of a large amount of small fragments, while trypsin is prone to produce intermediate-sized polypeptides. The presence of these latter fragments contributes positively to the modified colloidal emulsifying and stabilising functionality of the protein materials obtained by trypsin digestion.

7.5 The impact of the protein structure

So far, we have mostly captured the common features of modified whey protein and soy protein materials as emulsifying and stabilizing agents. Nonetheless, these materials also displayed some contrasting behaviours (as seen in Chapter 4 and Chapter 5), arising from the different states of the parental intact proteins in the solution.

First of all, the hydrolysates derived from whey protein and soy protein behave differently in their solubility post digestion by enzyme. For milk whey protein which can readily dissolve down to “almost” individual protein molecules, the action of both trypsin and alcalase was seen to cause a reduction in the solubility (at all tested pH conditions). This is suggested to be the result of an averaging effect for the influence of pH on the protein solubility, arising from the production of a mixture of polypeptides (having a distribution of *pI* values). Whereas the solubility was significantly improved for soy protein following hydrolysis. Nonetheless, the solubility here only refers to the apparent solubility, but not the amount of protein material that is truly dissolved. As most commercially available plant derived proteins are present in the form of colloidal-sized protein aggregates in the solution, the reduction of soy protein particle size largely leads to such increase in the apparent solubility.

Moreover, the Maillard reaction products (i.e. MRPs) made with whey protein/polypeptide and those with soy protein/polypeptide, formed following conjugation with polysaccharide, also exhibited distinct functional properties. The former became highly soluble at pH conditions close to *pI*, without formation of any visible protein aggregates, in comparison to their non-bonded counterparts. The emulsion droplets fabricated by these MRPs were all able to remain well dispersed during pH adjustment. On the other hand, all the conjugated soy protein materials did

not show a significant enhancement in their solubility at pI . Particularly, the MRPs made between the non-hydrolysed (but ultrasonicated) SPI and maltodextrin (i.e. SSPI-MD) became extremely insoluble. This is most likely attributed to the large amount of protein aggregates present in the soy protein samples, which does not allow for chemically reactive sites (i.e. $-NH_2$) on protein backbone to be sufficiently exposed nor an intimate mixing of biopolymers on a molecular scale. Therefore, the Maillard reaction between soy protein/polypeptide and maltodextrin becomes restricted. Other obstacles to the efficiency of reaction could come from the non-protein components which bind the protein chains and shield the chemically reactive sites. This insufficient level of conjugation, in the final produced emulsifiers, was responsible for the flocculated morphology of the emulsions stabilized by conjugated soy protein materials.

7.6 Conclusions and outlook

The ultimate aim of this project is to form plant based emulsifiers that are capable of producing and stabilising submicron sized O/W emulsion systems under challenging environmental conditions (e.g. low pH, high salt, etc.), by the route of protein hydrolysis, followed by conjugation with polysaccharides. To achieve this, enzymes with a high level of selectivity are found to be much more beneficial in producing suitable polypeptides. In the following stage of conjugation reaction between protein/polypeptide and polysaccharide, one requires a good mixing between these two biopolymers, almost down to molecular scales.

When it comes to vegetable proteins, the major issue of synthesizing MPRs is the delicate choice of the level of hydrolysis. If too little, then the solubility of the plant protein would remain poor, with the presence of a large number of aggregated proteins. Thus, it would not be possible to achieve a molecular-scaled uniform mixture of protein fragments with polysaccharides, which is an important prerequisite for good reaction efficiency in obtaining suitable conjugates via heating process. Yet, a high DH is equally undesirable as it leads to the production of many small peptides, which will deteriorate the overall colloidal performance. One possible way to overcome such issue is to remove those large and small undesirable components from the protein hydrolysates via ultrafiltration (based on molecular weight of the peptide) in future. Similar studies for other plant proteins (e.g. pea protein) and comparisons with animal

derived ones (e.g. α_{s1} - and β -casein) in future would be most helpful to solidify and support the conclusions that have been arrived at in the current research work.

Whilst a non-charged linear polysaccharide (i.e. maltodextrin) is used throughout the entire project, conjugation with polysaccharide having a more sophisticated structure (e.g. charged or branched) is worthy of future investigations both from a theoretical (though the stiffness of chains is not considered in the currently applied SCF calculations) and experimental perspectives, to see whether the protein/polypeptide with superior emulsifying and stabilizing capacities could be generated.

To conclude, the conjugates of protein and polysaccharide are capable of inducing strong steric stabilization to O/W systems under a wide variety of environmental stresses. They are not only effective emulsifying and stabilizing agents to potentially replace the currently used expensive emulsifiers (e.g. Gum Arabic) in beverage industry (Williams et al., Akhtar et al., 2017), but also promising wall materials for encapsulating lipophilic bioactive compounds (e.g. curcumin, essential oils) (Araiza-Calahorra et al., 2018, Majeed et al., 2015). Moreover, turning vegetable proteins into suitable biopolymer-based emulsifying agents via the current strategy (i.e. protein hydrolysis followed by conjugation with polysaccharides), is likely to provide additional positive biological effects (e.g. antioxidant and immunomodulating activities), due to the health-enhancing properties of the bioactive peptides which may be released from enzymatic hydrolysis of the parental vegetable proteins (Wang et al., 2005, Gibbs et al., 2004).

List of Abbreviations

a_w : water activity

BCA: bicinchoninic acid

BSA: bovine serum albumin

DE: dextrose equivalent

DH: degree of hydrolysis

DLS: Dynamic Light Scattering

DTNB: 5,5'-Dithiobis-(2-nitrobenzoic acid)

DTT: dithiothreitol

DX: dextran

EAI: emulsifying activity index

E/S ratio: enzyme-to-substrate ratio

ESI: emulsion stability index

K_a : acid dissociation constant

pI : isoelectric point

MD7: maltodextrin with a dextrose equivalent number of 4-7

MRPs: Maillard reaction products

M_w : molecular weight

MWCO: molecular weight cut-off

OPA: o-phthalaldehyde

O/W: oil-in-water

RH: relative humidity

SCF: self-consistent field

SDS: sodium dodecyl sulphate

SDS-PAGE: sodium dodecyl sulphate polyacrylamide gel electrophoresis

SPI: soy protein isolate

SSA1: hydrolysed ultrasonicated soy protein isolate obtained by the action of alcalase at DH 2.5%

SSA1-MD: conjugates made from SSA1 and maltodextrin

SSA2: hydrolysed ultrasonicated soy protein isolate obtained by the action of alcalase at DH 5.5%

SSA2-MD: conjugates made from SSA2 and maltodextrin

SSA3: hydrolysed ultrasonicated soy protein isolate obtained by the action of alcalase at DH 8.0%

SSA3-MD: conjugates made from SSA3 and maltodextrin

SSPI: ultrasonicated soy protein isolate

SSPHs: hydrolysed ultrasonicated soy protein isolate

SP10: ultrasonicated soy protein fragments (obtained by the action of trypsin) in the molecular size range of < 10 kDa

SP10-MD: conjugates made from SP10 and maltodextrin

SR10: ultrasonicated soy protein fragments (obtained by the action of trypsin) in the molecular size range between 10~30 kDa

SR10-MD: conjugates made from SR10 and maltodextrin

SR30: ultrasonicated soy protein fragments (obtained by the action of trypsin) in the molecular size range of > 30 kDa

SR30-MD: conjugates made from SR30 and maltodextrin

SST1: hydrolysed ultrasonicated soy protein isolate obtained by the action of trypsin at DH 2.5%

SST1-MD: conjugates made from SST1 and maltodextrin

SST2: hydrolysed ultrasonicated soy protein isolate obtained by the action of trypsin at DH 5.5%

SST2-MD: conjugates made from SST2 and maltodextrin

SST3: hydrolysed ultrasonicated soy protein isolate obtained by the action of trypsin at DH 8.0%

SST3-MD: conjugates made from SST3 and maltodextrin

TNBS: trinitrobenzenesulfonic acid

TNB: 5-thio-2-nitrobenzoic acid

WA1: hydrolysed whey protein isolate obtained by the action of alcalase at DH 2.5%

WA1-MD: conjugates made from WA1 and maltodextrin

WA2: hydrolysed whey protein isolate obtained by the action of alcalase at DH 5.5%

WA2-MD: conjugates made from WA2 and maltodextrin

WA3: hydrolysed whey protein isolate obtained by the action of alcalase at DH 8.0%

WA3-MD: conjugates made from WA3 and maltodextrin

WPHs: whey protein hydrolysates

WPI: whey protein isolate

WP10: whey protein fragments (obtained by the action of trypsin) in the molecular size range of < 10 kDa

WP10-MD: conjugates made from WP10 and maltodextrin

WR10: whey protein fragments (obtained by the action of trypsin) in the molecular size range between 10~30 kDa

WR10-MD: conjugates made from WR10 and maltodextrin

WR30: whey protein fragments (obtained by the action of trypsin) in the molecular size range of > 30 kDa

WR30-MD: conjugates made from WR30 and maltodextrin

WT1: hydrolysed whey protein isolate obtained by the action of trypsin at DH 2.5%

WT1-MD: conjugates made from WT1 and maltodextrin

WT2: hydrolysed whey protein isolate obtained by the action of trypsin at DH 5.5%

WT2-MD: conjugates made from WT2 and maltodextrin

WT3: hydrolysed whey protein isolate obtained by the action of trypsin at DH 8.0%

WT3-MD: conjugates made from WT3 and maltodextrin

Appendix I

Here we provide a more detailed discussion of the self-consistent-field (SCF) theory and calculations on the prediction of the most probable density profiles of various species at equilibrium and the corresponding colloidal interaction potentials mediated by the polymeric chains between the particles.

There are two contributions to the free energy of a system, the enthalpic term and the entropic term (Akinshina et al., 2008, Ettelaie et al., 2014). The former derives from the interactions between different species in the system and is in principle easy to model and compute. The latter however is much more difficult to cope with theoretically, given that a polymer is normally composed of tens or even hundreds or thousands of monomeric segments. This allows such macromolecules to adopt many internal configurations. When polymeric chains interact with each other, the problem becomes a complex many-body problem, with the configuration adopted by one chain also influencing that taken by its neighbouring macromolecules. In order to make progress, a non-interacting system and a set of auxiliary fields $\psi^\alpha(r)$ are considered instead (Ettelaie et al., 2014, Ettelaie et al., 2016, Ettelaie et al., 2003). The non-interacting system comprises of equivalent polymers (i.e. polymer chains that have the same size and sequence of monomer residues as the interacting polymers), as well as all the other monomeric species (ions, solvent, etc.) with the same bulk concentrations as in the interacting system. The difference is that all the species in the non-interacting system are considered to not interact with each other, but instead only interact with a set of external fields $\psi^\alpha(r)$ (Ettelaie et al., 2014). These auxiliary fields $\psi^\alpha(r)$ are specified for each type of monomers at every layer between the two surfaces and only act on their corresponding type of monomers (Ettelaie et al., 2003). In this way, an interacting many-body problem is replaced with that of individual chains interacting with external fields. This latter is far easier to tackle theoretically (Ettelaie et al., 2014). Through tuning those external fields, the concentration profiles $\phi_i^\alpha(r)$ of the non-interacting system could be adjusted until they satisfy certain constraints. These constraints, when satisfied, can be shown to lead to the desired concentration profiles of the equivalent interacting system that minimize the free energy (Ettelaie et al., 2014, Ettelaie et al., 2016, Akinshina et al., 2008). Those above are the general

principles of how to solve the free energy of a real system and sort out the concentration profiles for the minimum free energy.

For convenience, in our project here, the free energy is calculated in units of per surface area a_0^2 and expressed in reference to the free energy of a uniform profile in the bulk (Ettelaie et al., 2014, Akinshina et al., 2008). For an arbitrary set of density profiles $\phi_i^\alpha(r)$ of each monomer species between two planar surfaces at a distance L apart, immersed in a polymer solution, the free energy of the system is obtained by equation (1) (Ettelaie et al., 2014, Akinshina et al., 2008),

$$\begin{aligned} \frac{\Delta F}{k_B T} = & - \int_0^L \left[\sum_i \frac{1}{N_i} \sum_\alpha (\phi_i^\alpha(r) - \Phi_i^\alpha) \right] dr - \int_0^L \left[\sum_\alpha \psi^\alpha(r) \sum_i \phi_i^\alpha(r) \right] dr \\ & + \frac{1}{2} \int_0^L \left[\sum_{ij} \sum_{\alpha \neq \beta} \chi_{\alpha\beta} (\phi_i^\alpha(r) - \Phi_i^\alpha) (\phi_j^\beta(r) - \Phi_j^\beta) \right] dr \\ & + \frac{1}{2} \int_0^L \left[\psi_{el}(r) \sum_\alpha q_\alpha \sum_i \phi_i^\alpha(r) \right] dr + \sum_i \sum_\alpha \chi_{\alpha s} [\phi_i^\alpha(1) + \Phi_i^\alpha(L)] \quad (1) \end{aligned}$$

The $\phi_i^\alpha(r)$ and Φ_i^α in equation (1) represent the concentration of monomers of type α that make up polymer i , in layer r and in bulk, respectively. The layer number r ($1 \leq r \leq L$) represents the distance of each layer measured relative to one of the surfaces (see **Figure 2.1**). The quantities $\psi^\alpha(r)$ are the mean fields that are specified for each type of monomers in every layer between the surfaces. The $\chi_{\alpha\beta}$ is the Flory-Huggins interaction parameter between monomers of types α and β . Similarly, $\chi_{\alpha s}$ is the Flory-Huggins interaction parameter between monomers of type α and the surface, which indeed describes the adsorption energy when a monomer of type α comes into contact with the surface. The number of residues that constitutes polymers of type i is denoted as N_i . For a solvent molecule or an ion, N_i is taken to be 1 (i.e. a single monomeric species with a degree of polymerization of 1). Finally, $\psi_{el}(r)$ represents the electrostatic fields across the gap between the two planar surfaces.

The first two terms in equation (1) account for the entropic contribution to free energy of the system, which derives from the number of different possible spatial and conformational arrangements of all species (i.e. polymers, ions and solvents) in the

system, when a particular set of density profiles $\phi_i^\alpha(r)$ for all the monomer species is given (Ettelaie et al., 2014). This entropic term is obtained with the aid of the non-interacting system introduced (as described previously).

The last three terms in equation (1) involve the enthalpic contribution to free energy that is associated with any given set of density profiles $\phi_i^\alpha(r)$ for each type of monomers (Ettelaie et al., 2014). These are the results of molecular interactions, which include the short-ranged interactions that occur only between neighbouring monomers, the longer ranged electrostatic interactions between the charged monomer species and also the interaction energy due to the adsorption of hydrophobic monomers onto the hydrophobic surfaces (Ettelaie et al., 2014, Akinshina et al., 2008, Ettelaie et al., 2008).

The set of mean fields $\psi^\alpha(r)$ in equation (1) is expressed as below (Ettelaie et al., 2008, Ettelaie et al., 2016, Ettelaie et al., 2014),

$$\psi^\alpha(r) = \psi_h(r) + \sum_i \sum_\beta \chi_{\alpha\beta} (\phi_i^\beta(r) - \Phi_i^\beta) + q_\alpha \psi_{el}(r) + \chi_{\alpha s} (\delta_{r,1} + \delta_{r,L}) \quad (2)$$

where $\psi_h(r)$ is the hard core potential, arising from the crowding effect of monomers in layer r . It ensures the incompressibility of the fluid system, assumed in this work (Ettelaie et al., 2014, Ettelaie et al., 2008). The other components include all possible interactions between different types of monomers and those with the hydrophobic surfaces.

A given set of mean fields $\psi^\alpha(r)$ will result in a corresponding set of density profiles $\phi_i^\alpha(r)$, which can be calculated with the aid of the segment density function $G_i(r, s)$. The quantity $G_i(r, s)$ is the probability of finding a fragment of polymer i which consists of the first s monomers of the polymer chain with the s^{th} ($1 \leq s \leq N_i$) monomer ending in layer r ($1 \leq r \leq L$). The s monomers can be chosen from either end of the chain. As a result of the connectivity of the polymer, consecutive monomers have to reside on adjacent layers or within the same layer. So $G_i(r, s)$ is obtained by equation (3) below (Akinshina et al., 2008, Ettelaie et al., 2016),

$$G_i(r, s) = \exp\left(-\psi^{t_i^\alpha(s)}(r)\right) [\lambda_{-1}G_i(r-1, s-1) + \lambda_0G_i(r, s-1) + \lambda_1G_i(r+1, s-1)] \quad (3)$$

In the above equation, the function $t_i^\alpha(s)$ is defined here to indicate the type to which the s^{th} monomer of polymer i belongs. To simplify the calculations and prevent a proliferation of parameters, the twenty or so amino acid residues of proteins will be grouped into six different categories, depending on the nature of their side chains (Leermakers et al., 1996). The sugar unit that makes up polysaccharides, the solvent molecules, the positive and negative ions, as well as other species that may exist in the system, are regarded as separate monomeric types, as earlier work (Akinshina et al., 2008, Ettelaie et al., 2008). The coefficients λ in the above equation is related to the possible number of positions for the $(s+1)^{th}$ monomer that is connected to the s^{th} monomer residing in layer r . Based on a cubic lattice model, in the absence of interactions between monomers, the values are $\lambda_{-1} = \lambda_1 = 1/6$ and $\lambda_0 = 4/6$ (Akinshina et al., 2008, Ettelaie et al., 2016), as illustrated in **Figure A.1**. That is to say, there are one possible position in layer $(r+1)$ and one in layer $(r-1)$, and a further four in layer r available to the $(s+1)^{th}$ monomer, so as to ensure it remains connected to the s^{th} monomer that is already placed in layer r .

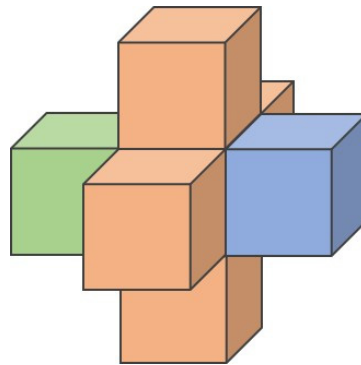


Figure A.1 Schematic illustration of possible positions for the $(s+1)^{th}$ monomer that is connected to the s^{th} monomer in a cubic lattice model. If the s^{th} monomer resides in the middle layer r (yellow colour), then the $(s+1)^{th}$ monomer can be placed at any of the four positions in the same layer r , or the one position in layer $(r-1)$ (green colour), or the one position in layer $(r+1)$ (blue colour).

With the use of composition law and equation (3), density profiles $\phi_i^\alpha(r)$ for each monomer species α belonging to the polymer i , everywhere in the gap, can be determined for a set of arbitrarily applied mean fields $\psi^\alpha(r)$ by equation (4) below (Ettelaie et al., 2016, Ettelaie et al., 2014),

$$\phi_i^\alpha(r) = \frac{\Phi_i^\alpha}{N_i} \sum_{s=1}^{N_i} \frac{G_i^f(r, s) G_i^b(r, N_i - s + 1)}{\exp(-\psi^{t_i^\alpha(s)}(r))} \quad (4)$$

The suffix '*f*' and '*b*', denote 'forward' and 'backward' calculation of the segment density functions respectively, i.e. $G_i^f(r, s)$ and $G_i^b(r, s)$, distinguishing the two ends of the polymer chain from which the s monomers are counted (Ettelaie et al., 2014, Akinshina et al., 2008). Obviously for a homopolymer or a symmetrical chain, this distinction is not necessary and the segment densities calculated from either end would be identical. However, this is often not the case in our study here. For solvent molecules and ions, which are considered as single monomers, equation (4) is simply reduced to,

$$\phi_\alpha(r) = \Phi_\alpha \exp(-\psi^\alpha(r)) \quad (5)$$

In order to solve the most probable concentration profiles $\phi_i^\alpha(r)$ of various species in the gap between two planar surfaces, the free energy in equation (1) has to be minimized, subjected to an additional constraint satisfying the incompressibility of all the species in the system (Ettelaie et al., 2014). This constraint means that the sum of the volume fractions of all monomer species, for every lattice site in the model system, has to add up to one, as shown below in equation (6) ,

$$\sum_i \sum_\alpha \phi_i^\alpha(r) = \sum_i \sum_\alpha \Phi_i^\alpha = 1 \quad (6)$$

Minimization of free energy, under the above constraint expressed in equation (6), will be achieved when the hard core potential $\psi_h(r)$ attains the same value for every type of monomers in layer (Akinshina et al., 2008, Ettelaie et al., 2008). From a mathematical point of view, the hard core potential $\psi_h(r)$ is the Lagrange multiplier associated with the constraint of incompressibility in equation (6) (Ettelaie et al., 2008).

Now it is clearly seen from the above equations that, to obtain the density profiles $\phi_i^\alpha(r)$ through equation (4), we will have to know the mean fields $\psi^\alpha(r)$. On the other hand, the set of fields $\psi^\alpha(r)$ in equation (2) depends on the unknown density distributions $\phi_i^\alpha(r)$ of all types of monomers, in turn. To obtain both sets of quantities, i.e. fields and density profiles, involves solving a set of non-linear equations in a self-consistent manner by an iterative process (Akinshina et al., 2008, Ettelaie et al., 2008). One normally starts the iteration with a set of initially guessed fields $\psi^\alpha(r)$ for each type of monomer in every layer. These values are used in equation (4) to obtain a set of density profiles $\phi_i^\alpha(r)$, from which a new set of fields $\psi^\alpha(r)$ is calculated using equation (2) and compared with the previous set (Ettelaie et al., 2016, Ettelaie et al., 2014). This process is repeated until the difference of both $\phi_i^\alpha(r)$ and $\psi^\alpha(r)$ in two consecutive iterations is within a required degree of accuracy. That is to say, convergence has been achieved. At this point, the desired equilibrium density profiles $\phi_i^\alpha(r)$ and the corresponding mean fields $\psi^\alpha(r)$, which minimize the free energy, have been determined for the specified separation distance between the two hydrophobic surfaces (Ettelaie et al., 2014, Akinshina et al., 2008, Ettelaie et al., 2016).

Such calculations are done for a series of separations between the two planar surfaces. Finally, the interaction potential (per unit area a_0^2) between two surfaces immersed in a polymer solution, due to the presence of adsorbed polymers, is obtained by equation (7) below (Ettelaie et al., 2014),

$$V(r) = \Delta F(r) - \Delta F(\infty) \quad (7)$$

where we take the value of ΔF when two surfaces are sufficiently apart as $\Delta F(\infty)$.

It is to note that the interaction potentials obtained from equation (7) are indeed the interactions between two flat surfaces. These values have to be further manipulated using Derjaguin approximation (Hunter, 2001a, Ettelaie et al., 2014),

$$V_{particle}(r) = -\pi R \int_L^\infty V(r) dr \quad (8)$$

so as to gain the mediated interaction potentials between two spherical colloidal particles/droplets of radius R .

The interaction potentials induced as a result of adsorbed polymer layers, obtained from equation (8), are then combined with the attractive van der Waals forces, which are always present between colloidal particles, irrespective of the behaviors of the polymers. The van der Waals interactions are easily calculated with the aid of the following equation (Everett, 1988j, McClements, 2015c),

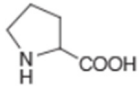
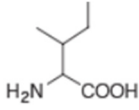
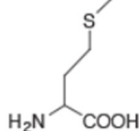
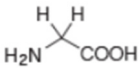
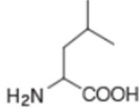
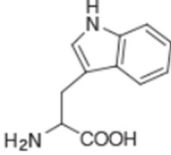
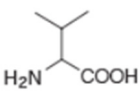
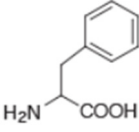
$$V_{van\ der\ Waals} = -\frac{AR}{12r} \quad (8)$$

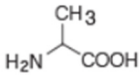
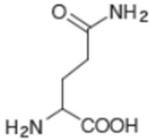
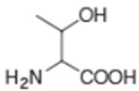
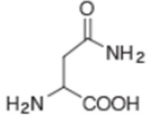
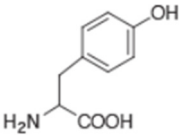
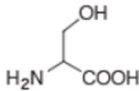
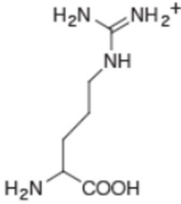
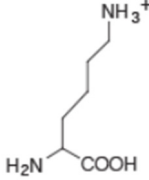
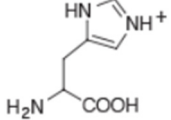
which is valid for equal-sized droplets of radius R , at a separation distance of r apart. A in the above equation is the composite Hamaker constant and is taken as $1\ k_B T$, typical of edible oils in O/W emulsions (Ettelaie et al., 2014). The value of A depends on the ease of polarizability of both the material in the droplets and that in the dispersion medium (Everett, 1988j, McClements, 2015c).

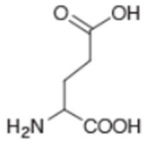
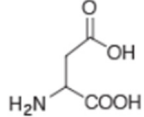
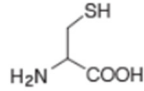
Eventually from the above calculations, the total interaction potential between two dispersed droplets coated with adsorbed polymers in an aqueous solution, can be generated and plotted against the separation distance between the droplets. Such graphs provide useful information on the colloidal stabilizing abilities of polymers. Moreover, the density profiles of polymers, as well as the average distance of each polymer segment can also be determined from these calculations, and are often plotted in conjugation with the induced interaction potential profiles, in order to provide further data on the structural characteristics of the adsorbed polymers that form the interfacial films.

Appendix II

A list of the abbreviations, full names and structures of the amino acids (Belitz et al., 2009) and their classification, based on their degree of hydrophobicity, the nature of charge and the value of their pK_a , is provided in the table below.

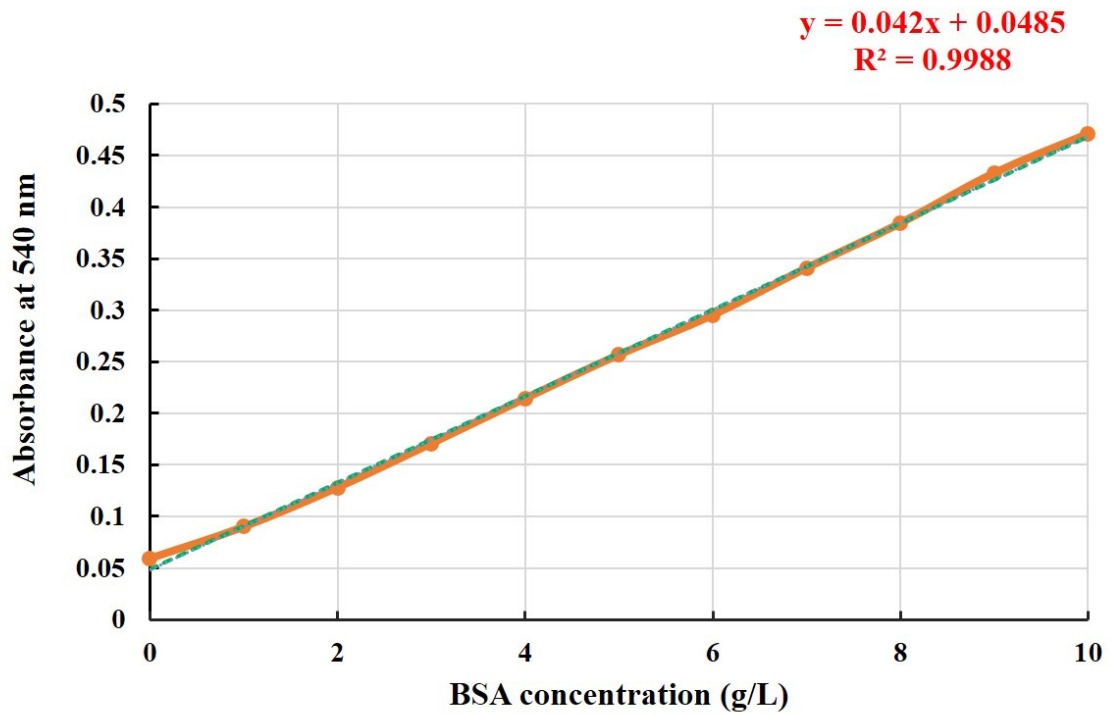
Group	Abbreviation	Full name	Structure
1 - Hydrophobic	Pro	Proline	
	Ile	Isoleucine	
	Met	Methionine	
	Gly	Glycine	
	Leu	Leucine	
	Trp	Tryptophan	
	Val	Valine	
	Phe	Phenylalanine	

	Ala	Alanine	
2 - Polar non-charged	Gln	Glutamine	
	Thr	Threonine	
	Asn	Asparagine	
	Tyr	Tyrosine	
	Ser	Serine	
3 - Positively charged	Arg	Arginine	
	Lys	Lysine	
4 - Histidine	His	Histidine	

5 - Negatively charged	Glu	Glutamic acid	
	Asp	Aspartic acid	
	Cys	Cysteine	

Appendix III

A standard curve of the absorbance (at 540 nm) against protein content (g/L), produced using bovine serum albumin (BSA) as a reference protein, is shown below, in order to determine the protein solubility in the tested samples.



Appendix IV

Citric acid monohydrate ($C_6H_8O_7 \cdot H_2O$, $M_w = 210.14$ g/mol) and trisodium citrate dihydrate ($C_6H_5O_7Na_3 \cdot 2H_2O$ $M_w = 294.12$ g/mol) are used to prepare the buffering systems at pH 3.0 and 4.5. Recipe for the preparation of 1 L buffer with a low background electrolyte concentration of 20 mM is given in the table below (Dawson et al., 1986). The appropriate amounts of the two chemicals are respectively weighed and dissolved in roughly 400 mL deionised water. The obtained two solutions are transferred to a 1 L volumetric flask and made to exactly 1 L with deionised water. The buffer should be well mixed before use.

pH	$C_6H_8O_7 \cdot H_2O$ (g)	$C_6H_5O_7Na_3 \cdot 2H_2O$ (g)
3.0	3.446	1.059
4.5	1.870	3.265

Monopotassium phosphate (KH_2PO_4 , $M_w = 136.09$ g/mol) and disodium phosphate (Na_2HPO_4 , $M_w = 141.98$ g/mol) are used to prepare the buffering system at pH 7.5. Recipe for the preparation of 1 L buffer with a low background electrolyte concentration of 20 mM is given in the table below (Dawson et al., 1986). The appropriate amounts of the two chemicals are respectively weighed and dissolved in roughly 400 mL deionised water. The obtained two solutions are transferred to a 1 L volumetric flask and made to exactly 1 L with deionised water. The buffer should be well mixed before use.

pH	KH_2PO_4 (g)	Na_2HPO_4 (g)
7.5	0.384	2.388

Bibliography

- Adler-Nissen, J. 1976. Enzymic hydrolysis of proteins for increased solubility. *Journal of Agricultural and Food Chemistry*, **24**(6), pp.1090-1093.
- Adler-Nissen, J. 1986. Methods in food protein hydrolysis. In: Adler-Nissen, J. ed. *Enzymic hydrolysis of food proteins*. London: Elsevier, pp.110-169.
- Adler-Nissen, J., Eriksen, S. and Olsen, H. 1983. Improvement of the functionality of vegetable proteins by controlled enzymatic hydrolysis. *Plant Foods for Human Nutrition*, **32**(3), pp.411-423.
- Adler-Nissen, J. and Olsen, H.S. 1979. The influence of peptide chain length on taste and functional properties of enzymatically modified soy protein. In: Pour-Ei, A. ed. *Functionality and protein structure*. ACS Symposium Series, pp.125-146.
- Ahmedna, M., Prinyawiwatkul, W. and Rao, R.M. 1999. Solubilized wheat protein isolate: Functional properties and potential food applications. *Journal of Agricultural and Food Chemistry*, **47**(4), pp.1340-1345.
- Akhtar, M. and Dickinson, E. 2003. Emulsifying properties of whey protein–dextran conjugates at low pH and different salt concentrations. *Colloids and Surfaces B: Biointerfaces*, **31**(1), pp.125-132.
- Akhtar, M. and Dickinson, E. 2007. Whey protein–maltodextrin conjugates as emulsifying agents: An alternative to gum arabic. *Food Hydrocolloids*, **21**(4), pp.607-616.
- Akhtar, M. and Ding, R. 2017. Covalently cross-linked proteins & polysaccharides: Formation, characterisation and potential applications. *Current Opinion in Colloid & Interface Science*, **28**(1), pp.31-36.
- Akinshina, A., Ettelaie, R., Dickinson, E. and Smyth, G. 2008. Interactions between adsorbed layers of alpha(s1)-casein with covalently bound side chains: A self-consistent field study. *Biomacromolecules*, **9**(11), pp.3188-3200.
- Al-Hakkak, J. and Al-Hakkak, F. 2010. Functional egg white–pectin conjugates prepared by controlled maillard reaction. *Journal of Food Engineering*, **100**(1), pp.152-159.
- Ames, J.M. 1992. The maillard reaction. In: Hudson, B.J.F. ed. *Biochemistry of food proteins*. London: Elsevier Applied Science, pp.99-153.
- Araiza-Calahorra, A., Akhtar, M. and Sarkar, A. 2018. Recent advances in emulsion-based delivery approaches for curcumin: From encapsulation to bioaccessibility. *Trends in Food Science & Technology*, **71**(1), pp.155-169.
- Arora, A. and Damodaran, S. 2011. Removal of soy protein-bound phospholipids by a combination of sonication, β -cyclodextrin, and phospholipase a2 treatments. *Food Chemistry*, **127**(3), pp.1007-1013.
- Atkinson, P.J., Dickinson, E., Horne, D.S., Leermakers, F.A.M. and Richardson, R.M. 1996. Theoretical and experimental investigations of adsorbed protein structure at a fluid interface. *Berichte der Bunsengesellschaft für Physikalische Chemie*, **100**(6), pp.994-998.
- Atkinson, P.J., Dickinson, E., Horne, D.S. and Richardson, R.M. 1995. Neutron reflectivity of adsorbed β -casein and β -lactoglobulin at the air/water interface. *Journal of the Chemical Society, Faraday Transactions*, **91**(17), pp.2847-2854.
- Azeredo, H.M.C. and Waldron, K.W. 2016. Crosslinking in polysaccharide and protein films and coatings for food contact – a review. *Trends in Food Science & Technology*, **52**(1), pp.109-122.

- Banta, R.A., Collins, T.W., Curley, R.A., Young, P.W., Holmes, J.D. and Flynn, E.J. 2018. Nanopatterned protein-polysaccharide thin films by humidity regulated phase separation. *Journal of Colloid and Interface Science*, **532**171-181.
- Belitz, H.D., Grosch, W. and Schieberle, P. 2009. *Food chemistry*, Berlin, Springer.
- Boland, M. 2011. Whey proteins. In: Phillips, G.O. & Williams, P.A. eds. *Handbook of food proteins*. Cambridge: Elsevier Science & Technology, pp.30-55.
- Bos, M.A. and Van Vliet, T. 2001. Interfacial rheological properties of adsorbed protein layers and surfactants: A review. *Advances in Colloid and Interface Science*, **91**(3), pp.437-471.
- Burger, T.G. and Zhang, Y. 2019. Recent progress in the utilization of pea protein as an emulsifier for food applications. *Trends in Food Science & Technology*, **86**(1), pp.25-33.
- Burgos-Díaz, C., Wandersleben, T., Marqués, A.M. and Rubilar, M. 2016. Multilayer emulsions stabilized by vegetable proteins and polysaccharides. *Current Opinion in Colloid & Interface Science*, **25**(1), pp.51-57.
- Cheison, S.C., Leeb, E., Toro-Sierra, J. and Kulozik, U. 2011. Influence of hydrolysis temperature and pH on the selective hydrolysis of whey proteins by trypsin and potential recovery of native alpha-lactalbumin. *International Dairy Journal*, **21**(3), pp.166-171.
- Chen, B., Li, H., Ding, Y. and Suo, H. 2012. Formation and microstructural characterization of whey protein isolate/beet pectin coacervations by laccase catalyzed cross-linking. *LWT - Food Science and Technology*, **47**(1), pp.31-38.
- Chen, H., Ji, A., Qiu, S., Liu, Y., Zhu, Q. and Yin, L. 2018a. Covalent conjugation of bovine serum albumin and sugar beet pectin through maillard reaction/laccase catalysis to improve the emulsifying properties. *Food Hydrocolloids*, **76**(1), pp.173-183.
- Chen, L., Chen, J., Ren, J. and Zhao, M. 2011a. Effects of ultrasound pretreatment on the enzymatic hydrolysis of soy protein isolates and on the emulsifying properties of hydrolysates. *Journal of Agricultural and Food Chemistry*, **59**(6), pp.2600-2609.
- Chen, L., Chen, J., Ren, J. and Zhao, M. 2011b. Modifications of soy protein isolates using combined extrusion pre-treatment and controlled enzymatic hydrolysis for improved emulsifying properties. *Food Hydrocolloids*, **25**(5), pp.887-897.
- Chen, L., Chen, J., Wu, K. and Yu, L. 2016. Improved low pH emulsification properties of glycated peanut protein isolate by ultrasound maillard reaction. *Journal of Agricultural and Food Chemistry*, **64**(27), pp.5531-5538.
- Chen, L., Chen, J., Yu, L., Wu, K. and Zhao, M. 2018b. Emulsification performance and interfacial properties of enzymically hydrolyzed peanut protein isolate pretreated by extrusion cooking. *Food Hydrocolloids*, **77**(1), pp.607-616.
- Chen, W., Liang, G., Li, X., He, Z., Zeng, M., Gao, D., Qin, F., Goff, H.D. and Chen, J. 2019. Impact of soy proteins, hydrolysates and monoglycerides at the oil/water interface in emulsions on interfacial properties and emulsion stability. *Colloids and Surfaces B: Biointerfaces*, **177**(2), pp.550-558.
- Chobert, J.M., Bertrand-Harb, C. and Nicolas, M.G. 1988. Solubility and emulsifying properties of caseins and whey proteins modified enzymatically by trypsin. *Journal of agricultural and food chemistry*, (5), pp.883-892.
- Coupland, J. 2014a. Molecules. In: Coupland, J. ed. *An introduction to the physical chemistry of food*. Berlin: Springer, pp.19-40.
- Coupland, J. 2014b. Polymers. In: Coupland, J. ed. *An introduction to the physical chemistry of food*. Berlin: Springer, pp.107-129.

- Coupland, J. 2014c. Surfaces. In: Coupland, J. ed. *An introduction to the physical chemistry of food*. Berlin: Springer, pp.69-76.
- Courthaudon, J.-L., Dickinson, E. and Dalgleish, D.G. 1991. Competitive adsorption of β -casein and nonionic surfactants in oil-in-water emulsions. *Journal of Colloid and Interface Science*, **145**(2), pp.390-395.
- Dawson, R.M.C., Elliot, D.C., Elliot, W.H. and Jones, K.M. 1986. *Data for biochemical research*, Oxford, Clarendon Press.
- de Oliveira, F.C., Coimbra, J.S.D.R., de Oliveira, E.B., Zuñiga, A.D.G. and Rojas, E.E.G. 2016. Food protein-polysaccharide conjugates obtained via the maillard reaction: A review. *Critical Reviews in Food Science and Nutrition*, **56**(7), pp.1108-1125.
- Delahaije, R., Gruppen, H., van Nieuwenhuijzen, N.H., Giuseppin, M.L.F. and Wierenga, P.A. 2013. Effect of glycation on the flocculation behavior of protein-stabilized oil-in-water emulsions. *Langmuir*, **29**(49), pp.15201-15208.
- Dickinson, E. 1992a. Emulsions. In: Dickinson, E. ed. *An introduction to food colloids*. Oxford: Oxford University Press, pp.82-110.
- Dickinson, E. 1992b. Emulsions. In: Dickinson, E. ed. *An introduction to food colloids*. Oxford: Oxford University Press, pp.82-88.
- Dickinson, E. 1992c. The field of study. In: Dickinson, E. ed. *An introduction to food colloids*. Oxford: Oxford University Press, pp.1-5.
- Dickinson, E. 1992d. The field of study. In: Dickinson, E. ed. *An introduction to food colloids*. Oxford: Oxford University Press, pp.1-29.
- Dickinson, E. 1992e. *An introduction to food colloids*, Oxford, Oxford University Press.
- Dickinson, E. 1992f. Proteins at liquid interfaces. In: Dickinson, E. ed. *An introduction to food colloids*. Oxford: Oxford University Press, pp.140-155.
- Dickinson, E. 1992g. Rheology. In: Dickinson, E. ed. *An introduction to food colloids*. Oxford: Oxford University Press, pp.51-76.
- Dickinson, E. 1992h. Structure and composition of adsorbed protein layers and the relationship to emulsion stability. *Journal of the Chemical Society, Faraday Transactions*, **88**(20), pp.2973-2983.
- Dickinson, E. 1997. Flocculation and competitive adsorption in a mixed polymer system relevance to casein-stabilized emulsions. *Journal of the Chemical Society. Faraday transactions*, **93**(13), pp.2297-2301.
- Dickinson, E. 2008. Interfacial structure and stability of food emulsions as affected by protein-polysaccharide interactions. *Soft Matter*, **4**(5), pp.932-942.
- Dickinson, E. 2011. Mixed biopolymers at interfaces: Competitive adsorption and multilayer structures. *Food Hydrocolloids*, **25**(8), pp.1966-1983.
- Dickinson, E. 2015. Colloids in food: Ingredients, structure, and stability. *Annual Review of Food Science and Technology*, **6**(1), pp.211-233.
- Dickinson, E. 2019. Strategies to control and inhibit the flocculation of protein-stabilized oil-in-water emulsions. *Food Hydrocolloids*, **96**(1), pp.209-223.
- Dickinson, E., Horne, D.S., Phipps, J.S. and Richardson, R.M. 1993. A neutron reflectivity study of the adsorption of beta-casein at fluid interfaces. *Langmuir*, **9**(1), pp.242-248.
- Dickinson, E., Horne, D.S., Pinfield, V.J. and Leermakers, F.A.M. 1997a. Self-consistent-field modelling of casein adsorption comparison of results for α s1-casein and β -casein. *Journal of the Chemical Society, Faraday Transactions*, **93**(3), pp.425-432.
- Dickinson, E., Murray, B.S. and Stainsby, G. 1988a. Coalescence stability of emulsion-sized droplets at a planar oil-water interface and the relationship to protein film

- surface rheology. *Journal of the Chemical Society, Faraday Transactions 1: Physical Chemistry in Condensed Phases*, **84**(3), pp.871-883.
- Dickinson, E., Pinfield, V.J., Horne, D.S. and Leermakers, F.A.M. 1997b. Self-consistent-field modelling of adsorbed casein. Interaction between two protein-coated surfaces. *Journal of the Chemical Society. Faraday transactions : physical chemistry & chemical physics*, **93**(9), pp.1785-1790.
- Dickinson, E. and Semenova, M.G. 1992. Emulsifying properties of covalent protein-dextran hybrids. *Colloids and Surfaces*, **64**(3), pp.299-310.
- Dickinson, E. and Stainsby, G. 1988b. Emulsion stability. In: Dickinson, E. & Stainsby, G. eds. *Advances in food emulsions and foams*. London: Elsevier, pp.1-44.
- Diftis, N. and Kiosseoglou, V. 2006. Physicochemical properties of dry-heated soy protein isolate–dextran mixtures. *Food Chemistry*, **96**(2), pp.228-233.
- Diftis, N.G., Biliaderis, C.G. and Kiosseoglou, V.D. 2005. Rheological properties and stability of model salad dressing emulsions prepared with a dry-heated soybean protein isolate–dextran mixture. *Food Hydrocolloids*, **19**(6), pp.1025-1031.
- Dill, K.A. and Bromberg, S. 2003a. Entropy & the boltzmann law. In: Dill, K.A. & Bromberg, S. eds. *Molecular driving forces: Statistical thermodynamics in chemistry and biology*. New York, London: Garland, pp.81-92.
- Dill, K.A. and Bromberg, S. 2003b. Extremum principles predict equilibria. In: Dill, K.A. & Bromberg, S. eds. *Molecular driving forces: Statistical thermodynamics in chemistry and biology*. New York, London: Garland, pp.29-38.
- Dill, K.A. and Bromberg, S. 2003c. Laboratory conditions & free energies. In: Dill, K.A. & Bromberg, S. eds. *Molecular driving forces: Statistical thermodynamics in chemistry and biology*. New York, London: Garland, pp.131-148.
- Dill, K.A. and Bromberg, S. 2003d. Polymer solutions. In: Dill, K.A. & Bromberg, S. eds. *Molecular driving forces: Statistical thermodynamics in chemistry and biology*. New York, London: Garland, pp.593-608.
- Dill, K.A. and Bromberg, S. 2003e. Polymers resist confinement & deformation. In: Dill, K.A. & Bromberg, S. eds. *Molecular driving forces: Statistical thermodynamics in chemistry and biology*. New York;London;: Garland, pp.685-698.
- Ding, R., Valicka, E., Akhtar, M. and Ettelaie, R. 2017. Insignificant impact of the presence of lactose impurity on formation and colloid stabilising properties of whey protein–maltodextrin conjugates prepared via maillard reactions. *Food Structure*, **12**(1), pp.43-53.
- Doucet, D., Otter, D.E., Gauthier, S.F. and Foegeding, E.A. 2003. Enzyme-induced gelation of extensively hydrolyzed whey proteins by alcalase: Peptide identification and determination of enzyme specificity. *Journal of Agricultural and Food Chemistry*, **51**(21), pp.6300-6308.
- Drapala, K.P., Auty, M.A.E., Mulvihill, D.M. and O' Mahony, J.A. 2015. Influence of lecithin on the processing stability of model whey protein hydrolysate-based infant formula emulsions. *International Journal of Dairy Technology*, **68**(3), pp.322-333.
- Drapala, K.P., Auty, M.A.E., Mulvihill, D.M. and O'Mahony, J.A. 2016. Performance of whey protein hydrolysate–maltodextrin conjugates as emulsifiers in model infant formula emulsions. *International Dairy Journal*, **62**(1), pp.76-83.
- Dubey, R., Shami, T.C. and Bhasker Rao, K.U. 2009. Microencapsulation technology and applications. *Defence Science Journal*, **59**(1), pp.82-95.
- Dunlap, C.A. and Cote, G.L. 2005. Beta-lactoglobulin-dextran conjugates: Effect of polysaccharide size on emulsion stability. *Journal of Agricultural and Food Chemistry*, **53**(2), pp.419-423.

- Ellman, G.L. 1959. Tissue sulfhydryl groups. *Archives of Biochemistry and Biophysics*, **82**(1), pp.70-77.
- Ettelaie, R. 2003. Computer simulation and modeling of food colloids. *Current Opinion in Colloid & Interface Science*, **8**(4), pp.415-421.
- Ettelaie, R., Akinshina, A. and Dickinson, E. 2008. Mixed protein-polysaccharide interfacial layers: A self consistent field calculation study. *Faraday discussions*, **139**(1), pp.161-178.
- Ettelaie, R., Akinshina, A. and Maurer, S. 2012. Mixed protein-polysaccharide interfacial layers: Effect of polysaccharide charge distribution. *Soft Matter*, **8**(29), pp.7582-7597.
- Ettelaie, R., Dickinson, E. and Murray, B.S. 2005. Self-consistent-field studies of mediated steric interactions in mixed protein + polysaccharide solutions. In: Dickinson, E. ed. *Food colloids - interactions, microstructure and processing*. Royal Society of Chemistry, pp.74-84.
- Ettelaie, R., Holmes, M., Chen, J. and Farshchi, A. 2016. Steric stabilising properties of hydrophobically modified starch: Amylose vs. Amylopectin. *Food Hydrocolloids*, **58**364-377.
- Ettelaie, R., Murray, B.S. and James, E.L. 2003. Steric interactions mediated by multiblock polymers and biopolymers: Role of block size and addition of hydrophilic side chains. *Colloids and Surfaces B: Biointerfaces*, **31**(1), pp.195-206.
- Ettelaie, R., Zengin, A. and Lee, H. 2014. Fragmented proteins as food emulsion stabilizers: A theoretical study. *Biopolymers*, **101**(9), pp.945-958.
- Ettelaie, R., Zengin, A. and Lishchuk, S.V. 2017. Novel food grade dispersants: Review of recent progress. *Current Opinion in Colloid & Interface Science*, **28**(1), pp.46-55.
- Evans, M., Ratcliffe, I. and Williams, P.A. 2013. Emulsion stabilisation using polysaccharide-protein complexes. *Current Opinion in Colloid & Interface Science*, **18**(4), pp.272-282.
- Everett, D.H. 1988a. Some important properties of colloids. 1. Kinetic properties. In: Everett, D.H. ed. *Basic principles of colloid science*. London: Royal Society of Chemistry, pp.89-93.
- Everett, D.H. 1988b. Some important properties of colloids. 2. Scattering of radiation. In: Everett, D.H. ed. *Basic principles of colloid science*. London: Royal Society of Chemistry, pp.95-104.
- Everett, D.H. 1988c. Some important properties of colloids. 2. Scattering of radiation. In: Everett, D.H. ed. *Basic principles of colloid science*. London: Royal Society of Chemistry, pp.104-107.
- Everett, D.H. 1988d. Some important properties of colloids. 3. Rheology. In: Everett, D.H. ed. *Basic principles of colloid science*. London: Royal Society of Chemistry, pp.110-126.
- Everett, D.H. 1988e. What are colloids? In: Everett, D.H. ed. *Basic principles of colloid science*. London: Royal Society of Chemistry, pp.1-10.
- Everett, D.H. 1988f. Why are colloidal dispersions stable? 1. Basic principles. In: Everett, D.H. ed. *Basic principles of colloid science*. London: Royal Society of Chemistry, pp.25-29.
- Everett, D.H. 1988g. Why are colloidal dispersions stable? 1. Basic principles. In: Everett, D.H. ed. *Basic principles of colloid science*. London: Royal Society of Chemistry, pp.19-24.

- Everett, D.H. 1988h. Why are colloidal dispersions stable? 2. Interparticle forces. In: Everett, D.H. ed. *Basic principles of colloid science*. London: Royal Society of Chemistry, pp.45-50.
- Everett, D.H. 1988i. Why are colloidal dispersions stable? 2. Interparticle forces. In: Everett, D.H. ed. *Basic principles of colloid science*. London: Royal Society of Chemistry, pp.36-45.
- Everett, D.H. 1988j. Why are colloidal dispersions stable? 2. Interparticle forces. In: Everett, D.H. ed. *Basic principles of colloid science*. London: Royal Society of Chemistry, pp.30-36.
- Everett, D.H. 1988k. Why are colloidal dispersions stable? 2. Interparticle forces. In: Everett, D.H. ed. *Basic principles of colloid science*. London: Royal Society of Chemistry, pp.36-53.
- Fang, Y., Li, L., Inoue, C., Lundin, L. and Appelqvist, I. 2006. Associative and segregative phase separations of gelatin/κ-carrageenan aqueous mixtures. *Langmuir*, **22**(23), pp.9532-9537.
- Fleer, G.J., Cohen Stuart, M.A. and Scheutjens, J.M.H.M. 1996. Polymers at interfaces. *Journal of the American Chemical Society*, **118**(43), pp.10678-10678.
- Freer, E.M., Yim, K.S., Fuller, G.G. and Radke, C.J. 2004. Interfacial rheology of globular and flexible proteins at the hexadecane/water interface: Comparison of shear and dilatation deformation. *The Journal of Physical Chemistry B*, **108**(12), pp.3835-3844.
- Friedman, M. 1996. Food browning and its prevention: An overview. *Journal of Agricultural and Food Chemistry*, **44**(3), pp.631-653.
- Fukushima, D. 2004. Soy proteins. In: Yada, R.Y. ed. *Proteins in food processing*. Cambridge: Elsevier Science & Technology, pp.123-145.
- Garti, N., Madar, Z., Aserin, A. and Sternheim, B. 1997. Fenugreek galactomannans as food emulsifiers. *LWT - Food Science and Technology*, **30**(3), pp.305-311.
- Gasteiger, E., Hoogland, C., Gattiker, A., Duvaud, S., Wilkins, M.R., Appel, R.D. and Amos, B. 2005. Protein identification and analysis tools on the expasy server. In: Walker, J.M. ed. *The proteomics protocols handbook*. Totowa, NJ: Humana Press, pp.571-607.
- Genovese, M.I., Barbosa, A.C.L., Pinto, M.D.S. and Lajolo, F.M. 2007. Commercial soy protein ingredients as isoflavone sources for functional foods. *Plant Foods for Human Nutrition*, **62**(2), pp.53-58.
- Gibbs, B.F., Zougman, A., Masse, R. and Mulligan, C. 2004. Production and characterization of bioactive peptides from soy hydrolysate and soy-fermented food. *Food Research International*, **37**(2), pp.123-131.
- Gornall, A.G., Bardawill, C.J. and David, M.M. 1949. Determination of serum proteins by means of the biuret reaction. *The Journal of Biological Chemistry*, **177**(2), pp.751-766.
- Graham, D. and Phillips, M. 1980. Proteins at liquid interfaces. V. Shear properties. *Journal of Colloid and Interface Science*, **76**(1), pp.240-250.
- Gu, F.L., Kim, J.M., Abbas, S., Zhang, X.-M., Xia, S.-Q. and Chen, Z.-X. 2010. Structure and antioxidant activity of high molecular weight maillard reaction products from casein–glucose. *Food Chemistry*, **120**(2), pp.505-511.
- Guan, J.-J., Qiu, A.-Y., Liu, X.-Y., Hua, Y.-F. and Ma, Y.-H. 2006. Microwave improvement of soy protein isolate–saccharide graft reactions. *Food Chemistry*, **97**(4), pp.577-585.

- Guzey, D. and McClements, D.J. 2006. Formation, stability and properties of multilayer emulsions for application in the food industry. *Advances in Colloid and Interface Science*, **128-130**227-248.
- Hansen, R.E. and Winther, J.R. 2009. An introduction to methods for analyzing thiols and disulfides: Reactions, reagents, and practical considerations. *Analytical Biochemistry*, **394**(2), pp.147-158.
- Hashemi, M.M., Aminlari, M. and Moosavinasab, M. 2014. Preparation of and studies on the functional properties and bactericidal activity of the lysozyme–xanthan gum conjugate. *LWT - Food Science and Technology*, **57**(2), pp.594-602.
- Hirst, L.S. 2013a. Colloidal materials. In: Hirst, L.S. ed. *Fundamentals of soft matter science*. Boca Raton: CRC Press, pp.152-156.
- Hirst, L.S. 2013b. Colloidal materials. In: Hirst, L.S. ed. *Fundamentals of soft matter science*. Boca Raton: CRC Press, pp.159-162.
- Hirst, L.S. 2013c. Colloidal materials. In: Hirst, L.S. ed. *Fundamentals of soft matter science*. Boca Raton: CRC Press, pp.156-159.
- Hou, C., Wu, S., Xia, Y., Phillips, G.O. and Cui, S.W. 2017. A novel emulsifier prepared from acacia seyal polysaccharide through maillard reaction with casein peptides. *Food Hydrocolloids*, **69**(1), pp.236-241.
- Huang, X., Kakuda, Y. and Cui, W. 2001. Hydrocolloids in emulsions: Particle size distribution and interfacial activity. *Food Hydrocolloids*, **15**(4), pp.533-542.
- Hunter, R.J. 2001a. *Foundations of colloid science*, Oxford, Oxford University Press.
- Hunter, R.J. 2001b. Nature of colloidal dispersions. In: Hunter, R.J. ed. *Foundations of colloid science*. Second ed. New York: Oxford University Press, pp.1-3.
- Ipsen, R., Otte, J., Sharma, R., Nielsen, A., Gram Hansen, L. and Bruun Qvist, K. 2001. Effect of limited hydrolysis on the interfacial rheology and foaming properties of β -lactoglobulin a. *Colloids and Surfaces B: Biointerfaces*, **21**(1), pp.173-178.
- Isaschar-Ovdat, S. and Fishman, A. 2018. Crosslinking of food proteins mediated by oxidative enzymes – a review. *Trends in Food Science & Technology*, **72**(1), pp.134-143.
- Isaschar-Ovdat, S., Rosenberg, M., Lesmes, U. and Fishman, A. 2015. Characterization of oil-in-water emulsions stabilized by tyrosinase-crosslinked soy glycinin. *Food Hydrocolloids*, **43**(4), pp.493-500.
- Jia, J., Ma, H., Zhao, W., Wang, Z., Tian, W., Luo, L. and He, R. 2010. The use of ultrasound for enzymatic preparation of ace-inhibitory peptides from wheat germ protein. *Food Chemistry*, **119**(1), pp.336-342.
- Jiang, S.-J. and Zhao, X.-H. 2010. Transglutaminase-induced cross-linking and glucosamine conjugation in soybean protein isolates and its impacts on some functional properties of the products. *European Food Research and Technology*, **231**(5), pp.679-689.
- Jiang, S.-J. and Zhao, X.-H. 2011. Transglutaminase-induced cross-linking and glucosamine conjugation of casein and some functional properties of the modified product. *International Dairy Journal*, **21**(4), pp.198-205.
- Jiménez-Castaño, L., Villamiel, M. and López-Fandiño, R. 2007. Glycosylation of individual whey proteins by maillard reaction using dextran of different molecular mass. *Food Hydrocolloids*, **21**(3), pp.433-443.
- Jung, J. and Wicker, L. 2012. Laccase mediated conjugation of heat treated β -lactoglobulin and sugar beet pectin. *Carbohydrate Polymers*, **89**(4), pp.1244-1249.

- Jung, J. and Wicker, L. 2014. B-lactoglobulin conformation and mixed sugar beet pectin gel matrix is changed by laccase. *LWT - Food Science and Technology*, **55**(1), pp.9-15.
- Kasran, M., Cui, S.W. and Goff, H.D. 2013. Covalent attachment of fenugreek gum to soy whey protein isolate through natural maillard reaction for improved emulsion stability. *Food Hydrocolloids*, **30**(2), pp.552-558.
- Kato, A. 2002. Industrial applications of maillard-type protein-polysaccharide conjugates. *Food Science and Technology Research*, **8**(3), pp.193-199.
- Kato, A., Mifuru, R., Matsudomi, N. and Kobayashi, K. 1992. Functional casein-polysaccharide conjugates prepared by controlled dry heating. *Bioscience, Biotechnology, and Biochemistry*, **56**(4), pp.567-571.
- Kato, A., Minaki, K. and Kobayashi, K. 1993. Improvement of emulsifying properties of egg white proteins by the attachment of polysaccharide through maillard reaction in a dry state. *Journal of Agricultural and Food Chemistry*, **41**(4), pp.540-543.
- Kato, A., Shimokawa, K. and Kobayashi, K. 1991. Improvement of the functional properties of insoluble gluten by pronase digestion followed by dextran conjugation. *Journal of agricultural and food chemistry*, **39**(6), pp.1053-1056.
- Kilara, A. and Vaghela, M.N. 2004. Whey proteins. In: Yada, R.Y. ed. *Proteins in food processing*. Cambridge: Elsevier Science & Technology, pp.72-99.
- Kim, H.J., Decker, E.A. and McClements, D.J. 2002a. Impact of protein surface denaturation on droplet flocculation in hexadecane oil-in-water emulsions stabilized by beta-lactoglobulin. *Journal of Agricultural and Food Chemistry*, **50**(24), pp.7131-7137.
- Kim, H.J., Decker, E.A. and McClements, D.J. 2002b. Role of postadsorption conformation changes of beta-lactoglobulin on its ability to stabilize oil droplets against flocculation during heating at neutral ph. *Langmuir*, **18**(20), pp.7577-7583.
- Kim, S.Y., Park, P.S.W. and Rhee, K.C. 1990. Functional properties of proteolytic enzyme modified soy protein isolate. *Journal of Agricultural and Food Chemistry*, **38**(3), pp.651-656.
- Kuipers, B.J.H. 2007. *Aggregation of peptides in soy protein isolate hydrolysates : The individual contributions of glycinin- and β -conglycinin-derived peptides*.
- Lee, J.C. 2002a. Isolated thermal systems. In: Lee, J.C. ed. *Thermal physics: Entropy and free energies*. River Edge, N.J: World Scientific, pp.15-50.
- Lee, J.C. 2002b. Systems in contact with a thermal reservoir. In: Lee, J.C. ed. *Thermal physics: Entropy and free energies*. River Edge, N.J: World Scientific, pp.51-79.
- Lee, S.W., Shimizu, M., Kaminogawa, S. and Yamauchi, K. 1987. Emulsifying properties of peptides obtained from the hydrolyzates of β -casein. *Agricultural and Biological Chemistry*, **51**(1), pp.161-166.
- Leermakers, F.A.M., Atkinson, P.J., Dickinson, E. and Horne, D.S. 1996. Self-consistent-field modeling of adsorbed β -casein: Effects of ph and ionic strength on surface coverage and density profile. *Journal of Colloid And Interface Science*, **178**(2), pp.681-693.
- Li, C., Huang, X., Peng, Q., Shan, Y. and Xue, F. 2014. Physicochemical properties of peanut protein isolate–glucomannan conjugates prepared by ultrasonic treatment. *Ultrasonics Sonochemistry*, **21**(5), pp.1722-1727.
- Li, W., Zhao, H., He, Z., Zeng, M., Qin, F. and Chen, J. 2016. Modification of soy protein hydrolysates by maillard reaction: Effects of carbohydrate chain length

- on structural and interfacial properties. *Colloids and Surfaces B: Biointerfaces*, **138**(1), pp.70-77.
- Li, Y., Le Maux, S., Xiao, H. and McClements, D.J. 2009. Emulsion-based delivery systems for tributyrin, a potential colon cancer preventative agent. *Journal of Agricultural and Food Chemistry*, **57**(19), pp.9243-9249.
- Lifshits, I.M., Grosberg, A.Y. and Khokhlov, A.R. 1978. Some problems of the statistical physics of polymer chains with volume interaction. *Reviews of Modern Physics*, **50**(3), pp.683-713.
- Liu, F. and Tang, C.-H. 2014. Emulsifying properties of soy protein nanoparticles: Influence of the protein concentration and/or emulsification process. *Journal of agricultural and food chemistry*, **62**(12), pp.2644.
- Liu, M. and Damodaran, S. 1999. Effect of transglutaminase-catalyzed polymerization of β -casein on its emulsifying properties. *Journal of Agricultural and Food Chemistry*, **47**(4), pp.1514-1519.
- Liu, Y., Qiu, S., Li, J., Chen, H., Tatsumi, E., Yadav, M. and Yin, L. 2015. Peroxidase-mediated conjugation of corn fiber gum and bovine serum albumin to improve emulsifying properties. *Carbohydrate Polymers*, **118**(1), pp.70-78.
- Liu, Y., Selig, M.J., Yadav, M.P., Yin, L. and Abbaspourrad, A. 2018a. Transglutaminase-treated conjugation of sodium caseinate and corn fiber gum hydrolysate: Interfacial and dilatational properties. *Carbohydrate Polymers*, **187**26-34.
- Liu, Y., Selig, M.J., Yadav, M.P., Yin, L. and Abbaspourrad, A. 2018b. Transglutaminase-treated conjugation of sodium caseinate and corn fiber gum hydrolysate: Interfacial and dilatational properties. *Carbohydrate Polymers*, **187**(1), pp.26-34.
- Liu, Y., Yadav, M.P., Chau, H.K., Qiu, S., Zhang, H. and Yin, L. 2017. Peroxidase-mediated formation of corn fiber gum-bovine serum albumin conjugates: Molecular and structural characterization. *Carbohydrate Polymers*, **166**(1), pp.114-122.
- Liu, Y., Zhao, G., Zhao, M., Ren, J. and Yang, B. 2012. Improvement of functional properties of peanut protein isolate by conjugation with dextran through maillard reaction. *Food Chemistry*, **131**(3), pp.901-906.
- Luo, Y., Pan, K. and Zhong, Q. 2014. Physical, chemical and biochemical properties of casein hydrolyzed by three proteases: Partial characterizations. *Food Chemistry*, **155**(1), pp.146-154.
- Ma, X., Chen, W., Yan, T., Wang, D., Hou, F., Miao, S. and Liu, D. 2020. Comparison of citrus pectin and apple pectin in conjugation with soy protein isolate (spi) under controlled dry-heating conditions. *Food Chemistry*, **309**125501.
- Magrane, M., Martin, M.J., O'Donovan, C. and Apweiler, R. 2005. Protein sequence databases. In: Walker, J.M. ed. *The proteomics protocols handbook*. Totowa, NJ: Humana Press, pp.609-618.
- Majeed, H., Bian, Y.-Y., Ali, B., Jamil, A., Majeed, U., Khan, Q.F., Iqbal, K.J., Shoemaker, C.F. and Fang, Z. 2015. Essential oil encapsulations: Uses, procedures, and trends. *RSC Advances*, **5**(72), pp.58449-58463.
- Martins, S.I.F.S., Jongen, W.M.F. and van Boekel, M.A.J.S. 2000. A review of maillard reaction in food and implications to kinetic modelling. *Trends in Food Science & Technology*, **11**(9), pp.364-373.
- Mat, D.J.L., Cattenoz, T., Souchon, I., Michon, C. and Le Feunteun, S. 2018. Monitoring protein hydrolysis by pepsin using ph-stat: In vitro gastric digestions in static and dynamic ph conditions. *Food Chemistry*, **239**(2), pp.268-275.

- Matemu, A.O., Kayahara, H., Murasawa, H. and Nakamura, S. 2009. Importance of size and charge of carbohydrate chains in the preparation of functional glycoproteins with excellent emulsifying properties from tofu whey. *Food Chemistry*, **114**(4), pp.1328-1334.
- Matsumura, Y., Sirison, J., Ishi, T. and Matsumiya, K. 2017. Soybean lipophilic proteins — origin and functional properties as affected by interaction with storage proteins. *Current Opinion in Colloid & Interface Science*, **28**(1), pp.120-128.
- McClements, D.J. 2004. Protein-stabilized emulsions. *Current Opinion in Colloid & Interface Science*, **9**(5), pp.305-313.
- McClements, D.J. 2010. Emulsion design to improve the delivery of functional lipophilic components. *Annual Review of Food Science and Technology*, **1**(1), pp.241-269.
- McClements, D.J. 2012. Advances in fabrication of emulsions with enhanced functionality using structural design principles. *Current Opinion in Colloid & Interface Science*, **17**(5), pp.235-245.
- McClements, D.J. 2015a. Appearance. In: McClements, D.J. ed. *Food emulsions: Principles, practices, and techniques*. Third ed. Boca Raton: CRC Press, pp.489-496.
- McClements, D.J. 2015b. Characterization of emulsion properties. In: McClements, D.J. ed. *Food emulsions: Principles, practices, and techniques*. Third ed. Boca Raton: CRC Press, pp.623-675.
- McClements, D.J. 2015c. Colloidal interactions. In: McClements, D.J. ed. *Food emulsions: Principles, practices, and techniques*. Third ed. Boca Raton: CRC Press, pp.55-82.
- McClements, D.J. 2015d. Colloidal interactions. In: McClements, D.J. ed. *Food emulsions: Principles, practices, and techniques*. Third ed. Boca Raton: CRC Press, pp.58-64.
- McClements, D.J. 2015e. Colloidal interactions. In: McClements, D.J. ed. *Food emulsions: Principles, practices, and techniques*. Third ed. Boca Raton: CRC Press, pp.64-70.
- McClements, D.J. 2015f. Colloidal interactions. In: McClements, D.J. ed. *Food emulsions: Principles, practices, and techniques*. Third ed. Boca Raton: CRC Press, pp.70-76.
- McClements, D.J. 2015g. Colloidal interactions. In: McClements, D.J. ed. *Food emulsions: Principles, practices, and techniques*. Third ed. Boca Raton: CRC Press, pp.88-89.
- McClements, D.J. 2015h. Colloidal interactions. In: McClements, D.J. ed. *Food emulsions: Principles, practices, and techniques*. Third ed. Boca Raton: CRC Press, pp.76-80.
- McClements, D.J. 2015i. Colloidal interactions. In: McClements, D.J. ed. *Food emulsions: Principles, practices, and techniques*. Third ed. Boca Raton: CRC Press, pp.80-82.
- McClements, D.J. 2015j. Context and background. In: McClements, D.J. ed. *Food emulsions: Principles, practices, and techniques*. Third ed. Boca Raton: CRC Press, pp.9-18.
- McClements, D.J. 2015k. Emulsion flavor. In: McClements, D.J. ed. *Food emulsions: Principles, practices, and techniques*. Third ed. Boca Raton: CRC Press, pp.462-463.

- McClements, D.J. 2015l. Emulsion ingredients. In: McClements, D.J. ed. *Food emulsions: Principles, practices, and techniques*. Third ed. Boca Raton: CRC Press, pp.151-166.
- McClements, D.J. 2015m. Emulsion ingredients. In: McClements, D.J. ed. *Food emulsions: Principles, practices, and techniques*. Third ed. Boca Raton: CRC Press, pp.125-142.
- McClements, D.J. 2015n. Emulsion ingredients. In: McClements, D.J. ed. *Food emulsions: Principles, practices, and techniques*. Third ed. Boca Raton: CRC Press, pp.142-151.
- McClements, D.J. 2015o. Emulsion rheology. In: McClements, D.J. ed. *Food emulsions: Principles, practices, and techniques*. Third ed. Boca Raton: CRC Press Inc, pp.383-432.
- McClements, D.J. 2015p. Emulsion stability. In: McClements, D.J. ed. *Food emulsions: Principles, practices, and techniques*. Third ed. Boca Raton: CRC Press, pp.293-307.
- McClements, D.J. 2015q. Emulsion stability. In: McClements, D.J. ed. *Food emulsions: Principles, practices, and techniques*. Third ed. Boca Raton: CRC Press, pp.318-323.
- McClements, D.J. 2015r. Emulsion stability. In: McClements, D.J. ed. *Food emulsions: Principles, practices, and techniques*. Third ed. Boca Raton: CRC Press, pp.324-325.
- McClements, D.J. 2015s. Emulsion stability. In: McClements, D.J. ed. *Food emulsions: Principles, practices, and techniques*. Third ed. Boca Raton: CRC Press, pp.323-324.
- McClements, D.J. 2015t. Emulsion stability. In: McClements, D.J. ed. *Food emulsions: Principles, practices, and techniques*. Third ed. Boca Raton: CRC Press, pp.325-327.
- McClements, D.J. 2015u. Emulsion stability. In: McClements, D.J. ed. *Food emulsions: Principles, practices, and techniques*. Third ed. Boca Raton: CRC Press, pp.358-365.
- McClements, D.J. 2015v. Emulsion stability. In: McClements, D.J. ed. *Food emulsions: Principles, practices, and techniques*. Third ed. Boca Raton: CRC Press, pp.289-293.
- McClements, D.J. 2015w. Emulsion stability. In: McClements, D.J. ed. *Food emulsions: Principles, practices, and techniques*. Third ed. Boca Raton: CRC Press, pp.334-346.
- McClements, D.J. 2015x. Molecular characteristics. In: McClements, D.J. ed. *Food emulsions: Principles, practices, and techniques*. Third ed. Boca Raton: CRC Press, pp.29-53.
- McNamee, B.F., O'Riorda, E.D. and O'Sullivan, M. 1998. Emulsification and microencapsulation properties of gum arabic. *Journal of Agricultural and Food Chemistry*, **46**(11), pp.4551-4555.
- Meinders, M.B.J., Kloek, W. and van Vliet, T. 2001. Effect of surface elasticity on ostwald ripening in emulsions. *Langmuir*, **17**(13), pp.3923-3929.
- Milczek, E.M. 2018. Commercial applications for enzyme-mediated protein conjugation: New developments in enzymatic processes to deliver functionalized proteins on the commercial scale. *Chemical Reviews*, **118**(1), pp.119-141.
- Moore, J.C., Devries, J.W., Lipp, M., Griffiths, J.C. and Abernethy, D.R. 2010. Total protein methods and their potential utility to reduce the risk of food protein

- adulteration. *Comprehensive Reviews in Food Science and Food Safety*, **9**(4), pp.330-357.
- Moulik, S.P. 1996. Micelles: Self-organized surfactant assemblies. *Current Science*, **71**(5), pp.368-376.
- Mu, L., Zhao, M., Yang, B., Zhao, H., Cui, C. and Zhao, Q. 2010. Effect of ultrasonic treatment on the graft reaction between soy protein isolate and gum acacia and on the physicochemical properties of conjugates. *Journal of agricultural and food chemistry*, **58**(7), pp.4494-4499.
- Mulcahy, E.M., Fargier-Lagrange, M., Mulvihill, D.M. and O'Mahony, J.A. 2017. Characterisation of heat-induced protein aggregation in whey protein isolate and the influence of aggregation on the availability of amino groups as measured by the ortho-phthaldialdehyde (opa) and trinitrobenzenesulfonic acid (tnbs) methods. *Food Chemistry*, **229**66-74.
- Murray, B.S. 2002. Interfacial rheology of food emulsifiers and proteins. *Current Opinion in Colloid & Interface Science*, **7**(5), pp.426-431.
- Murray, B.S. 2011. Rheological properties of protein films. *Current Opinion in Colloid & Interface Science*, **16**(1), pp.27-35.
- Nagano, T., Hirotsuka, M., Mori, H., Kohyama, K. and Nishinari, K. 1992. Dynamic viscoelastic study on the gelation of 7 s globulin from soybeans. *Journal of Agricultural and Food Chemistry*, **40**(6), pp.941-944.
- Nakamura, A., Takahashi, T., Yoshida, R., Maeda, H. and Corredig, M. 2004. Emulsifying properties of soybean soluble polysaccharide. *Food Hydrocolloids*, **18**(5), pp.795-803.
- Nakamura, S., Kato, A. and Kobayashi, K. 1991. New antimicrobial characteristics of lysozyme-dextran conjugate. *Journal of Agricultural and Food Chemistry*, **39**(4), pp.647-650.
- Nash, A.M., Eldridge, A.C. and Wolf, W.J. 1967. Fractionation and characterization of alcohol extractables associated with soybean proteins. Nonprotein components. *Journal of Agricultural and Food Chemistry*, **15**(1), pp.102-108.
- Nishinari, K., Fang, Y., Guo, S. and Phillips, G.O. 2014. Soy proteins: A review on composition, aggregation and emulsification. *Food Hydrocolloids*, **39**(2), pp.301-318.
- Niu, L.Y., Jiang, S.T., Pan, L.J. and Zhai, Y.S. 2011. Characteristics and functional properties of wheat germ protein glycosylated with saccharides through maillard reaction. *International Journal of Food Science & Technology*, **46**(10), pp.2197-2203.
- Nursten, H.E. 2005. Inhibition of non-enzymic browning in foods. In: Nursten, H.E. ed. *The maillard reaction : Chemistry, biology and implications*. Cambridge: Royal Society of Chemistry, pp.152-160.
- O'Regan, J. and Mulvihill, D.M. 2010a. Heat stability and freeze-thaw stability of oil-in-water emulsions stabilised by sodium caseinate-maltodextrin conjugates. *Food Chemistry*, **119**(1), pp.182-190.
- O'Regan, J. and Mulvihill, D.M. 2010b. Sodium caseinate-maltodextrin conjugate hydrolysates: Preparation, characterisation and some functional properties. *Food Chemistry*, **123**(1), pp.21-31.
- O'Regan, J. and Mulvihill, D.M. 2013. Preparation, characterisation and selected functional properties of hydrolysed sodium caseinate-maltodextrin conjugate. *International Journal of Dairy Technology*, **66**(3), pp.333-345.

- Oliver, C.M., Melton, L.D. and Stanley, R.A. 2006. Creating proteins with novel functionality via the maillard reaction: A review. *Critical Reviews in Food Science and Nutrition*, **46**(4), pp.337-350.
- Panyam, D. and Kilara, A. 1996. Enhancing the functionality of food proteins by enzymatic modification. *Trends in Food Science & Technology*, **7**(2), pp.120-125.
- Parkinson, E.L., Ettelaie, R. and Dickinson, E. 2005. Using self-consistent-field theory to understand enhanced steric stabilization by casein-like copolymers at low surface coverage in mixed protein layers. *Biomacromolecules*, **6**(6), pp.3018-3029.
- Petkov, J.T., Gurkov, T.D., Campbell, B.E. and Borwankar, R.P. 2000. Dilatational and shear elasticity of gel-like protein layers on air/water interface. *Langmuir*, **16**(8), pp.3703-3711.
- Pezennec, S., Gauthier, F., Alonso, C., Graner, F., Croguennec, T., Brulé, G. and Renault, A. 2000. The protein net electric charge determines the surface rheological properties of ovalbumin adsorbed at the air-water interface. *Food Hydrocolloids*, **14**(5), pp.463-472.
- Pirestani, S., Nasirpour, A., Keramat, J., Desobry, S. and Jasniewski, J. 2017. Effect of glycosylation with gum arabic by maillard reaction in a liquid system on the emulsifying properties of canola protein isolate. *Carbohydrate Polymers*, **157**(4), pp.1620-1627.
- Pugnaroni, L.A., Dickinson, E., Ettelaie, R., Mackie, A.R. and Wilde, P.J. 2004. Competitive adsorption of proteins and low-molecular-weight surfactants: Computer simulation and microscopic imaging. *Advances in Colloid and Interface Science*, **107**(1), pp.27-49.
- Pugnaroni, L.A., Ettelaie, R. and Dickinson, E. 2003. Growth and aggregation of surfactant islands during the displacement of an adsorbed protein monolayer: A brownian dynamics simulation study. *Colloids and Surfaces B: Biointerfaces*, **31**(1), pp.149-157.
- Qi, M., Hettiarachchy, N.S. and Kalapathy, U. 1997. Solubility and emulsifying properties of soy protein isolates modified by pancreatin. *Journal of Food Science*, **62**(6), pp.1110-1115.
- Qu, W., Zhang, X., Han, X., Wang, Z., He, R. and Ma, H. 2018. Structure and functional characteristics of rapeseed protein isolate-dextran conjugates. *Food Hydrocolloids*, **82**(2), pp.329-337.
- Rao, J. and McClements, D.J. 2012. Impact of lemon oil composition on formation and stability of model food and beverage emulsions. *Food Chemistry*, **134**(2), pp.749-757.
- Ren, C., Tang, L., Zhang, M. and Guo, S. 2009. Structural characterization of heat-induced protein particles in soy milk. *Journal of agricultural and food chemistry*, **57**(5), pp.1921.
- Rivas, H.J. and Sherman, P. 1984. Soy and meat proteins as emulsion stabilizers. 4. The stability and interfacial rheology of o/w emulsions stabilised by soy and meat protein fractions. *Colloids and Surfaces*, **11**(1), pp.155-171.
- Rocco, R.M. 2006. Proteins by the biuret reaction. In: Rocco, R.M. ed. *Landmark papers in clinical chemistry*. Amsterdam: Elsevier, pp.233-250.
- Rufián-Henares, J.A. and Morales, F.J. 2007. Functional properties of melanoidins: In vitro antioxidant, antimicrobial and antihypertensive activities. *Food research international*, **40**(4), pp.995-1002.

- Samoto, M., Maebuchi, M., Miyazaki, C., Kugitani, H., Kohno, M., Hirotsuka, M. and Kito, M. 2007. Abundant proteins associated with lecithin in soy protein isolate. *Food chemistry*, **102**317-322.
- Scheutjens, J.M.H.M. and Fleer, G.J. 1979. Statistical theory of the adsorption of interacting chain molecules. 1. Partition function, segment density distribution, and adsorption isotherms. *The Journal of Physical Chemistry*, **83**(12), pp.1619-1635.
- Scheutjens, J.M.H.M. and Fleer, G.J. 1980. Statistical theory of the adsorption of interacting chain molecules. 2. Train, loop, and tail size distribution. *The Journal of Physical Chemistry*, **84**(2), pp.178-190.
- Schratter, P. and Cutler, P. 2004. Purification and concentration by ultrafiltration. In: Cutler, P. ed. *Protein purification protocols*. Second ed. Totowa, NJ: Humana Press, pp.101-116.
- Schröder, A., Berton-Carabin, C., Venema, P. and Cornacchia, L. 2017. Interfacial properties of whey protein and whey protein hydrolysates and their influence on o/w emulsion stability. *Food Hydrocolloids*, **73**(1), pp.129-140.
- Selinheimo, E., Lampila, P., Mattinen, M.-L. and Buchert, J. 2008. Formation of protein-oligosaccharide conjugates by laccase and tyrosinase. *Journal of Agricultural and Food Chemistry*, **56**(9), pp.3118-3128.
- Shu, Y.-W., Sahara, S., Nakamura, S. and Kato, A. 1996. Effects of the length of polysaccharide chains on the functional properties of the maillard-type lysozyme-polysaccharide conjugate. *Journal of Agricultural and Food Chemistry*, **44**(9), pp.2544-2548.
- Singh, R., Lamoureux, G.V., Lees, W.J. and Whitesides, G.M. 1995. Reagents for rapid reduction of disulfide bonds. *Methods in enzymology*, **251**(1), pp.167.
- Skorepova, J. and Moresoli, C. 2007. Carbohydrate and mineral removal during the production of low-phytate soy protein isolate by combined electroacidification and high shear tangential flow ultrafiltration. *Journal of agricultural and food chemistry*, **55**(14), pp.5645-5652.
- Srinivas, P.R. 2012. Introduction to protein electrophoresis. In: Kurien, B.T. & Scofield, R.H. eds. *Protein electrophoresis: Methods and protocols*. Totowa, NJ: Humana Press, pp.23-28.
- Tamm, F., Herbst, S., Brodkorb, A. and Drusch, S. 2016. Functional properties of pea protein hydrolysates in emulsions and spray-dried microcapsules. *Food Hydrocolloids*, **58**204-214.
- Tang, C.-H. 2017. Emulsifying properties of soy proteins: A critical review with emphasis on the role of conformational flexibility. *Critical Reviews in Food Science and Nutrition*, **57**(12), pp.2636-2679.
- Tavano, O.L. 2013. Protein hydrolysis using proteases: An important tool for food biotechnology. *Journal of Molecular Catalysis B: Enzymatic*, **90**1-11.
- Tcholakova, S., Denkov, N.D., Ivanov, I.B. and Campbell, B. 2006. Coalescence stability of emulsions containing globular milk proteins. *Advances in Colloid and Interface Science*, **123**(2), pp.259-293.
- Thanh, V.H., Okubo, K. and Shibasaki, K. 1975. Isolation and characterization of the multiple 7s globulins of soybean proteins. *Plant physiology*, **56**(1), pp.19-22.
- Tirok, S., Scherze, I. and Muschiolik, G. 2001. Behaviour of formula emulsions containing hydrolysed whey protein and various lecithins. *Colloids and Surfaces B: Biointerfaces*, **21**(1), pp.149-162.
- van der Ven, C., Gruppen, H., de Bont, D.B.A. and Voragen, A.G.J. 2001. Emulsion properties of casein and whey protein hydrolysates and the relation with other

- hydrolysate characteristics. *Journal of Agricultural and Food Chemistry* **49**(10), pp.5005-5012.
- van Koningsveld, G.A., Gruppen, H., de Jongh, H.H.J., Wijngaards, G., van Boekel, M.A.J.S., Walstra, P. and Voragen, A.G.J. 2001. Effects of pH and heat treatments on the structure and solubility of potato proteins in different preparations. *Journal of Agricultural and Food Chemistry*, **49**(10), pp.4889-4897.
- Vu Huu, T. and Shibasaki, K. 1979. Major proteins of soybean seeds. Reversible and irreversible dissociation of β -conglycinin. *Journal of Agricultural and Food Chemistry*, **27**(4), pp.805-809.
- Wagner, J.R., Sorgentini, D.A. and Añón, M.C. 2000. Relation between solubility and surface hydrophobicity as an indicator of modifications during preparation processes of commercial and laboratory-prepared soy protein isolates. *Journal of agricultural and food chemistry*, **48**(8), pp.3159.
- Wang, Q. and Ismail, B. 2012. Effect of maillard-induced glycosylation on the nutritional quality, solubility, thermal stability and molecular configuration of whey protein. *International Dairy Journal*, **25**(2), pp.112-122.
- Wang, W. and De Meija, E.G. 2005. A new frontier in soy bioactive peptides that may prevent age - related chronic diseases. *Comprehensive Reviews in Food Science and Food Safety*, **4**(4), pp.63-78.
- Wang, W. and Zhong, Q. 2014. Properties of whey protein–maltodextrin conjugates as impacted by powder acidity during the maillard reaction. *Food Hydrocolloids*, **38**(1), pp.85-94.
- Wijmans, C.M., Leermakers, F.A.M. and Fleer, G.J. 1994. Multiblock copolymers and colloidal stability. *Journal of Colloid And Interface Science*, **167**(1), pp.124-134.
- Williams, P.A. and Phillips, G.O. Gum arabic. In: Phillips, G.O. & Williams, P.A. eds. *Handbook of hydrocolloids*. Second ed.: Woodhead Publishing, pp.155-168.
- Winther, J.R. and Thorpe, C. 2014. Quantification of thiols and disulfides. *Biochimica et Biophysica Acta (BBA) - General Subjects*, **1840**(2), pp.838-846.
- Wong, B.T., Day, L. and Augustin, M.A. 2011. Deamidated wheat protein–dextran maillard conjugates: Effect of size and location of polysaccharide conjugated on steric stabilization of emulsions at acidic pH. *Food Hydrocolloids*, **25**(6), pp.1424-1432.
- Wooster, T.J. and Augustin, M.A. 2006. B-lactoglobulin–dextran maillard conjugates: Their effect on interfacial thickness and emulsion stability. *Journal of Colloid And Interface Science*, **303**(2), pp.564-572.
- Wooster, T.J. and Augustin, M.A. 2007. The emulsion flocculation stability of protein–carbohydrate diblock copolymers. *Journal of Colloid And Interface Science*, **313**(2), pp.665-675.
- Wrolstad, R.E. 2012. Browning reactions. In: Wrolstad, R.E. ed. *Food carbohydrate chemistry*. Ames, Iowa: Blackwell, pp.60-68.
- Wu, W.U., Hettiarachchy, N.S. and Qi, M. 1998. Hydrophobicity, solubility, and emulsifying properties of soy protein peptides prepared by papain modification and ultrafiltration. *Journal of the American Oil Chemists' Society*, **75**(7), pp.845-850.
- Xu, D., Yuan, F., Gao, Y., McClements, D.J. and Decker, E.A. 2013. Influence of pH, metal chelator, free radical scavenger and interfacial characteristics on the oxidative stability of β -carotene in conjugated whey protein–pectin stabilised emulsion. *Food Chemistry*, **139**(1), pp.1098-1104.

- Xu, J., Han, D., Chen, Z., Li, M. and Jin, H. 2018. Effect of glucose glycosylation following limited enzymatic hydrolysis on functional and conformational properties of black bean protein isolate. *European Food Research and Technology*, **244**(6), pp.1111-1120.
- Xu, K. and Yao, P. 2009. Stable oil-in-water emulsions prepared from soy protein-dextran conjugates. *Langmuir*, **25**(17), pp.9714-9720.
- Yang, Y., Cui, S.W., Gong, J., Guo, Q., Wang, Q. and Hua, Y. 2015. A soy protein-polysaccharides maillard reaction product enhanced the physical stability of oil-in-water emulsions containing citral. *Food Hydrocolloids*, **48**(1), pp.155-164.
- Yin, B., Wang, C., Liu, Z. and Yao, P. 2017. Peptide-polysaccharide conjugates with adjustable hydrophilicity/hydrophobicity as green and pH sensitive emulsifiers. *Food Hydrocolloids*, **63**(1), pp.120-129.
- Yu, J., Wang, G., Wang, X., Xu, Y., Chen, S., Wang, X. and Jiang, L. 2018a. Improving the freeze-thaw stability of soy protein emulsions via combining limited hydrolysis and maillard-induced glycation. *LWT-Food Science and Technology*, **91**(1), pp.63-69.
- Yu, J., Wang, G., Wang, X., Xu, Y., Chen, S., Wang, X. and Jiang, L. 2018b. Improving the freeze-thaw stability of soy protein emulsions via combining limited hydrolysis and maillard-induced glycation. *LWT*, **91**63-69.
- Zha, F., Dong, S., Rao, J. and Chen, B. 2019. Pea protein isolate-gum arabic maillard conjugates improves physical and oxidative stability of oil-in-water emulsions. *Food Chemistry*, **285**(1), pp.130-138.
- Zhang, A., Yu, J., Wang, G., Wang, X. and Zhang, L. 2019a. Improving the emulsion freeze-thaw stability of soy protein hydrolysate-dextran conjugates. *LWT-Food Science and Technology*, **116**.
- Zhang, B., Guo, X., Zhu, K., Peng, W. and Zhou, H. 2015. Improvement of emulsifying properties of oat protein isolate-dextran conjugates by glycation. *Carbohydrate Polymers*, **127**(1), pp.168-175.
- Zhang, J., Wu, N., Yang, X., He, X. and Wang, L. 2012a. Improvement of emulsifying properties of maillard reaction products from β -conglycinin and dextran using controlled enzymatic hydrolysis. *Food Hydrocolloids*, **28**(2), pp.301-312.
- Zhang, Q., Li, L., Lan, Q., Li, M., Wu, D., Chen, H., Liu, Y., Lin, D., Qin, W., Zhang, Z., Liu, J. and Yang, W. 2019b. Protein glycosylation: A promising way to modify the functional properties and extend the application in food system. *Critical Reviews in Food Science and Nutrition*, **59**(15), pp.2506-2533.
- Zhang, X., Qi, J.-R., Li, K.-K., Yin, S.-W., Wang, J.-M., Zhu, J.-H. and Yang, X.-Q. 2012b. Characterization of soy β -conglycinin-dextran conjugate prepared by maillard reaction in crowded liquid system. *Food Research International*, **49**(2), pp.648-654.
- Zhang, Y., Tan, C., Abbas, S., Eric, K., Zhang, X., Xia, S. and Jia, C. 2014a. The effect of soy protein structural modification on emulsion properties and oxidative stability of fish oil microcapsules. *Colloids and Surfaces B: Biointerfaces*, **120**(1), pp.63-70.
- Zhang, Y., Tan, C., Abbas, S., Eric, K., Zhang, X., Xia, S. and Jia, C. 2014b. The effect of soy protein structural modification on emulsion properties and oxidative stability of fish oil microcapsules. *Colloids and Surfaces B: Biointerfaces*, **120**63-70.
- Zhang, Y., Tan, C., Zhang, X., Xia, S., Jia, C., Eric, K., Abbas, S., Feng, B. and Zhong, F. 2014c. Effects of maltodextrin glycosylation following limited enzymatic

- hydrolysis on the functional and conformational properties of soybean protein isolate. *European Food Research and Technology*, **238**(6), pp.957-968.
- Zhang, Y., Zhou, F., Zhao, M., Lin, L., Ning, Z. and Sun, B. 2018. Soy peptide nanoparticles by ultrasound-induced self-assembly of large peptide aggregates and their role on emulsion stability. *Food Hydrocolloids*, **74**(1), pp.62-71.
- Zhao, G., Liu, Y., Zhao, M., Ren, J. and Yang, B. 2011. Enzymatic hydrolysis and their effects on conformational and functional properties of peanut protein isolate. *Food Chemistry*, **127**(4), pp.1438-1443.
- Zhu, C.-Y., Wang, X.-P. and Zhao, X.-H. 2015. Property modification of caseinate responsible to transglutaminase-induced glycosylation and crosslinking in the presence of a degraded chitosan. *Food Science and Biotechnology*, **24**(3), pp.843-850.
- Zhu, D., Damodaran, S. and Lucey, J.A. 2008. Formation of whey protein isolate (wpi)-dextran conjugates in aqueous solutions. *Journal of Agricultural and Food Chemistry*, **56**(16), pp.7113-7118.